The Resistance Increase of a Ship in Waves

J.J. Blok

Printed by:
Grafisch Bedrijf Ponsen & Looijen BV, Wageningen

The Resistance Increase of a Ship in Waves

Proefschrift
ter verkrijging van de graad van doctor
aan de Technische Universiteit Delft,
op gezag van de Rector Magnificus,
Prof. Drs. P.A. Schenck,
in het openbaar te verdedigen
ten overstaan van een commissie
aangewezen door het College van Dekanen
op donderdag 10 juni 1993
te 14.00 uur

door

Jan Jacobus Blok

geboren op 13 juni 1947 te Voorburg,
Scheepsbouwkundig Ingenieur.

Dit Proefschrift is goedgekeurd door de Promotor:
Prof. Ir. J. Gerritsma

Aan mijn ouders
Annejuul
Marloes
Merle

Table of Contents

Stellingen

1. De weerstandsverhoging van een schip in golven wordt voor het grootste gedeelte veroorzaakt door de relatieve verticale waterbeweging rond de boeg.

2. Uit model experimenten en uit mathematische modelering blijkt dat de krachten, die verantwoordelijk zijn voor de weerstandverhoging van een varend schip in recht van voren komende golven, in hoofdzaak werken op het gedeelte van de boeg dat zich ten gevolge van de relatieve verticale waterbeweging afwisselend boven en onder water bevindt.

3. De relatieve verticale waterbeweging aan de boeg van een schip bevat een aanzienlijke bijdrage van de interactie tussen de instationaire en de stationaire component van de stroming. Deze interactie wordt aan het wateroppervlak zichtbaar door de 'dynamische opstuwing' van het water. Het verschijnsel wordt geregeerd door de ongestoorde relatieve verticale waterbeweging en neemt in betekenis toe naarmate de spantvorm aan de boeg meer uitwaaiering vertoont.

4. Vanuit het oogpunt van toegepaste weerstand in golven heeft een scherpe boeg de voorkeur in korte golven en een ronde boeg de voorkeur in lange golven.

5. In die gevallen waarin het snelheidsverlies van een schip ten gevolge van wind en golven sterker van de vaarrichting afhangt dan de bijbehorende verlenging van de baan, dient het varen van een zig-zag koers te worden aanbevolen.

6. Het niet-lineaire gedrag van de buigende momenten en de dwarskrachten in de romp van een varend schip in golven kan beschreven worden met het Wiener-Volterra model met medenemen van termen tot en met de derde orde. Hiermee kan met name het verschil tussen het 'hogging' en het 'sagging' moment verklaard worden.

7. De moderne trend bij het ontwerpen van constructies om empirisch verworven kennis te vervangen door rationele probabilistische ontwerp methoden met het doel te komen tot lichtere constructies, leidt niet alleen tot een toeneming van de zekerheid bij de ontwerper maar ook tot een afgenomen feitelijke zekerheid van de integriteit van de constructie.

8. De trends tot individualisering van de samenleving en de beoogde integratie van Europa staan haaks op elkaar, omdat beide een tegengesteld beroep doen op het solidariteitsgevoel met de medemens.

9. Voor het gelijktijdig verwerken van informatie uit diverse bronnen (gesprekken, telefoon, krant, en kabel TV) is het verleidelijk om de principes van 'multi-channel sampling' toe te passen; men dient zich daarbij echter bewust te zijn van het grote risico van volstrekt foute interpretatie ten gevolge van de gebruikte bemonstering.

10. Waar centraal wordt geleid wordt decentraal geleden.

11. De veel gehoorde stelling, dat kennis van de geschiedenis ons helpt het heden te begrijpen, dient uitgebreid te worden met het omgekeerde.

12. Aangezien voor de gezondheid van de mens voeding uit vis beter is dan uit vlees dienen de Schermer, Beemster, Purmer en Wormer wederom te worden ingericht voor het kweken van vis in plaats van vlees. Dat de watersport recreatie hier tevens van meeprofiteert moet gezien worden als een bijkomend voordeel.

13. Bij het verklaren van fysische verschijnselen dient van alle mogelijke verklaringen de meest eenvoudige als eerste te worden beschouwd.

14. De belangstelling van de locale bevolking naar amateur-tekenkunst in het vrije veld is in West-Europa omgekeerd evenredig met de leeftijd en met de breedtegraad.

Stellingen behorend bij proefschrift van J.J.Blok:
"The Resistance Increase of a Ship in Waves",
10 juni 1993

A full-body bulk carrier in waves from ahead.

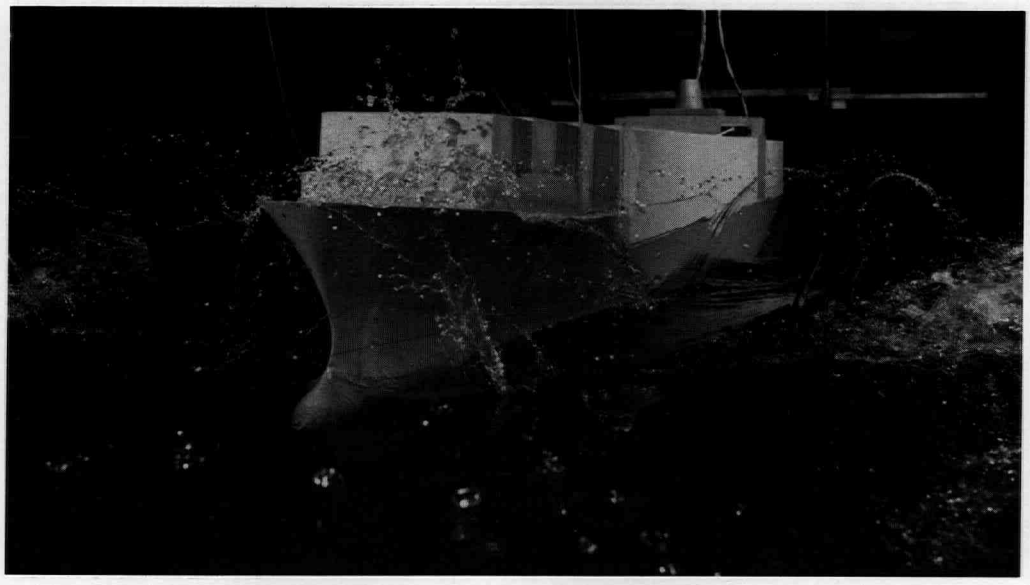

A model of a large containership in high waves.

The oceanographic research ship Hr. Ms. Tydeman showing her boot-topping in a seaway, [Courtesy Royal Netherlands Navy].

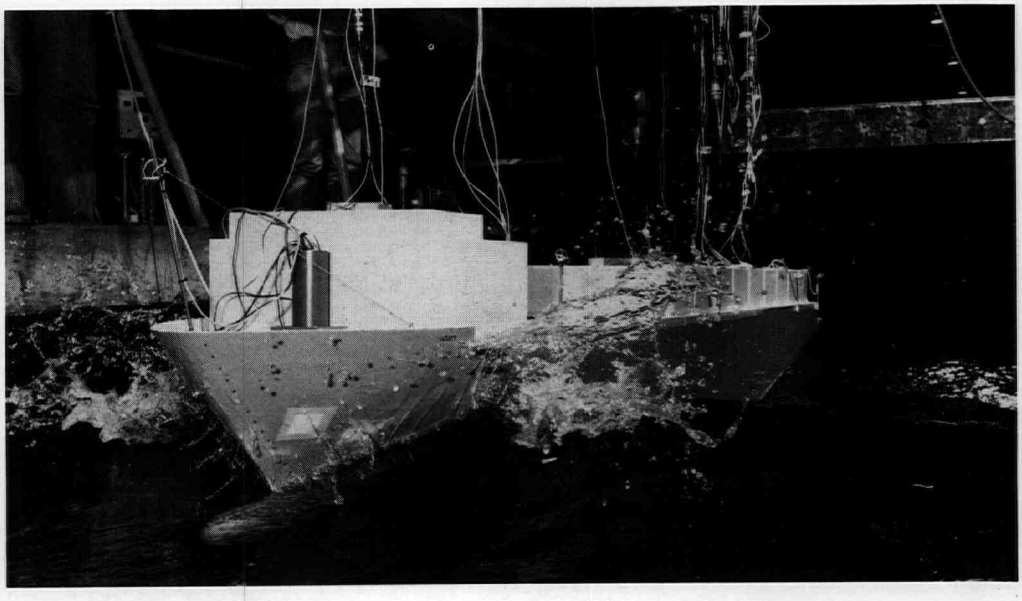

A model of a hatchcoverless containership undergoing seakeeping experiments, [Courtesy Fincantieri, Trieste].

A heavy-load ship in a moderate seaway; view taken from jack-up drilling rig deck cargo, looking forward at the bow,
[Courtesy Dock-Express Shipping B.V., Rotterdam].

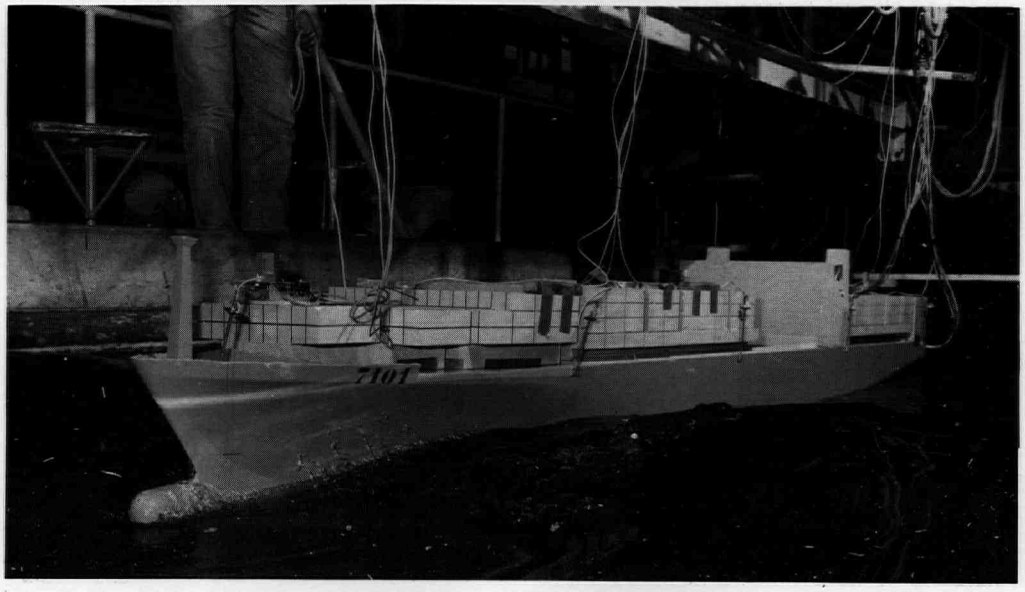

A model of a 265 m long open containership in bow quartering seas,
[Courtesy Nedlloyd Lines, Rotterdam].

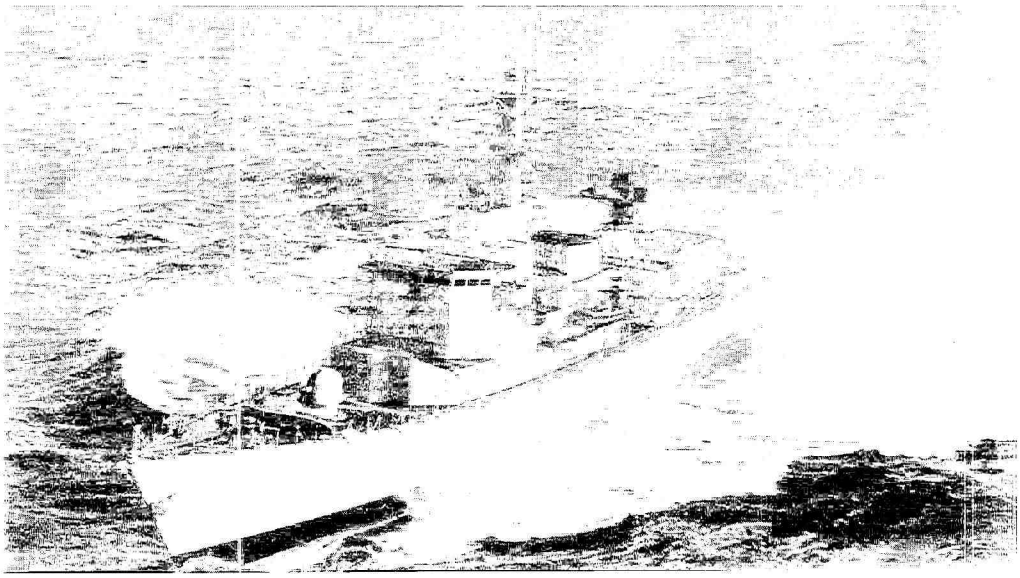

Chapter 1

Introduction

1.1 Resistance components

A ship at speed experiences a resistance force due to the two fluids, water and air. Even though the density of air is almost a thousand times less than that of water, the resulting resistance forces can be of equal order of magnitude, due to the higher air flow velocity (velocity squared law) and the usually larger 'sail' area of the ship above the water.

The resistance in air and in water, can fundamentally be split up into tangential forces and normal forces, the former from viscous origin, the latter from potential (pressure) origin. For the present investigation we will be dealing with the resistance in water only.

Under truly ideal flow conditions the paradox of d'Alembert holds, which implies that no hydrodynamic force acts on a body moving with constant translational velocity in an infinite, inviscid, and irrotational fluid. Hence it takes no work or energy to proceed a body in a fluid. Unfortunately, the flow condition in reality is less than 'ideal' and it takes considerable effort to move a ship through the water. The main effect stemming from friction due to the viscosity of the fluid and from the wave system set up on the surface of the fluid.

It is historically a practical expedient that the resistance in water is decomposed into the resistance in undisturbed calm water plus a variety of additional effects. Usually the extra effects result in an increase of the resistance, but occasionally one may find a reduction of the resistance.

The extra effects on top of calm water resistance will be due to:

- an existing incident fluid velocity (current),
- non-uniformity or instationarity of the fluid (surface waves),
- roughness of the surface of the body,
- a change in attitude (trim, heel, drift angle),
- resistance of appendages (rudder, propeller struts, bilge keels, fins, sonar dome, intakes),
- bottom effects (shallow water effects).

It is very often assumed that the extra resistance components can be superimposed onto one another, though great care is to be exercised with respect to the possible interferences.

In real ships virtually always all resistance components are present to some degree, and it is not possible to isolate their influence and study them separately. Here model experiments come into their own because they offer the possibility of systematic experiments to separate the resistance components and isolate the independent contributing parts.

The scaling of model test results from a small model to a big ship continues to be of major concern, even though some procedures have been established and have gained wide application, perhaps more for practical reasons and by international consensus than for fundamental reasons.

In the model experiment one has to comply with a number of scaling laws of which the Reynolds law for viscous effects and the Froude scaling law for accelerations related effects are well-known. Different scaling laws and factors apply to the conversion of data from model experiment to full scale values for the various components of resistance.

The extra resistance component that results from gravity waves on the surface of the fluid is the subject of our interest inasmuch as it represents a formidable resistance force to the progress of the ship, when there are waves, (viz. Photo 1-1).

Fortunately enough, periods of stormy weather with waves are separated by even longer spells of fine weather, which does not, however, distract from the importance of the subject because periods with moderate seaways will persist much longer.

It will be made clear later (Section 1.5) just to how much this resistance can amount for some typical ship types under light, moderate and heavy weather conditions.

Photo 1-1: A Standard Frigate in heavy weather.
(Courtesy Royal Netherlands Navy)

1.2 Propulsion components

Apart from the resistance, all the aforementioned influences also have a bearing on the propulsion of the ship. This need not have been the case. If the propulsive power were imparted to the ship from outside the air and water fluids, such as a ship towed from a line, no interference would probably take place.

However, the most common way of propelling a ship is by imparting a certain backward momentum to the fluid and thereby obtaining a forward force on the ship. This can most effectively be done by 'some rotary device' in the water, the heaviest fluid. This can either be an internal pump (waterjet) or an external pump (propeller or paddle wheel). In some instances the momentum is imparted to the lighter fluid by air-screws, because the ship's limited draft does not allow the fitting of an underwater screw, as in hovercraft.

Since the propelling device is in the water the causes of extra resistance will also affect the propulsion (viz. Photo 1-2).

Another example of interference between resistance and propulsion is that a more powerful propeller sucks the water towards it at a higher velocity thereby increasing the frictional resistance along the aftbody, and also altering the flow separation.

Propeller effectiveness and efficiency are generally influenced by the same factors that also affect resistance. Yet the propulsion side is outside our scope of research, and we will leave it at these remarks.

Photo 1-2: Oscillatory ship motions and orbital wave motion will produce an oscillatory inflow into the propeller [open containership model in waves, courtesy Verolme Shipyard Heusden B.V.]

1.3 Added resistance

Let us define the subject of our investigation more precisely. Assume the ship to progress on a calm fluid in an upright fashion, no heel, no trim, at constant speed. The so-called 'calm water resistance' then experienced is our 'datum' resistance.

Let us further assume there to exist an incident wave pattern on the surface of that fluid, harmonic or random, from one oblique angle or from various angles. The effect these waves have on the resistance of the ship is the subject of our investigation.

For a better understanding of the phenomenon involved we confine ourselves to waves from ahead, both because this is the most demanding condition and causes the largest resistance increase and also because the symmetric case is the first to come in for an investigation; directional spreading and short-crest-

edness of wave components are further complicating factors to be deferred to a later stage.

The instationary water motion (instationary both in an earth-bound reference frame as well as in a ship-bound reference frame) results in a change in the potential (pressure) resistance. It can be shown that the frictional resistance increase is at least an order of magnitude smaller than the potential effect and can be left out of the picture (Section 5.1).

Under the influence of the harmonic sinusoidal waves the normal pressure that any point on the underwater hull of the ship experiences is an oscillatory quantity with very small, if not zero, mean value. The oscillation is partly due to the incident wave orbital motion and associated pressure variation, and partly because of the oscillatory ship motions set up by the waves. Conversely, just because each point experiences an oscillatory pressure they combine to a force capable to set the total ship in motion.

It has long been thought that the oscillatory force on the ship as a whole was bound to have also zero time mean value, because the pressures have zero mean, or very nearly so. Further thought, however, spurred by experimental observation and by energy and momentum considerations, has given the insight that indeed a sizeable, non-zero, time-averaged mean force value will occur, what model experiments had shown to exist already.

In the broad sense the ultimate goal of the research on this subject is to obtain the relation between the total ship resistance and the hull form, for a range of ship speeds and for all possible wave conditions. In the present study we will only address a part of it and investigate the 'added resistance due to waves' and its physical origin.

1.4 History

Historically ship hull forms were compared on resistance in calm water alone, because it was in the past quite impossible to define the highly irregular and random nature of the waves in useful terms and characterize it by a few numbers. Now that we have acquired spectral analysis as a tool to deal with the irregular nature of the sea waves, and obtained the link with regular sinusoidal waves, the effect that waves have on a ship can be investigated in a more rational manner.

Early studies on the subject of wave added resistance and its effect on slowing down of the ship were carried out by Kent [1-1], Möckel [1-2] and Lewis [1-3]. The studies were based on observations made at sea and a vast amount of logbook data was analyzed to obtain statistical data on the speed loss in particular. The diagram shown in Figure 1-1 based on work by Lewis and Morrison [1-4] and [1-5] shows the dramatic slowing down of Victory-type ships in rough seas.

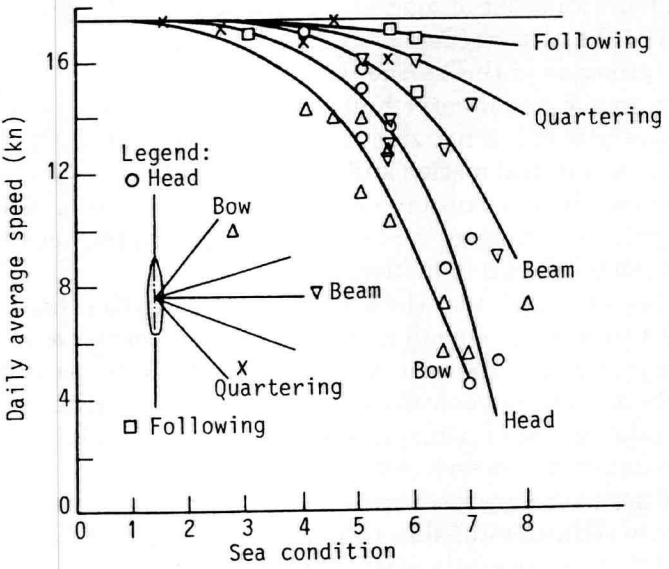

Figure 1-1: Reduction of speed of Victory-type ships in rough sea approaching from various directions [1-4].

In a naval context the added resistance due to waves has been a factor of importance in some major sea battles (Salamis [1-6] and North Cape [1-7]). More recently reports deal with the added resistance as a major hindrance to fleet operations, viz. Kehoe [1-8] and Comstock et al. [1-9].

1.5 Nowadays

The knowledge of added resistance due to waves and the possibility to minimize it by changes in ship particulars and hull form has stirred up the operator's interest in optimizing ships in this respect. Some idea of the order of magnitude that we are talking about is given in the Figure 1-2. Knowledge about the relation between added resistance and hull size and form can lead to hull forms more efficient in waves.

It is shown for a number of ships types that in moderate seaways at speeds not far below the designed service speed the added resistance is responsible for up to 50 percent of the total resistance. It depends very much on the service speed, the shape of the resistance curve and the overload characteristics of the propeller whether the speed can be maintained in waves or not.

In even higher wave and wind cases the master of the ship is forced to 'voluntarily' reduce speed or change heading on account of extreme effects like 'bow pounding', 'water on the deck' or 'propeller tip out of the water' occurring too often.

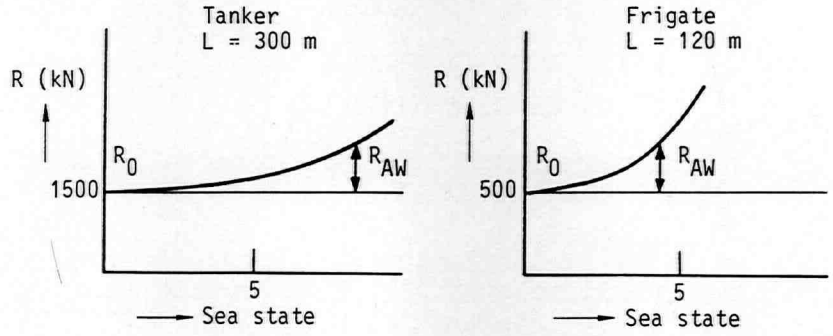

Figure 1-2: Resistance increase as a function of sea state for a tanker and a frigate at their design speed.

A trend can be discerned towards 'designing for service conditions' in which the probability of occurrence of storms along the projected trade route of the ship is taken into account in making a selection of the best hull form, i.e. the hull is not selected on basis of low calm water resistance alone.

In the 1980's ships were generally given lower service speeds so that the resistance increase due to waves and its importance has even relatively increased.

Since in sea transportation the fuel cost continues to represent a large proportion of the total operating costs, great emphasis continues to be laid on low overall resistance and efficient propulsion. For a great number of commodities the ship remains the cheapest and often the only means of transportation over long distances which can be deployed in a flexible manner.

Chapter 2

Review of literature on resistance increase in waves

2.1 General overview

In the present section an overview is given of the literature that has been published in the recent past on the subject of added resistance due to waves.

Historically the added resistance due to waves was considered as an extra 'drag' on top of the calm water resistance and in the estimation of the necessary engine power an allowance was made for service conditions, involving waves and wind.

With the advent of the spectral analysis techniques and the breakthrough of Seakeeping as a branch of science in its own right in the 1950's the opportunity opened up to make rational predictions of wave added resistance for realistic seaways. These estimates were at that time mostly based on results of model tests conducted in either regular waves or in irregular waves.

The extension of spectral analysis techniques to the propulsion quantities like thrust and torque led to ways of predicting the extra thrust, torque or horsepower to drive the ship at a constant mean speed in waves or conversely to obtain the speed loss for a given installed power and prevailing seaway.

Later in the 1950's, as the potential theory applications to seakeeping became more in existence, attempts were made to compute added resistance as a follow-up to ship motions.

In the present time a good deal of literature exists on the subject by which added resistance can be computed in a truly theoretical fashion.

Basically added resistance theories can be split up into five categories:

a. theories based on energy conservation considerations,
b. theories based on momentum considerations,
c. theories based on pressure integration over the wetted surface,
d. theories based on the 'ray' theory of reflection,
e. computational models based on regression on model experiment data.

This split-up is by no means very rigorous, as combinations of various approaches do arise.

All theories, except the last, are based on potential theory. The most common theoretical methods for added resistance of a ship in regular waves are either derived by using the equations for conservation of energy or change of momentum in the fluid, or by directly integrating the pressure over the wetted ship surface. The procedures are mostly based on a description involving a perturbation scheme where the first order motions and loads are obtained as a first approximation. The added resistance is found as the time average of the longitudinal force.

The method of direct pressure integration has the advantage of being easier to comprehend and understand the physical phenomena of added resistance.

Most theories are based on some kind of slenderness assumption, which makes them questionable to apply to blunt ships.

Theories under 'a' are based on the fact that potential damping energy can only be radiated by surface waves emanating away from the ship. The energy that the ship radiates through surface waves is equated to the work that the ship does on the fluid. This work can only be drawn from the propulsive power. The theory can be either two-dimensional (2-D) or three-dimensional (3-D), the radiated waves being obtained from a strip theory application or from a full 3-D description.

Theories under 'b' make use of the momentum equation applied to a volume of fluid surrounding the ship, the wetted hull forming the inner boundary, the outer boundary being situated at infinity or at sufficiently large distance from the ship.

The force exerted by the waves on the ship can be expressed in terms of the integrated change of momentum of the fluid flowing through the control boundary. With the use of the Green's theorem the integration over the inner boundary (the hull) can be shifted to the outer boundary so as to finally result in one integration solely over a suitable control surface at infinity. For this integration to be carried out and to obtain tangible results some measure of slenderness of the ship is usually adopted, and the potentials are usually replaced by their much simpler asymptotic behaviour at infinity.

Theories under 'c' are also based on the potential theory. The fluid in the vicinity of the body is described by a suitable singularity distribution over the hull surface. Using the Bernoulli equation the pressure on the hull is obtained from the flow velocities whereupon the force on the ship is obtained through direct integration. In some of the cases the integration over the hull is exchanged for an integration over a control surface far away from the ship by using Green's theorem. In this way the far field behaviour of the potentials is used in the integration.

Theories under 'd' make use of the 'ray' theory to derive expressions for the mean force on a ship in very short waves. In very short waves it is assumed that the sole source of added resistance is the complete reflection of the waves on -most importantly- the bow.

Computational methods under 'e' are invariably based on regression on a large number of model tests in as far as the added resistance can be made dependent upon a limited number of descriptive ship parameters like length, beam, draft, block coefficient and other form coefficients and service conditions like speed and sea state. Within a certain class of ship type, for which in particular the block coefficient and form coefficients are constrained to a narrow band, methods of this kind have considerable value. One attempt is known to exist in which models of this kind for various ship types were merged together into one computational model.

The potential theory models based on the same approach are all virtually similar in their initial formulation, and their assumptions. Yet in practice it is found that, depending on the simplifications and the numerical evaluation of the solution, results are obtained that can be widely different because of the nature and the accuracy of the input information and the inherent manipulation of the input data.

In the following sections we will summarize the main points of a great number of interesting studies in this field. We have grouped them according to the main aspects of the approach. It must be said however, that considerable overlap is sometimes present between the theories.

2.2 Energy methods

In the computation method proposed by Gerritsma and Beukelman [2-24] the mean added resistance is obtained by equating the work done by the mean added resistance force to the energy radiated by the oscillating ship in the form of gravity waves.

In keeping with the strip theory approach the radiated energy is expressed in terms of the sectionwise (2-D) damping coefficients multiplied with the squared vertical velocity of the section. A major point of the method is the choice of the relative vertical velocity rather than the absolute velocity, which ties in closely with the 'relative motion concept', one of the building blocks of the strip theory. An interesting result of this concept is that in short waves, where the ship motions cease to exist, still an added resistance is computed because of the remaining incident waves. It is also noteworthy that the relative velocity is squared in the expression so that the mean added resistance due to an oscillating ship in calm water and due to a restrained ship in waves cannot be superimposed. Rather the total relative velocity should be taken and squared.

It was shown by Maruo [2-53] that by simplifying the full potential theory expression the formula of Gerritsma-Beukelman could be obtained.

A thorough correlation is presented with the results of model experiments on a fast cargo ship and the results appear to correlate well for the case of head seas and for speeds of up to Fn = 0.30. The method has been found to work well for narrow as well as beamy ships, at low and at high speed. In general it was found that the higher the motion damping the better the results.

A further correlation with experimental data on the container ship hull form S-175 in the ITTC study also showed good correlation for waves oblique on the bow [2-27].

For following waves an analysis of the method has been presented by Journée [2-36] who carried out experiments on the same fast cargo ship in following waves. The experiments showed the mean added resistance to be still positive but otherwise very small.

A full-scale correlation of the method was done in the study by Beukelman and Buitenhek [2-8], reporting on the full-scale trials of the container ship 'Atlantic Crown'. The correlation, however, is hampered by the impossibility to measure resistance on a ship sailing at sea so that the results had to be correlated in terms of power, with all the disturbing factors like propulsive efficiency, and propeller factors playing a role, and masking the correlation. Also the wave buoys could not measure wave direction, which made the analysis more complex.

An extensive correlation of the method with model test data was carried out by Gerritsma, Beukelman and Glansdorp [2-25]. The study was concerned with a variation of the L/B ratio ranging from 4 to 20 and apart from the added resistance all hydrodynamic coefficients were obtained in the horizontal and the vertical mode. The comparison with added resistance data for head seas and for speeds up to Fn = 0.30 exhibits quite good correlation even for the fullest ship, except for very short wave length.

A fundamental study to investigate the method in depth was undertaken by Beukelman [2-6, 2-7] who carried out model experiments on rectangular and triangular slender cylinders in head waves which showed an unexpectedly large discrepancy in the added resistance correlation with the predictions on basis of the Gerritsma-Beukelman theory [2-24]. The discrepancy is possibly due to the three-dimensional effects around the bow and stern, made to appear small in comparison to the contribution of the mid-body. It was also felt that for the rectangular cylinder the neglect of viscous effects could have led to an underestimation of the damping and thereby to overestimation of the first order motions and the added resistance around pitch resonance. The accuracy of the prediction was found to depend heavily on the damping; if the added resistance was calculated on basis of the measured damping the results were much better in line with the experimental results, as Beukelman showed [2-101].

Kholodilin and Yurkov [2-37] proposed a method which is based on energy considerations. The work carried out by the added resistance force is equated to the change of energy within a control volume. The change of energy is expressed in terms of an integration of derivatives of the incident and the disturbance potentials over the mean wetted hull. The method can easily be hooked-up to a strip theory computer program.
A very limited correlation using experimental data on a Series 60 ship having a block coefficient of 0.70 is provided and shows good correlation for the wave length about equal to the ship length.

Loukakis and Sclavounos [2-46] have proposed an extension to the method of Gerritsma-Beukelman [2-24] for the calculation of added resistance. Their method is also capable to compute the drift forces in oblique waves as it includes the effect of lateral motions. A limited correlation is provided for the S-175 container ship in various wave headings. Even though the computations did not include the lateral motions the results showed a reasonable correlation with experiments over the intermediate wave length range.

2.3 Momentum methods

Maruo [2-47 to 2-50] has formulated a theoretical derivation of the mean forces on a ship at speed in waves, based on potential theory. He was one of the first to explore the subject in depth. With the use of the Lagally theorem an expression was derived for the force on the ship's hull in terms of the Kochin function, which is the Green's representation expression for a specific hull form in terms of potentials of incident wave and radiated waves and derivatives thereof, to be evaluated on the wetted surface. Linear potential theory and linearized boundary conditions are used in the formulation of the problem. Time-averaging of the

longitudinal force expression leads to the mean added resistance force due to waves.

A key point in the application of the method is to obtain the Kochin function, which can only be numerically approximated through the use of a singularity distribution. In order to obtain tangible results the singularity distribution is further reduced to a centreplane distribution of sources, and eventually to a line distribution of sources along the length of the ship. Use of the strip theory and Froude-Krilov pressures to obtain information on ship motions is necessary to obtain the source strengths to feed into the expression.

Eventually an expression is derived composed of six terms, involving the heave and pitch motion, the incident wave, and coupling terms between them.

The method is cumbersome to apply from the practical viewpoint and the accuracy of the method depends strongly on how well the linear ship motion problem is solved.

In a later study Maruo [2-51] shows that the principle of conservation of energy for a control volume around the ship leads to an energy balance between the work done in propelling the ship and the energy carried away by the surface gravity waves.

For the zero ship speed case Maruo [2-52] showed that the expression can be simplified and conforms closely to the expression due to Havelock [2-31] for the drift force. Based on considerations of energy conservation Maruo states: *"The increase in resistance (due to waves) is the sum of the drift force (on a restrained ship) and the resistance due to oscillations of the ship (in an otherwise calm sea)"*.

In an extension study [2-52] he shows that the same results can also be obtained from momentum considerations, because the Lagally theorem can be viewed as a variant of the momentum equation for fluids.

Maruo [2-53] also showed that by simplifying his potential theory expression the formula due to Gerritsma-Beukelman could be obtained.

Maruo [2-48, 2-50] was the first to derive an expression for the added resistance due to irregular waves as a logical extension to the spectral analysis formulation used in linear ship motion theory. The added resistance being a quadratic function of wave amplitude could be treated by spectral analysis which is also a quadratic process. Although it produced a very practical method, it was nevertheless theoretically not entirely sound, as Vassilopoulos pointed out [2-102].

A systematic series of computations based on Maruo's simplified method of a line distribution of singularities was carried out by Brown et al. [2-12] for

destroyer hull forms. They modified the method by also including a vertical line distribution of sources at each section. The results showed remarkably little speed influence on the added resistance, which was attributed to the flat aft-body sections the effect of which could not be represented very well by a vertical line distribution.

A correlation due to Loukakis [2-44] for a Series 60 hull form shows a fair correspondence between computations and measurements due to Sibul [2-77]. Differences were in the order of 30 percent over the whole range of wave length, the theory overpredicting the measurements. Comparisons between model test data and Maruo's theory were also made by Wang [2-97] and Beck [2-4].

A recent extension to his method was published by Maruo and Iwase [2-55] in 1980 in which the expression for added resistance is extended to also include oblique wave headings. Like for the head sea case the solution is expressed in terms of a line distribution of sources. The computational results do not show an appreciable added resistance in short waves, contrary to experimental results. The correlation he provides with data due to Yamanouchi and Ando [2-98] is very limited and not convincing.
Maruo and Ishii [2-54] have simplified the original formula by Maruo [2-48] considerably by using a high frequency assumption consistent with strip theory. The ship is represented in a simplified manner by a distribution of singularities along a line. They have used both the energy and the momentum equations. The procedure is valid for any wave length and any wave direction, however the procedure is unfortunately difficult to apply in practice and the accuracy is dependent upon how well the linear problem is solved.

Takagi, Hosoda and Higo [2-85] have derived the same formula as Maruo and Ishii by the use of the equations of momentum and energy and using other control surfaces than Maruo.

Maruo and Iwase [2-55] have also presented a prediction formula for the added resistance in oblique waves, which can be viewed as a high frequency approximation to his original formulation. The correlation with experimental data was fair in waves from ahead and poor in waves from the stern quarter, most probably due to the high frequency assumption.

The work of Newman [2-65] has been instrumental for much subsequent work on added resistance. He formulated expressions for the steady drift force and moment on a ship in waves at zero speed. The use of the momentum equation led to expressions in terms of the Kochin functions. Although his work on mean forces was confined to the zero forward speed case, the work was used by others

as a departure point for deriving expressions applicable to the non-zero forward speed case, for instance Lin and Reed [2-43].

In a most thorough and revealing study Newman [2-66] discussed the interaction between a ship and the waves in terms of the Green's theorem in a most comprehensive way. The expressions of Maruo and Haskind are derived in a logical way out of Green's theorem.

The theory of Joosen [2-35] is an extension of the work of Maruo and Newman. The mean added resistance is obtained from the momentum equation applied to a control volume around the ship hull, and can be expressed in terms of the Kochin function. The problem remains to derive this function for an arbitrary ship shape. Joosen solved this by assuming the ship to be slender and proceeds to expand the expression obtained by Maruo in an asymptotic series with respect to the slenderness parameter. By supposing the speed to be low (Fn = order ε) he removes the speed effect altogether. The influence of forward speed is later added as an afterthought by taking the encounter frequency instead of the wave frequency.

A limited comparison with data of Series 60 experiments is provided. It is shown that for low block ships the theory grossly underpredicts the experiments, whilst for full block ships the theory is capable of predicting the added resistance at the conspicuous hump due to synchronous pitching but not the sizeable value at wave length shorter than the ship length. If a simple expression for the diffraction effect in short waves is added (taken from Havelock [2-31]) the computations seem to match the experiments better, though the correlation is not conclusive.

Hosoda [2-33] proposed a method for the computation of the added resistance in regular waves from oblique headings, which is essentially based on theory of Maruo [2-47]. The Kochin function that needs to be evaluated before the added resistance can be calculated is approximated by a singularity distribution on the ship's centreplane. On basis of the strip theory the source strength of the singularities is determined by the relative velocity between the fluid and the ship. The location and the phase of the singularities are determined so as to produce a radiated wave equal to the one that the two-dimensional section would produce at infinity.

Numerical calculations of the added resistance in regular oblique waves were presented for a container ship of the SR-108 type for a speed of Fn = 0.2 in waves from various headings.

A correlation is provided between the calculated added resistance and experimental results of thrust increase obtained on a free-running model. The correlation is not convincing though.

One of the conclusions of his work was that the contribution of the lateral motions to the added resistance is relatively small. According to this conclusion it is justified that the added resistance in oblique waves be calculated on the basis of the extension of the prediction methods for head seas, as also done by Fujii-Takahashi [2-19] and by Gerritsma-Journée [2-27].

Ohkusu [2-67] attempted to extend the wave-cut method of obtaining the wave resistance of a model in steady forward motion in calm water to the unsteady wave field generated by a heaving and pitching model in waves. The wave field is measured in the far field by an array of wave probes, and is used to directly obtain the energy flux of the waves far away from the model. The wave measurement is linearly decomposed into Kochin functions associated with the radiated waves due to the six modes of motion and the diffracted waves due to scattering of the incident waves.

The thus measured Kochin functions of the radiated waves correlate well to the Kochin functions computed using slender-body theory, as due to Ogilvie-Tuck. However, the Kochin function of the diffraction waves cannot be predicted by slender-body theory, as for instance shown by Adachi [2-1]. As a consequence, the Kochin function of the combined radiation and diffraction waves does not correlate so well with the experimentally obtained Kochin function.

The added resistance of the model can directly be obtained from the measured Kochin functions, since the Kochin functions in Maruo's formulation can be obtained from the Fourier transform of the wave record. Ohkusu [2-68] found that the added resistance computed from the total flux of the theoretical wave field is in good agreement with that derived from the spectrum of the measured wave field. It is shown to correlate reasonably well with the directly measured value, which can be interpreted as proof that the wave added resistance is a truly potential effect and has as a consequence little to do with viscous effects. Although the experiments were only concerned with a full tanker-like ship type sailing at low speed, the method as a whole appears to underscore the value of the Kochin function.

Another study undertaken by Ohkusu [2-70] was concerned with the diffraction of short waves on a ship having a blunt bow. The method takes account of the interaction between the incident and the diffracted waves with the steady flow field around the bow, and can be considered as an extension of Faltinsen's theory [2-16] for very short waves. A 'ray' theory is used to obtain an expression for the diffracted waves which are assumed to have been generated by complete reflection of the incident waves on the bow.

The comparison of computed added resistance data to experimental results due to Fujii-Takahashi [2-19] still shows a considerable discrepancy, although the trend with bow bluntness seems to have been predicted well.

The work of Fujii and Takahashi [2-18, 2-19, 2-20] was mainly concerned with waves in the short and very short wave length regime. This is important for blunt ship forms sailing in short waves like VLCCs in moderate sea conditions. They elaborated upon Maruo's final expression which is based on a approximation of the Kochin function through a line distribution of sources.

They propose to divide the added resistance into two parts. One part is added resistance due to ship motions and another part is added resistance due to wave reflection on the bow (or stern in following waves). The split-up is questionable, yet from the practical viewpoint it is an expedient since the frequencies of the ship motion regime and the reflection regime are fairly well separated. It is in principle possible to derive one expression for both wave length ranges if for instance the first order motions and loads are calculated by a three-dimensional source distribution method.

The added resistance due to ship motions may be calculated by conventional methods, while Fujii-Takahashi have derived a quasi-rational method for the resistance increase due to the reflection on the bow.

Their formula gives a correct asymptotic behaviour for very short waves and zero speed, as long as the ship's surface is vertical at the waterline. The effect of finite draft and forward speed is only included in an approximate way by multiplication by a quasi-analytical formula.

For the very short wave length range they assumed that the added resistance of a ship with forward velocity can be described by an expression analogous to the expression derived by Havelock [2-30] for the wave drift force on a vertical cylinder without forward speed. The forward speed effect is accounted for by an empirical coefficient to be determined from experimental data.

Experiments in short waves were carried out on four models of different bow form and were used to obtain data on added resistance to derive an empirical 'tuning coefficient'. The data was also used to correlate the computational results with. An expedient way to describe the effect of bow form is found in the concept of the 'bluntness coefficient', which is devised to describe the form of the waterline in the fore-body in a single coefficient. The experimental data shows a clear trend of the added resistance with the bluntness of the bow for a given wave length. The correlation of the computational results to the measurement data is rather weak notwithstanding the inclusion of the empirical factor in the method.

Fijii and Takahashi have also drawn the attention to the added resistance of fine ship forms, which can be rather high when the Froude number is high and

the wave length is small. This is an important point for fast and slender container ships. No theoretical method is currently available to explain this experimental finding.

A formulation based on the momentum theory has been proposed by Ankudinov [2-2, 2-3]. He applied the momentum equation to a control volume around the ship. The expressions from which he departs are similar to the ones Newman has derived and involve an integration over the body surface. Eventually an expression is obtained involving the Kochin functions. The integration over the hull can be removed and exchanged for an integration over a surface at infinity for which purpose it is sufficient to know the far field asymptotic behaviour of the potentials.

Eventually an expression is obtained which is very nearly similar to the Havelock formulation but for the fact that Ankudinov uses the total excitation, including diffraction effects, where Havelock uses only the incident wave excitation.

The method, which is in principle valid for any wave heading, can easily be incorporated in a conventional ship motion prediction program. A very scanty correlation with experimental data is provided which seems to suggest a good correspondence.

An approximation is given for a slender ship in head waves using Mitchell's approximation for a thin ship for moderate speed (Fn = 0.15).

Salvesen [2-72, 2-73] has derived relations for the second order steady-state forces and moments exerted on a ship sailing in oblique regular waves. The forces and moments are expressed as products of the ship motion responses, the oscillatory potential and the incident wave potential, which are all first order quantities. The oscillatory potential has been expressed in terms of the two-dimensional sectional potentials by applying strip theory assumptions.

The problem of solving the diffraction potential is circumvented by using the Haskind relations so that the exciting forces can be expressed in terms of the two-dimensional potentials.

The final expression contains three terms; one resembles the expression due to Havelock and involves the incident wave force, a second term of similar form adds the effect of diffraction, while a third term boils down to an integration of the two-dimensional damping coefficient over the ship length.
Numerical results that are given show some interesting trends; the added resistance is larger in waves from the bow quarter than in waves from ahead, which is also found in experiments. The correlation with experimental data for oblique waves is extremely limited and not convincing, if only because of an apparent lack of such experimental data.

In the work of Lin and Reed [2-43] equations for the horizontal force and the yawing moment are derived for a ship moving with a constant speed into waves approaching under an oblique angle. The analysis is developed within the context of a linearized ship motion and infinitesimal wave theories for an ideal fluid. The momentum equation is used to obtain expressions for the force and moment in terms of the far field potential. This far field potential is expressed in terms of the potential on the mean surface by means of Green's theorem in conjunction with the proper Green's function. An asymptotic form of the Green's function is used to finally express the force and moment in terms of the Kochin functions, which require knowledge of the forced oscillation and diffraction potentials at the mean position of the ship surface. To obtain numerical results the strip theory method due to Salvesen et al. is used.

The authors have presented neither numerical results nor correlation with experimental data.

As an extension to this work Kim [2-38] has developed a numerical procedure for the computations based on the same theory. Only a limited correlation is provided with experimental data obtained for a Series 60 hull, the computations overpredicting the measurements.

For the short wave length range Kwon [2-40] has devised a method of prediction of speed based on calculation of the reflection of the incident waves, in an approach similar to the Fujii-Takahashi method. The effect of forward speed and finite draft was introduced in the form of a correction.

Wada and Baba [2-104] proposed a calculation method that can be viewed as a modification of the Fujii-Takahashi method and the method due to Faltinsen et al. [2-16]. The method can be applied to large full ships in arbitrary wave directions, the formula of Sakamoto and Baba [2-105] is used to take account of the curved flow effect around a full ship's bow.

2.4 Pressure integration methods

Havelock [2-29] has done pioneering work in 1937 in a first attempt to obtain an expression for the added resistance from the theoretical side. He derived an expression for the horizontal force acting on a thin ship moving among waves at constant velocity. Within the order of approximation he concludes that the extra force due to the existence of waves was a periodic force so that there was no mean resistance augmentation from the waves. In a second attempt [2-30] to come to grips with the subject he investigated the reflection of waves by the ship. In the derivation he arrived at an added resistance which was much to small to be a possible explanation of the physical processes involved.

Later Havelock [2-31] made use of the fact that the extra resistance due to waves is closely related to the pitching of the ship, at least in head waves. He obtained an expression in terms of the pitch and heave exciting forces, the motions and the phase angles between them. In the derivation he assumes the pressure on the hull to comply with the Froude-Krilov hypothesis.
Although he ignores the diffraction effects altogether, inasmuch as he uses only the excitation due to the incident waves, the theory has been shown to give results which are of the right order of magnitude. Obviously in the short wave regime the predicted added resistance goes to zero while experiments would still show a considerable contribution to the added resistance.

A comparatively simple method was proposed by Boese [2-11], who composes the mean added resistance of two components.

The first part is derived from integration of the pressures associated with the heave and pitch motion, and is essentially a second order term associated with the rotation of the vertical force vector in a space-fixed system of axes. A second part is obtained from integration of the relative vertical motion around the waterline, and can be viewed as a correction on the first part. The deformation of the wave by the presence of the ship is not taken into account in the evaluation of the relative motion.

In this method Boese has neglected the quadratic velocity term in the Bernoulli equation and a term arising from using the pressure on the instantaneous position of the wetted surface instead of using the pressure on the average position of the ship. The method is fairly simple to implement in a strip theory program, but may only be used for the case of head waves, although in principle it could be extended to other modes of motion as well.

The comparison of the calculated data to model measurements, due to Nakamura et al. [2-60] and Sibul [2-76 to 2-83], shows a fair correlation, the computation in most cases exceeding the experiment.

Faltinsen et al. [2-16] propose an asymptotic theory for small wave length that takes into account the forward speed effect. In contrast to the Fujii-Takahashi method [2-19], in which the added resistance is thought to be composed of two parts, namely one part related to the heave and pitch motion and another part related to the reflection of waves on the bow, the method of Faltinsen is essentially one expression valid for all wave lengths. The method is based on the integration of the hydrodynamic pressure over the hull. The influence of the stationary perturbation potential and the interactions with the oscillatory potentials are neglected.

The formulation for the pressure is derived up to the second order and expressed in a Taylor series about the mean position of the ship. The final expression for the force contains a major component due to the relative motion

around the waterline plus terms containing spatial derivatives of the local acceleration giving rise to a second order force and a mean value.

The final expression has a good deal in common with the formula derived by Boese [2-11], yet it is more extensive, as it also includes the effect of horizontal motions. They also have not discarded the velocity squared term in the Bernoulli equation and have included the effect of integrating over the instantaneous wetted surface, in contrast to the Boese method.

The effect of oblique waves can also be studied because terms dependent on horizontal motion are included so that mean transverse force and mean yawing moment can also be obtained.

The authors [2-16] have derived a separate formula for the added resistance in very short waves, so they do not invoke the 'relative motion hypothesis' to construct a solution to the diffraction problem. The hull is considered as a flat wall of infinite dimensions upon which the wave is reflected. Through the use of the energy conservation concept and an approximation consistent with slender body theory a formulation is obtained for the mean force which can be decomposed into longitudinal and lateral forces and a yawing moment. The resulting formula is similar in appearance to the one due to Fujii-Takahashi, yet differences exist in the term that describes the forward speed effect.

It is as of yet uncertain which method correlates better with experimental data. Fujii and Takahashi showed a good correlation with experimental data of their own, yet only for a wave length to ship length ratio of 0.5. However, it would seem that the theory is better applicable to even shorter waves, but no validation is given.

For the Faltinsen method some correlation is provided with the experimental results of Strom-Tejsen et al. [2-84], for various wave headings. The correlation is in general better for the longer wave lengths. For the very short waves the validity of the method is not fully borne out by the comparison, if only because experimental data for very short wave lengths are non-existent.

The added resistance in the short wave length range is still underpredicted, like for most other theories.

Faltinsen [2-17] (1983) has proposed a different scheme for the bow flow and the resulting added resistance of slender ships at high speed in short waves from ahead. He analyzed the flow by means of matched asymptotic expansions. The near field solution implies solving a two-dimensional Laplace equation with complete free-surface conditions. A solution technique with fundamental sources and dipoles is used. The comparison with experimental results for a Wigley hull and a Series 60 hull does not show a satisfactory correspondence for

the steady part of the bow flow. The comparison for the unsteady part with experimental data for a $C_B = 0.60$ ship hull does not correlate too well.

In a recent study Faltinsen et al. [2-103] have investigated the added resistance of very high speed catamarans. It was assumed that the separation of the hulls and the speed would be high enough to justify the hulls being treated as monohulls. In the method of prediction of the added resistance some effect of the interference with the stationary flow field has been included. The calm water resistance is expressed in terms of a Taylor's expansion to the ship motions heave and pitch and the coefficients are calculated by stationary flow calculations for different drafts and trim angles. The effect of viscous resistance is included by applying the ITTC-1957 formula to the instantaneous wetted surface and the instantaneous speed, taking account of the wave orbital velocity. The predictions are correlated with experiments for a frigate at very high speed and the term describing the interaction with the steady flow appears to make a significant contribution.

In a recent contribution by Lee [2-41] a finite difference method is used to calculate the wave diffraction effects in head seas. For short waves it is assumed that the waves are completely reflected at the ship's hull surface, and that the potential flow varies with depth as an exponential function. The potential of the steady flow is approximated by assuming a double body solution based on the method of Hess and Smith [2-32]. The unsteady potential is defined using linearized boundary conditions and solved in a finite difference scheme. The method is restricted to head seas.

A similar method is applied to longer waves, which in contrast to short waves are only incompletely reflected by the hull. In this case the slender body theory and the method of matched asymptotic expansions are used. The method is suitable only for ship speeds in excess of the wave phase velocity.

The mean wave added resistance is obtained from the calculated diffraction waves and compared to measurements.

The comparison with experimental data due to Blume [2-9] shows a fair correlation for lower speed cases and a large discrepancy for higher ship speeds. The hull form was a rather full ship with a wedge type bow and stern form.

In recent times the numerical computation of ship motions and related quantities through time-domain analysis has been gaining importance, see for instance Nakos and Sclavounos [2-108, 2-109] and Liapis and Beck [2-110]. These methods are based on finite element and finite difference schemes and have the advantage that non-linear equations can be treated. Yet for unsteady flow related quantities they require still a very large computing time. A number of publications have covered ship motions, added mass, damping and wave forces,

yet no application as to the second order quantity of wave added resistance has yet been published.

2.5 Ray theory methods

Naito et al. [2-59] made a study of the added resistance in the very short wave range. They invoked the ray-tracing technique to obtain a description of the diffracted wave field. With this technique the interaction between the steady and the unsteady flow field can be studied. The diffracted waves that cannot propagate into the far field, on account of their wave length and celerity, are bound to break. The discrepancy observed between the results obtained from a far field wave pattern analysis and measured added resistance is attributed to the energy loss due to wave breaking and consequent wave energy loss. The approach is, in a way, similar to the Fujii-Takahashi method and a 'bluntness factor' is used to derive a tuning factor to bring the computational results in line with the measured results. The experiments included testing of a captive model in head waves alternatively fitted with three different bow forms, ranging from a wedge bow to a very blunt bow. The correlation shows that generally the predicted values underestimate the measurements, the discrepancy being larger for the blunt bow than for the wedge bow.

As a further extension Naito and Takagi [2-106] derived a simplified formula based on slender ship theory. It is claimed that the formula should give a good estimation in the case of middle and long wave length, yet experimental data does not really support this.

2.6 Regression models

The work of Jinkine and Ferdinande [2-34] is one of the few examples of regression models available in the field of added resistance due to waves.

The method has drawn upon experimental data from ship model tests as published by various authors. The expression is valid for cargo ships of fine hull form, and applies to the case of head seas and to speed of up to Fn = 0.30. The expression obtained, which should be considered as entirely empirical, contains but one coefficient, to be evaluated from an experiment. Average 'default' values of the coefficient will enable the user to predict the added resistance in an entirely calculatory manner.

The method is confined to the wave length region around synchronous pitching for which an abundance of data on added resistance is present in the literature. The conspicuous hump in the function for wave length to ship length ratios around unity lends itself for a treatise as done for wave spectra, using a normalization function.

A 'goodness of fit' evaluation is obtained by applying the method to the original experimental data set from which it was derived in the first place. No correlation is provided with other data from outside the original data set.

An elaborate empirical study, applicable to a wide parameter range, was developed by Schifrin [2-74] on the basis of regression on model experiments. The method can be used for slender high-speed ships and for blunt slow-speed ships alike. Moreover the method can also be applied to wave angles other than head seas. The method employs a base hull of standard parameters and uses correction functions for deviating parameters of speed, pitch gyradius, length/draft ratio and block coefficient. The method is in its application more universal than the Jinkine-Ferdinande method.

In the work of Thiel [2-87] a comparison is made of two empirical methods to compute the added resistance, the method of Moor and Murdey and the method due to Schifrin [2-74]. Both methods are also compared with a series of model experiments. Even though the empirical methods are capable to predict the conspicuous hump in the added resistance curve at a wave length corresponding to synchronous pitching, a discrepancy remains. The difference may for some wave lengths amount to a factor of two. The irregular wave spectrum smoothes out the larger discrepancies though.

In the main it was concluded that the Schifrin method has more potential as a prediction tool than the Moor-Murdey method, because of its greater applicability due to its wider parameter range and because of the use of the standard ITTC wave spectrum. Also it was found that the two methods agreed better for high seaways than for low seaways, where in fact the accurate prediction is of more practical importance.

Netsvetaev [2-63] has presented a method to predict added resistance by estimating the response operator from experiments and to evaluate the added resistance in irregular waves in a straightforward manner.

2.7 Experimental studies

The experiments carried out by Yoshioka [2-100] were meant to obtain the extra resistance due to a steady heel angle and due to dynamic rolling motion in calm water of a model of a cargo ship at speed. Although the added resistance did not amount to much, an interesting finding was that the rolling would exaggerate the magnitude of the humps and hollows in the resistance curve and that there existed a speed range for which the resistance under dynamic rolling was actually less than for a model not rolling. No explanation was given for this phenomenon.

Ueno et al. [2-88 to 2-92] carried out a most complete model experiment program in which the effect of the motions heave, roll, pitch and yaw on the ahead resistance of a model in calm water was determined.

The ship motions did in general all produce an increase of the resistance. The extra resistance depended strongly on ship speed, the oscillation amplitude and period and also on the ship type. If expressed in percentage of the 'base line' calm water resistance the oscillatory motions would produce an increase ranging from 10 percent (roll, heave, yaw) to as much as 50 or even 100 percent for pitching; all for realistic amplitude and period cases.

On the basis of model tests they derived regression formulae to predict the amount of added resistance for various ship types. Although the studies provide a wealth of material, the physical situation is rather artificial, however it draws the attention to the overriding importance of the pitching motion in producing added resistance due to ship motions.

An extensive experimental study was executed by Blume and Kracht [2-10] into the effect of a bulbous bow on the behaviour in waves in general and the propulsive performance in particular.

A systematic series of models was tested, varying the L/B and B/T ratio for hulls having a block coefficient in the range from 0.57 to 0.76. The models were fitted with various bulbous bows forming part of a systematic series. Tests were conducted in regular head waves to obtain ship motions and accelerations as well as thrust, torque and RPM.

As to the findings, the added thrust is usually assumed to be proportional to wave amplitude squared, yet this relation was not found to apply to all cases. The power coefficient would drop as low as 1.5 in some cases. It was observed that this power coefficient for ships with a bulbous bow was lower than for ships without a bulbous bow. In a seaway the bulb cannot set up a steady flow that causes cancellation of the hull wave by the bulb wave. This non-presence of the beneficial effect is attributed to the seaway and incorporated in the added resistance due to waves.

The effect of a bulb on added thrust depends for the most part on the block coefficient and on the wave length. The results were made available in the form of design charts. The major overall finding was that up to Beaufort 6 seaways the bulbous-bow fitted ship has almost the same seakeeping qualities as the bulb-less ship, so that the bulbous-bow design may be based on smooth water considerations alone. For higher seaways the bulb-fitted ship will be worse off and it was advised to make the bulb not too large.

The influence of bilge keels and bilge vanes on the ahead resistance of a ship in calm water was studied by Gadd [2-21]. He carried out systematic rolling

experiments, decay tests and forced rolling tests, on a trawler hull. The results indicated a marked increase of the resistance that could amount to as much as 20 percent. It was determined that about half of this augmentation could be attributed to extra resistance due to rolling of the bare hull and half to the effect of the bilge keels. Since bilge keels reduce the rolling they may be expected to also reduce the added resistance due to rolling, even though the keels must incur some extra resistance of their own; no data was given on this aspect though.

The work of Sibul [2-76 to 2-83] was for the most part concerned with extensive series of model experiments. He investigated the effect of such parameters as wave steepness and block coefficient on added resistance, the pros and cons of the constant thrust method versus the constant velocity method for added resistance experiments in waves, as well as the effect of irregularity of waves. The data obtained provided a wealth of material for subsequent investigators to correlate computational methods with and validate their theories, yet it should be kept in mind that the experiments were done on rather small models - about 1.3 m (5 ft) in length - which must have had some effect on the accuracy of the added resistance obtained.

2.8 Overview studies

The work of Gatzer and Fröhlich [2-22] deals with a comparison between model experiments and computations. The theoretical methods compared were the Jinkine-Ferdinande regression method [2-34] and the Schifrin empirical method [2-74]. These were compared to the potential theory based models of Salvesen [2-72], Boese [2-11], Kholodilin and Yurkov [2-37] and Loukakis and Sclavounos [2-46]. The results of the methods, in terms of added resistance, were compared to experiments for a fast cargo ship. It was found that the regression model of Jinkine-Ferdinande gave the best correlation with experiments while Schifrin came out second best.

In a review on the subject Hearn et al. [2-107] compares various computational schemes, both 2-D and 3-D, for the calculation of added resistance. Both near field and far field procedures are presented. Comparisons of the computational results with experimental results shows that in general all methods come fairly close, yet all schemes fail to predict the added resistance in short waves.

Overall it may be concluded that the literature on the subject of added resistance due to waves contains an abundance of mathematical theories that, when put to the test, show varying degrees of correlation with experimental data. In addition, literature shows a limited amount of experimental data, in particular for short waves. A good deal of studies should be classed under the heading of 'synthesis' rather than 'analysis' and contribute little to the physical insight into

the matter. A considerable amount of work is yet to be done to obtain a full understanding of the subject.

Chapter 3

Some major trends in resistance increase due to waves

Our knowledge on added resistance due to waves is for the most part based on systematic model experiments. The work of Gerritsma et al. [3-1] gave insight into the relationship between the various propulsion characteristics: resistance, thrust, torque, revolutions and power and their dependency on speed and wave properties, wave length and wave height.

Systematic model tests including variations of ship particulars were carried out by Vossers et al. [3-2] and Sibul [3-3].

From the viewpoint of signal analysis the added resistance is an oscillatory signal. In first instance it was studied in harmonic sinusoidal waves because this approach had also produced most valuable insight into the subject of ship motions in waves.

However, an important difference exists between the added resistance and the ship motions. For the motions the large oscillations are of greater importance than the mean value, which is usually a very small quantity that goes almost unnoticed amidst the large oscillations.

In contrast, for the added resistance the large oscillations constitute an alternating propelling and resisting force resulting in an oscillatory 'surging' motion. This oscillation is of little interest but the mean value, which can be really large, constitutes the most important quantity directly responsible for the speed loss.

There exist various ways in which experiments on added resistance can be carried out in the model basin. In practice there are two usual approaches. One

approach is to enforce a constant speed on the model and tow the model by a flexible connection that allows heave and pitch motions to be made, yet restricts the model in all other modes of motion, most importantly surging. The other way is to tow the model by a constant mean force applied for instance by a solid weight on a line over a pulley. The latter way has the advantage of realistic 'surging' motion, yet the dynamic influence of the suspended weight is not accounted for correctly. A better approach is to use a constant tension winch to keep the tow force truly constant, notwithstanding the surging motion.

Since the surging in head waves has been shown to have negligible effect on the mean of the added resistance, the first method is to be preferred, because of the advantage of subtracting the resistance in calm water from the resistance in waves for exactly the same constant speed.

In studying the dependence of added resistance upon the characteristics of the ship and the seaway the following points are of interest:

- influence of wave length c.q. wave frequency,
- influence of wave height c.q. wave amplitude,
- influence of wave heading relative to the ship,
- influence of ship speed,
- influence of ship size,
- influence of ship main particulars,
- influence of ship hull form.

Experimental studies carried out in the past to investigate these influences have brought to light some very interesting relationships, which will be touched upon below.

3.1 The influence of wave length, c.q. wave frequency

The added resistance is a function of wave length or wave frequency, and attains a maximum value where a dominant ship motion is also maximum.
In waves of which the length is equal to the ship length the ship pitches heavily, resulting in large added resistance, as indicated in Figure 3-1.

3.2 The influence of wave height

The added resistance is approximately proportional to the square of the wave height. If the wave height increases, then also the water pressure and the surface area on which this pressure acts increase. Their combined integrated effect results in a mean force that goes up with the square of the wave height.

The wave height squared law relation is quite well borne out by the Figure 3-2 showing model test results on a cargo ship in waves from ahead.

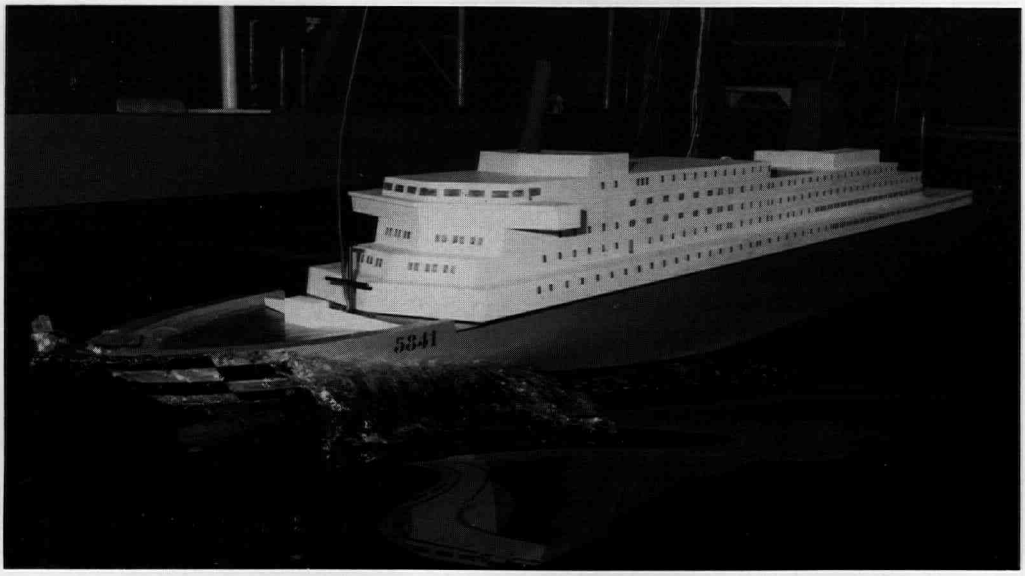

Photo 3-1: Wave height and wave length influence the ship motions. A model of the HAL cruise ship 'Nieuw Amsterdam' undergoing seakeeping tests. [Courtesy Chantiers de l'Atlantique, St. Nazaire]

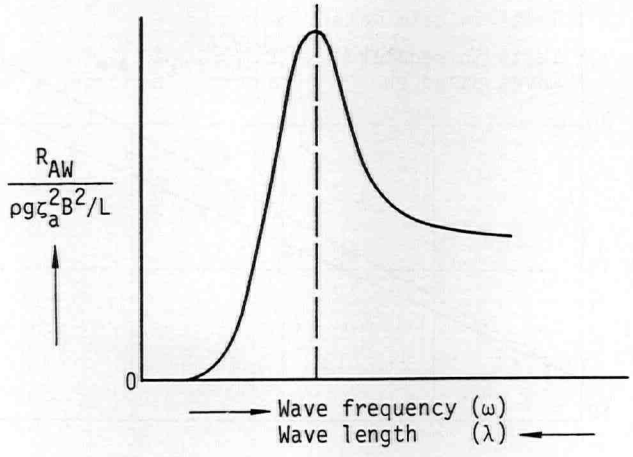

Figure 3-1: Transfer function of added resistance indicating region of large extra resistance.

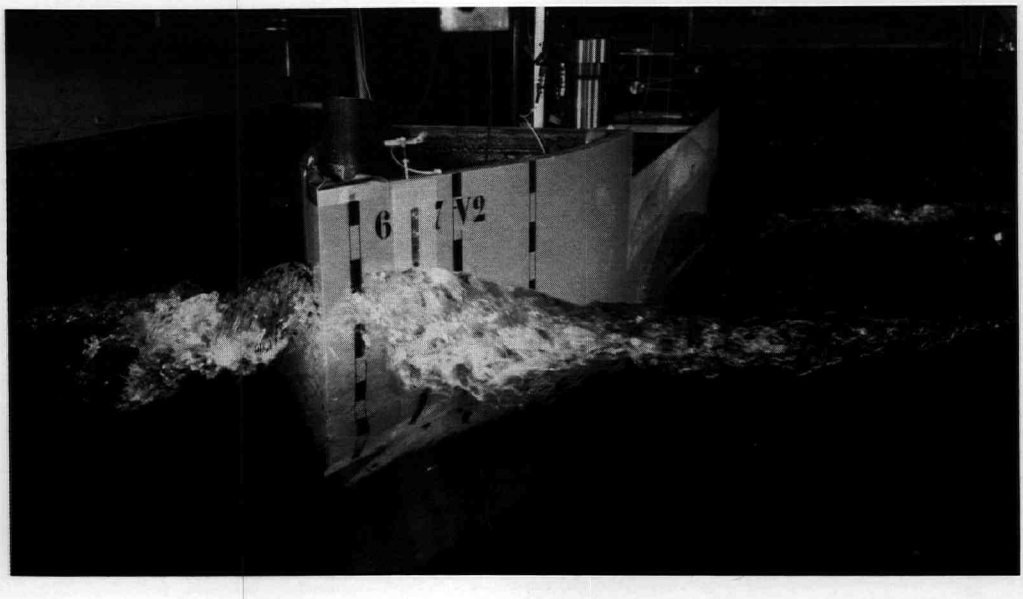

Photo 3-2: The added resistance increases proportional with the wave height squared because the wetted area and the pressure on it increase [7-9].

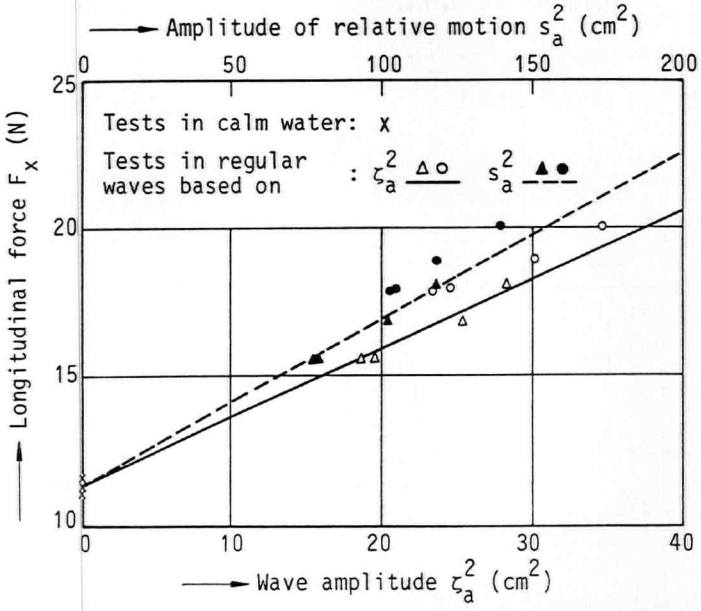

Figure 3-2: Added resistance plotted as a function of wave amplitude squared showing a straight line.

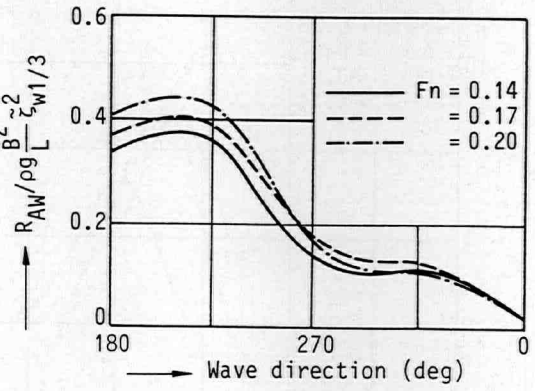

Figure 3-3: Added resistance plotted as a function of wave direction for an LNG carrier in sea state 7.

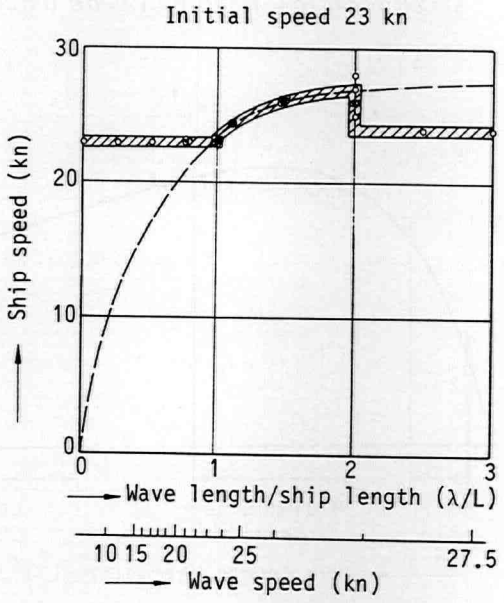

Figure 3-4: Speed as a function of wave length and wave height in following waves for a fast container ship model.

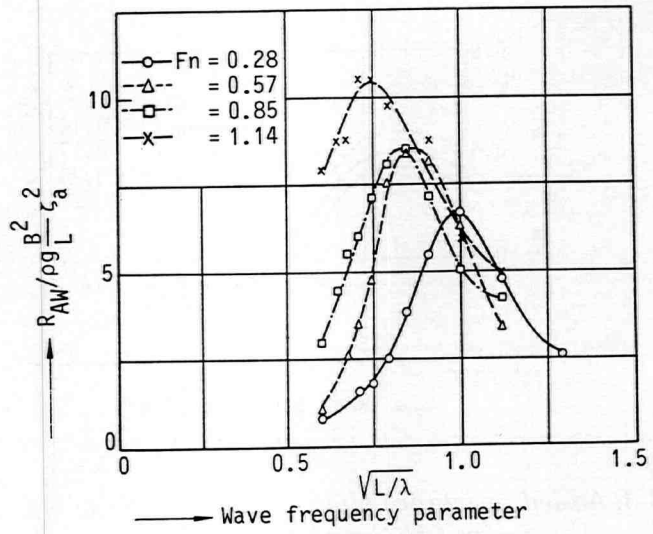

Figure 3-5: Non-dimensional added resistance as a function of speed for a fast frigate in head waves [3-5].

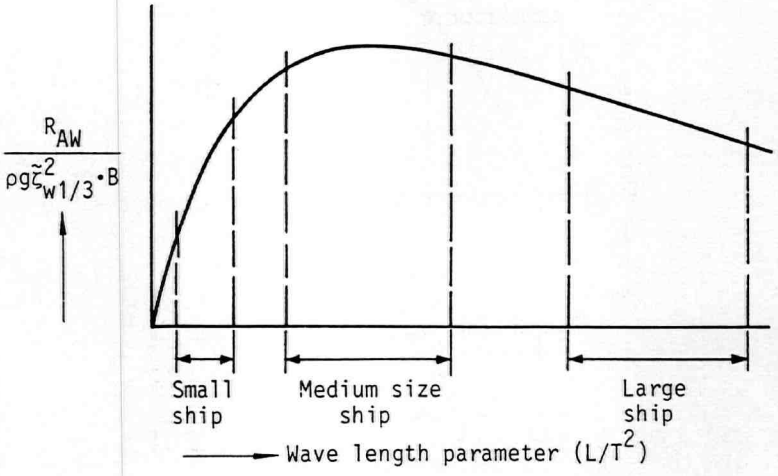

Figure 3-6: Non-dimensional added resistance function showing regions of operation of ships of different size.

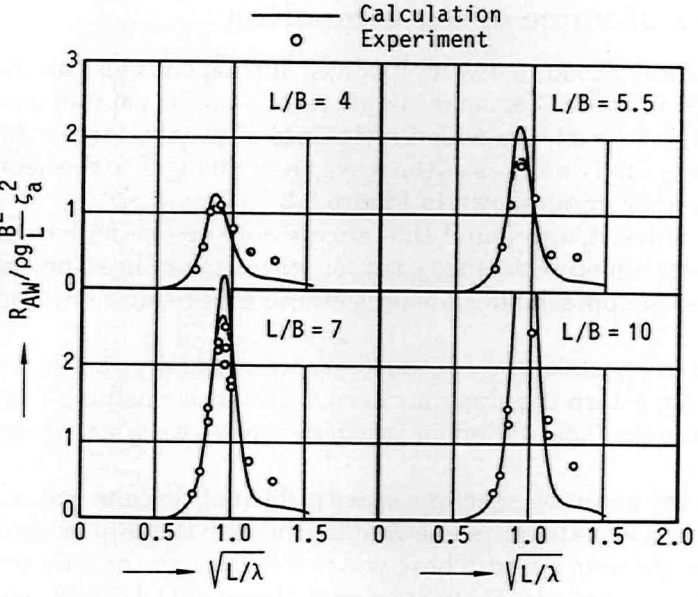

Figure 3-7: The influence of Length and Beam on wave added resistance [3-4].

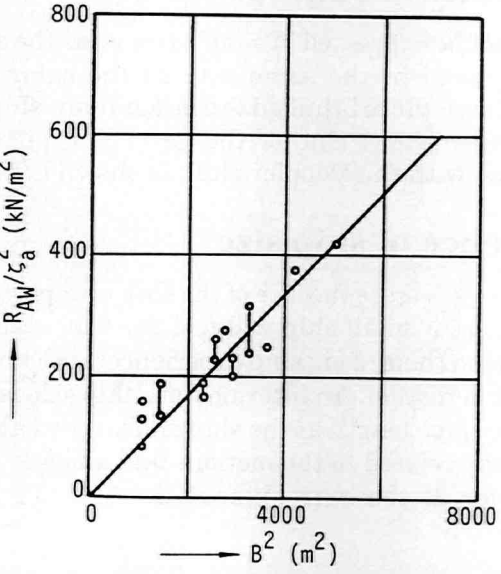

Figure 3-8: Added resistance as a function of beam for tanker hull forms.

3.3 The influence of wave heading

The effect of wave heading is very involved and depends also on the wave length and on the ship speed. Yet some simple trends can be pointed out.

For a ship at speed, the added resistance is usually largest for waves from ahead and gradually reduces as the wave angle changes to the beam and further to the stern quarter, as shown in Figure 3-3.

For long ships it was found that waves oblique on the bow can produce a slightly larger added resistance than for waves taken head-on. In beam waves there still is an appreciable added resistance as a result of rolling, and yawing motion.

In waves from astern the added resistance is usually very low.
In waves from astern the ship may even experience a helping force pushing the ship up to a higher speed than for which the power were set, as shown in Figure 3-4.
In this case the power was set for a speed of 23 knots in calm water. Some regular waves having a wave length somewhat longer than the ship length had a velocity higher than the ship speed. These waves would push the ship up to a speed of 27 knots. Waves that propagate at an even higher speed would overtake the ship without much 'pushing' effect on the ship.

3.4 The influence of ship speed

This influence cannot be expressed in simple terms, as the added resistance does not increase with speed in the same way as the calm water resistance. In principle the added resistance is linked to the dominant ship motion and exhibits the same speed dependency. One of the governing factors is the encounter frequency associated with the Doppler shift as shown in Figure 3-5.

3.5 The influence of ship size

For a given moderate sea state the size of the ship is important to her seakeeping characteristics. Where a small ship will feel the waves as long waves and will float up and down with them, a big ship experiences the same waves as relatively short and is not set in motion. An intermediate ship size is at a disadvantage as the waves are of the same length as the ship and large motions result. The added resistance is in a way related to the motions and a bigger ship is relatively less affected by the waves, as shown in Figure 3-6.

3.6 The influence of ship main particulars

The effect of the main particulars (length, beam and draft) is difficult to ascertain separately from the influence of hull form proper, because a change in a linear dimension is invariably attended by a change in form. Yet from systematic studies it was found that the beam is the ruling quantity, and the draft is of lesser importance.
It appears that both length and beam are important for the added resistance due to waves, as shown in Figure 3-7 and 3-8.

3.7 The influence of hull form

The effect of the major hull form coefficients C_B, C_M, C_P, C_{WP}, C_{VP} on added resistance is mainly in an indirect way, as the form influences ship motions on which the added resistance in turn strongly depends.

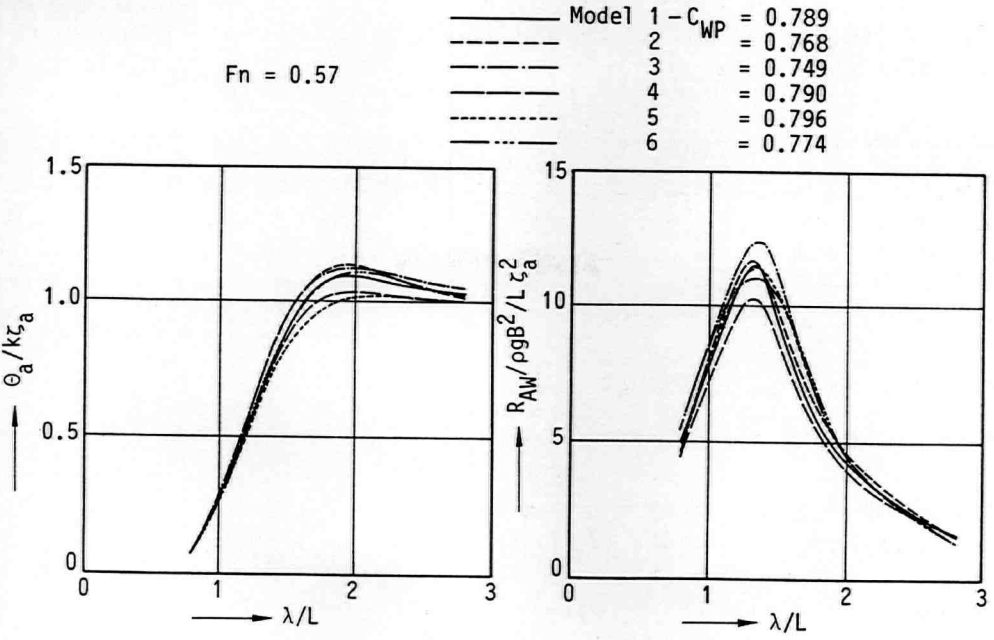

Figure 3-9: The influence of waterplane area coefficient C_{WP} on pitch angle and on added resistance [3-5].

This page intentionally left blank

Chapter 4

The objective of the study

4.1 The hypothesis

Most mathematical models set up to predict the added resistance due to waves are based on a functional dependancy of some kind between the added resistance as the 'output' and the ship motions as the 'input'. The ship motion input is either used in the potential theory based models to obtain the source strength for each section of the ship, or in energy based models to obtain the amplitude of the outgoing damping wave, on basis of which eventually the added resistance is computed.

Indeed a strong resemblance exists between added resistance and ship motions as a function of wave frequency as shown below.

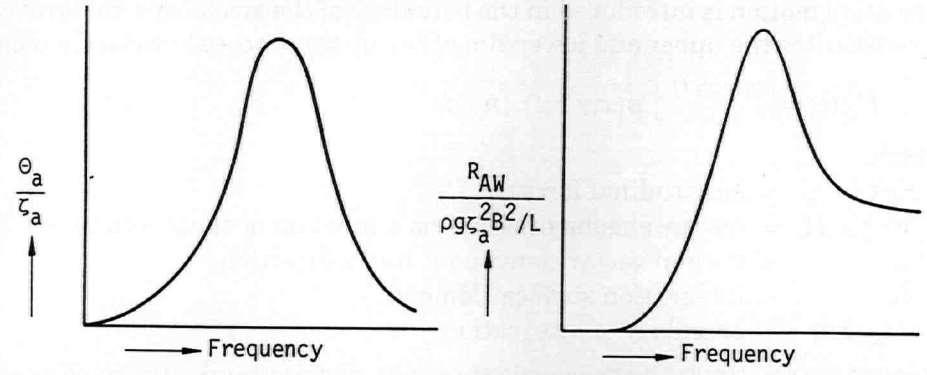

Figure 4-1: Transfer functions of pitch and added resistance [Ref. 9-7]

An even stronger correspondence can be shown to exist between the relative vertical motion of the water surface at the forebody and the added resistance as shown below.

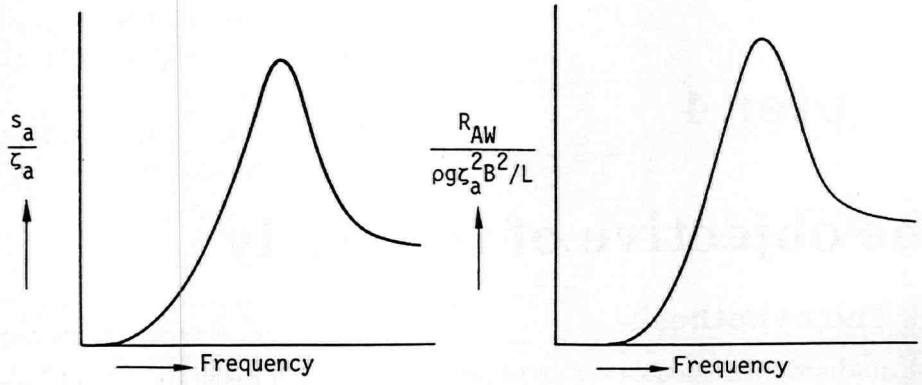

Figure 4-2: Transfer functions of relative forebody motions and added resistance [Ref. 9-7]

It is hypothesized that this represents a most important input- output relation, which can be made plausible as follows.

The longitudinal force on the ship, as a time-dependent quantity, can be written as an integration of the pressure over the wetted part of the ship hull. The relative motion is introduced in the boundary of the space-wise integration, as it constitutes the upper and lower rim of the instantaneously wetted surface.

$$F_x(t) = \int^{s(x,y,z;t)} p(x,y,z;t) \cdot n_x \, ds$$

in which:

$F_x(t)$	=	longitudinal force
$p(x,y,z;t)$	=	instantaneous pressure as a function of space and time
n_x	=	normal vector component into x direction
ds	=	integration surface element
$s(x,y,z;t)$	=	boundary of integration

In principle, if the time- and space-wise pressure distribution on the moving ship hull in a seaway is known, as well as the relative motion, the added resistance can easily be obtained as the time-averaged mean value in the longitudinal direction.

The time-averaged mean value becomes:

$$\overline{Raw} = \overline{F_x(t)} = 1/T \int_0^T F_x(t)\, dt$$

In order to evaluate the above integration we shall have to investigate the following subjects:

1. The expression for the pressure p(x,y,z;t), taking into account the ship motions related pressure variations as well as the pressures due to incident, radiated and diffracted wave patterns.
2. The expression for the relative vertical motion s(x,y,z;t) which constitutes the boundaries of integration, taking the same pressure components into account.
3. The relative contributions of bow and stern.

All of these subjects were approached from the experimental side to obtain insight into the 'physicalities' of the subject and thence to structure the mathematical model. It is the objective of the study to verify the hypothesis and to obtain insight into the physical aspects of the subject.

4.2 The lay-out of the study

The study was laid out along the following four stepping stones.

1. An initial investigation of seakeeping data of a variety of ship types to obtain data to support the hypothesis on the relation between added resistance and relative motions. [Section 7.2]
2. Model experiments to investigate the relative motions, the forces on the hull, and the instationary pressure distribution at the bow to structure the mathematical model. [Section 7.3, 7.4, 7.5] Further model experiments to study the influence of main particulars, bow form and wave direction on the added resistance. [Section 7.6, 7.7, 7.8]
3. The formulation of a mathematical model on the basis of the insight gained from the model experiments. The formulation is based on potential theory and has been programmed on computer. [Chapter 8]
4. The correlation of computed results to experimental results. [Chapter 9]

4.3 Some explanatory notes

Experiment and Theory

Quite often a theory is developed first and afterwards some experiments are carried out to validate the theory. The present study was done the other way around. A number of experimental programmes were carried out to obtain insight into the details of the flow and to understand how the mean added resistance is generated by the flow in the first place. Subsequently the theory was set up as a description of the knowledge gained from the experiments. Eventually computations based on the theory were correlated with the initial experiments as well as with 'outside' experiments.

The 'near field' approach

In setting up a theory for the prediction of a global quantity like the mean added resistance in waves one has the choice between a 'near field' and a 'far field' approach. In the 'far field' approach one uses an integral formulation such as conservation of energy or conservation of momentum for a control surface at a great distance from the ship. The present approach of pressure integration over the wetted surface that we have chosen is a 'near field' approach. This offers the possibility to incorporate detailed experimental insight into the theory.

The 'dynamic swell-up'

The relative motion between the ship and the water surface is usually computed as a combination of incident wave and vertical ship motions: heave, pitch and sometimes also roll. However, the relative vertical motion along the length of the ship, and in particular at the bow, is much more than the combined effect of ship motions and incident waves. Even when the 'upwash' effect of radiated waves and diffracted waves is included the relative motion is still underpredicted for a ship at speed. This led to the identification of the 'dynamic swell-up' as an effect brought about by the interaction between the relative motion due to ship motion and incident wave on the one hand and the stationary bow wave system on the other hand. This 'dynamic swell-up' is shown to be a sizeable quantity and since it enters into the added resistance in a squared form its importance becomes even greater.

The pressure distribution

For a ship at zero speed the ship motion, radiation and diffraction problems have to first order been solved [Ref. 4-1, 4-2, 4-3]. If the time-dependent potential is known, the time- dependent free surface elevation is obtained from the pressure in the Z=0 plane, which in turn is taken equal to the time derivative of the potential, owing to the linearized Bernoulli equation. The tacit assumption being

that, even though the free surface depends on time, the instantaneous vertical distribution of the pressure at any moment follows the hydrostatic distribution. Hence if the relative motion is known, so is the vertical pressure distribution. For a ship at forward speed, however, the pressure on the hull is not related to the free surface through the hydrostatic line. The pressure distribution on the hull is not only related to ship motions, incident, radiated and diffracted waves, but also related to the stationary flow field due to forward ship speed.

Added resistance

A sailing ship in a seaway experiences the largest added resistance in waves from ahead. In addition it was reasoned that the major 'driving effects' would show up in the case of head waves without blurring or masking side effects from other degrees of freedom that would probably produce interesting wave effects, yet would not make a major contribution to the resistance. For that reason the study has been confined to that important wave heading: head seas. At some future time the findings can perhaps be generalized to other wave headings.

Importance of the bow and the stern

For a ship in waves from ahead the relative vertical motion at the bow is about three to five times larger than at the stern. It was pointed out that the relative motion enters into the added resistance in a squared form, so it will be understood that the contribution of the forebody will be an order of magnitude (10) times larger than the contribution of the aftbody. The parallel midbody of the ship does not contribute to the added resistance as its surface normal has no component in the longitudinal direction. Therefore a separate experimental study was done to check the importance of the bow over that of the stern, which was indeed shown.

4.4 The novel aspects of the present study

To the knowledge of the author the present study is the first investigation of the relation between relative motion and added resistance due to waves, taking account of the stationary and instationary pressure distribution and dynamic swell-up effects.

This page intentionally left blank

Chapter 5

The physical origin of wave added resistance

The resistance of a ship sailing in calm water is composed of a potential part and a viscous part, the magnitudes of which depend on hull form and ship speed. In a broad sense it can be said that they are of equal importance. For a ship sailing in waves, gravity waves that is, the resulting ship motions are for the most part the result of potential effects. The only exception being rolling in which a strong viscous influence has been identified. In line with ship motion theory, the wave added resistance is invariably assumed to be of potential origin, in fact this is always taken for granted. It may be well to assemble the proof and the support of this assumption and to touch upon a few important aspects. We shall do so along the lines of the following stepping stones:

1. Estimation of mean added frictional resistance in waves,
2. Comparison of model experiments at different scales,
3. Investigation of oscillatory tow force of models,
4. Full scale trials investigation.

5.1 Estimation of mean added frictional resistance in waves

The added resistance due to waves is generally considered as a quantity of potential origin. Prediction formulations based on potential theory can give a fair estimate of the values measured in a model basin and if the added resistance

is accepted as being of potential origin, then it follows that the Froude scaling law applies. In the following we shall derive an approximate expression for the frictional part of the mean added resistance due to waves. We shall assume the same formulation as applies to stationary frictional resistance and also assume the stationary frictional resistance coefficient to apply. This is a simplification, since in reality the boundary layer also becomes instationary and the flow separation at the stern, which may happen for full ship forms with too strong curvature of the lines in the aftbody, may also become time-dependent. Little, if anything, is known about this behaviour under wave- enforced instationary conditions and for the sake of this estimation we therefore have to assume the stationary friction coefficient and a formulation as follows:

$$R = C_f \cdot \tfrac{1}{2}\rho V^2 \cdot A \tag{5.1}$$

The bottom of the ship is left out of the consideration, only the sides are taken into account, because most wave action is confined to the region around the waterline.

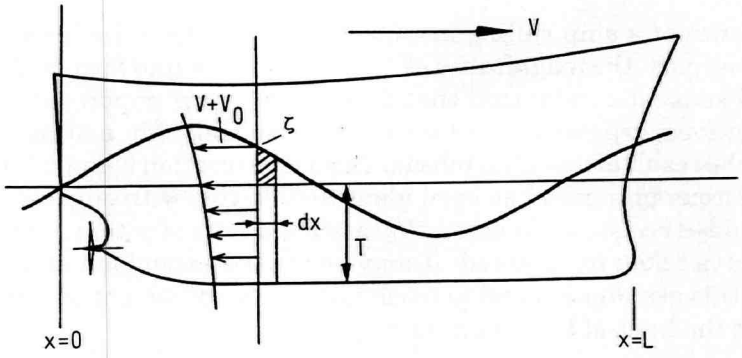

Figure 5-1: Wave profile and flow velocity profile.

The time-dependent velocity V is the result of the main flow to which the orbital wave velocity is added. The time-dependent wetted area A is the result of the harmonically oscillating water surface elevation. Since the waves are in most cases longer than the draught, the attenuation of orbital motion with depth is neglected. It therefore follows from Figure 5.1 that:

$$R = C_f \cdot \rho \cdot \int_0^L (T + \zeta)\,(V + V_0)^2\, dx \tag{5.2}$$

in which:

Cf	=	frictional coefficient for stationary flow according to ITTC-1957,
ρ	=	specific density of the fluid
L	=	lenght of the ship
T	=	draught of the ship
ζ	=	wave elevation
V	=	ship velocity
V_0	=	wave orbital velocity

Through application of the appropriate expressions for harmonic wave motion, and taking the time-wise and length-wise integration, it follows that:

$$\overline{R} = 2\pi\rho g \cdot C_f \cdot \zeta_a{}^2 \cdot \frac{L}{\lambda}\left(\frac{T}{2} + \frac{V}{\omega}\right) \tag{5.3}$$

in which further:

ζ_a	=	wave amplitude
λ	=	wave length
ω	=	wave circular frequency

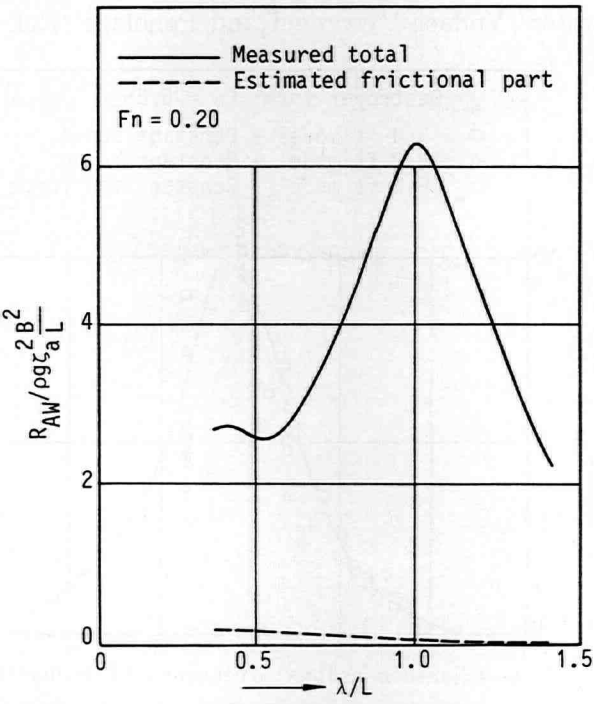

Figure 5-2: Transfer function of wave added resistance of an LNG carrier in head waves showing total value as measured and frictional contribution as estimated.

So we can write for the transfer function:

$$R \,/\, \rho g \zeta_a{}^2 \frac{B^2}{L} = 2\pi C_f \cdot \left(\frac{L}{B^2}\right) \cdot \left(\frac{L}{\lambda}\right) \cdot \left(\frac{T}{2} + \frac{V}{\omega}\right) \tag{5.4}$$

For a typical example of a model that was tested in the Seakeeping Basin (Ref. Section 7.2.1) the total mean added resistance as measured and the frictional part of it as estimated with the above formulation are compared in Figure 5-2.

Even taking the approximative nature of the formula into account it follows that the mean wave added resistance contains only a small contribution from viscous effects and is for the most part of potential origin.

5.2 Comparison of model experiments at different scales

An effective approach to determine the physical origin of the added resistance lies in model experiments at different scales. In the study of calm water resistance researchers have gone to great length in this respect and even went as far as towing a real ship behind another ship. (W.Froude 1874: corvette HMS Greyhound (Ref. 5-1). Similar experiments were done on the ships 'Simon Bolivar','Lucy Ashton','Yudachi','Wrangel',and 'Penelope' (Ref. 5-2).

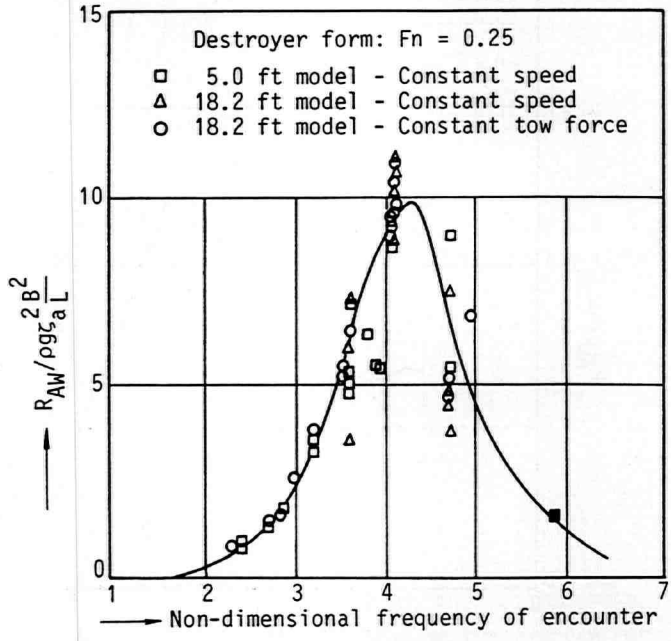

Figure 5-3: Transfer function of added resistance derived of model experiments at different scale [Ref. 5-3]

On the wave added resistance similar experiments are non- existent. Yet a number of model test programmes have been carried out with models which were quite different in size. An important case was reported by Strom-Tejsen et al (Ref. 5-3) who compared results obtained on a 1.50 m (5.2 ft) model to similar experiments on a 5.50 m (18.2 ft) model. The results in terms of added resistance transfer function, reprocuced in Figure 5-3, are compared on a basis of the Froude scaling law and the results are shown to correlate well. It should be kept in mind that the mean wave added resistance is a second order quantity and hence its measurement is fraught with a greater inaccuracy than first order quantities. The similarity between the data is good, considering that completely different towing tanks and techniques were used to perform the experiments. This supports the assumption that the wave added resistance is of potential origin.

5.3 Investigation of oscillatory tow force of models

In section 7.6.1 of the following we shall discuss a model test programme on cargo ship hull forms that was carried out on towed models, and for details we refer to that section. The models were towed at constant speed using a central tow cylinder so that in waves the oscillatory time history of the tow force was recorded. It is common practice to separate out the mean value and to disregard the oscillatory force since it is of no relevance to the mean added resistance.

For the sake of the present argument we have investigated the phase angle between the first order longitudinal force and the wave. A phase angle is invariably expressed on a time basis, in degrees, yet it can also be expressed in space coordinates. In that case the question is to find the position of the wave crest at the moment when the longitudinal oscillatory tow force is maximum. It was found for a number of model sizes that for all applicable wave lengths the maximum first order longitudinal force coincides with the position of the wave crest on the forebody. These results are shown in Figure 5-4.

From the frictional resistance point of view a dominance of the bow is inconceivable, certainly not for all wave length cases. From the potential resistance point of view this observation does make sense because the vertical water motion at the bow is larger than at the stern and also the x-normal at the one-quarter length forward is largest. So the fact that the maximum first order oscillatory longitudinal force occurs when the wave crest sits under the bow, such irrespective of wave length, can be viewed as support of this force being of potential nature.

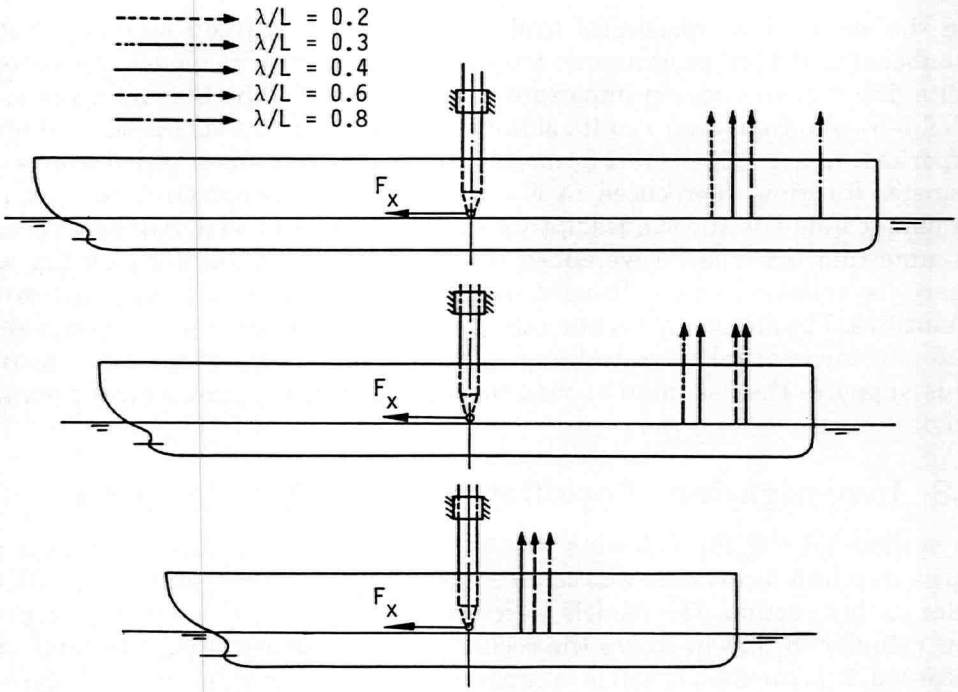

Figure 5-4: Position of wave crest when longitudinal force is maximum.

The added resistance is a second order force and as such it may stem from an entirely different physical origin. Yet, because both first and second order forces have been shown to be strongly related to the relative vertical motion of the water on the hull, Figure 5-4 can be viewed as an indication that both forces draw on the same - potential - origin.

5.4 Full scale trials investigation

In a more complex way full scale trials can serve as evidence of mean added resistance as a potential effect. For this purpose we have to use synthesis rather than analysis, and the reasoning rests on the following points:

- added resistance is intimately related to added thrust at model scale,
- added thrust at model scale can be used to compile a prediction of the speed loss in waves on a basis of Froude's law of similitude,
- speed loss predictions obtained on basis of model test results correlate well with full scale trials results.

The first point holds as long as the propeller remains in the water, which is the case for low and moderate seaways. The thrust and torque measured in waves

could quite well be mapped in the open water diagram of the propeller, see for instance Moor and Murdey (Ref. 5-4) and Van Sluijs and Dommershuijzen (Ref.5-5). Essentially this means that the thrust deduction coefficient obtained in calm water applies quite well to the case of moderate seaways.

The second point covers a well-established procedure to predict the sustained sea speed in waves, hence the speed loss, on basis of propeller thrust measurements in waves. The measurement of torque is in most cases inpracticable on the comparatively small seakeeping models on account of propeller size, propeller availability and measurement accuracy. Therefore the procedure rests on thrust rather than torque. The intersection of the required thrust curve with the curve of the thrust the engine and propeller can deliver yields the sustained sea speed. For more details about this procedure see Van Slijs and Dommershuijzen (Ref. 5-5).

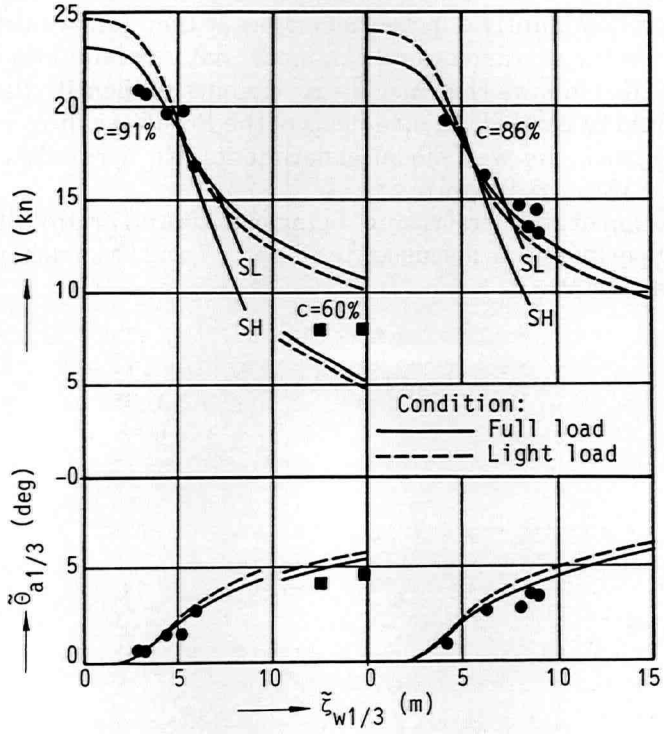

Figure 5-5: Predicted and measured speed and pitch angle of m.s. Dart Europe in head waves [Ref. 5-6].

The third point is the most complex, because speed loss obtained on full scale trials is the result of a whole range of effects ranging from wave added resistance to wind resistance, rudder effect, changing propulsion efficiency and engine torque limitation. If the full scale data is to be correlated to model data the model predicted speed loss is to be based on synthesis of all effects that are present. Studies of this kind have been undertaken in the past and the degree of correlation justifies the methods and assumptions made. See for instance Journée (Ref. 5-6), from which Figure 5-5 has been drawn.

So in conclusion, when the speed loss in reality matches the prediction, it justifies the various components of the prediction, one of these components being the assumption that added resistance due to waves is of potential origin.

5.5 Concluding remark

From the foregoing investigation it can be concluded that the wave added resistance is predominantly of potential origin. It then follows that the scaling law that governs the extrapolation from model data to ship data is the Froude scaling law. It also follows that model experiments to identify the wave added resistance should be carried out on a basis of the Froude scaling law, which ties in quite nicely with the way model experiments are normally carried out to obtain the calm water resistance.

The assumption of added resistance being of potential origin is the departure point for the experiments as discussed in Chapter 7 and the mathematical model as explained in Chapter 8.

Chapter 6

Some aspects of stationary and instationary potential flow

In the present chapter we shall discuss some aspects of stationary and instationary potential flow in as far as it is of relevance to the flow around the bow. The points discussed here will be useful in understanding the experiments of Chapter 7 and they also form the basis of the mathematical model to be discussed in Chapter 8.

6.1 Reference frames

A flow is called instationary when its velocity in a given point varies with time. It should be noted that the instationarity of a flow has just as much to do with the flow itself as with the frame of reference in which it is described. The flow of water around a ship at speed in calm water is stationary in a ship-based system of axes and instationary in an earth-based system of axes.

In the general case of a ship travelling through a propagating wave field, thereby making motions in all six degrees of freedom, the flow is considered as instationary. No reference frame can be constructed in which the total flow becomes stationary; had this been the case it would have been an enormous simplification of the ship motion problem.

6.2 The Bernoulli equation

For the case that the fluid flow is unsteady, irrotational, incompressible and the velocity and the external body force can be derived from a gradient field, the

Euler momentum equation can be integrated with respect to the space coordinates to yield the Bernoulli equation:

$$\Phi_t + \tfrac{1}{2}V^2 + \frac{p}{\rho} + gX_3 = c(t) \tag{6.1}$$

in which:

Φ_t = time-wise derivative of the velocity potential
V = velocity of the fluid
p = pressure
ρ = fluid density
g = acceleration due to gravity
X_3 = vertical coordinate with respect to earth-fixed axes
$c(t)$ = a constant, dependent upon time.

The above expression is typically in a space-fixed system, but it can easily be transposed on to the steady translating axes using the Galilei transformation:

$$\Phi_t = \frac{\partial}{\partial t}\Phi(\overline{X}, t) = \left(\frac{\partial}{\partial t} - U\frac{\partial}{\partial x_1}\right)\varphi(\overline{x}, t) \tag{6.2}$$

where $\Phi(\overline{X}, t)$ is the velocity potential defined on space-fixed axes and $\varphi(\overline{x}, t)$ is the potential defined on steadily moving axes. In doing so we arrive at:

$$\varphi_t - U\varphi_{x_1} + \tfrac{1}{2}(\nabla\varphi \cdot \nabla\varphi) + \frac{p}{\rho} + gx_3 = \frac{p_a}{\rho} \tag{6.3}$$

where the gradient is to be taken in the steady moving axes. If we set the ship speed to zero the two coordinate systems coincide and the expression becomes identical with the one above. An elaborate treatise will be found in Lamb [6-1], Batchelor [6-2] and Newman [6-3].

6.3 Stationary flow

The Bernoullian of bow flow

For a ship sailing at a constant speed on a fixed draft the flow field will be stationary, apart from turbulency in the boundary layer and the wake and some other effects that do not concern us here. On a macro scale it is stationary. The stationarity is axes-bound and holds only for a system of axes with respect to the ship, i.e. we hold the ship fixed and let the fluid flow along the ship. Since our interest lies mainly in the bow region, the points that we would like to make are in most cases illustrated by the flow around the bow.
For this case we can write the Bernoullian:

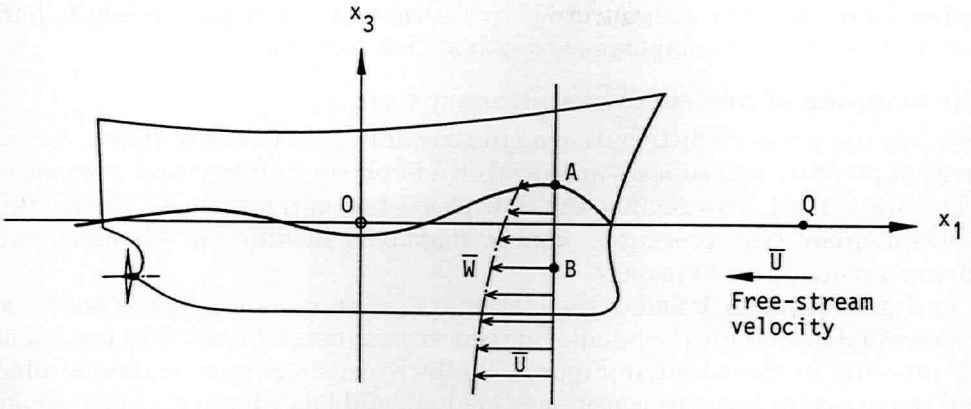

Figure 6.1: Schematic diagram of bow wave velocity field.

$$p_{total} + \tfrac{1}{2}\rho W^2 + \rho g x_3 \quad = \text{total head} \quad = p^* + \tfrac{1}{2}\rho U^2 \tag{6.4}$$

in which p^* is the piezometric height which for the present case where the free surface coincides with the $x_3 = 0$ plane equals the atmospheric pressure.

For the present case it is convenient to set the total head equal to the sum of the atmospheric pressure p_a and the velocity head $\tfrac{1}{2}\rho U^2$ which is the total head at point Q in the undisturbed upstream flow.

Using the Bernoullian we can obtain the relationship between the pressures on the bow as shown above. We may simply delete the atmospheric pressure on both sides of the above equation so that p becomes the pressure in excess of the atmospheric pressure.

For the point A on top of the bow wave we find:

$$p_A + \tfrac{1}{2}\rho W_A{}^2 + \rho g x_{3A} = \tfrac{1}{2}\rho U^2 \tag{6.5}$$

Since in the free surface $p_A = 0$ the height of the bow wave is equal to:

$$x_{3A} = -\frac{1}{2g}(W_A{}^2 - U^2) \tag{6.6}$$

In words, it is the 'velocity defect' that causes the bow wave to rise.

For a point B in the fluid, below A, we obtain likewise:

$$p_B = -\tfrac{1}{2}\rho\,(W_B{}^2 - U^2) - \rho g x_{3B} \tag{6.7}$$

So that here the pressure is governed by the velocity defect and the depth in the gravity field (not the submergence depth at that location).

The mapping of pressures of stationary flow

To study the pressure distribution on the bow it is most useful to take a vertical array of pressure transducers arranged on a forebody station where one expects a bow wave crest. To visualize the flow properties at a station on the bow the relevant quantities (pressures) can be displayed in different fashions, each having a merit in some respect.

In Figure 6.2 (a, b, c and d) the stationary pressure on the bow is shown for the nominal draft (only the middle line concerns us here). Figure 6.2a represents the pressure as measured, in Figure 6.2b the hydrostatic zero reading is added and the pressure becomes continuous (as it should be). Figure 6.2c is a variant of 6.2b showing the decomposition of hydrostatic pressure and velocity squared term. Finally Figure 6.2d shows the full decomposition of the pressure in hydrostatic, velocity squared and pressure increase term. All of these figures are in a ship-fixed system of axes.

In Figure 6.3 (b and d), numbered to keep it comparable to the previous Figure 6.2 the pressures are shown in space-fixed travelling axes. It is only the middle line that concerns us here, and since the ship is restrained in the vertical sense both reference frames coincided and the middle line in both diagrams are similar for this case.

A number of systematic model test programs were carried out to obtain pressure data in the bow region. See Section 7.5 for a more detailed discussion.

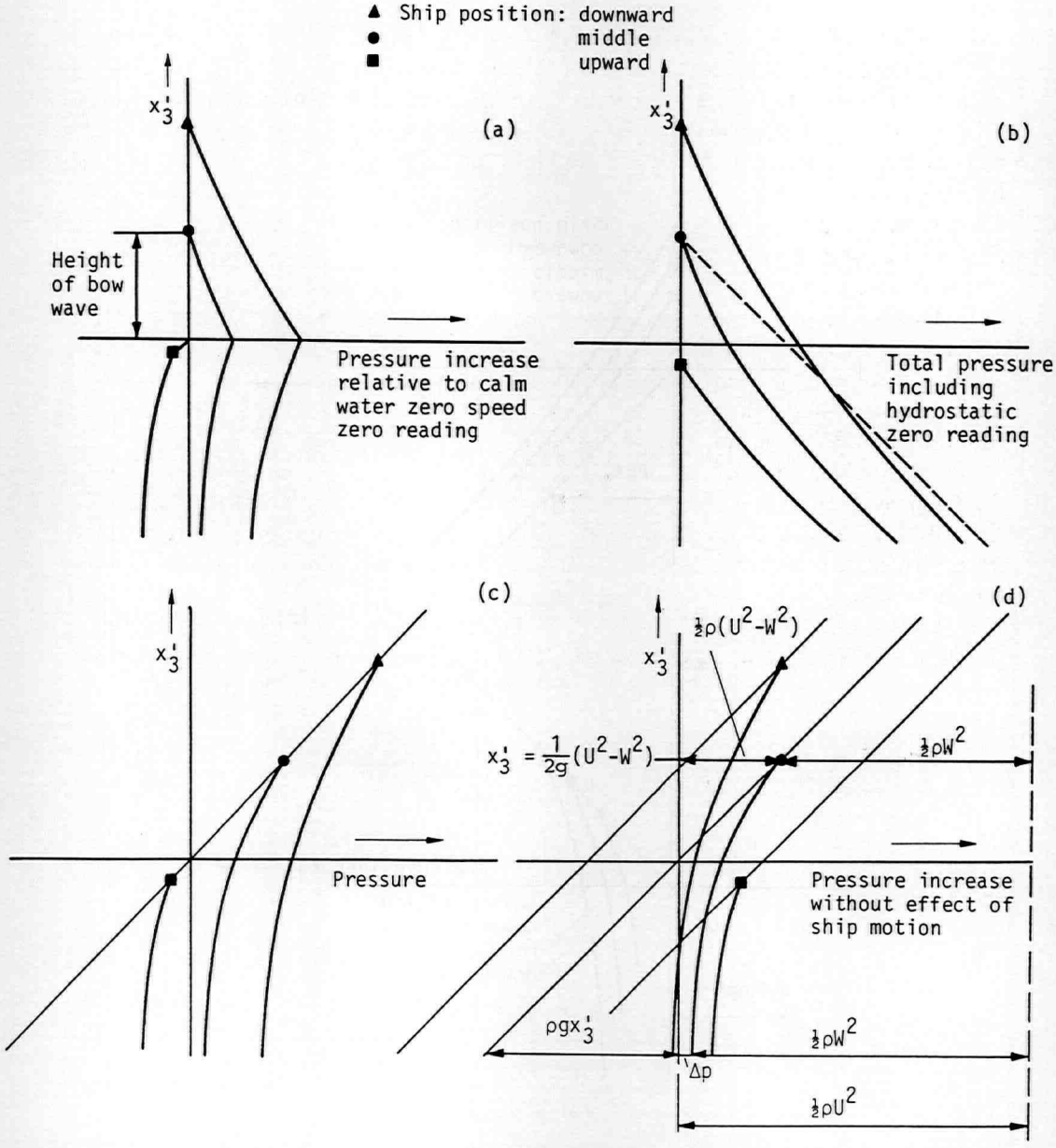

Figure 6.2: Pressure curves in a ship-fixed system of axes for a ship in three vertical positions in calm water at speed.

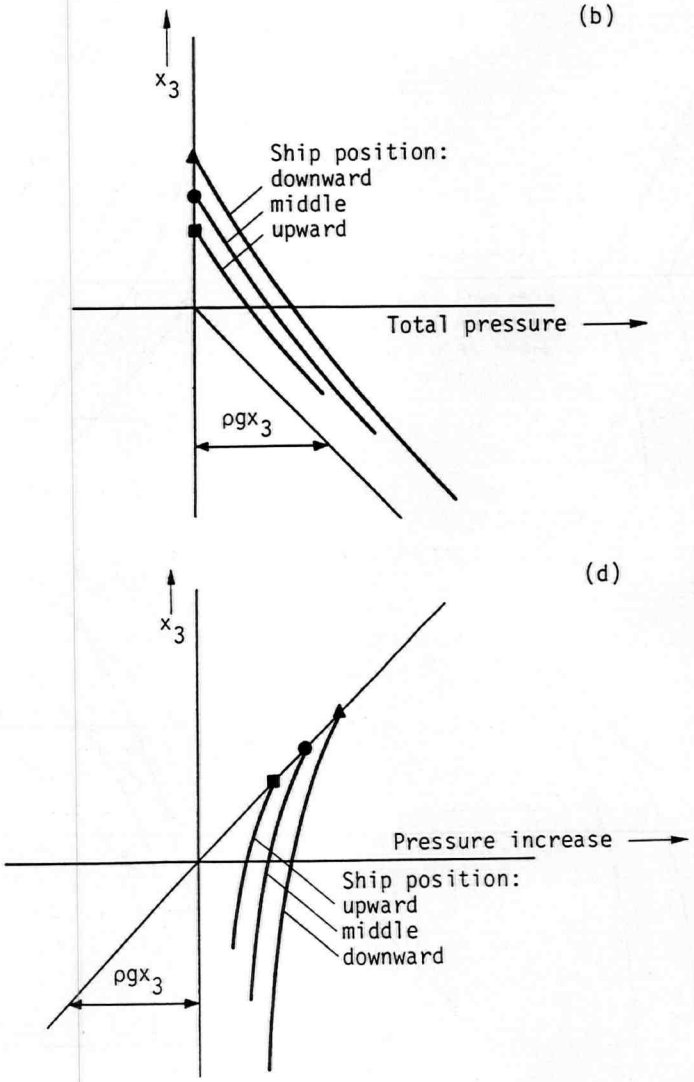

Figure 6.3: Pressure curves in space-fixed travelling axes for a ship in three vertical positions in calm water at speed.

6.4 Instationary flow

The Bernoullian of instationary bow flow

Assume the ship to be sailing at a constant speed on a fixed draft. Also assume that the incoming flow field is not stationary, but changes with time and place and that its surface also undulates in time and space. The Bernoulli equation that applies to this case has been expressed in equation (6.3). Irrespective of the complexity of the problem of solving for the describing potential function that governs the flow velocity field we can map some characteristics of the flow, by taking a measured pressure record and comparing this to the record of the stationary flow.

The pressure at some level in the oscillatory flow is:

$$p = -\rho(\varphi_t - U\varphi_{x_1}) - \tfrac{1}{2}\rho(\nabla\varphi \cdot \nabla\varphi) + p_a - \rho g x_3 \qquad (6.8)$$

The last two terms are constant for some level in the fluid. The difference found between the stationary and instationary Bernoullian is due to dynamic effects, i.e. the local and convective acceleration terms and the velocity squared term. At the free surface they make their presence manifest by a free surface rise or a surface drop. In the fluid a continuous change of velocity, in magnitude and direction, and pressure takes place.

A pressure gauge mounted in the hull can yield most useful data, yet in a ship-based system of axes.

The mapping of pressures of instationary flow

In the instationary case of a ship sailing into head waves and pitching and heaving the external wave forces acting upon the ship vary with time in an oscillatory manner and so do the motions and the reaction forces that are set up by the motions. It was found that the motions bear - to leading order- a linear relationship to the wave amplitude, a finding which has been used for instance as the basis for strip theory.

If the linearity works well for wave forces and motions it should have a basis in the pressures. For the mapping of the results of pressure measurements we have to reconsider the systems of axes. Strictly speaking a measurement device to record the pressure on the hull is fixed to the ship and gives a read-out in ship-based axes.

Suppose the point in question moves up and down over a known vertical distance (because of heaving and pitching), the instantaneous pressure lines related to the uppermost and downmost position are as also shown in Figure 6.2. The vertical motion enforces a change of the Bernoullian on the measured pressures that can be removed. In this fashion the results of pressure measurements can be plotted in a way as shown in Figure 6.2d. This figure applies to a

point on the bow of a ship making vertical oscillations with respect to a calm water surface.

We can take this one step further if we consider Figure 6.2d. The pressure shown is the pressure variation due to the vertical motion of the hull, but the change in hydrostatic pressure is removed as being a (too) obvious component. The system of axes can also be changed. If we shift the axes (of the plot) vertically over the distance of the oscillation we obtain a plot that relates to a system of fluid-based travelling axes. This is shown in Figure 6.3d. The pressure curves in this figure can be obtained by a pressure transducer held outside the hull at a constant depth under the water surface and travelling with the ship. Because of the obvious interference with the flow, this is an impossible proposition from the measurement side. As the ship is moved up and down in a stepwise fashion the pressure transducer would remain in place, and the results of such measurements would be as plotted in Figure 6.3d. For a truly instationary case where the bow makes up and down motions and an incident wave system is present the (absolute) rigid body motion of the hull-mounted pressure transducer can be removed and the results plotted in the same diagram.

A number of systematic model test programs were carried out to obtain pressure data for the bow region. See Section 7.5 for a more detailed discussion.

6.5 Quasi-stationary flow

The long wave case

Suppose a ship is sailing on flat calm water on which a very long sinusoidal wave is superimposed. The wave is long in the sense that the wave length is many times greater than the ship length. Suppose the ship is held fixed in space-fixed axes, so that the passing of the long wave crest can also be viewed as sailing at 'just a deeper draft'. If the wave is very long indeed, the flow should be similar to the steady flow for that deeper draft, because a long wave in deep water exhibits only negligible particle orbital velocity. The stationary (bow) wave system related to the nominal draft changes very slowly into a stationary wave system related to the deeper draft, the dynamics of this change can be neglected and at any time the flow is stationary.

The exact expression for the free surface elevation of point A (see Figure 6.4) above the initial calm water level $x_3 = 0$ follows from Bernoulli:

$$\zeta = -\frac{1}{g}\left(\Phi_t + \tfrac{1}{2}(\nabla\Phi)^2 \right) \tag{6.9}$$

When the total potential is decomposed into the nominal steady flow potential φ° and a potential describing the change φ of $O(\varepsilon)$ then the rise of surface can be

written as:

$$\zeta = -\frac{1}{g}(\varphi_t + \overline{W}\cdot\nabla\varphi) - \frac{1}{2g}(W^2 - U^2)\Big|_{x_3=\zeta} \tag{6.10}$$

See also Section 7.5 for further details.

This expression has to be evaluated at the unknown level $x_3 = \zeta$. Since the expression holds on a unknown surface we have to apply a suitable Taylor expansion with respect to a known (lower) boundary in order to obtain a tractable solution. Two parameters show up for this linearization:

- the field coordinate x_3;
- the amplitude of the incoming wave ζ_a, which presents a rise in water level, hence draft.

At first sight it would seem that the field coordinate x_3 suffices. Linearization with respect to x_3 means that if an additional 'layer of water' is added on top of $x_3 = 0$, the velocity curve W is extrapolated from W_A to W_B' in a linear fashion.

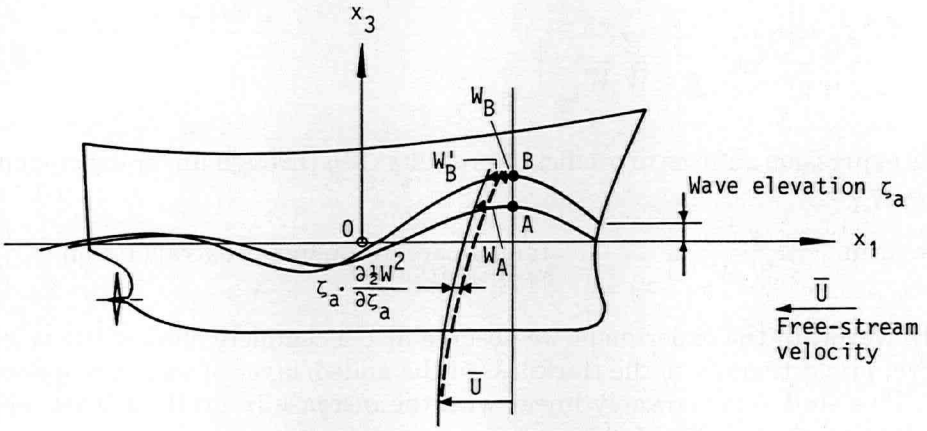

Figure 6.4: Diagram to illustrate linearization of bow wave velocity related to wave elevation.

This linearization would read:

$$\zeta = -\frac{1}{2g}(W^2 - U^2)\Big|_{x_3=\overline{\zeta}} - \frac{1}{g}(\varphi_t + \overline{W}\cdot\nabla\varphi)\Big|_{x_3=\overline{\zeta}}$$

$$- \frac{1}{g}(\zeta - \overline{\zeta})\,\overline{W}\cdot\overline{W}_{x_3}\Big|_{x_3=\overline{\zeta}} \tag{6.11}$$

so that:

$$\zeta - \overline{\zeta} = -\frac{\varphi_t + \overline{W}\cdot\nabla\varphi}{g}\cdot\frac{g}{g + \overline{W}\cdot\overline{W}_{x_3}}\Big|_{x_3=\overline{\zeta}} \tag{6.12}$$

Since φ represents the long incident wave we have:

$-\frac{\varphi_t}{g} = \zeta_a$, the incident wave amplitude

$\nabla\varphi \cong 0$, for a long wave and the expression reduces to:

$$\zeta - \overline{\zeta} = \zeta_a \cdot \frac{g}{g + \overline{W}\cdot\overline{W}_{x_3}}\Big|_{x_3=\overline{\zeta}} \tag{6.13}$$

This expression suffices to predict the velocity W_B' through linear extrapolation from W_A.

The term $\frac{g}{g + \overline{W}\cdot\overline{W}_{x_3}}\Big|_{x_3=\overline{\zeta}}$ taking care of the linear extrapolation.

However, in the experiment we observe also a complete shift of the velocity curve, proportionally to the thickness of the added 'layer of water', see Section 6.3. This shift is remarkably linear with the increase in draft, at least for the bow region as experiments have shown.

For a good prediction of the true velocity W_B instead of W_B' this effect should not be neglected and it appears that both linearizations should be used together. This aspect is important for the shaping of the mathematical model and this point is further illustrated in Section 7.5 and in Chapter 8.

The slow heave case

If a ship at speed is forcibly made to heave very slowly in flat calm water we have the opposite of the foregoing case. The change in (bow) wave system set up by the deeper draft will in all respects be similar to the wave system set up by the very long wave, at least in the vicinity of the ship. The only difference would seem to lie in the coordinate system, a pressure transducer mounted in the hull would not be able to tell the difference, so the description should be very nearly similar to the foregoing case.
Also for this case we may write:

$$\zeta = -\frac{1}{g}(\varphi_t + \overline{W}\cdot\nabla\varphi) - \frac{1}{2g}(W^2 - U^2)\Big|_{x_3=\zeta} \tag{6.14}$$

Here φ represents the small potential describing the changing of the flow in the entire flow domain as the ship goes from the nominal draft to a deeper draft.
We have:

$\varphi_t \equiv 0$ because the downward movement is executed very slowly;

$\nabla\varphi$ = the change of velocity in a space-fixed point under water. This can to first approximation be written as:

$$\nabla\varphi = z_a \frac{\partial \overline{W}}{\partial z_a}\ , \text{ so that}$$

$$\overline{W}\cdot\nabla\varphi = z_a \frac{\partial}{\partial z_a}(\tfrac{1}{2}W^2) \tag{6.15}$$

Using these we can write:

$$\zeta = -\frac{z_a}{g}\frac{\partial}{\partial z_a}(\tfrac{1}{2}W^2) - \frac{1}{2g}(W^2 - U^2)\Big|_{x_3=\zeta} \tag{6.16}$$

$$\zeta = -\frac{1}{2g}(W^2 - U^2) - \frac{z_a}{g}\frac{\partial}{\partial z_a}(\tfrac{1}{2}W^2)$$

$$-(\zeta - \overline{\zeta})\frac{\partial}{\partial x_3}\left\{\frac{1}{2g}(W^2 - U^2) + \frac{z_a}{g}\frac{\partial}{\partial z_a}(\tfrac{1}{2}W^2)\right\}\Big|_{x_3=\overline{\zeta}} \tag{6.17}$$

If we neglect the term containing the second derivative as being $O(\varepsilon^2)$ we obtain:

$$\zeta - \overline{\zeta} = \left[\frac{-z_a \frac{\partial}{\partial z_a}(\tfrac{1}{2}W^2)}{g} \right] \cdot \left[\frac{g}{g + \overline{W} \cdot \overline{W} x_3} \right] \Bigg|_{x_3 = \overline{\zeta}} \tag{6.18}$$

The first ratio represents the decrement in kinetic energy which is linearly extrapolated along the velocity line W with the field coordinate, as indicated by the second term, indicated in Figure 6.5.

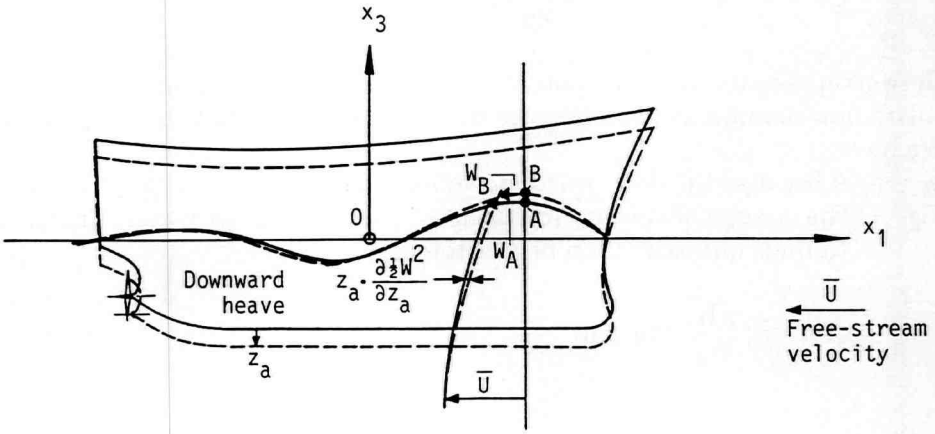

Figure 6.5: Diagram illustrating extrapolation of the velocity related to heaving.

6.6 A proposed linearization scheme

The two foregoing flow cases, the long wave crest inducing a deeper draft on the fixed ship and the slow downward heave movement in calm water are, as one can imagine, in terms of flow dynamics, entirely similar. Yet the expressions for the surface rise are dissimilar, even if one takes account of the difference in reference frame.

The reason is obvious. In the long wave case we have introduced the small potential φ containing only the incident wave. Yet some disturbance potential representing the reaction of the flow to the deeper immersion should have been added. The existence of such a reaction is obvious from the slow heave case, yet in the long wave case it was not yet included.

So the long wave case is to be amended by a term that takes into account the changing of the flow deep inside the fluid domain, on account of the thin layer of water that is added at the top. If an appropriate potential is defined to describe this change, the surface rise will read for the long wave case, in line with the slow heave case:

$$\zeta - \overline{\zeta} = \zeta_a - \frac{\zeta_a}{g}\frac{\partial}{\partial \zeta_a}(\tfrac{1}{2}W^2) \cdot \frac{g}{g + \overline{W}\cdot\overline{W}_{x_3}}\Bigg|_{x_3=\overline{\zeta}} \tag{6.19}$$

This formula shows the need for a Taylor's expansion into two coordinates. The first is a linearization with respect to the field coordinate x_3 which we can view as extrapolating the velocity line from W_A to W_B' in Figure 6.4. This leads to the denominator in expression (6.19). The second linearization is with respect to the increase in draft ζ_a that modifies the flow in the entire domain. This second linearization showed up in a natural way in the slow heave case, we could show that it should also have been included in the long wave case. Combining the two it follows that in the more general case it represents a linearization with respect to the 'change of draft' or the 'relative motion', which is composed of both incident wave and heave, (the other motion, pitching, follows a likewise reasoning).

It is fair to say that in the long wave case the small first order potential φ should have included the sum of both incident wave and the flow perturbation with draft, or better relative motion. In that case the linearization with respect

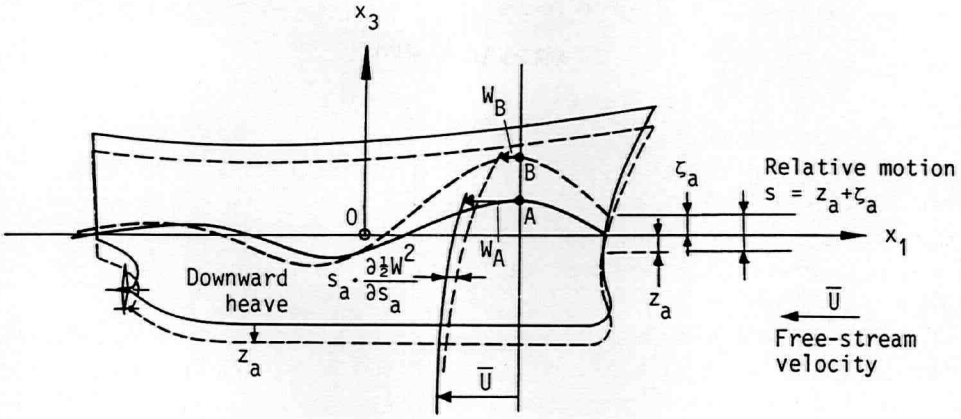

Figure 6.6: Diagram illustrating linearization scheme related to the relative motion.

to the field coordinate x_3 would have led automatically to formula (6.19) and there would not have been a need for the second linearization. However, we have to include this effect somewhere, otherwise it will be lost.

In Section 8 a boundary value problem is formulated that will lead to a solution for the first order potential φ. In order to include the physical effect that was observed in the model experiments, i.e. a strong dependency of the flow on the relative motion, the double linearization scheme will be used in deriving the boundary conditions for this problem. In that way a potential will be defined that describes the observed physical effect.

Chapter 7

The Model Experiments

7.1 General summary of model experiment series and procedures

7.1.1 Summary of model experiment series

In the present section the main points are discussed of no less than 10 model experiment series covering work on 19 hull forms. The greater part of the work was concerned with the investigation of flow effects around the forebody. The studies were concerned with the following subjects:

-section 7.2:	relative water motion at the bow
	7.2.1: LNG carrier
	7.2.2: high speed frigate
	7.2.3: survey of data files (40 hulls)
-section 7.3:	relative motion and dynamic swell-up for a frigate
-section 7.4:	forebody effect of a wedge type bow model
-section 7.5:	pressure distribution at the bow
	7.5.1: wedge type bow model
	7.5.2: Wigley models (2)

In addition systematic model experiments are discussed here that shed some light on the influence of ship and wave characteristics, covering the following subjects and experimental series:

-section 7.6:	ship main particulars
	7.6.1: cargo ships (3)
	7.6.2: systematic frigates (5)

-section 7.7: bow form
7.7.1: bulk carriers (4)
7.7.2: cargo ships (3)
-section 7.8: wave direction
7.8.1: LNG carrier
7.8.2: cargo ship

Some of the studies in the latter group are of a confidential nature, yet permission has been granted by the sponsors to display general details of the experimental programme and a limited amount of data results, in a self-contained form. This confidential work includes a multi-year research programme to the order of the NSMB Cooperative Research on Ships (CRS), carried out to investigate the effect of short waves (Section 7.6.1, 7.7.2, 7.8.2). It also includes confidential work known as the Fast Displacement Ship (FDS) Series, a multi-year research programme under the joint sponsorship of the Royal Netherlands Navy, the United States Navy, the Royal Australian Navy and MARIN. This work was concerned with a systematic variation of main particulars (Section 7.2.2 and 7.6.2)

7.1.2 Summary of model experiment procedures

For a better understanding of the experiments and the results to be presented in this section it will be useful to very briefly describe the laboratories, the test setup and the instrumentation.

Most experiments were performed in the Seakeeping Laboratory of MARIN, which measures 100*24*2.5 metres in length, width and waterdepth respectively. A towing carriage can travel on rails along the length of the basin at a maximum speed of 4 m/s. Some experiments in waves were carried out in the High Speed Towing Tank, which measures 220*4*3.6 metres in length, width, and waterdepth respectively. This basin is admirably suited for the testing of high speed ship models, because the towing carriage can travel at much higher speeds of up to 15 m/s, sufficient to test fast craft at Froude numbers of up to 2.0.

Two series of experiments (Section 7.5.2) were carried out in the Ship Hydromechanic Laboratory of the Delft University of Technology, in a towing basin measuring 150*4*3m in length, width and water depth respectively.

Various ways of towing the model were employed. In some cases the model was towed by a pulling wire in which a force transducer and a spring were inserted. A system of soft linear springs rigged in beamwise direction would keep the model on course without adding a longitudinal force to the model. Another option was to tow the model by means of an air-lubricated heave cylinder and a universal joint, fixing the model in sway, yaw and surge, while allowing heave, pitch and roll, which is a better procedure for high speed testing.

Both basins are equipped with wavemakers. The Seakeeping Laboratory has a wave generator of the flap type. To generate regular longitudinal waves from ahead the generator is run at constant rate of rotation so that the flaps make a sinusoidal movement with the prescribed period. The amplitude of the wave is governed by the stroke of the flap. Irregular wave spectra can also be generated. The High Speed Towing Basin has a hydraulically operated wave generator, which can also be used to generate regular sinusoidal waves and irregular seaways conforming to a prescribed spectrum.

Experiments in regular-sinusoidal-waves were usually done for a wave length range from $\lambda/l = 0.5$ to 2.0. For high speed models it was necessary to test in even longer waves. For the studies specifically done in short waves a wave length range from $\lambda/L = 0.2$ to 0.8 was used. Wave height would usually be such that neither the bow would come out of the water, nor would any water be shipped on the deck. To this end the wave amplitude was restricted to about 1 to 2 percent of the model length. Except for the experiments in section 7.8 all experiments were done in waves from ahead.

The weight distribution of the model is usually adjusted in air on a low-mass oscillating bench. The model is placed on the bench in such a way that the position of the C.O.G. coincides with the axis of the bench. The bench is set in oscillation and the radius of gyration in longitudinal direction - for pitch- is adjusted by measuring the period of oscillation of the bench. An alternative approach is to suspend the model from two wires (bifilar pendulum) and to take the period of oscillation as a measure for the pitch gyradius. The transverse metacentric height is adjusted in water by a heeling experiment, the transverse radius of gyration is usually checked by measuring the natural period of roll from the record of a roll extinction test.

The measurements comprised the all-important resistance, measured by a strain-gauge transducer, from which the added resistance was to be established. In addition vertical ship motions, heave and pitch, were measured as reference channels and invariably also the relative vertical water motion at some forebody station was measured by means of a resistance type wave probe, usually fitted to one or both sides of the model bow at station 18 or 19. As is usual in such experiments, the undisturbed wave amplitude was measured about a model length in front of the model. Since the recording equipment was installed on the towing carriage, cable connections were used to relay the measurements from the model to the carriage. The data recording took place on computer as well as on UV paper for quick on-the-spot inspection.

For the experiments in regular waves the test duration was set by the required number of oscillations and the time needed for the transient to dampen. To account for the latter the measurements would start only after some ten oscillations had passed. For the measurements proper an equal number of oscillations was sufficient to determine the amplitude and phase of the various

signals by means of Fourier analysis. For the resistance, which also showed a sinusoidal character, only the mean value was of interest.

Prior to the experiments in waves a series of runs had to be made in still water for the measurement of the still water levels of the various quantities. Although this was a minor detail for the ship motions it was necessary for the resistance. After subtracting the constant still water resistance from the mean total resistance in waves, for the same forward speed, a value for the mean wave-added resistance was obtained.

The test result of resistance increase is in the diagrams invariably denoted by RAW (Resistance Added in Waves). In most diagrammes it has been non-dimensionalized by $\rho g \zeta_a^2 \, . \, l$. In this expression ρg are included to obtain a force, which is in keeping with the Froude scaling law. The dependency on wave amplitude squared (ζ_a^2) has been shown before (Section 3.2). The dependency on a characteristic length l is clearly required for dimensional homogeneity. The quantity B^2/L is often used as a characteristic length, however some other choice may be made as well. More about this is said in Section 3.6 and in Section 7.6.2.

7.2 A study on added resistance and relative motions

In Section 4.1 it was hypothesized that a close relationship would exist between the wave added resistance and the vertical relative motions on the forebody. Some limited evidence was shown to support this idea. In the present section we shall expand on this idea and bring it on a stronger footing by showing that the experimental evidence is consistent and not related to a specific ship type, speed or wave condition. In this section test results are shown of two widely different experimental model series, covering tests on an LNG-carrier and on a high speed frigate.

7.2.1 Experiments on the model of an LNG-carrier

For the present test programme a model of a 125,000 m3 LNG- carrier was used, at a scale factor of 1 to 70. The model was outfitted with bilge keels and the instruments necessary to do the measurements of heave,pitch,relative motion and added resistance. The weight distribution of the model corresponded to a full load draught of 11.5 m on an even keel. The main particulars of the ship and the pertaining weight distribution are given in Table 7.2.1-1. The bodyplan of the model is shown in Figure 7.2.1-1.

Denomination	Symbol	Unit	Model	Prototype
Length	L	m	3.900	273.00
Breadth	B	m	0.600	42.00
Draught, even keel	T	m	0.164	11.50
Displacement volume	∇	m^3	0.2878	98.740
Block coefficient	C_B	-	0.749	0.749
Midship section coefficient	C_M	-	0.991	0.991
Waterline coefficient	C_{WL}	-	0.805	0.805
Longitudinal centre of gravity from aft perpendicular	$\overline{AG}$	m	1.981	138.66
Centre of gravity above base	$\overline{KG}$	m	0.196	13.70
Metacentric height	$\overline{GM}$	m	0.057	4.00
Longitudinal gyradius	k_{yy}	%L	24	24
Transverse gyradius	k_{xx}	%B	35	35
Natural heave period	T_z	s	1.12	9.4
Natural pitch period	T_Θ	s	1.12	9.4
Natural roll period	T_ϕ	s	1.91	16.0

Table 7.2.1-1: Main particulars of LNG-carrier.

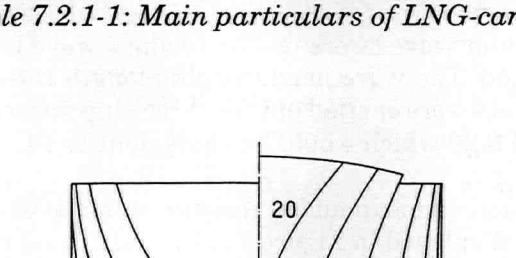

Figure 7.2.1-1: Bodyplan of LNG carrier.

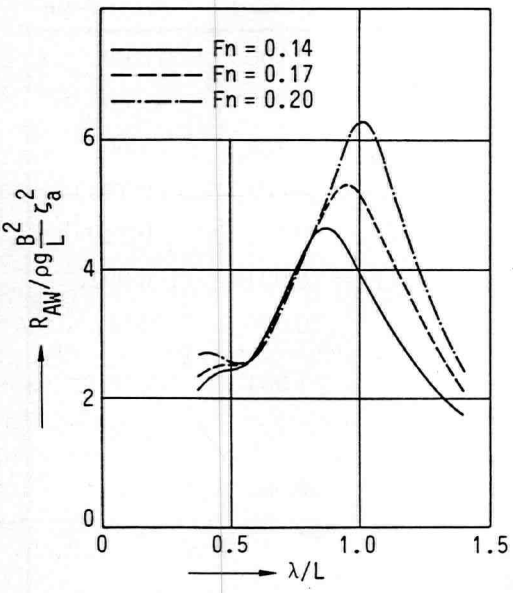

Figure 7.2.1-2

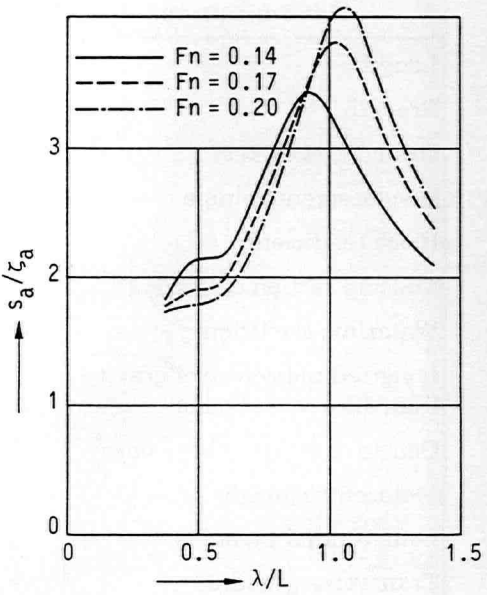

Figure 7.2.1-3

Transfer functions of resistance increase and relative motion (Station 19) of LNG carrier in regular head waves.

The experiments were performed in the Seakeeping Laboratory. For the present test programme regular waves were used covering a wave length to ship length ratio from 0.37 to 1.40. The wave height to ship length ratio corresponded to 1 to 50. The experiments were carried out for three ship speeds, corresponding to Fn. = 0.14; 0.17 and 0.20 which would be equivalent to 14, 17 and 20 knots for the real ship.

The results obtained on mean added resistance in waves and on the relative forebody motion are displayed in Figure 7.2.1-2 and 7.2.1-3 respectively. Figure 7.2.1-2 shows the ordinate value of mean added resistance, non-dimensionalized as explained in Section 7.1.2, and plotted on an abscisse of wave length ratio, also in non-dimensional form. For the wave length ratio close to unity the conspicuous hump shows up which can be attributed to large synchronous ship motions heave and pitch.

In head waves the relative motion, Figure 7.2.1-3, exhibits a pronounced resonance peak at pitch resonance and, like pitching, the relative motion increases for increasing speed. The height of the peak of the relative motion function, between 3.5 and 4 times the wave amplitude, is not unusual for a ship of this type.

The added resistance in waves, Figure 7.2.1-2, depends on speed; the higher the speed the larger the wave added resistance and the curve shifts towards the longer wave length range. It is interesting to note in the head wave case that the speed dependency only exists in the long wave regime i.e. $\lambda/L > 1$ whilst in waves much shorter than the ship length the speed has only little effect.

A most striking correspondence has come to light between the wave added resistance and the relative motion at station 19. In principle there can be no argument about the fact that the wave added resistance is just and only the nett result of the hydrodynamic pressure distribution integrated around the body. In addition the relative motion at a certain location can be viewed as the visual expression of the pressure distribution underneath. However, as the diagrams Figure 7.2.1-2 and 7.2.1.3 show, the resistance is closely related to the relative motion on the forebody and this suggests that the relative motion is the main cause of the added resistance, rather than the ship motions themselves. The similarity between the added resistance curves and the relative motion curves is strong. We can construct a diagram in which the added resistance (RAW) is replotted on a non- dimensional basis of relative motion squared instead of wave amplitude squared. It will be obvious that in this case the relative motion depends on the particular forebody station chosen for the determination of the relative motions. This is not the same at all positions on the bow and it would perhaps make sense to use an effective or equivalent relative motion to take the spatial variation into account. Yet, that would come close to using a true pressure integration model, which is to be preferred. In Figure 7.2.1-4 it is clear that the resonance behaviour around $\lambda/L = 1$ has been removed and that added resis-

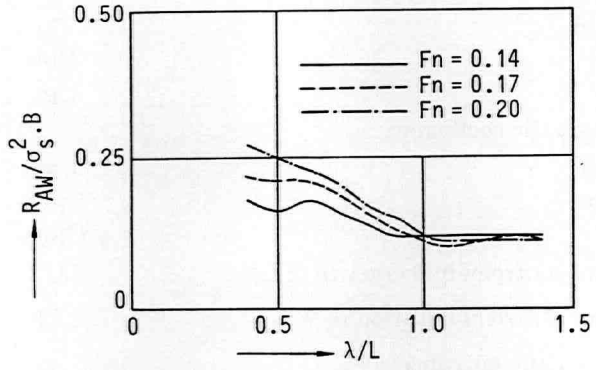

Figure 7.2.1-4: Resistance increase coefficient of LNG carrier.

tance is stronger related to relative motion at the forebody than to wave amplitude as such.
In Section 7.8.1 a continuation of the present study is reviewed from which it can be concluded that also for other oblique and following wave headings the relative motion forward remains a most determining quantity.

7.2.2 Experiments on the model of a high speed frigate

For the present test programme a 5 metre model of a frigate hull form was used. The model had a bare hull. Measurements comprised heave and pitch, relative motions at a number of forebody stations and wave added resistance. The main

Designation	Symbol	Model 5[A]
Length/Breadth	L/B	8
Breadth/Draught	B/T	4.0
Length/Draught	L/T	32
Blok coefficient:		
Total	C_B	0.396
Fore body	C_{BF}	0.327
Aft body	C_{BA}	0.465
Midship section coefficient	C_M	0.633
Waterplane coefficient:		
Total	C_{WP}	0.796
Fore body	C_{WPF}	0.600
Aft body	C_{WPA}	0.992
Horizontal prismatic coefficient:		
Total	C_P	0.626
Fore	C_{PF}	0.517
Aft	C_{PA}	0.735
Vertical prismatic coefficient:		
Total	C_{PV}	0.497
Fore	C_{PVF}	0.545
Aft	C_{PVA}	0.469
Longitudinal centre of buoyancy in % L_{PP}	LCB	-5.11
Longitudinal centre of flotation in % L_{PP}	LCF	-8.68
Angle of waterline entrance	iE	11.0°
Breadth transom/Breadth	-	0.96

Table 7.2.2-1: Form coefficients of high speed frigate.

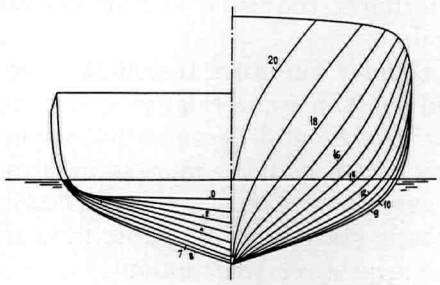

Figure 7.2.2-1: Body-plan of high speed frigate.

particulars and bodyplan of the frigate model used for the present test series are displayed in Table 7.2.2-1 and Figure 7.2.2-1.
The experiments in waves were carried out in the High Speed Towing Tank, following the general procedures as set forth in Section 7.1.2.

The regular waves spanned a wide wave length range from λ/L = 0.6 to 2.8; wave heights (double amplitude) were in most cases 2 percent of the model length. As to the speeds, the tests were carried out over a very wide speed range that corresponded to Froude numbers of Fn. = 0.285; 0.57; 0.855; 1.14. Concerning the heading, all tests were performed in regular waves from ahead.

Results were obtained on the mean added resistance in waves and the relative motion at the forebody at station 18. These are displayed in Figure 7.2.2-2 and

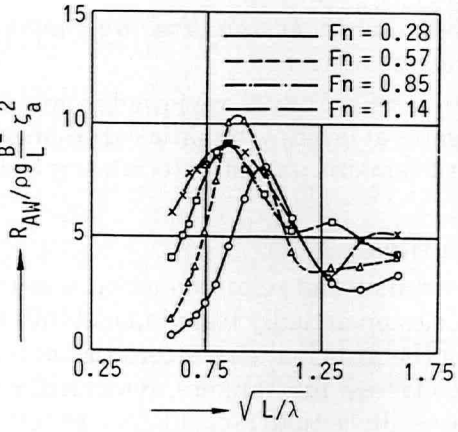

Figure 7.2.2-2

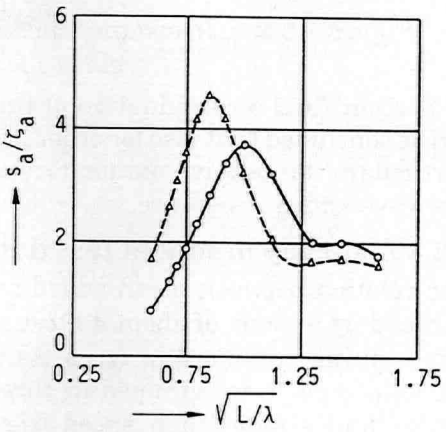

Figure 7.2.2-3

Transfer functions of resistance increase and relative motion (Station 19) of high speed frigate for various speeds in regular head waves.

7.2.2-3 respectively, adhering to the usual non-dimensionalization of the ordinate and the abscisse scale.
Also in the case of this slender hull form tested at extremely high speed, the similarity between added resistance and relative motion squared is large. When we call to mind the extremely great differences in speeds for which the frigate was tested this similarity becomes all the more interesting.

Like in the foregoing case of the LNG carrier the section for relative motion was chosen to be a forebody station, which exhibits in most cases the largest steady bow wave and the largest relative motions.

If we take the ratio of mean added resistance and relative motion squared we obtain Figure 7.2.2-4 in which the conspicuous resonance behaviour, related to synchronous pitching, disappears. In view of the high speed of the frigate model the similarity between the curves becomes all the more intriguing.

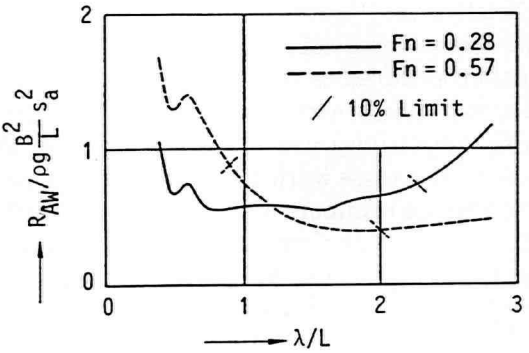

Figure 7.2.2-4: Resistance increase non-dimensionalized on basis of relative forebody motion.

In Section 7.6.2 a continuation of the present study is reviewed from which it can be concluded that also for other frigates at large systematic variation of main particulars the relative motion forward remains a most determining factor for the wave added resistance.

7.2.3 A survey of model test data files

The relation between mean added resistance and relative motion was further pursued by a study of about 40 test series on actually tested model hull forms, representing various ship types. As to the principal characteristics of the hull the ship types were grouped in three classes: full tankers, intermediate type ferries and slender high speed frigates. In actual fact all test programmes included in this data file survey were concerned with model tests in which the propeller thrust was measured on a free-running model instead of the resistance force on a towed model. However, research in this field has shown that, provided

that the propeller remains in the water, the mean wake and thrust deduction factor are very close to the calm water values, so that the trend of propeller thrust with some relevant parameters can be taken as representative of the resistance.

In Figure 7.2.3-1 scores of test data are plotted on a basis of ship speed. Since the tests were invariably carried out on self- propelled models in irregular waves a slightly different approach was used to non-dimensionalize the data. In this case the added thrust has been non-dimensionalized by the squared standard deviation of the relative motion multiplied by the ship's beam, which can be interpreted as the irregular wave equivalent of the quantity obtained in regular waves. As shown in the figure a distinction was made between low wave and high wave cases. The ratio between the relative motion of the forebody and the

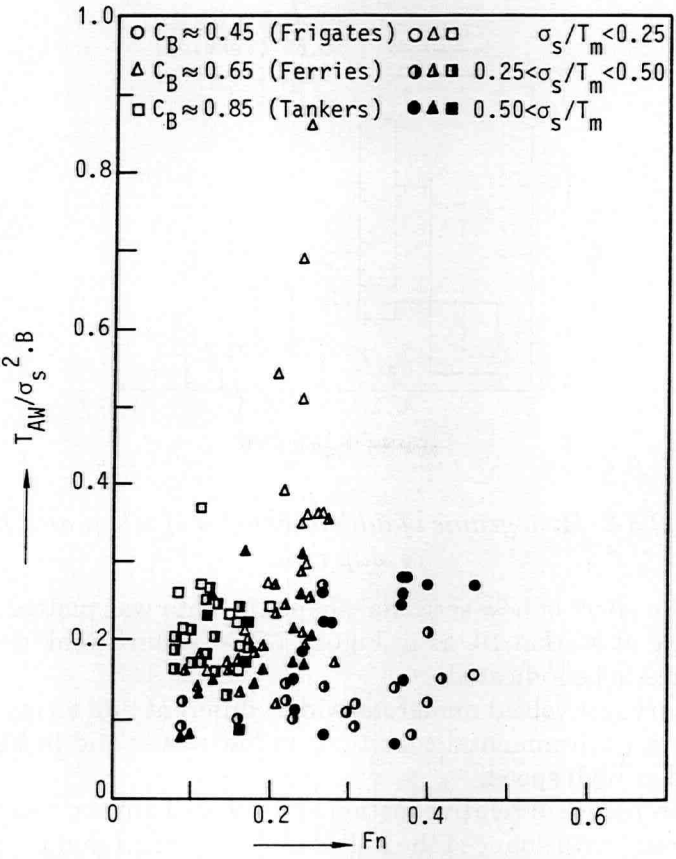

Figure 7.2.3-1: Added thrust coefficient correlated to Froude number for various ship types.

model draft was used to distinguish between low waves, moderate waves and high waves.
The data is clustered in a cloud around a value of 0.20 although the variation runs from as low as 0.1 to as high as 0.3, if we make an exception for a few outliers. The diagram tells us that the relative motion and the ship's beam are important parameters, but no apparent trend with speed can be made out.

As to the effect of ship type, the data has been grouped in three different classes, in Figure 7.2.3-2, corresponding with fullness and slenderness and a weak influence of fullness can be discerned. The blunt bow form of the tanker types of models appear to score consistently higher than the fine bow form of the frigates.

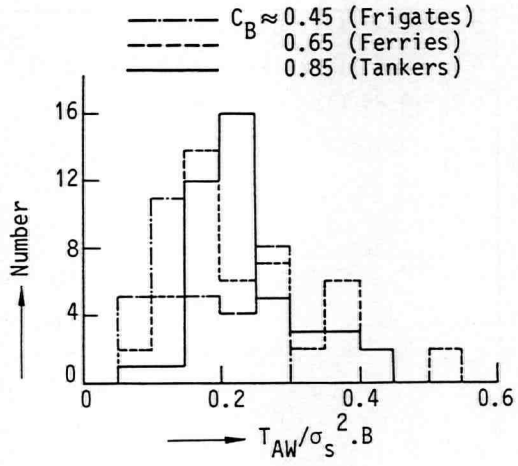

Figure 7.2.3-2: Histograms of added thrust coefficient as a function of ship type.

In search of the effect of bow sectional shape the data was plotted on a basis of bow flare angle at station 19, as in Figure 7.2.3-3. Some weak dependency on bow flare seems to be indicated.

This data survey involved numerous widely different hull forms tested under widely different environmental conditions in low waves and in high waves, at low speed and at high speed.

The major influence of relative motion and ship's beam are clear from Figure 7.2.3-1. The trend with shape of the hull is perhaps not all that easy to establish from a random set of hull forms, and it will take experiments on a systematisc series of hull forms to establish the influence of shape.

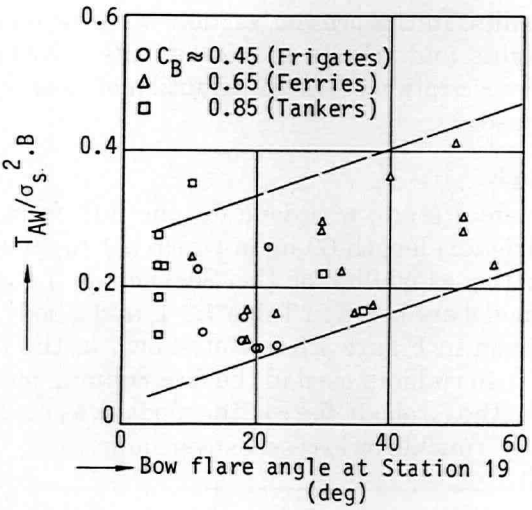

Figure 7.2.3-3: Added thrust coefficient correlated to bow flare for various ship types.

7.3 A study on relative motion and dynamic swell-up

A comprehensive investigation has been carried out into the vertical relative motion of the water surface along the bow of a frigate running in a seaway. In particular attention was focussed on the 'dynamic swell-up', i.e. the effect of water being pushed up around the bow higher than can be accounted for by considering ship motions heaving, pitching and incident wave alone.

The work was carried out under the sponsorship of the Royal Netherlands Navy and was published by Blok and Huisman in a paper read before the RINA in 1983 (Ref. 7-1).

The investigation included various kinds of experiments, like free-running tests in waves and still water, restrained model tests in waves and still water and oscillation tests in still water. Parallel to this, calculations as to ship motions and still water bow wave system were carried out.

On basis of the experiments and the calculations a 'swell-up coefficient' was defined and it was demonstrated that inclusion of this coefficient would greatly improve the prediction of relative motions at the bow and hence also related extreme forebody effects like probability of shipment of water and emergence of the forefoot out of the water.

Finally, the findings of the investigation were evaluated and synthesized into a design procedure that could easily be linked to the widely used strip theory method in ship motion calculation.

For a full description of the work we refer to reference (7-1) containing all the details and test results. In the present section we draw on this paper to show some of the highlights and results that constitute a stepping stone for our understanding and description of the contribution of the relative motion to the wave added resistance.

Experimental work

The whole experimental study was done for one hull form designated by the name of 'compact frigate', length 63 m, of which a 1 to 20 scale wooden model was made to suit the capability of the Seakeeping Laboratory. The main particulars of the model are listed in Table 7.3-1, and a body plan and stem and stern profile are given in Figure 7.3-1. Not shown in the figure are the twin propellers and the twin rudders used in the free-running model tests. As can be seen in Figure 7.3-1, the forebody flare of the model was moderate as is usual in frigates, without any knuckle or excessive overhang.

Denomination	Symbol	Unit	Magnitude
Length between perpendiculars	L	m	3.150
Breadth	B	m	0.450
Even keel draught	T	m	0.138
Displacement volume	∇	m^3	0.087
Block coefficient	C_B	-	0.449
Waterplane coefficient	C_W	-	0.795
Midship section coefficient	C_M	-	0.645
LCB aft of station 10	$\overline{AG}$	m	0.119
Centre of gravity above base	$\overline{KG}$	m	0.230
Metacentric height	$\overline{GM}$	m	0.040
Longitudinal gyradius in air	k_{yy}	% L	24
Natural heave period	T_z	sec.	0.783
Natural pitch period	T_Θ	sec.	0.783

Table 7.3-1: Main particulars of model of 'Compact Frigate'.

In the experiments as described in (Ref. 7-1 and 7-2) five distinctly different kinds of experiments were carried out to obtain the data in various ways that gave insight into the 'swell- up' phenomenon. These included:

-stationary tests: -free-running model in still water
-restrained model in still water
-instationary tests:-free-running model in waves
-restrained model in waves
-forcibly oscillating model in still water

The descriptive details of each test programme are summarized in Table 7.3-2.

Concerning measurement equipment, most importantly a series of relative motion wires were fitted to the bow to measure the water motion as indicated in Figure 7.3-1. These were of the resistance type and were laid in a groove in

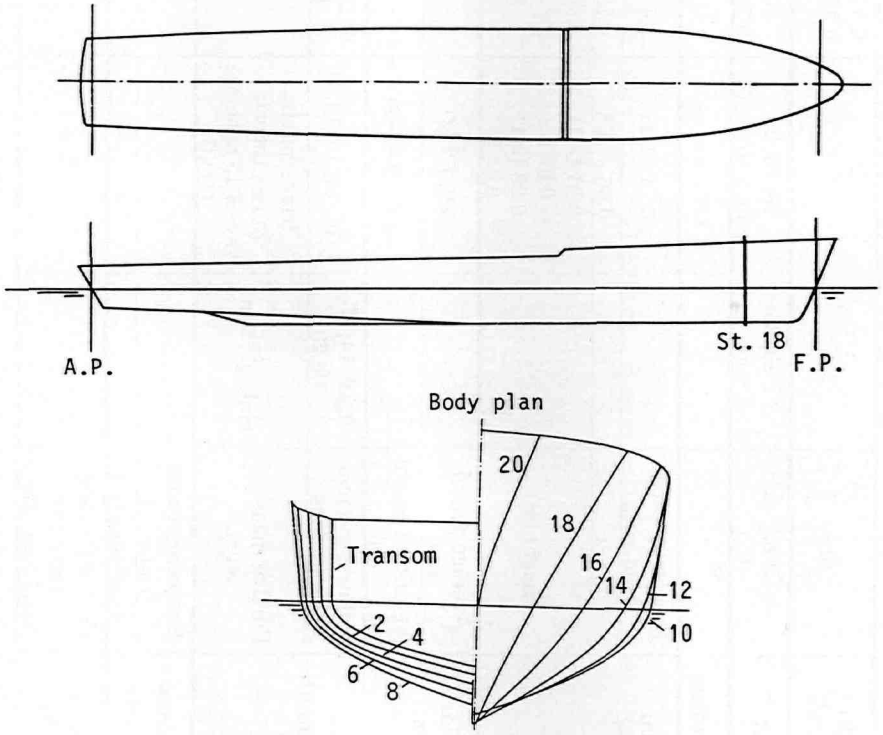

Figure 7.3-1: Bodyplan and profile of compact frigate.

Particulars		Test series: Free-Running in still water	Free-running in waves	Restrained in still water	Restrained in waves	Oscillation in still water
Draught (even keel)	(m)	2.75	2.75	2.75 (nominal); 3.35; 3.55; 3.75; 2.15; 1.95; 1.75	2.75	2.75
Speed	(kn.) (F_n)	15; 20; 25 0.30; 0.40; 0.50	15; 20; 25 0.30; 0.40; 0.50	15; 20; 25; 0.30; 0.40; 0.50	0; 15; 20; 25 0; 0.30; 0.40; 0.50	15; 20; 25 0.30; 0.40; 0.50
Wave heading		-	head waves	-	head waves	-
Regular waves	Frequency range (rad./sec.)	-	0.74 - 1.27	-	0.74 - 1.27	-
	L/λ	-	0.56 - 1.66	-	0.56 - 1.66	-
	Height (m)	-	0.01 L (1) 0.02 L 0.03 L (1) 0.04 L	-	0.02 L	-
Irregular waves	Average period (sec.)	-	5.9; 7.2 (2)	-	5.9	-
	Significant height (m)	-	1.31; 2.95 (2)	-	1.31	-
Measurements	Relative motions at stations	0; 10; 14; 16; 18; 20	0; 10; 14; 16; 18; 20	0; 10; 14; 16; 17; 18; 19; 20	0; 10; 14; 16; 17; 18; 19; 20	0; 10; 14; 16; 17; 18; 19; 20
	Further measurements	sinkage; trim	heave; pitch; surge; thrust; wave 3.15 m before C.O.G.	-	wave 3.15 m before C.O.G.	-
Oscillations heave mode	Frequency range (rad./sec.)	-	-	-	-	0.74 - 1.27
	Amplitude (m)	-	-	-	-	0.6; 0.8; 1.0
Oscillations pitch mode (3)	Frequency range (rad./sec.)	-	-	-	-	0.74 - 1.27
	Amplitude (deg.)	-	-	-	-	2.3

Table 7.3-2: Particulars of the various test programmes.

Notes: (1) for $L/\lambda = 0.83$ only
(2) for $F_n = 0.40$ only
(3) for $F_n = 0.40$ only

the hull so that they were flush with the shell. For the free-running tests, as well as for the oscillation tests, it was necessary to also monitor the heave and pitch motion.

A general impression of the experimental setup during oscillation tests in calm water is given in photo 7.3-1.

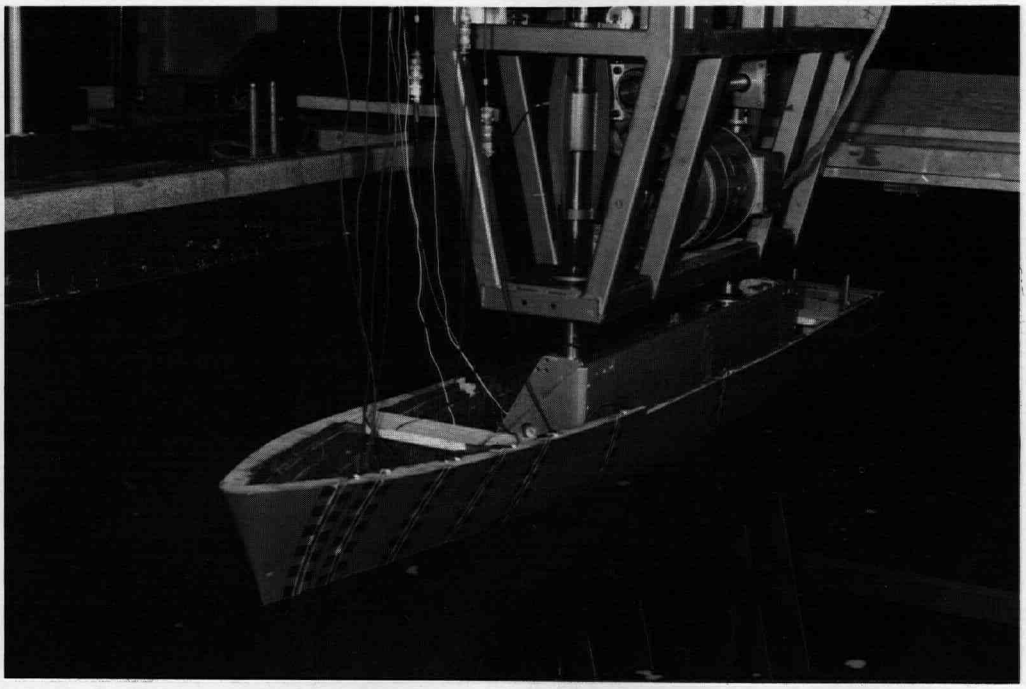

Photo 7.3-1: Model of compact frigate fitted to mechanical oscillator.

Swell-up

When a free-running model is tested in head waves the relative vertical motion between the water surface and the hull at the bow is found to be much more than can be accounted for on the basis of the vector summation of absolute motions heave, pitch and the incident wave amplitude. Clearly there is a magnification mechanism that causes the water to 'swell up' above, and below, what one would expect. This'swell-up' is caused by the very presence of the ship's hull that disturbs the incident wave, and it is customarily attributed to reflection and diffraction of the incoming waves as well as to the radiation of waves generated by the ship motions. A swell-up effect associated with the radiated

wave has been studied by Tasai (Ref. 7-14) , and by Vugts, (Ref. 7-15), yet their investigation dealt with zero ship speed potential effects solely.

It is shown in Ref. 7-1 that besides these well-known hydrodynamic effects there is more to it that has to be accounted for. This is defined as 'swell-up' and the reference was the first study to describe it thoroughly and to explain the origin.

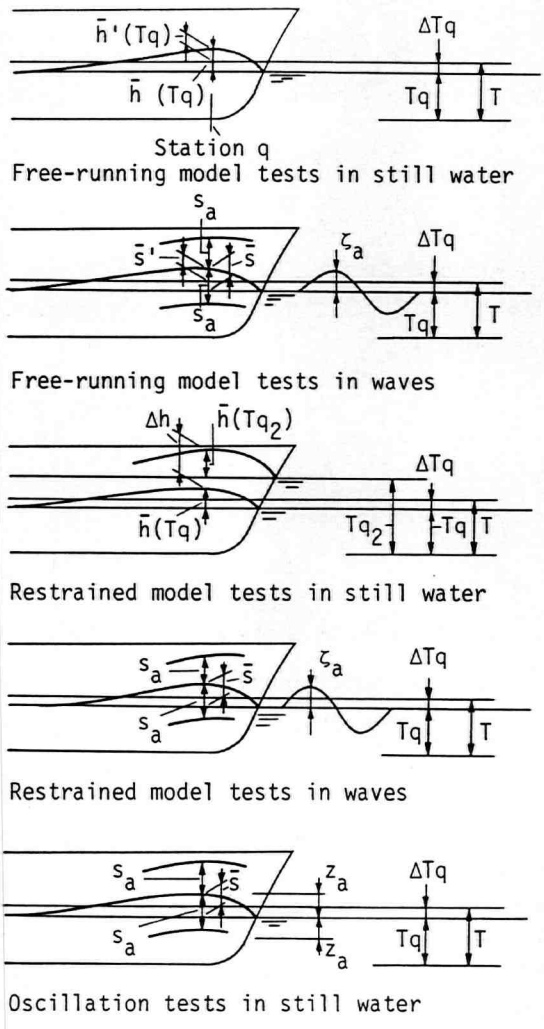

Figure 7.3-2: Bow wave and swellup quantities in various experiments.

In brief, the 'swell-up' is an effect brought about by the interaction of the stationary bow wave and the instationary local draught at the bow, which varies as a result of ship motions and incident waves.
The 'swell-up' effect is described in a formula as follows, see also Figure 7.3-2 :

$$S_a(T) = S_{0_a}(T)\left\{1 + \frac{h_a(Tq)}{S_{0_a}(T)}\right\} \qquad (7.3\text{-}1)$$

in which:

$S_a(T)$ = amplitude of relative motion
$S_{0a}(T)$ = amplitude of undisturbed relative motion
$h_a(Tq)$ = amplitude of steady bow wave variation
T = draught
Tq = local effective draught

The bracketed term is the 'swell-up coefficient' (SUC) and is usually in the order of 1.1 to 1.5 for the bow. If no swell-up occurs this factor reduces to unity since the disturbance function $h_a(Tq)$ vanishes.

Results

The first important finding was that, as the experimental results will show, the swell-up coefficient remains very nearly the same regardless of how the undisturbed relative motion has been brought about, either through heaving, pitching or incident waves, separately or combined, as Figure 7.3-3 shows, in particular for the longer waves. Consequently, the dependency of the swell-up on heave, pitch and incident undisturbed wave may be lumped onto a dependency on relative motion *per se* and the experiments show that the swell-up is to leading order a function of the relative motion. It was also found to be dependent upon forebody station and ship speed.

The second finding was that the 'swell-up' coefficient was remarkably independent of frequency as shown in Figure 7.3-3 and 7.3-4 . This led to a better understanding of the physicalities involved and can briefly be explained as follows. We consider the limiting case as the frequency goes to zero and the wave length becomes very long. We take equation 7.3-1 as a departure point and assume the ship to be running in calm water and assume a very small, nearly zero, frequency. When the ship is forcibly oscillated and as part of the downward cycle it is pushed down vertically, (and very slowly), such that the draught increases but the trim angle remains unaltered it can be seen that:

$$S_a(T) = \Delta Tq \left\{ 1 + \frac{\partial h_a(T)}{\partial T} \right\} \qquad (7.3\text{-}2)$$

in which:

$S_a(T)$ = relative motion amplitude as function of draught
ΔTg = increase in local effective draught
$h_a(T)$ = steady bow wave amplitude as a function of draught
T = draught

In words, at the greater draught the water swells up vertically over a distance equal to the difference in draught plus the difference in calm water bow wave height between the two draughts. Usually for the greater draught the bow has a blunter entrance angle and the bow wave is higher so that the bracket expression in equation 7.3-2 becomes larger than unity, hence:

$$SUC > 1$$

As the experimental results show, the bracketed swell-up coefficient expressed in equation 7.3-2 is very nearly equal to the one obtained from equation 7.3-1.

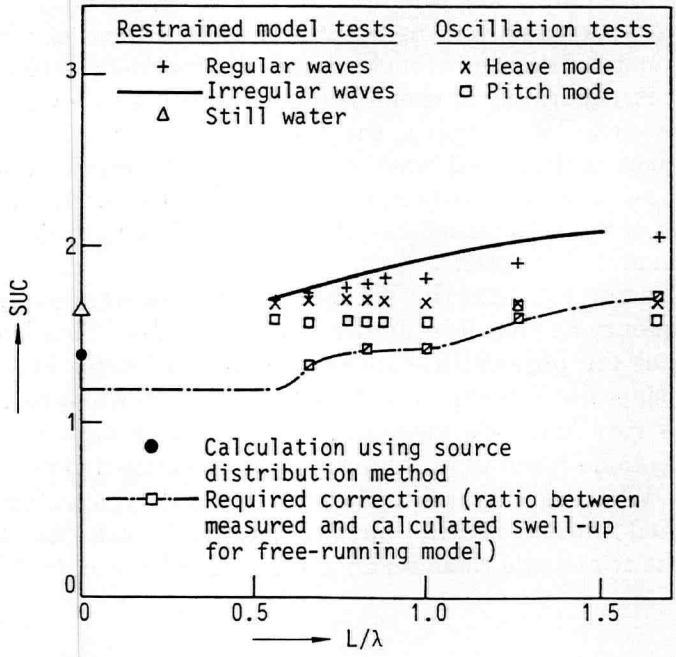

Figure 7.3-3: Comparison between swellup coefficients (SUC) at station 18 from various experiments (Fn = 0.40)

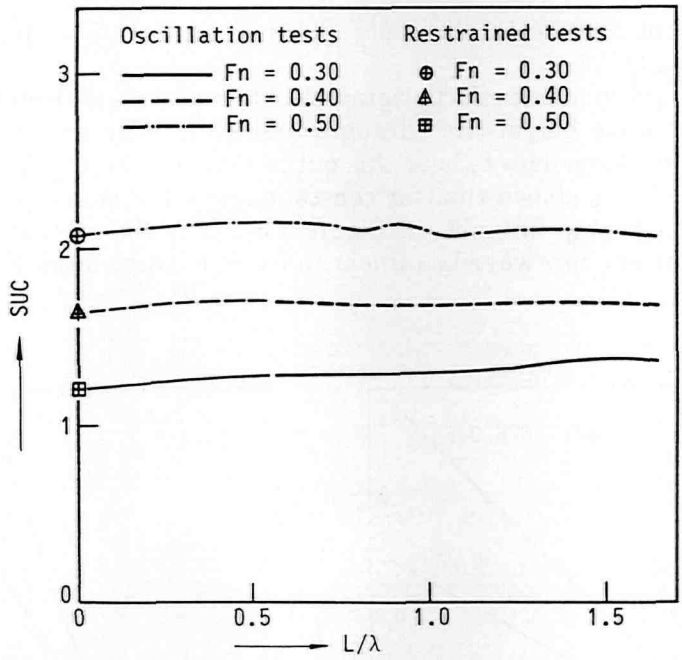

Figure 7.3-4: Swellup coefficient (SUC) at Station 18 based on oscillation tests in still water (heave mode) and restrained tests in still water.

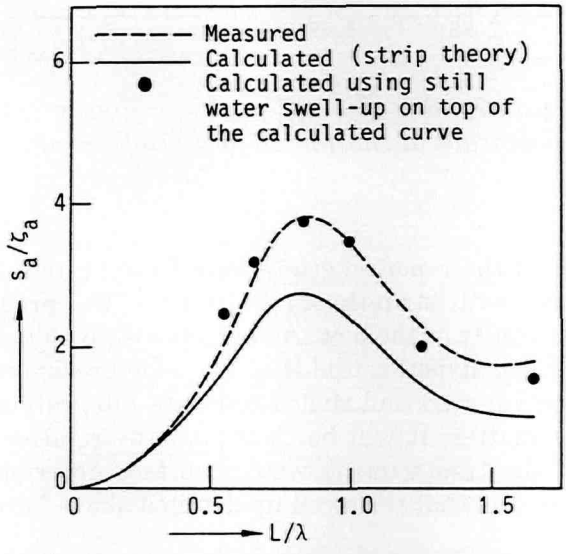

Figure 7.3-5: Correlation of measured and calculated relative motion at Station 18 for Fn = 0.40.

Some important experimental results drawn from Ref. (7-1) are depicted in Figures 7.3-3 and 7.3-4 .
The swell-up as a dynamic effect originates to a great extent from the variation of steady bow wave height with draught and eventually with instantaneous relative motion. Some data to bear this out is shown in Figure 7.3-6 and 7.3-7. In Figure 7.3-6 it is shown that for constant speed the steady bow wave is a linear function of ship draught, in Figure 7.3-7 it is shown that for constant draught the steady bow wave is a linear function of ship speed. For more data we refer to Ref. (7-1).

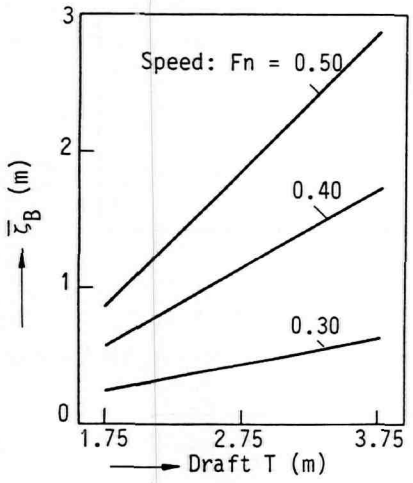

Figure 7.3-6

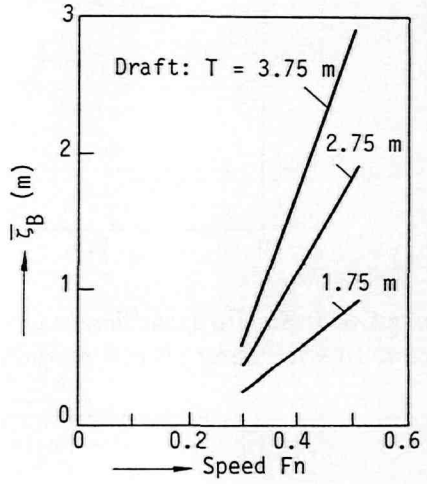

Figure 7.3-7

Stationary bow wave at Station 18 for various drafts and speeds.

Evaluation

The main findings of the reported study were forged into a tool that could be used in conjunction with strip-theory to improve the prediction of relative motion, most importantly at the bow. An example is given in Figure 7.3-5.

In Section 4.1 it was hypothesized that the added resistance was related to the relative motion squared and that a pressure integration approach would shed light on this matter. It will be clear that the relative motion plays an important role in the time-varying wetted surface description hence in the integration domain, and that the swell-up detailed above forms part of this.

7.4 A study on the influence of the bow

In this sub-section we shall briefly discuss the most important results of an experimental study carried out to investigate the forces on various parts of a model in waves. It was hypothesized in Section 4.1 that the mean wave added resistance in head waves is closely related to the relative motion at the bow. The present study was done to show that indeed the bow section makes the largest contribution to the mean wave added resistance.

Experiments on a wedge type bow model

The study formed part of the MARIN background research programme and a full description together with all results can be found in the MARIN report Ref. (7-8).

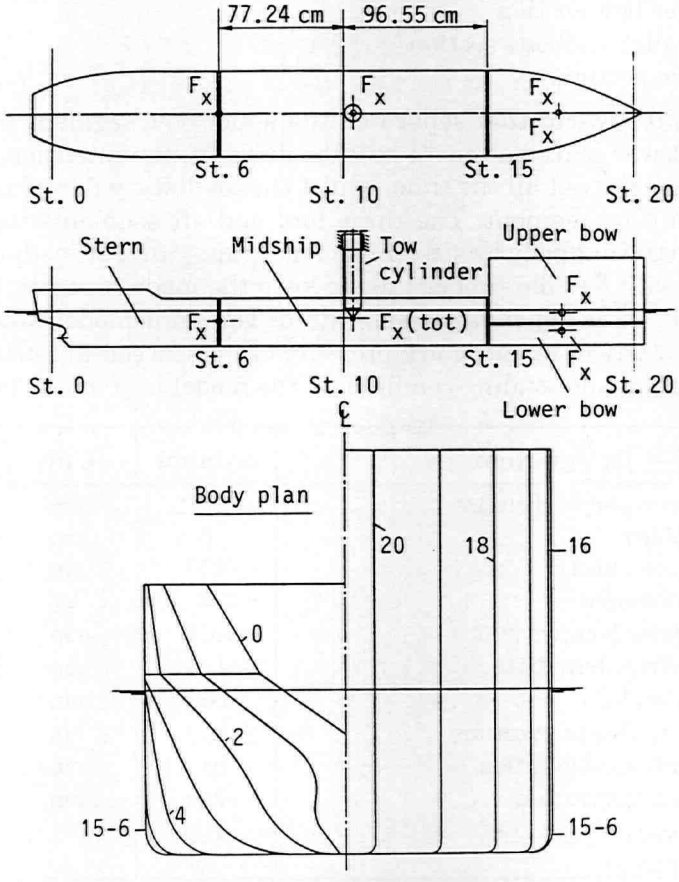

Figure 7.4-1: Bodyplan and segmentation of model with wedge type bow.

For the present test program a model was designed that would have normal lines in all respects, so it would demonstrate the preponderance of the bow over the stern without undue exaggeration. A set of lines was prepared that were reminiscent of a traditional cargo ship as shown in the bodyplan in Figure 7.4-1.

In the aftbody the sections were given an S-shape because interference from a transom stern was to be avoided. In the forebody the sections were U-shaped with vertical sides under water as well as above water. The bodyplan shows the absence of bow flare above the water. This was done to avoid breaking waves around the bow and the generation of spray that might have given anomalous readings on the forces and also interfered with visual observation. It had a parallel midbody segment that would not contribute to longitudinal forces,

The model was segmented into four different parts:

- an upper bow section
- a lower bow section
- a parallel midbody section
- a stern section

The horizontal saw-cut that separated the upper bow segment from the lower bow segment was placed at about half the draught, the intention being to keep the lower segment wet all the time, whilst the oscillatory flow would take place on the upper bow segment. The three fore and aft segments were connected separately to the midbody by six-component strain-gauge transducers. The gaps were sealed with flexible rubber tape to keep the model watertight. The model was bare hull, so no appendages were fitted. The same model would later on be used for the study of instationary pressures as discussed in Section 7.5.1. The main particulars and loading condition of the model is given in Table 7.4-1.

Designation	Symbol	Unit	Magnitude
Length between perpendiculars	LPP	cm	386.20
Breadth moulded	B	cm	58.60
Mean draft (even keel)	TM	cm	24.10
Displacement weight	W	kg	456.30
Centre of gravity forward st 0	LCG	cm	199.34
Centre of gravity above base	KG	cm	18.80
Metacentric height	GM	cm	4.56
Longitudinal radius of gyration	kyy	cm	94.60
Transverse radius of gyration	kxx	cm	20.70
Vertical radius of gyration	kzz	cm	95.20
Block coefficient	C_B	-	0.8365
Natural roll period	$T\phi$	s	2.02

Table 7.4-1: Particulars of wedge type bow model.

The model was tested in the Seakeeping Basin of MARIN following the general procedures as set forth in Section 7.1.2. It was towed by the air-lubricated tow cylinder to obtain a constant speed, the tow force being measured. In addition to the forces on the segments ship motions and relative motion at the forebody were also recorded.

The model was tested in regular waves spanning a range of $\lambda/L = 0.40$ to 1.50, which is sufficiently wide to include the short and long wave regime. All tests were done in waves from ahead. The wave heights used ranged from 1 to 3 percent of the model length. Most tests were done at a speed corresponding to Fn.= 0.20, some tests were done at Fn.= 0.10.

A selection of test results, drawn from the referenced report, Ref. 7-8, is shown in Figure 7.4-2 and 7.4-3.

The decomposition of the total mean wave added resistance force over the four segments of the model is shown in Figure 7.4-2. The mean longitudinal forces on the separate segments are seen to bear a quadratic relationship to the relative motion at the forebody. It is also clearly shown that the upper bow segment, which becomes alternatingly wet and dry, contributes most to the mean force.

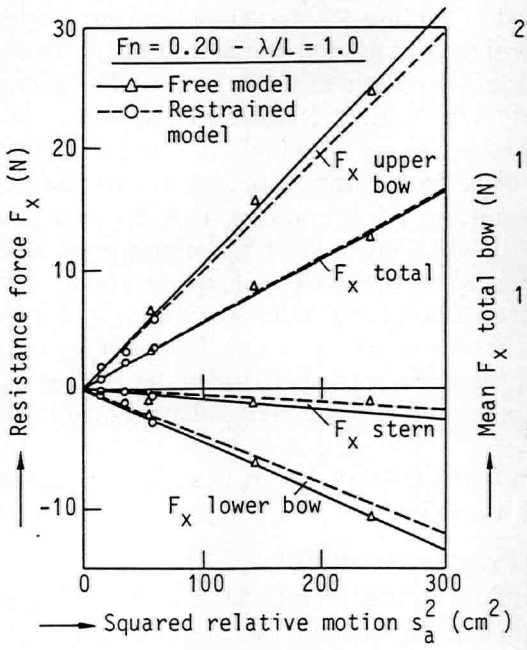

Figure 7.4-2

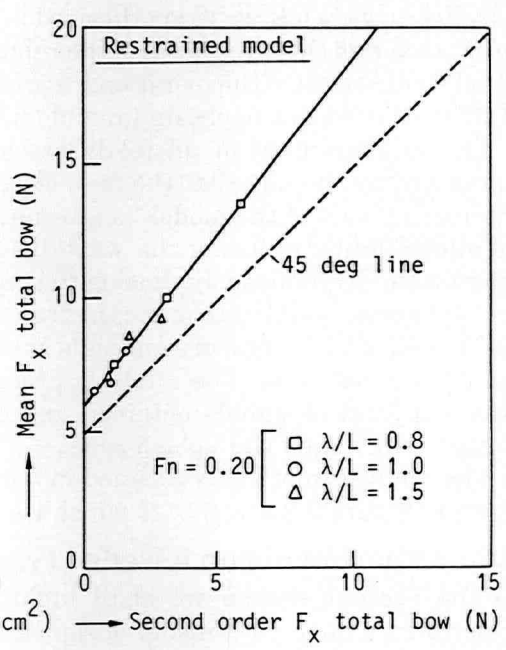

Figure 7.4-3

Comparison of longitudinal forces on segments and total bow forces from different experiments.

It is remarkable to see that the lower bow segment that remained wet all the time has a negative contribution so it tends to reduce the wave added resistance. Later in Section 7.5.1 we shall come across some pressure data that supports this result. As expected the stern contributes very little because it has only a very small relative motion amplitude itself. The good correspondence between results obtained on a free model and on a restrained model are further proof of the hypothesis of Section 4.1.

Further support for this view is given in Figure 7.4-3 where we show that for the longitudinal bow force the mean value bears an almost one to one relation to the second order force. This should indeed be the case if both originate from the same first order relative motion. It was also found that the second order relative motion was only very small so that it cannot have played a part in this respect.

7.5 A study on instationary pressure distribution

In this sub-section we shall briefly discuss the major aspects of two experimental studies that were done to investigate the instationary pressures on the bow of a model in waves. It was hypothesized in Section 4.1 that the mean wave added resistance was closely related to the relative motion at the bow, which is in turn a visible exponent of the instationary pressure field around the bow. The present studies were meant to obtain tangible information to substantiate this view.

The measurement of unsteady pressures on a model in a wave basin is hampered by the fact that the area close to the water surface -for us the most interesting part of the model- is alternatingly wet and dry. This drawback can be alleviated by reducing the wave height, but only at the expense of signal magnitude. By judiciously chosing the type of pressure transducer and by using an appropriate coating to make the transducers insensitive to the wet/dry effect and to related temperature and light intensity changes a useful set of measurements was obtained. The analysis procedure was specifically devised to cope with the kind of signals obtained and could produce spatial pressure curves consistent through the 'splash zone'.

The analysis method is outlined in Section 6 together with some explanatory figures (Figure 6-2 and 6-3) to which we refer.

7.5.1 Experiments on a wedge type bow model

In the present section we shall highlight the results of a series of model experiments done on a model designed to be suitable for the measurement of unsteady bow pressures. The study formed part of the MARIN background research programme and a full description together with all results can be found in the MARIN report Ref. (7-9).

The model was specifically designed for this purpose; it was the same model as used for the study on segment forces discussed herefore in section 7.4,

although for the present pressure measurements a new bow had to be built to accommodate all the pressure transducers. The model had a vertical wedge type bow to allow the fitting of a large array of transducers. This form of bow was chosen to avoid as much as possible bowflare spray that could mess up the pressure measurements and interfere with visual observations. The bodyplan and the instruments are shown in Figure 7.5.1-1 The main particulars and loading condition of the model is given in Table 7.4-1. The model was bare hull, so no appendages were fitted.

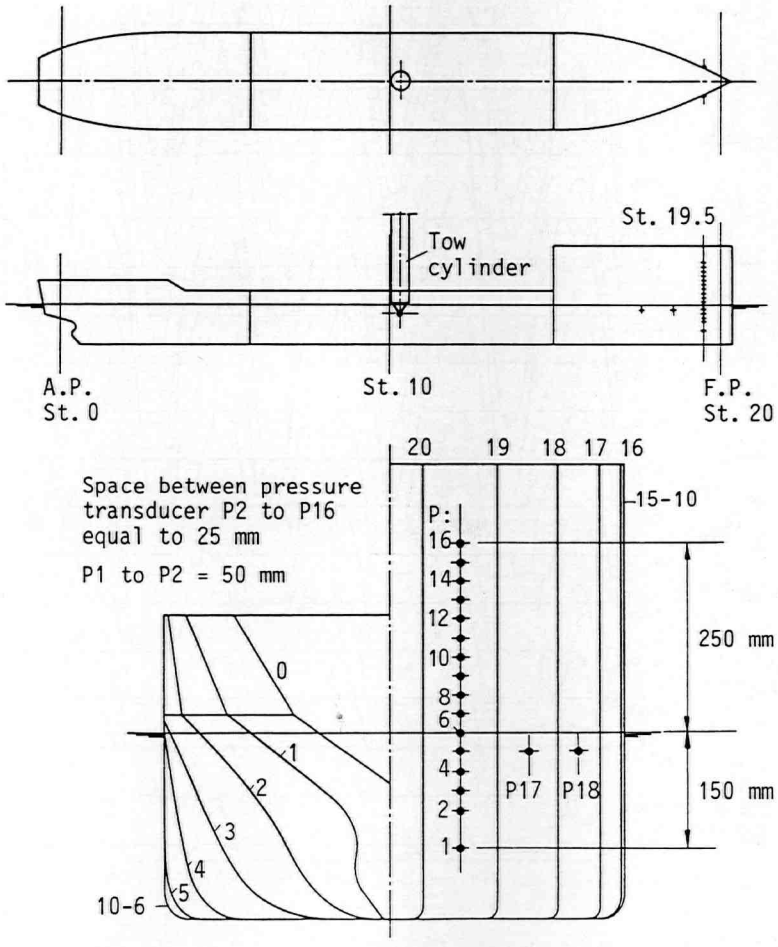

Figure 7.5.1-1: Bodyplan and pressure transducer layout of model with wedge type bow.

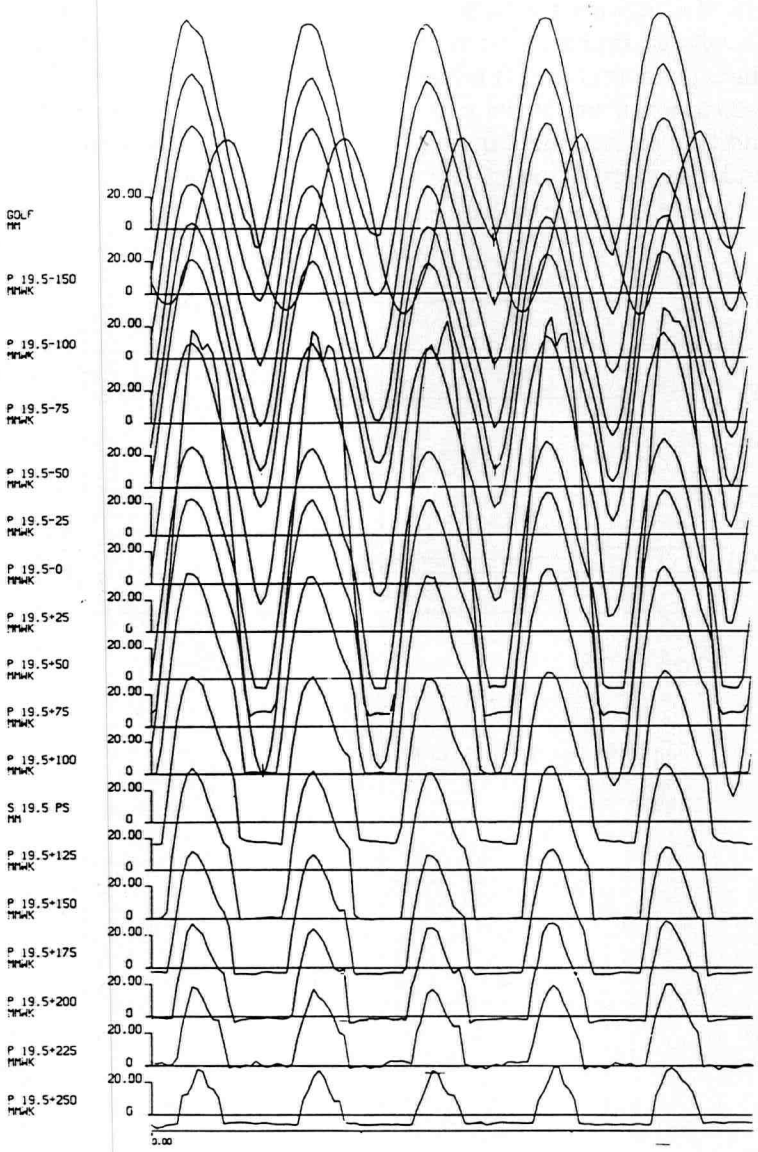

Figure 7.5.1-2: Example of time history records of pressures (head waves; $\lambda/L = 1.0$; $Fn = 0.30$).

The model was tested in the Seakeeping Basin of MARIN following the general procedures as set forth in Section 7.1.2. It was towed by the air-lubricated tow cylinder to obtain a constant speed, the tow force being measured. In addition ship motions and relative motion at the forebody were also recorded.

The model was tested in regular waves spanning a range of $\lambda/L = 0.40$ to 1.50, which is sufficiently wide to include the short and long wave regime. All tests were done in waves from ahead. A series of wave heights was used ranging from 0.5 to 2 percent of the model length. As to the speeds two speeds were used, corresponding to Fn. = 0.20 and 0.30.

A selection of test results, drawn from the referenced report, is shown in Figure 7.5.1-2 to 7.5.1-6.

A sample of the time traces of the pressure signals is shown in Figure 7.5.1-2.

The amplitudes of the pressure variations are shown in Figure 7.5.1-3 for the case of Fn. = 0.20 and a short wave length ratio of 0.40. Both the free model case and the restrained model case are shown in the figure which could be accomplished by cross- plotting the data and normalizing on a common basis of similar wave height or undisturbed relative motion. In the pressure lines the hydrostatic

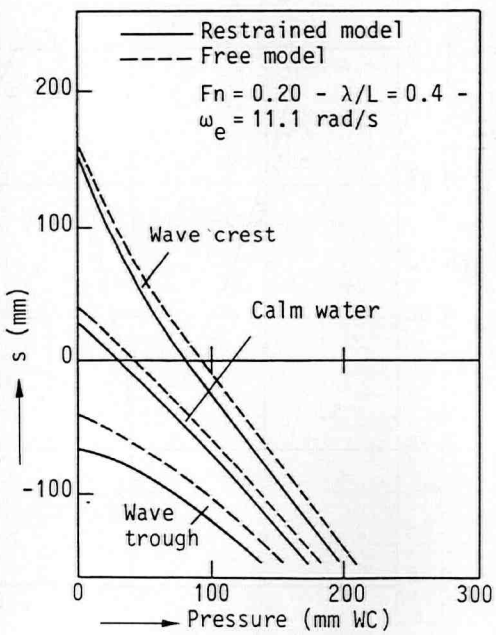

Figure 7.5.1-3

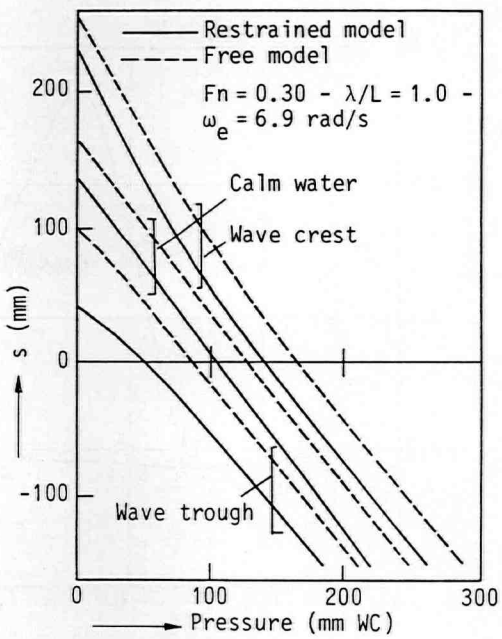

Figure 7.5.1-4

Comparison of pressure amplitude distribution for free and restrained tests in waves. (Pressure curve, bodyfixed type b, see Section 6.3 and 6.4).

pressure, zeroed out in the model test, has been added to make the lines continuous through the z=0 undisturbed watersurface.

It can be read from the pressure lines that as the water goes up and down along the bow the pressure variation on the underwater bow is much less than would be suggested by the relative motion visible at the watersurface. In fact, as the water rises with respect to the bow some body-fixed point underwater feels the hydrostatic pressure rise, but in addition that point moves into water that flows at a higher velocity with an associated pressure drop. The combined effect is that the pressure variations underwater are less than the relative motion amplitudes at the surface. It should be stressed that this is not the result of dynamic wave pressures reducing with depth since we see the same thing happening in longer waves as shown in Figure 7.5.1-4 for the case of the higher speed Fn. = 0.30 and a longer wave λ/L = 1.00. So it is entirely due to the gradients in the steady bow wave flow.

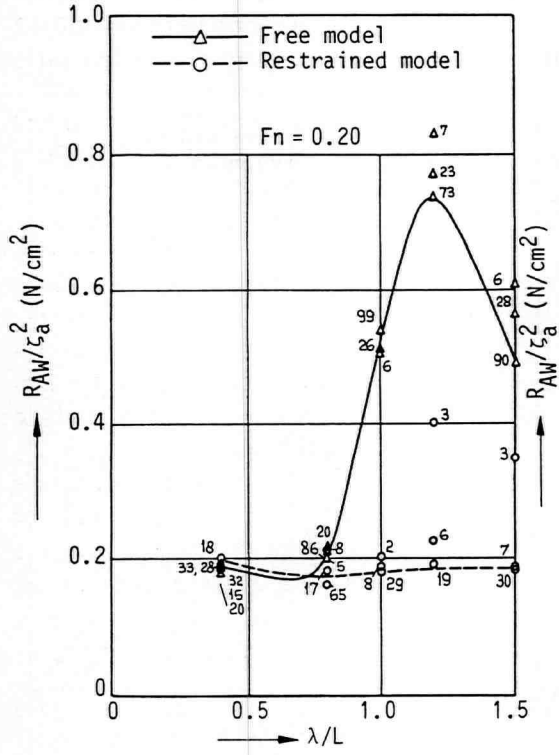

Figure 7.5.1-5

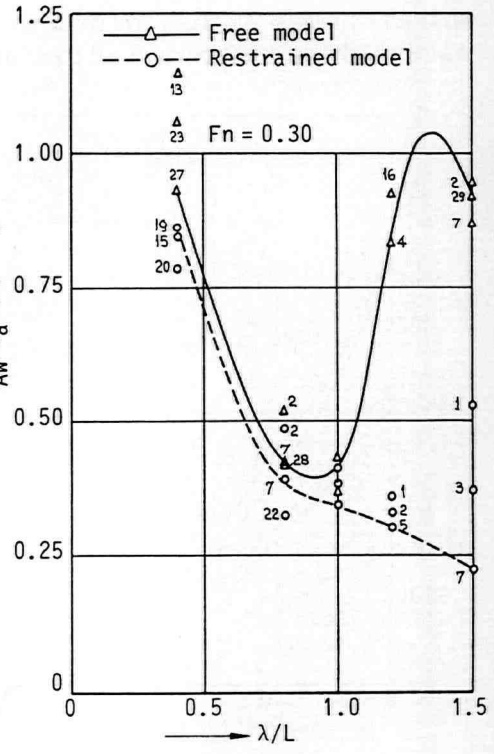

Figure 7.5.1-6

Transfer function of resistance increase on free and restrained model in waves.

The difference between the free model case and the restrained model case in Figure 7.5.1-3 is due to the trim down by the head that the free model experiences when making headway. It appears to be a constant shift.

In Figure 7.5.1-5 the added resistance transfer function is given both for the free model and for the restrained model for the lower speed of Fn. = 0.20.
It is interesting to note that the restrained model lacks the hump associated with pitching and resultant large relative motions. This supports the hypothesis that the added resistance depends on relative motion. The small print figures inscribed in the figure indicate the added resistance as a percentage of the calm water resistance. It is clear from the numbers that in particular for the larger wave heights the added resistance was sufficiently large to be established with a sufficient degree of accuracy.

The added resistance for the higher speed Fn. = 0.30 is given in Figure 7.5.1-6. When the speed is increased to Fn. = 0.30 the added resistance in short waves is seen to increase steeply. When we consult the results we find that this is not so much due to changes to the pressures underwater as well as to the much increased dynamic relative motion amplitudes.

Another aspect worth to note is that the mean value of the pressure as can be established from the analysis of the amplitudes seems to lie consistently lower than the mean pressure obtained in calm water. This ties in with the finding from the segmented model in Section 7.4 that the lower part of the bow experiences a mean force in waves which is less than the mean force in calm water, so relatively speaking the lower bow is sucked forward in waves. This is in line with the result that the bow trims down at speed so there must be a field of reduced mean pressure around the bow in waves as compared to calm water.

It should also be concluded that a linearization scheme to extrapolate the pressure from below the undisturbed waterplane into the actual fluid domain above has to take the relative motion into account because the latter is a major determinant for the flow pattern and the pressure distribution.

The data has been established on basis of cross-plotting the results of experiments for various wave amplitudes and normalizing the input in terms of constant wave amplitude or relative motion. The correspondence of the pressure line results for experiments done on a free model and on a restrained model in particular for waves at $\lambda/L = 1$ is a striking support for the 'relative motion hypothesis', which forms one of the building blocks of seakeeping theory.

7.5.2 Experiments on two WIGLEY form models

In the present section we shall discuss the main results of a series of model experiments done on two WIGLEY form models. The experiments were carried out by the Ship Hydromechanics Laboratory of the Delft University of Technology to investigate the global hydrodynamic properties -added mass, damping and wave forces- of the two hulls. In the context of the present thesis study the

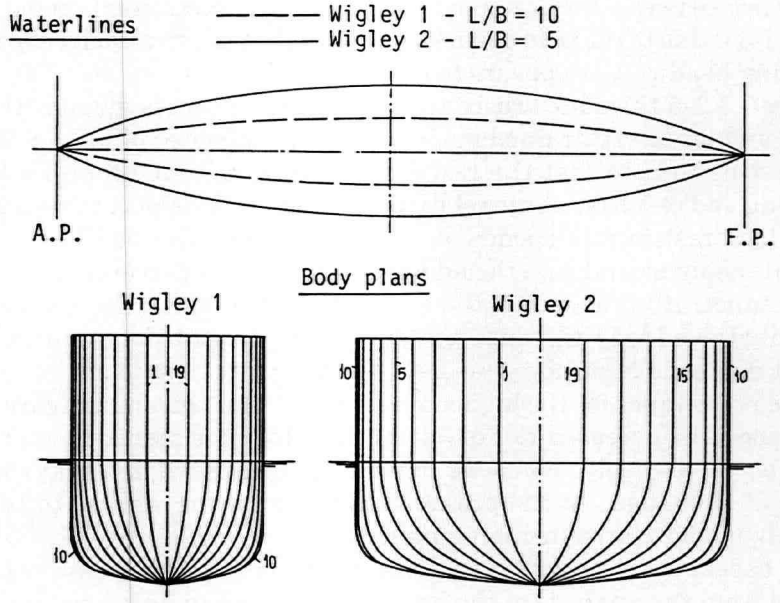

Figure 7.5.2-1: Waterlines and bodyplans of Wigley models.

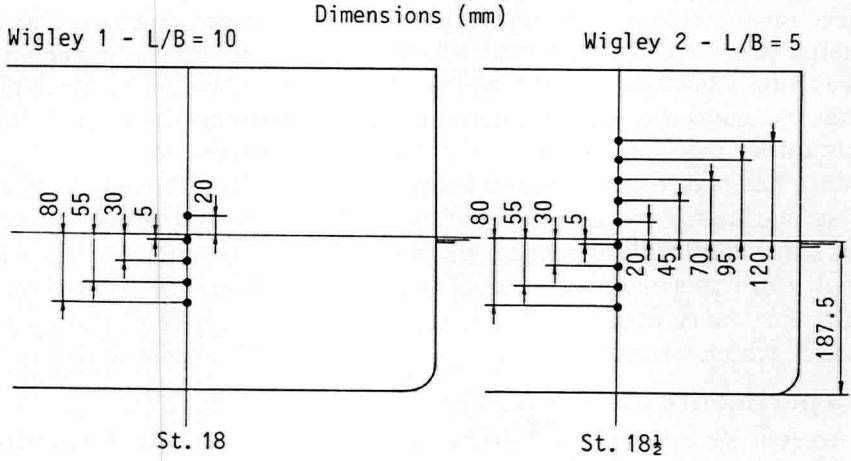

Figure 7.5.2-2: Layout of pressure transducers on the bows of the Wigley models.

opportunity was offered to cooperate and to investigate the added resistance and the dynamic pressures on the bow in the same test set-up. A full description together with all results can be found in the MARIN reports Ref. 7-6 and 7-7.

The two WIGLEY models were close relatives, one having an L/B = 10 the other model being twice as wide, having L/B = 5. The body- plans are shown in Figure 7.5.2-1. The models had a vertical wedge type bow that allowed the fitting of an vertical array of pressure transducers which are indicated in Figure 7.5.2-2. The WIGLEY 1 model had 5 transducers at station 18, the WIGLEY 2 model had 9 transducers at station 18½. This form of bow does not easily generate a breaking bow wave and spray so it allowed good visual observations to be made. The model was bare hull, no appendages were fitted. The main particulars and loading condition of the models are given in Table 7.5.2-1.

Hull particulars (Model values)	**Wigley 1 (L/B = 10)**	**Wigley 2 (L/B = 5)**
Length	3.00 m	3.00 m
Breadth	0.30 m	0.60 m
Draught	0.1875 m	0.1875 m
Displacement	94.7 dm^3	189.24 kg
Length/breadth	10	5
Length/draught	16	16
Block coefficient	0.561	0.561
Waterplane coefficient	0.693	0.693
Midship section coefficient	0.909	0.909

Table 7.5.2-1: Particulars of Wigley models.

The models were tested in the wave basin of the TU-Delft generally following similar procedures as set forth in Section 7.1.2 for the tests in the MARIN basins.

The experiments included oscillation tests in calm water in the heave and in the pitch mode, restrained model tests in regular head waves and finally experiments in regular head waves, the model being free to heave and pitch. For the TU-Delft investigation the model was outfitted with strain-gauge transducers in the oscillator struts to measure global hydrodynamic reaction forces and wave exciting forces, potentiometers to measure heaving and pitching motion and a wire type wave probe to measure wave elevation in front of the model. For the study into wave added resistance the model was also equipped with a wire type wave probe fitted to the side of the bow to measure relative

motion and an array of pressure transducers on the bow to measure the fluctuating hydrodynamic pressure on the bow as affected by forward ship speed, ship motions and incident waves.

The oscillator setup, while meant to obtain global hydrodynamic characteristics by oscillation tests in calm water and restrained tests in waves, was also ideally suited to investigate the local pressure distribution. Tests were done for various draughts and trim angles in a fixed position as well as at a number of oscillation frequencies and amplitudes.

The models were tested in regular waves spanning a wide range of $\lambda/L = 0.50$ to 2.00, which is sufficiently wide to include the short and long wave regime. All tests were done in waves from ahead. The wave heights used were about 1 percent of the model length. The speeds used were Fn. = 0.20, 0.30, 0.40 for the L/B = 10 model and Fn. = 0.20 for the L/B = 5 model. Oscillation frequencies ranged from 3 to 12 rad/sec. for a number of amplitudes.

A selection of test results, drawn from the referenced report, is shown in Figure 7.5.2-3 to 7.5.2-7 for the WIGLEY 1 model of L/B = 10. Most results shown apply to a speed of Fn. = 0.40. For realistic ships this may be rather high, yet it allowed us to clearly observe the various flow aspects through visual and electronic recording.

The effect of draught and speed on static bow wave height in calm water and level trim is shown in Figure 7.5.2-3. It is shown that for speeds in excess of Fn. = 0.20 the bow wave height increases linearly with the draught. The resulting

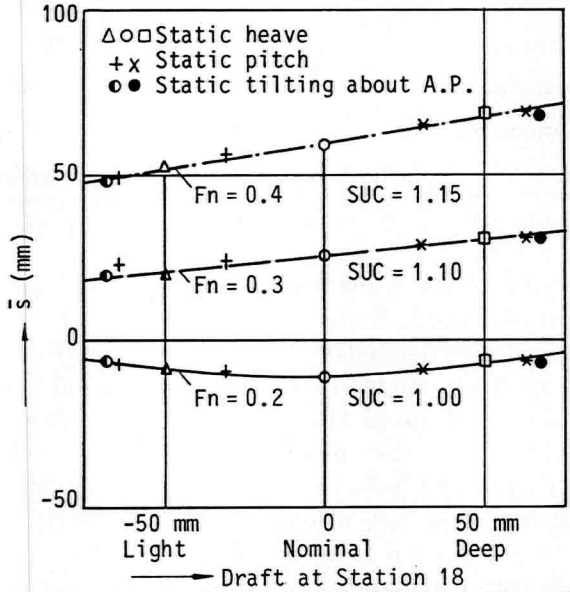

Figure 7.5.2-3: Stationary bow wave height as a function of draft and speed in calm water (Wigley 1).

swell-up coefficient (SUC) that can be obtained from the plot is only 1.1 to 1.15 due to the very fine bow form without any flare at higher elevations. It is also shown in the figure that for the bow wave crest at station 18 it does not make any difference whether the draught variation is effected through static heaving, pitching or rotation about a point at the aft perpendicular (APP), provided the absolute vertical motion at that station 18 is the same.

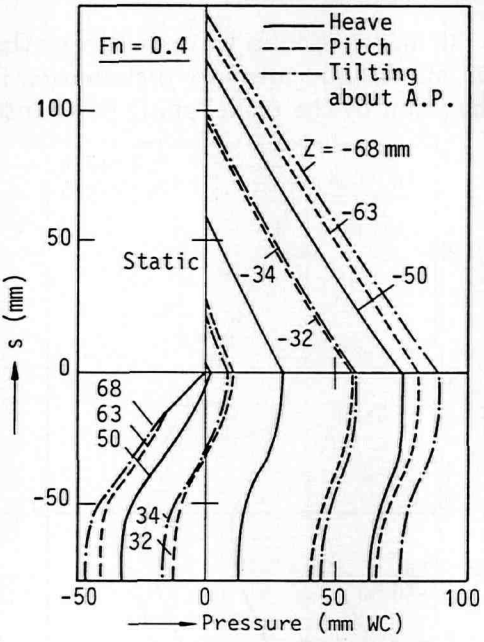

Figure 7.5.2-4

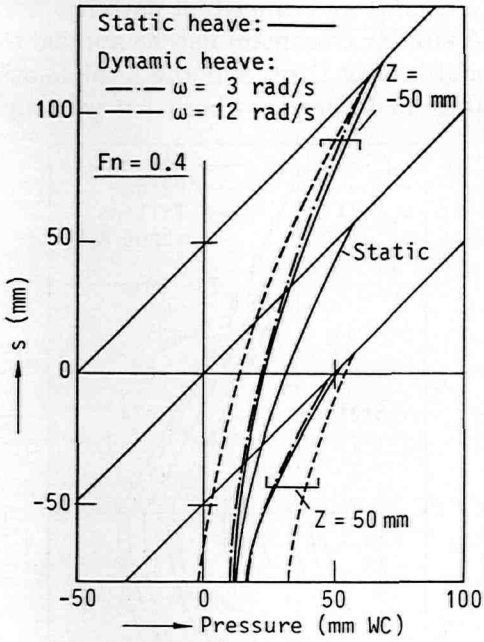

Figure 7.5.2-5

Comparison of pressure amplitude distributions from static and dynamic experiments for Wigley 1 (pressure curve, body fixed type a and d, see Section 6.3 and 6.4).

The local equivalence of static heave, pitch or tilting about the APP is not only found for the bow wave height but also for the vertical pressure distribution under the bow wave crest. In Figure 7.5.2-4 we show a type-a body-fixed diagram and we note that the pressure variation in the bow wave crest and deeper underwater down to about half the draught does not depend on the mode of motion. The absolute vertical motions are inscribed in the figure.

The pressure distribution along a vertical array of points for dynamic oscillation has a good deal in common with the static case, as Figure 7.5.2-5 shows. This is a type-d body-fixed diagram, in which the hydrostatic pressure variation and the velocity induced pressure variation are separated. For low frequency the pressure distribution very nearly coincides with the static case. For higher

frequency the curves are seen to depart from the static case in the sense that the variation in hydrostatic pressure is reduced by the dynamic component.

The local equivalence of static heave, pitch and tilting was also shown to exist for the dynamic case. In Figure 7.5.2-6 we show the results of dynamic oscillation tests for the three modes and for different amplitudes in a type-a body-fixed diagram. Even for the very high oscillation frequency of 12 rad/s. the curves fall in a similar and consistent pattern.

A similar treatment can be applied to the model tests in waves whereby the model is kept fixed. For the local relative motion and pressure distribution it makes no difference whether it is brought about by the model going down into

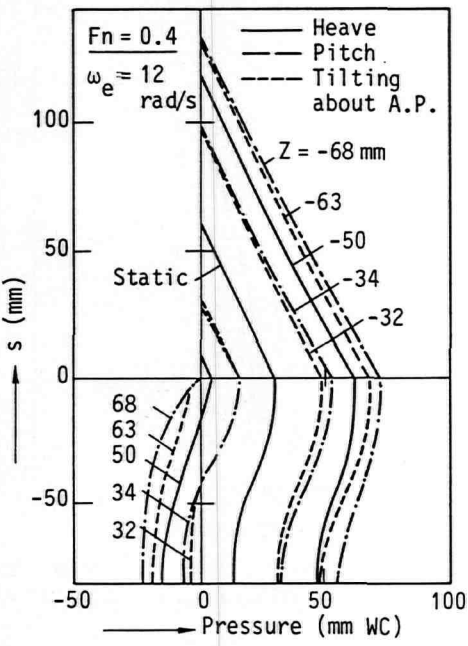

Figure 7.5.2-6

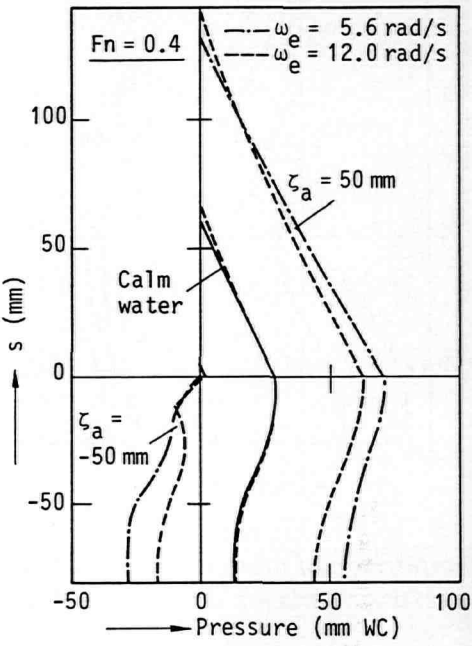

Figure 7.5.2-7

Comparison of pressure amplitude distribution for static and dynamic tests in calm water and in waves (Wigley 1, Fn = 0.40) (Pressure curve, body fixed type a, see Section 6.3 and 6.4).

the water or the incident wave crest going up. This equivalence, which was shown before for the relative motion in Section 7.3, was also shown to exist for the vertical pressure distribution. In Figure 7.5.2-7 we shown the results of restrained model tests in waves for two frequency cases and if we compare it to Figure 7.5.2-6 we note the strong similarity.

From Figures 7.5.2-7 and 7.5.2-6 we can also read the proof of the 'relative motion hypothesis' which plays such a dominant role in the theory of seakeeping.

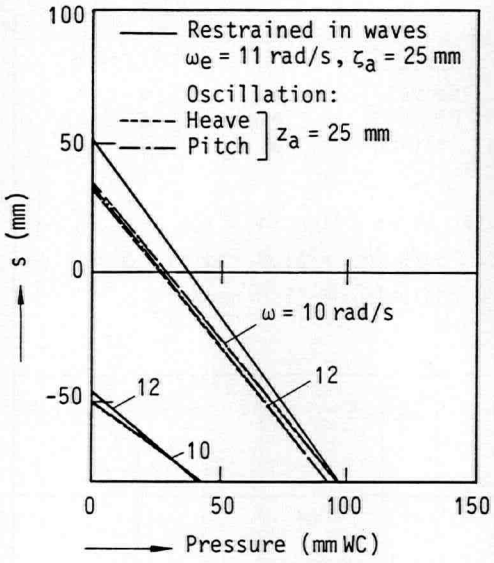

Figure 7.5.2-8

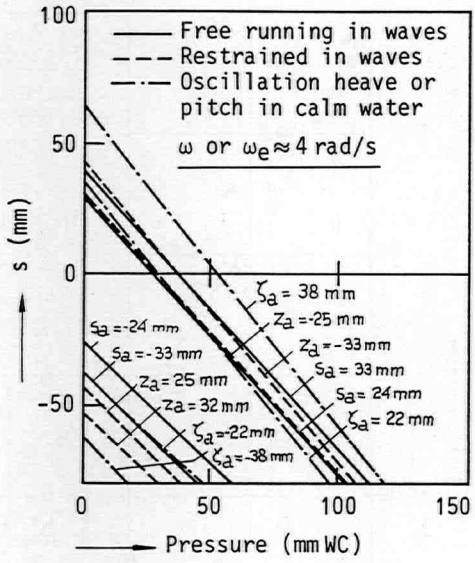

Figure 7.5.2-9

Comparison of pressure amplitude distribution from various dynamic experiments in calm water and in waves (Wigley 2, Fn = 0.20) (pressure curve, body fixed type b, see Section 6.3 and 6.4).

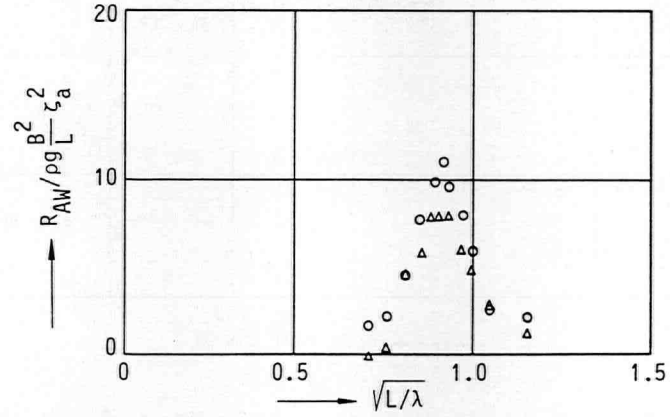

Figure 7.5.2-10: Transfer function of added resistance for Wigley 2 (head waves, Fn = 0.20).

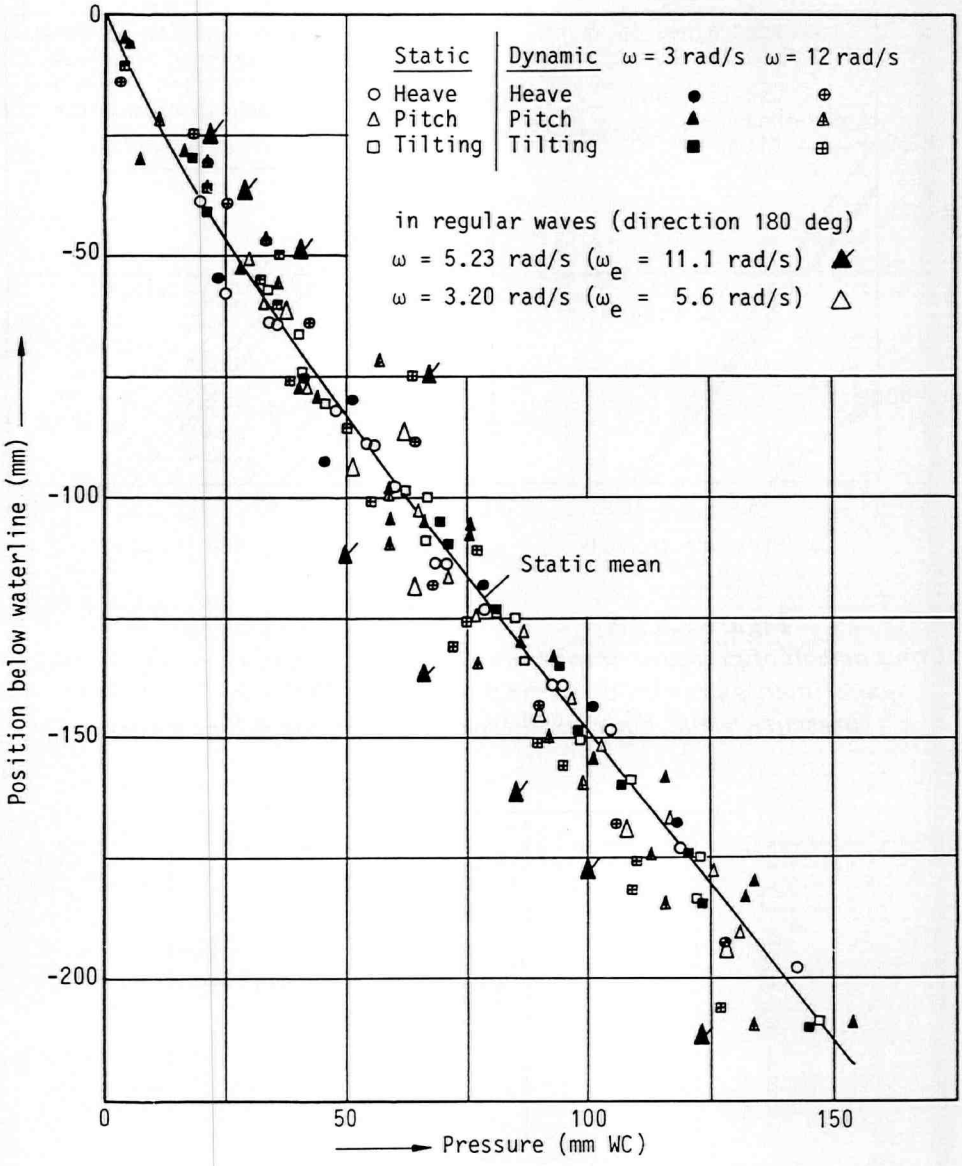

Figure 7.5.2-11: Comparison of pressure amplitude distributions from various experiments related to a system of axes in the free surface (Wigley 1, Fn = 0.40).

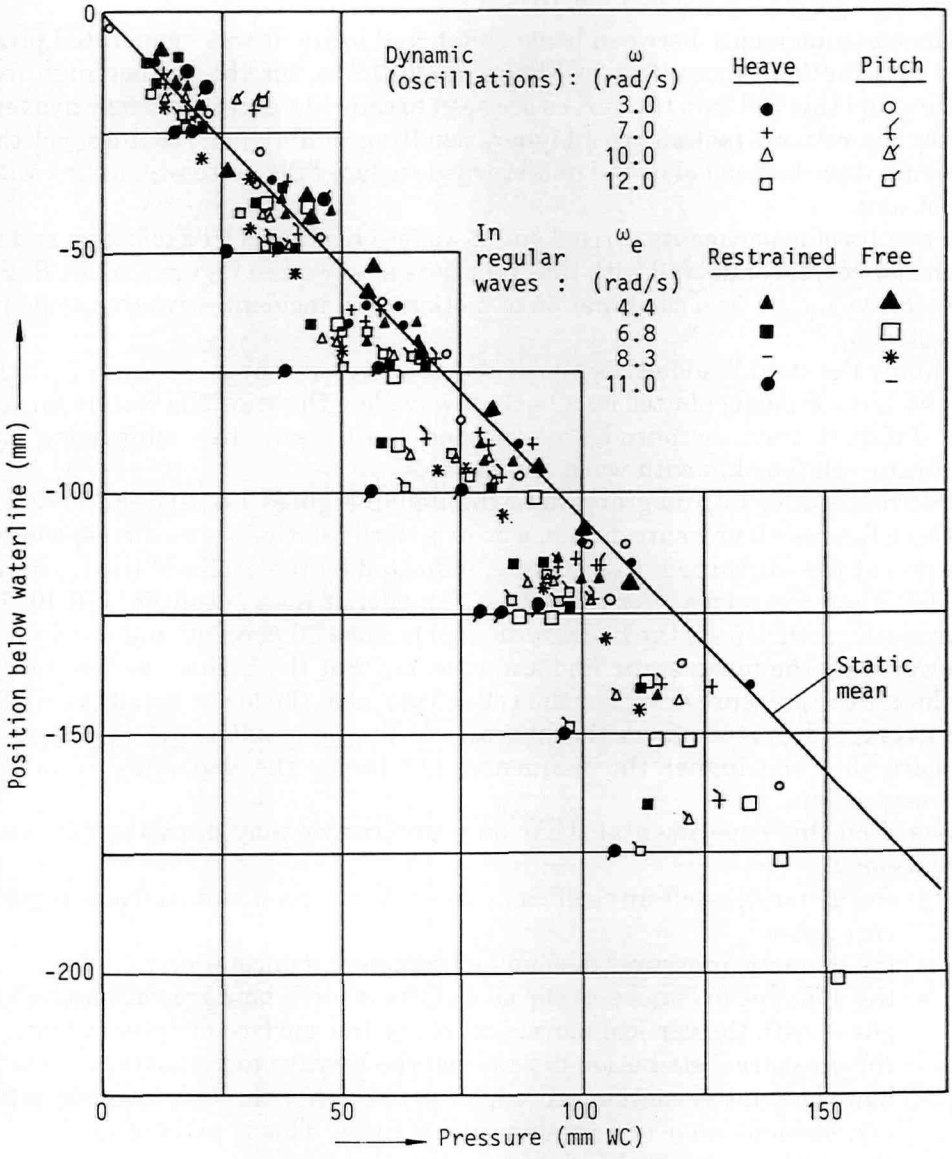

Figure 7.5.2-12: Comparison of pressure amplitude distributions from various experiments related to a system of axes in the free surface (Wigley 2, Fn = 0.20).

Some results for the WIGLEY 2, drawn from the referenced report, Ref. 7-7 , are shown in Figures 7.5.2-8 to 7.5.2-10.

The correspondence between heave, pitch and incident wave generated pressure distribution is manifest in Figure 7.5.2-8. Also for this rather high frequency and this full ship the curves are seen to coincide, except for the wave test where the relative motion rises higher, resulting in a higher swell-up, yet the pressure distribution below the undisturbed surface falls quite well in line with the others.

The results of experiments carried out in waves on a model free to heave and to pitch also corresponds well with the other data as shown in Figure 7.5.2-9. Since the relative motion is a combination of motions and incident wave this could be expected.

Finally the overall added resistance due to waves is shown in Figure 7.5.2-10 for the L/B = 5 model plotted on a basis of wave length ratio. The results for the two different wave amplitudes correspond quite well, thus supporting the quadratic relationship with wave amplitude.

Two most intriguing diagrams are exhibited in Figures 7.5.2-11 and 7.5.2-12. In these figures all pressure data has been plotted relative to the corresponding position of the -disturbed- free surface, indicated by the origin of the figure in the left hand top corner. For the L/B = 10 model at high speed Fn. = 0.40 the average departure from the hydrostatic line is some 30 percent, and the data is strewn along the mean static line and it seems that the higher the frequency, the larger the pressure drop. For the L/B = 5 model at the lower speed Fn. = 0.20 the average departure from the hydrostatic line is smaller, yet also here it appears that the higher the frequency, the larger the departure from the hydrostatic line.

Based on this experimental study on pressures we may draw the following conclusions:

- the dynamic swell-up coefficient depends on speed and on frequency of encounter.
- the dynamic pressures depend on frequency of encounter
- the dynamic pressures at the side of the model's bow are very much in phase with the vertical movement of the free surface directly over it.
- the pressure distribution depends on the relative motion irrespective of how the relative motion is brought about, either through heaving, pitching, incident wave or a combination of these. This is proof of the 'relative motion hypothesis' of ship motion theory.
- If a linearization scheme is to be devised to extrapolate the velocity field from the domain under the undisturbed z=0 plane to the actual free surface, it is necessary to use a double scheme, i.e. to linearize with respect to the field coordinate and also in addition to the undisturbed relative motion.

7.6 A study on the effect of main particulars

7.6.1 Experiments on the model of a cargo ship

In the present section we will briefly relate the outlines and some results of a series of model experiments in which the behaviour of the ship in short waves was studied. The attention was focussed in particular on the importance of main particulars on added resistance in short waves. The study was part of a multi-year research program to the order of the NSMB Cooperative Research on Ships (CRS). Since big ships often operate in relatively moderate seaways, with an average wave length shorter than the ship length, the main particulars are important.

For this series of experiments three models were designed and built. For the sub-series related here the model was segmented and could alternatively be fitted with two midbody sections or without any, as shown in Figure 7.6.1-1, so as to obtain three model lengths while keeping the bow and stern the same.

The model particulars are given in Table 7.6.1-1 and the body plan is shown in Figure 7.6.1-2.

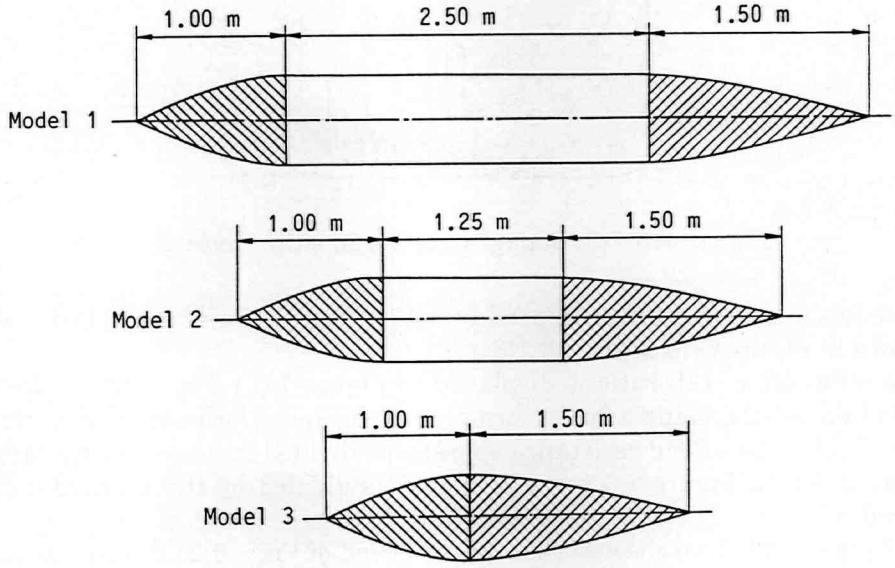

Figure 7.6.1-1: General layout of cargo ship models 1, 2 and 3.

Designation	Symbol	Unit	Model 1	Model 2	Model 3
Length between perpendiculars	Lpp	cm	500.0	375.0	250.0
Depth	D	cm	50.0	50.0	50.0
Breadth moulded	B	cm	62.5	62.5	62.5
Mean draft (Even keel)	T	cm	17.9	17.9	17.9
Displacement weight	W	n	4.149	2.794	1.439
Centre of gravity aft st 10	LCG	cm	13.1	12.7	12.7
Centre of gravity above base	KG	cm	21.0	21.0	21.0
Metacentric height	GM	cm	5.7	5.4	4.5
Longitudinal radius of gyration	Kyy	cm	120.0	90.0	60.0
Natural pitch period	TΘ	s	1.14	1.10	1.10

Table 7.6.1-1: Main particulars of cargo ship models 1, 2 and 3.

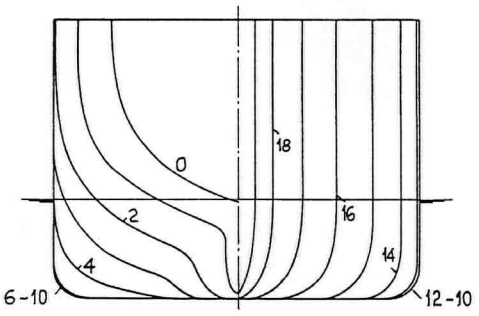

Figure 7.6.1-2: Bodyplan of cargo ship model 2.

The models were bare hull, no appendages were fitted. A selection of test results is shown in Figures 7.6.1-3 to 7.6.1-6.

The influence of L/B ratio is displayed in Figure 7.6.1-3 and 7.6.1-4 for the speed of Fn. = 0.21, being a fairly normal cruising speed for many ship types. In Figure 7.6.1-3 the added resistance operator is divided on basis of wave amplitude squared, in Figure 7.6.1-4 it is shown as divided by the relative motion squared.

In Figure 7.6.1-3 we observe that for the speed of Fn. = 0.21 the curves settle on a constant level in the intermediate wave length region around a wave length ratio of 0.5. The results of model 2 and 3 appear to coincide in this region, while model 1 lies higher.

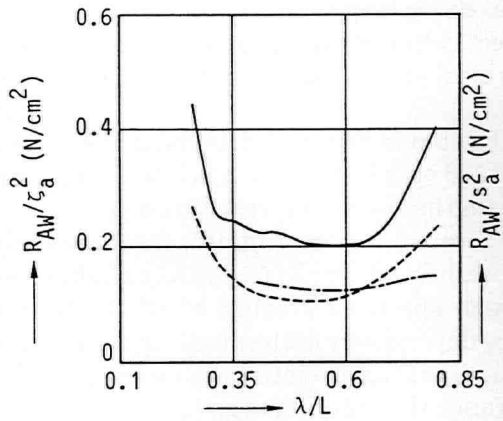

Figure 7.6.1-3

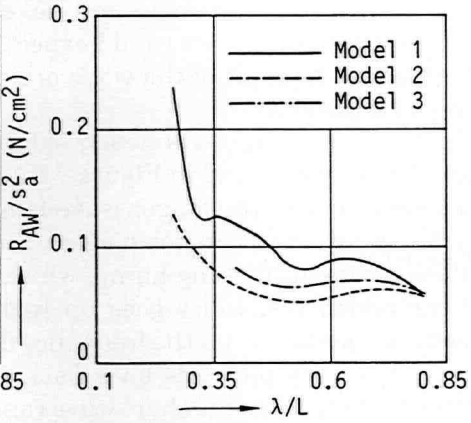

Figure 7.6.1-4

Transfer functions of added resistance based on wave amplitude and on relative motion amplitude (head waves; Fn = 0.21).

It would seem surprising that the curves are not spread in line with the L/B ratio, yet this can be explained as follows. In order to obtain instationary test results in the wave tank the tests for the three different model lengths are carried out on a basis of constant Froude number. This means that the longer model was tested at a higher speed in the basin. For the global effects of the steady wave system in calm water the Froude basis would also seem to be appropriate. However, the three models were fitted with exactly the same bow and for the dynamic swell-up in waves it is not so much the Froude number on a basis of ship length that matters as the Froude number on a basis of length of bow. The latter was higher for the longer model, thus leading to a higher dynamic swell-up.

If we consider Fn. = 0.21 and $\lambda/L = 0.5$ and we take the actual speed corrected for the wave orbital velocity we find that the water entrance velocity at the bow is almost 40 percent higher for the longest model as compared to the shortest model. In view of the strong speed dependency and weak frequency dependency of the swell-up coefficient (see also Section 7.3) it is therefore conceivable that model 1 incurs a higher swell-up hence a higher added resistance.

At the long wave end ($\lambda/L = 0.8$) we observe a neat disposition of the lines in Figure 7.6.1-3 which is directly in line with what we may expect as the wave length approaches the resonant pitching region.

At the very short wave length end of the scale (λ/L smaller than 0.3) the curves appear to go up again; this is attributed to the increase of the swell-up coefficient for the higher encounter frequencies.

If we consider the added resistance operator on basis of relative bow motion as in Figure 7.6.1-4 we observe an interesting pattern. The results of the added

resistance operator become more neatly arranged. For the longer waves the curves become flat, as we would expect, while for the shorter waves the curves still go up, as a result of the wave orbital velocity being higher in short waves than on long waves.

The influence of speed is clearly exhibited in Figure 7.6.1-5 on a basis of wave amplitude squared, and in Figure 7.6.1-6 on a basis of relative motion squared. It is shown that at the longer wave lengths the added resistance operator goes up with speed, and then down again because of the encounter frequency effect, and the resonant pitching hump, which lies around $\lambda/L = 1$. At the short wave end the added resistance goes up with speed on account of the high orbital velocity of the water and the frequency dependency of the swell-up for very short waves. When we plot this on a basis of relative motion squared, the curves become flatter, yet at the short wave range they remain to go up due to increased wave reflection on the bow.

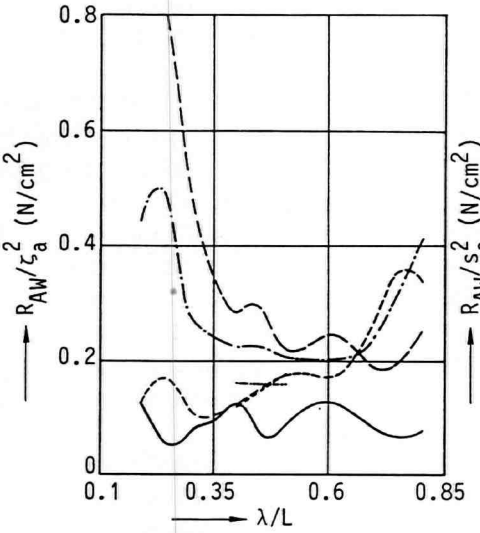

Figure 7.6.1-5

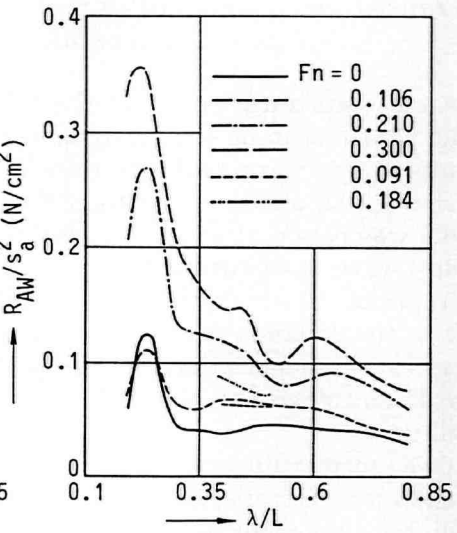

Figure 7.6.1-6

Transfer functions of added resistance based on wave amplidude and on relative motion amplitude (head waves; model 1).

7.6.2 Experiments on systematic frigate models

In the present section we will briefly discuss the outlines and some results of a systematic series of model experiments in which the seakeeping characteristics of high speed displacement vessels (frigates) were studied. The study, known as the FDS series was carried out as a multi-year research programme under the

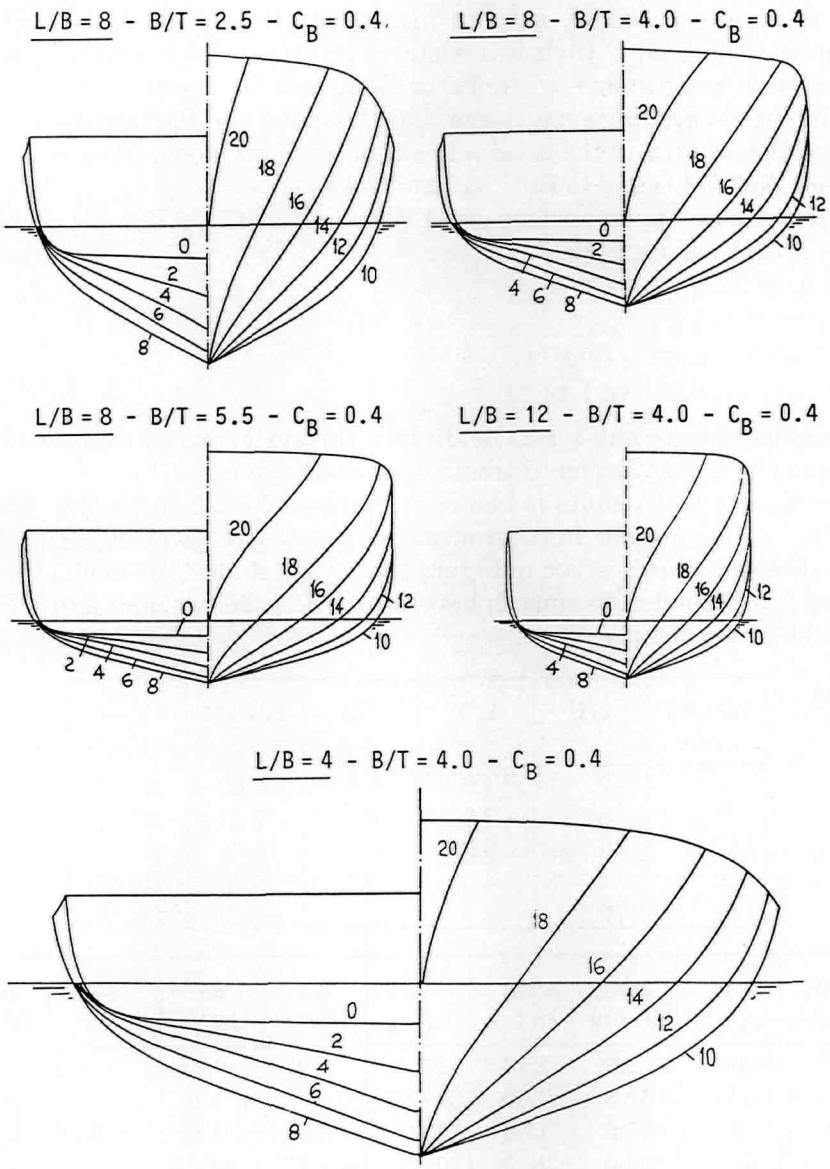

Figure 7.6.2-1: Bodyplans of high speed frigate models.

sponsorship of the Royal Netherlands Navy, the United States Navy, the Royal Australian Navy and MARIN.

For this systematic series of experiments a total of about 25 models were designed, built and tested, both to investigate their calm water resistance characteristics as well as their behaviour in waves. For a general treatise of the total research programme we refer to Blok and Beukelman (Ref. 7-3) who discussed the seakeeping aspects and Van Oossanen and Pieffers (Ref.7-10) who discussed the origin and the calm water aspects. For an overall review we refer to Robson (Ref. 7-11) and to Ref. 7-12 and 7-13.

The parameter space encompassed variation of the following parameters together with their ranges:

L / B	: 4 to 12
B / T	: 2.5 to 5.5
Cb	: 0.35 to 0.55
Fn.	: 0.285 to 1.14

Subsequent separate sub-series dealt with the systematic variation of waterplane area coefficient, prismatic coefficient and bilge keels.

A selection of test results is shown in Figures 7.6.2-2 to 7.6.2-6. The main particulars of the parent hull form, model no. 5a are given in Table 7.6.2-1, whereas the bodyplan is given in Figure 7.6.2-1. As shown, the model was round bilge and had a moderate smooth bow flare. The parent model had a B/T = 4, L/B = 8, and Cb = 0.40.

Model code	L/B	B/T	C_B	$L/\nabla 1/3$	k_{yy} in % L
5^A	8	4.0	0.4	8.62	25
7	8	2.5	0.4	7.37	25
8	8	5.5	0.4	9.58	25
9	4	4	0.4	5.43	25
10	12	4	0.4	11.29	25

Model code	L_{PP} in cm	B_{WL} in cm	T_M in cm	Δ in kg	T_z in s	b_z in %	T_Θ in s	b_Θ in %
5^A	500	62.5	15.6	193.3	1.05	0.24	0.99	0.14
7	500	62.5	25.0	312.5	-	0.26	-	0.19
8	500	62.5	11.4	142.0	0.92	0.31	0.90	0.21
9	400	100.0	25.0	400.0	1.23	0.15	1.38	0.14
10	600	50.0	12.5	150.0	0.75	0.10	0.80	0.17

Table 7.6.2-1: Main particulars of systematic frigate models.

Four systematic variants of this model were tested, two were varied in the vertical direction, to obtain a variation of B/T ratio for the same beam, two were varied in the length direction to obtain a variation of L/B ratio, keeping the cross section and bodyplan the same. The freeboard would be increased in proportion with the length though. The bodyplans of the models are shown in Figure 7.6.2-1.

We have included some diagrams to show the effect of parameter variation on the seakeeping characteristics, most importantly with respect to the relation between added resistance and relative motion on the forebody. In the present experimental series this is all the more manifest because the parameter variation was so wide. We have transformed some of the results on a different non-dimensional basis to highlight some interesting aspects of the relation between added resistance and relative motion.

The influence of B/T ratio and speed is displayed in Figures 7.6.2-2 and 7.6.2-3 for two speeds. The speeds are rather high, Fn. = 0.285 would correspond to about 20 knots for a navy frigate of current size, yet Fn. = 0.57 will be out of reach for most ships. As the results of the experiments show, the model having the highest B/T value exhibited the lowest motions, mainly on account of increased damping and a shorter natural pitch period. As the speed is increased the motions and consequently also the relative motions and added resistance increase, and the differences between the models are aggravated, see Figures 7.6.2- 2abc and 7.6.2-3abc

We have transformed the added resistance response function on a basis of relative motion squared for Fn. = 0.285, and it is shown that the conspicuous resonant pitch hump is removed and the curve becomes more straight (Figure 7.6.2-2d). So for the wave length range of interest the lines are fairly independent of wave length. The tails of the curves may go up but these are related to very small measurement values and must be fraught with higher inaccuracy. The 10 percent limit indicates resistance increase as percentage of calm water resistance. For the higher speed, Fn. = 0.57 a similar set of curves is given which show a clear tendency to rise for short waves (Figure 7.6.2-3d). This phenomenon was also observed in the experiments discussed in Section 7.6.1. It appears that for short waves and high speed the function becomes dependent upon the encounter frequency, an effect which is virtually absent at lower speed.

The influence of L/B ratio and speed is displayed in Figure 7.6.2-4 and 7.6.2-5 for the same two speeds. In this case we observe larger differences between the three models because the length is a major parameter in seakeeping. There are two ways of looking at this parameter variation: as a variation of length or a variation of midship section. Since the results are plotted on a basis of non-dimensional wave length we may consider these models as being of the same length and different beam (and draught). For the lower speed there is a considerable difference between the pitch motions of the models, mainly because of a considerable difference in natural pitch period (Figure 7.6.2-4a). In the relative motion

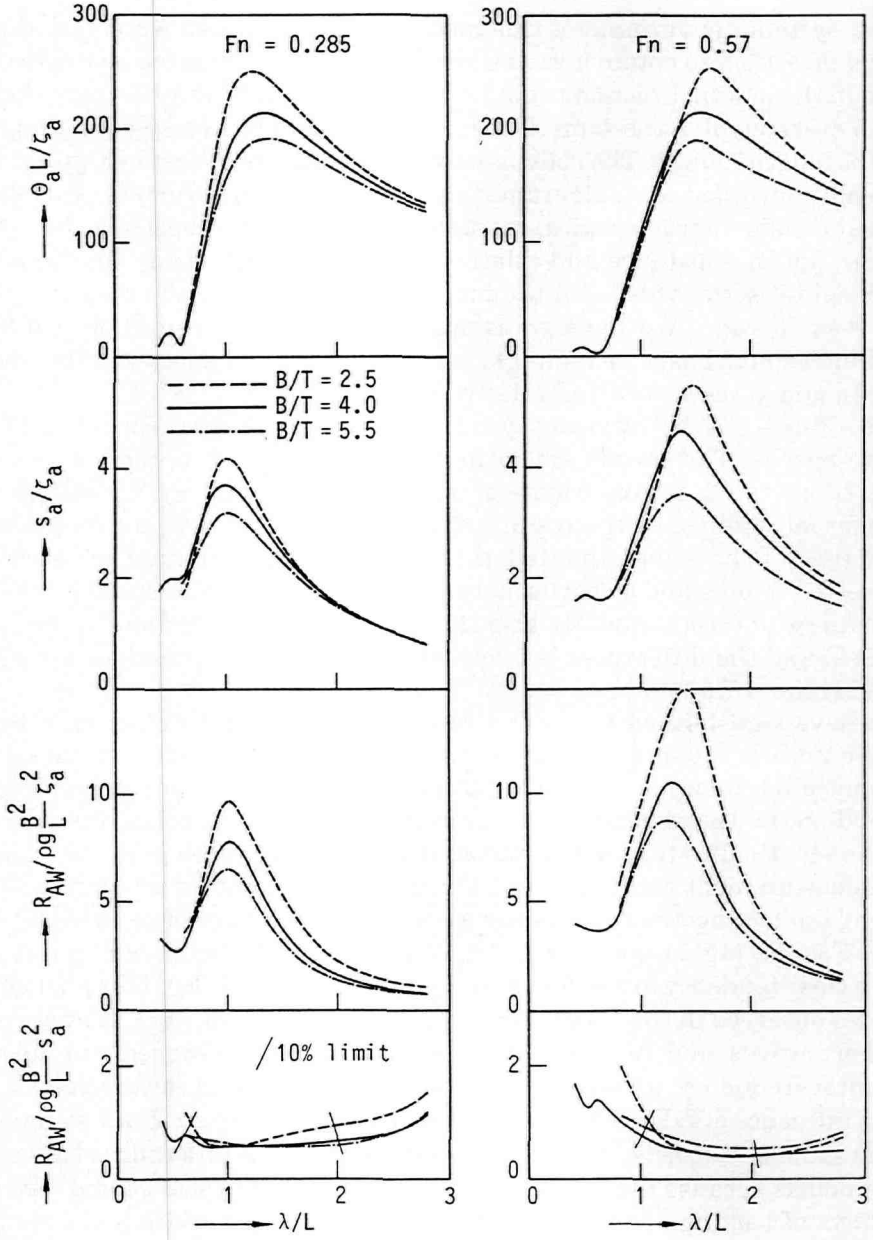

Figure 7.6.2-2 *Figure 7.6.2-3*

Transfer functions of pitch, relative motion and added resistance for three beam / draft ratios.

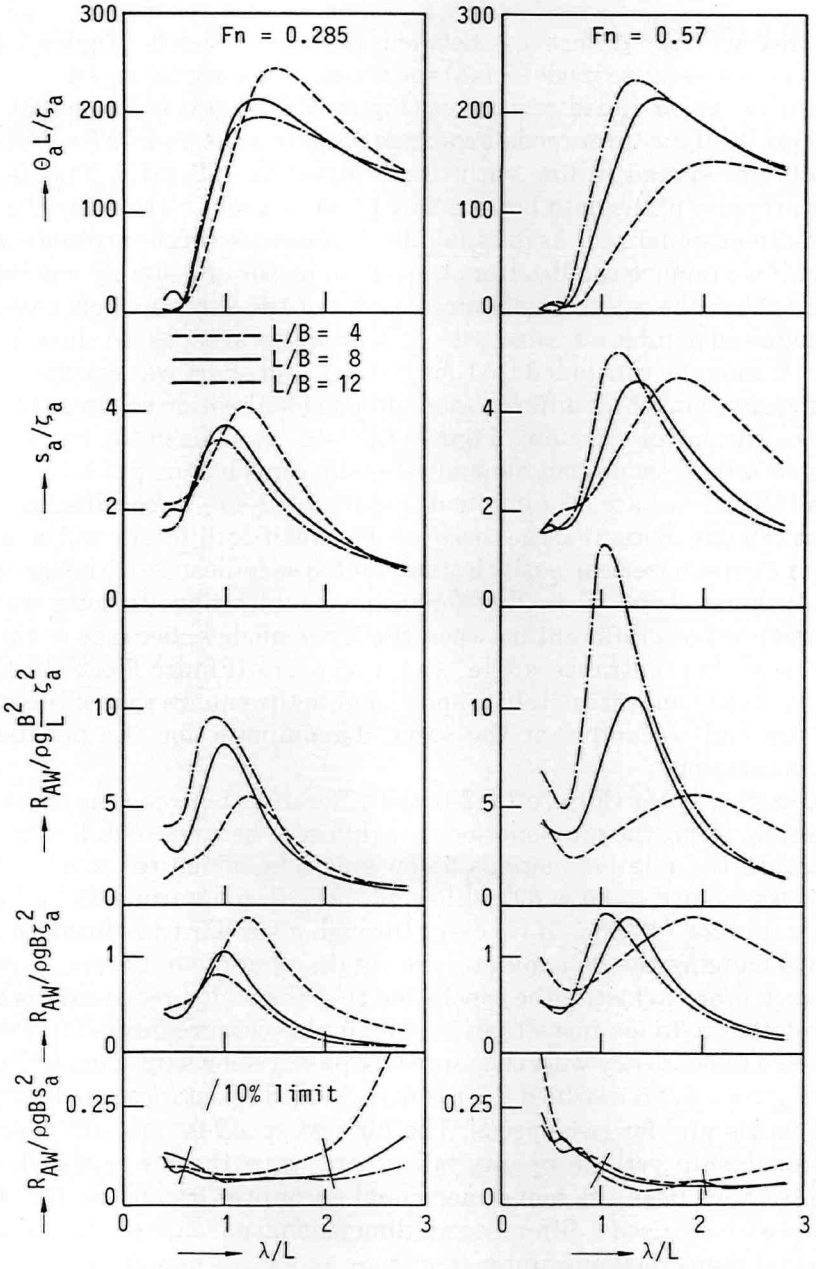

Figure 7.6.2-4

Figure 7.6.2-5

Transfer functions of pitch, relative motion and added resistance for three length / beam ratios.

we also observe large differences between the three models (Figure 7.6.2-4b), understandable because model 9 is three times as beamy as no. 10.

In the response of added resistance (Figure 7.6.2-4c) it is important to note that the results of the three models coincide for long waves, while for short waves the results are spread in line with their respective L/B ratio. This is not an inherent property of the data but is solely brought about by the way the results were non-dimensionalized. As is usual, the denominator of the ordinate includes B^2/L , yet if we remove the B/L from the denominator and simply use B instead we observe that the added resistance results of the three models coincide for short waves and exhibit a spread with L/B for long waves, as we show in Figure 7.6.2-4d. It must be concluded that long waves and short waves constitute two different regimes in which different non- dimensionalization schemes will apply. If we take the latter function, Figure 7.6.2-4d, as a basis to transform the ordinate on a relative motion denominator the conspicuous pitch hump disappears and the curves are straightened (Figure 7.6.2-4e). In conclusion, in short waves the relative motions of the three models are little different and beam times relative motion squared can easily be interpreted as indicative of the mean added resistance, hence be used in the non-dimensionalization. In long waves the relative motions are different between the three models, because of the differences in waterline entrance angle, and it appears (Figure 7.6.2-4b) that the relative motion is approximately proportional to the square root of the beam, so that in the end we arrive at the same denominator for the ordinate non-dimensionalization.

For the higher speed (Figure 7.6.2-5) the differences between the three models become really large, the pitch motions are different because of different natural pitch periods, the relative motions follow suit. The added resistance response functions are shown to be widely different, both in magnitude as in dominant frequency (Figure 7.6.2-5c). If we carry through a similar transformation of the curves by changing the denominator we obtain a bundle of curves, sufficiently close to each other to justify the conclusion that the added resistance is dependent on relative motions more than anything else (Figure 7.6.2-5e). For really high speed a dependency with encounter frequency shows up. This will be more clear in Figure 7.6.2-6 in which the results of added resistance are displayed for all five models and for two speeds. The highest speed is incredibly high for a displacement ship yet the results fall in line with the lower speed. On the abscisse we have used the non-dimensional encounter frequency. On the ordinate value we have used a different non-dimensional parameter, by also dividing by the non-dimensional encounter frequency on a basis of ship beam.

If we transform all added resistance data in this way all data is shown to collapse within a common band. Data points lying outside the resonance area are derived from very small measurement data.

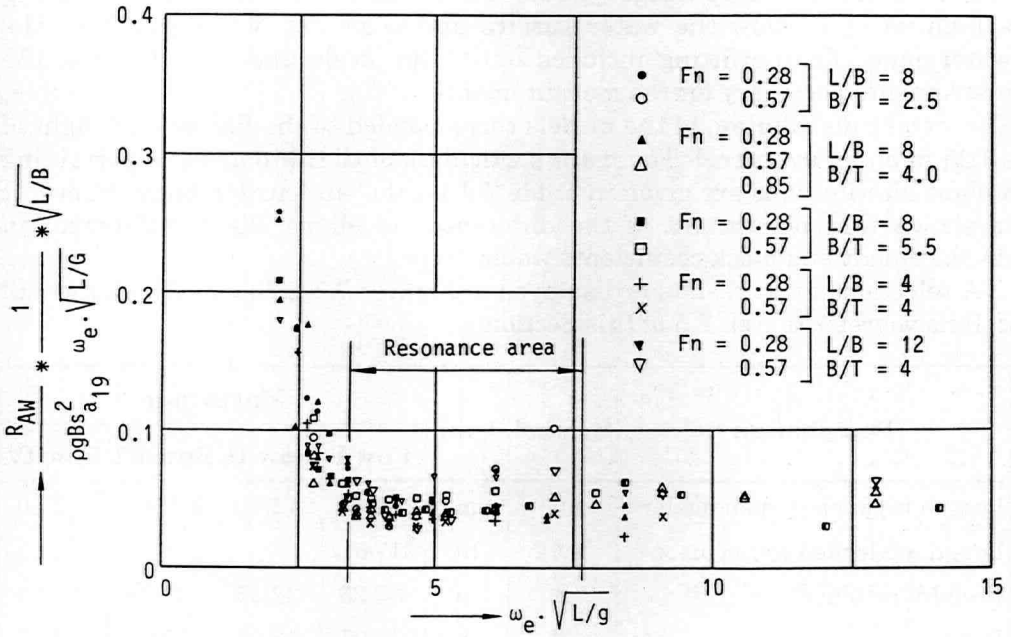

Figure 7.6.2-6: Non-dimensional resistance increase of systematic frigate models as function of non-dimensional encounter frequency

7.7 A study on the influence of forebody form

7.7.1 Experiments on the model of a bulk-carrier

Under this sub-heading we shall relate a model test program that was carried out to obtain experimental data on the mean added resistance due to waves, and most importantly we will show the effect of shape of the bow in waves having a length around the ship's length. For these waves conspicuous pitching is to be expected and as a consequence also the added resistance is highest.

For the present test program a model of a 76,000 tons bulk- carrier was used at a scale ratio of 1 to 55. For these experiments a total of four forebody forms were designed an built. They extended over about one quarter of the model

length and could be fitted to the same aftbody. The four forebody forms are shown in Figure 7.7.1-1 . As shown, there were two cylindrical bows, one of them with above water bow flare and one without. In addition there were two fine forms, one of which was a sharp wedge type bow and the other one was a fine bow having a bulbous bow below the water surface and a modest bow flare above the waterplane. The outfitting included only bilge keels and the fitting of the instruments necessary for the measurements.
The weight distribution of the models corresponded to the full load draught of 13.25 m on an even keel. The main particulars of the ship and the pertaining weight distributions are given in Table 7.7.1-1 for all four forebody shapes. It is shown that on account of the differences in shape slight differences in displacement and block coefficients would occur.

A selection of test results is displayed in Figures 7.7.1-2 and 7.7.1-3. For full details we refer to Ref. 7-5 of this Section.

Designation	Symbol	Unit	Magnitude			
			Bow I	Bow II	Bow III	Bow IV
Length between perpendiculars	L_{PP}	m	212.40	212.40	212.40	212.40
Length on loaded waterline	L_{WL}	m	217.0			
Breadth moulded	B	m	32.25	32.25	32.25	32.25
Draft	T	m	13.25	13.25	13.25	13.25
Displacement weight	Δ	m^3	76.500	76.350	76.350	71.700
Block coefficient	C_B	-	0.84	0.84	0.84	0.79
Centre of buoyancy forward of Station 10	$\overline{FB}$	m	5.18	5.0	5.0	0
Centre of gravity	$\overline{KG}$	m	10.34	10.34	10.34	10.34
Metacentric height	$\overline{GM}$	m	2.75	2.75	2.75	2.75
Longitudinal radius of gyration	k_{yy}	%L_{PP}	25.60	25.60	25.60	25.60

Bow I = Bulbous bow with bowflare
Bow II = Cylindrical bow with bowflare
Bow III = Cylindrical
Bow IV = Wedge

Table 7.7.1-1: Main particulars of bulk-carrier with bow form variation.

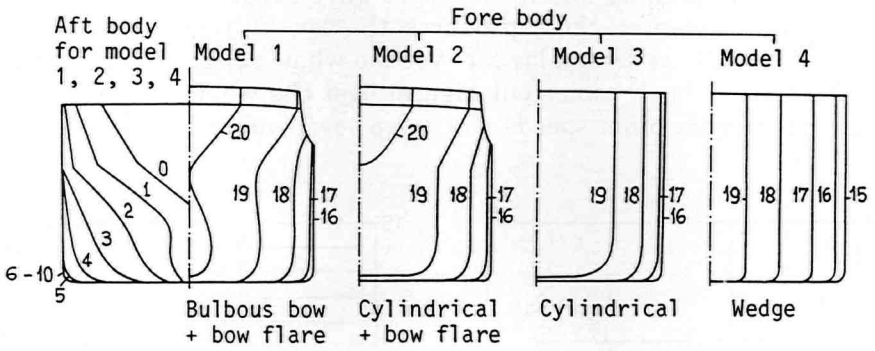

Figure 7.7.1-1: Bodyplans of four models.

The effect of bow shape

The 'raison d'etre' of this study was to investigate the influence of bow shape, for which four shapes were tested, two of them realistic shapes in use these days, the other two, having vertical sides, are perhaps more of academical interest, but certainly worth investigating to complete the picture. In spite of small differences in displacement it is felt that the main differences found can be attributed to shape rather than any other parameter as these differed comparatively little. An exception should perhaps be made for the wedge bow (No. 4), where differences in displacement amounted to 6 percent and the block coefficient was 0.79 as compared to 0,84 for the other ships. Like in any experimental study on ship models it is impossible to vary only one geometrical parameter at the time, while keeping all others the same.

The influence of bow shape on the ship motion heaving was shown to exist only in the long wave range dominated by the spring coefficient which depends on the waterplane area. The cylindrical bow (No.2) had the largest waterplane area forward and on account of its flare also more damping so that the motion came out lowest. All three ship speeds produce the same result in this respect, the fine forebody with the smallest waterplane area (wedge No. 4) gives the highest heave response. The same reasoning holds for pitching where the wide cylindrical bows No. 2 and 3 produce the lowest pitch, in the long wave range. It must be conceeded that the differences in pitch are rather small. The influence of bow shape on relative motion at station 19 is somewhat more pronounced, as shown in Figure 7.7.1-2 for the speed case of Fn. = 0.14. Since the basic ship motions heave and pitch do not exhibit such great variations between the models, the differences in relative motion can effectively be attributed to shape. It is shown that in the long waves the wide cylindrical bows (No.2 and No.3) have the lowest relative motion, while for the wave range around a wave length

to ship length ratio of unity and in the short wave range the wedge bow with sharp waterline entrance (No.4) produces the lowest relative motion. The cylindrical bow (No.3) is second lowest over the whole range. The bulbous bow with bowflare (bow No. 1) comes out highest over the whole range. The same trend exists also for the other speeds, the sharp bow invariably yields the lowest motion.

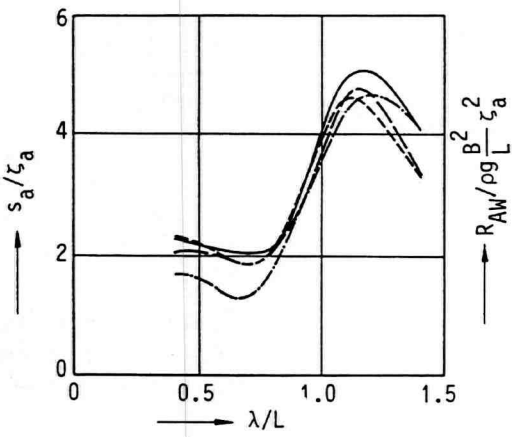

Figure 7.7.1-2

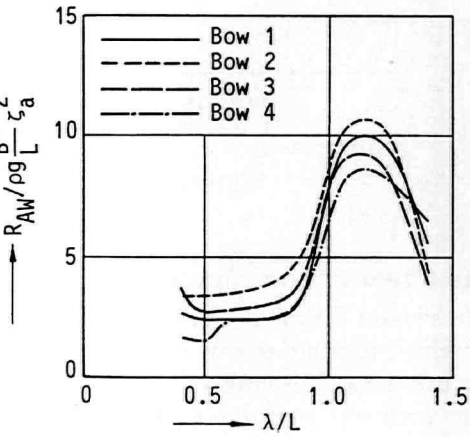

Figure 7.7.1-3

Transfer functions of relative motion (Station 19) and added resistance for four bow forms (head waves, Fn = 0.14).

The shape of the bow also has a marked effect on the wave added resistance as shown in Figure 7.7.1-3 again for the speed case of Fn. = 0.14. In the long wave range ($\lambda/L > 1.35$) some crossover points occur, but for all three speeds tested it may be concluded that the cylindrical bow with vertical sides (bow No. 3) produces the lowest wave added resistance with the other cylindrical bow with flare (bow No. 2) just a shade worse. In these long waves the sharper bows, the bulbous bow (No. 1) and the sharp wedge bow (No. 4) produce the highest wave added resistance. In the wave range $1.0 < \lambda/L < 1.35$, where the ship exhibits the largest pitch angles, the wedge bow (No. 4) is best at lower speeds and the cylindrical bow (No. 3) is best at higher speeds. In the short wave range, $\lambda/L <$ 1, again the curves exhibit some crossover points, but for all speeds combined we may say that the sharp bow (No. 4) scores lowest, followed closely by the sharp bulbous bow (No. 2) and the cylindrical bows score highest, the one with bow flare (No. 2) ranking at the top. By and large, taking all effects together it is evident that in short waves the sharp bows (No. 1 and 4) should be favoured as they produce the lowest added resistance, while in long waves the wider cylindrical forms (No. 2 and 3) produce the lowest wave added resistance.

Since large ships operate often in a moderate sea environment with waves being shorter than the ship length, it would make sense to adopt a comparatively sharp bow.

It is interesting to note the close correspondence between the relative motion and the wave added resistance. Not only in the shape of the response curves, but also in the conclusions on the bow shape. The score of the bow forms discussed above is fairly well in line with the score in relative motion. As we see from the response functions, the added resistance curves and the relative motion curves are very similar in shape and even the general trends and cross-over points are similar. We observe that in short waves the fine bow forms produces the lowest relative motion and the lowest added resistance and that in long waves the full cylindrical bows yield the lowest relative motion and the lowest added resistance. Another interesting point to note is that in the added resistance response curves the presence of bow flare tends to increase the added resistance. In the short wave range bow No. 3 (without bow flare) comes out better (lower) on added resistance than bow No. 2 (with bow flare) for exactly the same underwater hull shape. In the long wave range bow No. 2 also seems to be consistently higher. It should be noted that in bow No.2 the bow flare starts right at the load waterline so that at any forward speed the steady bow wave interferes with the bow flare.

As far as the sharp bows are concerned the presence of flare also appears to increase the added resistance although it should be noted that bows No.1 and No.4 had a different underwater hull which is bound to have influenced the results as well. So, in conclusion, we may safely say that the bow producing the lowest relative motion amplitude will also incur the lowest added resistance from waves. In short waves sharp bows should be favoured whilst in long waves cylindrical bows are the best on added resistance.

More specifically in long waves the cylindrical bow should not have any bow flare and in short waves the sharp bow should not have any flare nor bulbous bow.

The differences are by no means insignificant. In particular in the short wave region the choice of the bow can cut back on added resistance by 40 percent, in the longer wave range reductions of 20 percent are possible.

7.7.2 Experiments on the model of a cargo ship

The foregoing sub-heading 7.7.1 addressed the influence of bow form for a wave length range running from waves longer than the model to a wave length about half the model length. In the present series of experiments to be discussed here the wave length was considerably shorter, down to wave length ratios of only 20 percent of the model length.

Designation	Symbol	Unit	Model 1	Model 4	Model 5
Length between perpendiculars	Lpp	cm	500.00	500.00	500.00
Depth	D	cm	50.00	50.00	50.00
Breadth moulded	B	cm	62.50	62.50	62.50
Mean draft (Even keel)	T	cm	17.90	17.90	17.90
Displacement weight	W	N	4.149	4.424	4.689
Centre of gravity aft st 10	LCG	cm	13.10	1.34	10.63
Centre of gravity above base	KG	cm	21.00	21.00	21.00
Metacentric height	GM	cm	5.70	5.80	6.10
Longitudinal radius of gyration	Kyy	cm	120.00	120.00	120.00

Table 7.7.2-1: Main particulars of cargo ship models.

The present study on the influence of bow form on added resistance in short waves was part of a multi-year research programme to the order of the NSMB Cooperative Research on Ships (CRS).

For the present series of experiments a total number of 7 models were designed and built. For the sub-series to be related here the model was segmented and was fitted alternatively with three bow forms: a very fine slender bow with hollow waterline entrance, a wedge bow and a blunt almost cylindrical

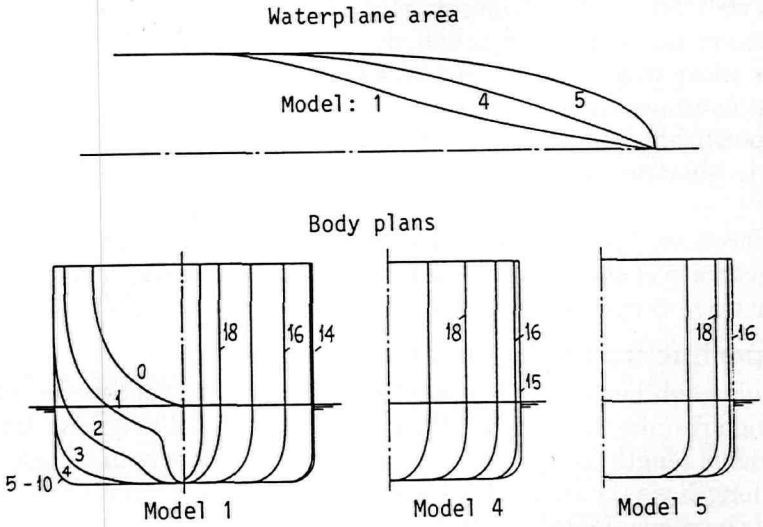

Figure 7.7.2-1: Bodyplans and waterlines forward for three cargo ship models.

bow. All bow forms had vertical sides. The model particulars are given in Table 7.7.2-1, while the bow forms are displayed in Figure 7.7.2-1 and Photo 7.7.2-1. The models were bare hull, no appendages being fitted.

Photo 7.7.2-1: Forebody sections of models.

A selection of test results is shown in Figures 7.7.2-2 and 7.7.2-3.
If we compare model No. 1, 4, and 5 we can obtain the influence of the bow form. All three models had the same midbody and aftbody, they all had a bow with vertical sides, the only difference lay in the shape of the forebody waterlines. When we compare the shape of the waterlines in Figure 7.7.2-1 we note that model 1 had a hollow S-curved waterline forward, model 4 had a wedge form, and model 5 had a blunt cylindrical bow.

The influence of bow form for the forward speed of Fn. = 0.21 is shown in Figure 7.7.2-2. At this speed the curves are well separated. It appears that the wedge type bow form No.4 exhibits the lowest added resistance. One would have thought that the even finer bow of model No. 1 would have shown an even smaller added resistance, but this was not the case, it is just a triffle higher. The blunt bow data lie, as expected, highest. The trends of the curves from model No. 4 to 1 to 5 exhibit a nice transition from the lowest curve to the highest as they are fairly separated.

In Figure 7.7.2-3 the added resistance data are related to the relative motion at the bow and the trend is completely reversed. Model No. 1 with a very fine bow lies highest and model No. 5 with a blunt bow lies lower. If we look back

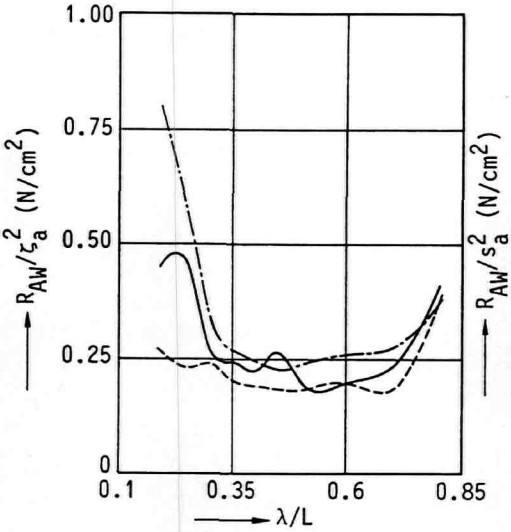

Figure 7.7.2-2

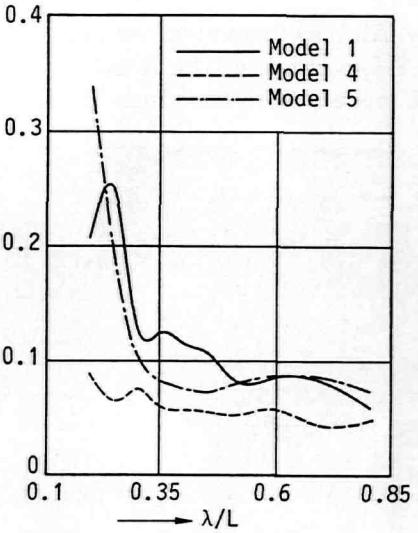

Figure 7.7.2-3

Transfer functions of added resistance based on wave amplitude and relative motion amplitude for three bow forms (head waves, Fn = 0.21).

into the relative motion data we note that relative motion is only little dependent on wave frequency and had about the following levels:

Model No.1:	Sa / ζ a = 1.5
Model No.4:	Sa / ζ a = 1.8
Model No.5:	Sa / ζ a = 1.6

The fuller waterline form of model No. 5 has a larger spring restoring coefficient in heave and pitch and as a result the absolute motions are slightly smaller. However in the short wave region the spring rate is of less concern and the ship motions play only a minor role. The deformation of the incident wave and the interaction with the bow wave is more important. On model No. 5 the blunt bow pushed a large bow wave in front of it and the wave probe that measured the relative motion happened to be located near the conspicuous bow wave trough that shows up for this Froude number. As a result the relative motion of model No. 5 is just not sufficient to describe the up and down water motion on the whole of the bow and that must have caused the reversal of the lines in Figure 7.7.2-3. In all other respects the curves are similar.

It could be concluded on basis of these experiments that:

- The effect of wave length on added resistance of a wedge bow and a blunt bow is in general similar to the trends observed for a fine bow,
- The effect of bow form on the wave added resistance depends on the speed and on the wave length range. The differences vary from a mar-

ginally few percent up to a 100 percent in the shortest waves where reflection plays a large role.
- Generally the added resistance of the blunt bow form was a good deal larger than for the wedge and fine bow form, of which the results were not as much different.

7.8 A study on the influence of wave direction

7.8.1 Experiments on the model of an LNG-carrier

Under this sub-heading we shall relate a model test program that was carried out to obtain experimental data on the mean added resistance due to waves coming from various directions. The experiments were a continuation of the test programme discussed in Section 7.2.1 to which we refer for a number of illustrations. The wave directions used in the experiments were waves from ahead (180°), the bow quarter (225°), the beam (270°), the stern quarter (45°) and from astern (0°).

For the present test series the same model of a 125,000 m3 LNG- carrier was used, at a scale factor of 1 to 70. The model was outfitted with bilge keels and the instruments necessary to do the measurements. The weight distribution of the model corresponded to a full load draught of 11.5 m on an even keel. The main particulars of the ship and the pertaining weight distribution are given in Table 7.2.1-1. The test setup and a bodyplan of the model are shown in Figure 7.2.1-1.

The experiments were carried out for three ship speeds, corresponding to Fn. = 0.14; 0.17 and 0.20 which would be equivalent to 14, 17 and 20 knots for the real ship. The wave headings were spread over 45 degree intervals and are denoted by 0 , 45, 270, 225, 180 degrees,

A selection of test results is shown in Figure 7.8.1-1 and 7.8.1-2. For full details we refer to Reference (7-4) of this section.

The effect of wave direction on motions

Wave direction has quite an impact on the ship motions. This is so because wave direction governs the juxtaposition of the wave length relative to the main axes of the ship, and as a result the contribution of wave energy to motions along or about these axes. As to heaving, the form of the response curve remains virtually the same for all headings although the level may vary; it has no dynamic amplification and is mainly dictated by wave exciting force. In oblique bow waves the whole heave curve is shifted towards the shorter wave length, because of the effective wave length coming into play. In beam waves heave is largest because all wave lengths are longer than the ship's beam, it even exhibits a peak, whereas waves from astern, right or oblique, produce less heave than from ahead mostly because of reduced pitch into heave coupling.

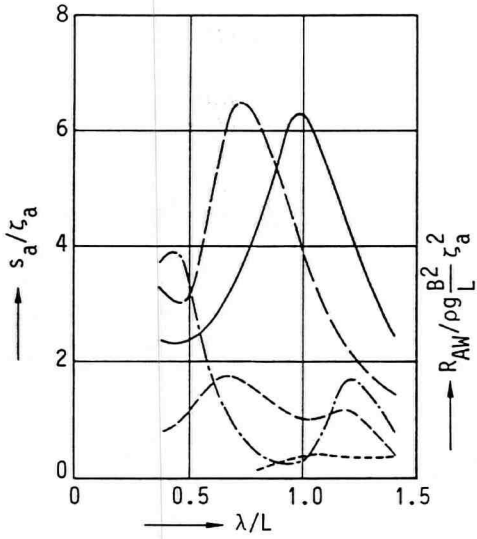

Figure 7.8.1-1

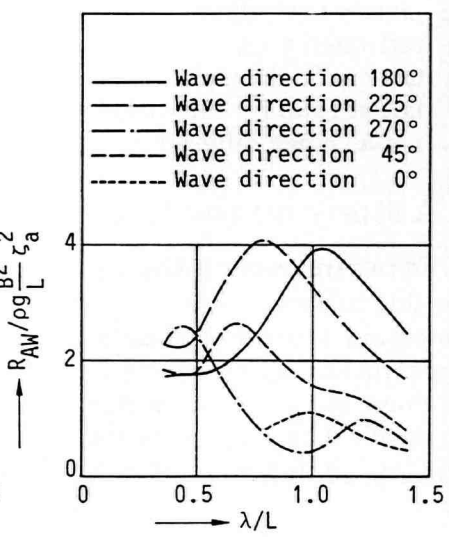

Figure 7.8.1-2

Transfer functions of relative motion and added resistance of LNG carrier for five wave headings (Fn = 0.20).

Pitching is largest in head waves and in bow quarter waves and less in waves from the stern sector and from the beam. In beam waves the pitching is understandably very small, in waves from the stern quarter or from dead astern the pitch response curve is basically similar to the ones for ahead waves, though generally lower on account of lower encounter frequency and reduced dynamics.

Rolling is largest in beam waves where we observe a conspicuous resonance peak at the natural period, and reduces quickly as the wave angle turns away from the beam. In stern quartering waves rolling exhibits two peaks. One of it is due to the roll natural period, the other one is related to the effective projected wave length being equal to the ship's length.

The horizontal motion surge is rather low in waves from ahead or from the bow angle, while it is much larger in waves from the stern quarter or in following waves. The reason for this is that in stern sector waves the waves of the same length as the ship run along with the ship and excite the ship at a very much lower frequency.

Sway and Yaw are largest in beam and stern quartering waves respectively, and do not exceed the water orbital motion in the water surface.

The effect of ship speed on motions

The speeds chosen for the experiments are in the realistic range for a ship of this size. The major effect of speed is that a certain wave length excites the ship

at a frequency higher or lower than the corresponding wave frequency, depending on whether the wave comes from the bow or the stern sector. This produces a shift of the response functions with respect to frequency.

Added resistance and relative motions

Some results of the experiments are shown in Figure 7.8.1-1 and 7.8.1-2. The relative motion at the bow is shown as well as the wave added resistance and the correspondance for each wave heading is clearly shown.

In waves from ahead (180°), the relative motion exhibits a pronounced resonance peak coincident with pitch resonance. In line with pitching the relative motion increases with speed. We observe a good deal of correspondence between relative motion and added resistance, the latter shows the same trends with wave length and also the same trend with speed. The speed effect is almost absent in short waves. The peak of the added resistance response function in non-dimensional form at pitch resonance is seen to reach a level of about 6 which is quite normal for this hull form. In short waves the function remains at a level of about half the height of the peak, as we often observe for many different hull forms.

In waves from the bow quarter (225°) the relative motion peaks at a shorter wave length due to the effective wave length principle, and we observe that the added resistance follows suit. The added resistance in bow quarter waves attains a higher peak than in head waves, as a result of larger relative motions. It is interesting to note the difference in relative motion between the seaward side (port side) and the leeward side (starboard). The latter is much lower since it is in the shadow region of the bow and does not feel the wave reflection. Curious enough, the mean value of the port and starboard relative motion is very close to the values recorded in head waves.

In waves from the beam (270°) the relative motion exhibits two peaks. The peak at the short wave length is associated with heaving and wave reflection, which in 270° is larger than in any other wave direction, in particular for short waves. The peak at the long wave side is associated with rolling resonance. It is interesting to note that for $\lambda/L = 0.5$ the relative motion on both sides of the bow is much more than can be accounted for by heave alone, yet, pitch and roll are very small and these high values must be the result of dynamic swell- up on the bow brought about by pure heaving. Again the values on the seaward side are much higher than on the leeward (starboard) side. It is also noteworthy that in the short wave regime the added resistance in beam waves is higher than in head seas, due to the lack of fore and aft symmetry that still produces a considerable resistance force, mainly due to reflection of waves on the ends of the ship.

In waves from the stern quarter (45°) the relative motion exhibits a rather oscillating behaviour that can only be attributed to rolling. The added resistance

is generally again in line with the relative motion, overall it is much lower than in waves from the forward sector.

In waves from dead astern (0°) the relative motion at the bow is a a flat curve for the lower speed and a peaked curve for the higher speed. The difference can only be attributed to a difference in surge that can bring about quite substantial differences in relative bow motions through the steady bow wave and dynamic swell-up phenomenon. The relative motion at the forebody is of the same magnitude as the wave amplitude.

These Figures 7.8.1-1 and 7.8.1-2 reveal the close correspondence between the wave added resistance and the relative motion at the bow typified by station 19. In principle there can be no argument about the fact that the wave added resistance is just and only the nett result of the hydrodynamic pressure distribution integrated around the body, and the relative motion is a visible exponent of this pressure in the fluid. So it must be concluded that the added resistance depends more on the relative motions than on the ship motions themselves.

7.8.2 Experiments on the model of a cargo ship

In the present section we shall discuss the details of a series of experiments meant to investigate the added resistance in very short waves approaching from various oblique headings on the bow.

The present experiments form part of a large multi-year research programme executed to the order of the NSMB Cooperative research on Ships (CRS).

For this model test programme a systematic series of models was designed and built, as discussed in Section 7.6.1. For the sub- series related here the parent hull form having a L/B = 6 (denoted no. 2) was used. For the model particulars we also refer to Section 7.6.1; main particulars are shown in Table 7.6.1-1 and body plan is given in Figure 7.6.1-2. As shown, the model had vertical sides in the forebody and a rather sharp bow with a vertical stem. The model was bare hull, no appendages were fitted.

Specifically for the present sub-series of experiments the test setup was modified to include two roller bar systems in fore and aft body to avoid swaying and yawing in oblique wave headings. This test setup allowed the model to freely heave and pitch without interfering with the tow force.

Because for short waves only the forward sector is of major concern the wave headings were confined to the forward sector and included 30, 45, and 60 degrees relative to the sailing direction. To this we may add the tests in head waves (Section 7.6.1) so that we have four data points to establish the effect of heading. The regular waves spanned the range of short wave lengths from λ/L = 0.2 to 0.8 ; wave heights (double amplitudes) ran from 1 to 4 percent of the model length. As to the speeds the tests were carried out for: Fn. = 0.21 and 0.30. A selection of the test results is shown in Figures 7.8.2-1 to 7.8.2-4.

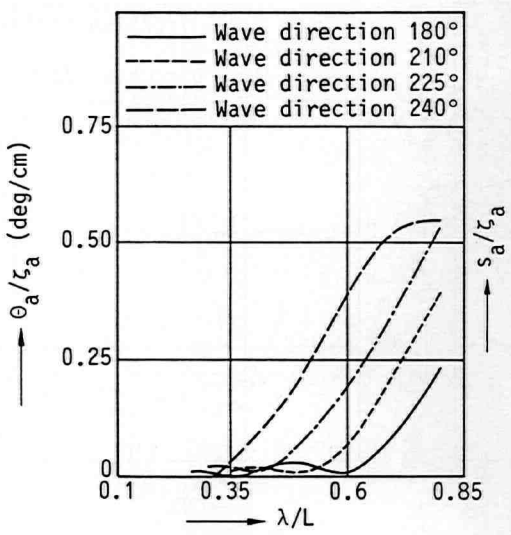

Figure 7.8.2-1

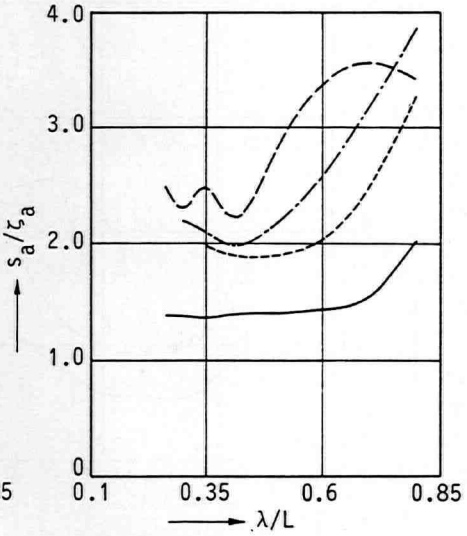

Figure 7.8.2-2

Transfer functions of pitch angle and relative motion (Station 18) for cargo ship model 2 in various wave headings from the bow quarter (Fn = 0.21).

The influence of wave heading on the pitch angle is shown in Figure 7.8.2-1. For very short waves the pitching is virtually zero, for waves having a length of more than half the ship length the pitch angle is seen to increase. The conspicuous hump at pitch resonance for wave length equal to ship length is just outside the figure. In this figure we also observe the effect of 'effective' wave length, i.e. for oblique wave angles the wave length felt by the ship is effectively longer than the nominal wave length and the pitching responds to that effective length.

The relative motion on the weather side of the bow is shown in Figure 7.8.2-2. It is composed of incident wave, disturbed wave, as well as ship motions, most dominantly pitch. A number of aspects are worthy of note. First the curves are always above unity, since this indicates the incident wave. Secondly, the 'spread' of the curves is fairly well in line with the response functions of pitching which is known to contribute greatly to the relative motion. Thirdly, for short waves, where the ship ceases to pitch, the curves remain on a constant level and have a tendency to rise again as for increasing obliquety the ship presents more of a barrier to the oncoming waves with consequently higher relative motion on the weather side.

Finally the wave added resistance is shown in Figure 7.8.2-3. It has a good deal in common with the relative motion. At the 'long' wave side the curves are spread in the same way as the (squared) relative motion, thus indicating the close relationship between the two. In the intermediate wave length range the

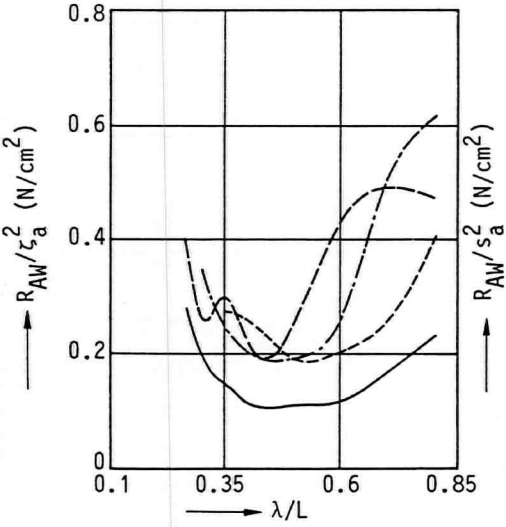

Figure 7.8.2-3

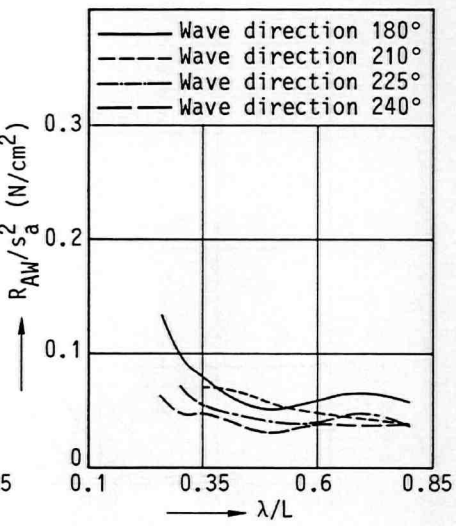

Figure 7.8.2-4

Transfer functions of added resistance based on wave amplitude and relative motion (Station 18) for cargo ship model 2 in various wave headings from the bow quarter (Fn = 0.21).

curves tend to coincide, which is also observed in the relative motion. For very short waves the added resistance operator goes up steeply, a trend that appears to go with the encounter frequency squared.

Bearing in mind the close relationship between added resistance and relative motion at the bow we have also non-dimensionalized the added resistance on basis of relative motion squared. The graphs are shown in Figure 7.8.2-4. It is interesting to note that the curves collapse on a common band (rather than a common line), which is fairly straight for the greater part of the wave length range. Probably one sole relative motion probe on the bow is too few to describe the flow around the bow and it may well be that if the relative motion had also been recorded on the lee-side of the bow and averaged with the relative motion on the weather side the correlation between the added resistance and relative motion would have been better.

At any rate, the wave added resistance in oblique waves shows a clear-cut trend with wave-length and appears intimately related to the relative motion on the forebody, just like we have shown for the head seas case, in Section 7.6.1.

Chapter 8

Hydrodynamic theory: The mathematical model

In the present chapter a mathematical model is derived for a number of reasons:

1. To describe the physical effects that we have observed in the model experiments.
2. To obtain insight in the components of the added resistance through study of the mathematical model.
3. To utilize the mathematical model to obtain numerical results that can be compared with model test data.

The theory has been split up in two parts. The first part of the theory is contained in the Appendix, as it deals with theoretical expressions that have been derived elsewhere. In this appendix we find details on the choice of the system of axes (Section A.1), expressions for the rigid body motions (Section A.2), the exact formulation of the boundary value problem within the framework of linear potential theory (Section A.3) and finally the formulation for the linearized boundary value problem (Section A.4). The expressions contained in the Appendix draw on the work of John [A-1], Stoker [A-2], Timman and Newman [A-3], Wehausen [A-4] and Wehausen and Laitone [A-5].

It has been included in the Appendix because it was used as the point of departure for our mathematical model, and will be useful for a better understanding as it contains definitions of axes and motions.

The second part of the theory is contained in the present Chapter 8. In this part we endeavour to describe the findings and observations from the various

experiments in a format of potential theory, and derive expressions for the mean wave added resistance from it. This part is contained in Section 8.3 to 8.9.

After having read Section 8.1 (Overview) and Section 8.2 (Introduction) it is recommended to first read the Appendix for the definitions of axes and motions before proceeding with Section 8.3.

8.1 General overview of the theory

In this overview we will briefly consider the various steps taken in the derivation. We refer to this Chapter 8 and to the Appendix.

In Section 8.2 the route is introduced along which we intend to attain our goal: to invoke potential theory to set up a boundary value problem, that can be solved for the unknown potential. Through the use of the Bernoulli equation the pressure in the fluid is obtained, and through integration of this pressure over a suitable region the total force on the ship can be resolved. This implies, as indicated in Chapter 4 already, that we are using a 'near field' approach.

$$\overline{F} = -\iint_A p\ \overline{n}\, dA \tag{8-1}$$

in which: $\overline{F}$ = force vector
p = hydrodynamic pressure
$\overline{n}$ = direction normal on the hull
A = wetted area.

In Section A.1 considerations are given on the choice of the system of axes. It is shown that three systems of axes are of relevance: a space-fixed and a body-fixed system, and in addition a so-called 'system of travelling axes', travelling with the mean position of the centre of gravity, yet the direction of the axes remaining fixed in space. It is this third system which is most useful for the description of our problem.

In Section A.2 the rigid body motions of the ship are described in the various systems of axes: body-fixed, space-fixed and travelling axes. Also the ship motions are expanded in a series expansion up to the second order, in anticipation of the need to use second order quantities in the description of the pressure and the integration boundary.

In Section A.3 the boundary value problem is formulated in an exact way, within the framework of linear potential theory. The boundary conditions can favourably be formulated in a system of travelling axes, yet the non-linear

character of the boundary condition at the free surface precludes solutions without further simplifications, as it reads:

$$\varphi_{tt} + 2\nabla\varphi \cdot \nabla(\varphi_t - U\varphi_{x_1}) + \tfrac{1}{2}\nabla\varphi \cdot \nabla(\nabla\varphi \cdot \nabla\varphi) +$$

$$+ g\varphi_{x_3} - 2U\varphi_{x_1 t} + U^2\varphi_{x_1 x_1} = 0 \qquad \text{on } x_3 = \zeta \quad \text{(A-30)}$$

In Section A.4 the boundary value problem is linearized in a way analogous to classical hydrodynamic theory, in which it is implied that the velocity potential of the flow, and all quantities to be derived from it - fluid velocity, pressure, wave height, hydrodynamic forces and motions of the ship - may be expanded in a convergent power series with respect to a small parameter:

$$\varphi = \varphi^{(0)} + \varepsilon\varphi^{(1)} + \varepsilon^2\varphi^{(2)} + 0(\varepsilon^3) \qquad \text{(A-34)}$$

where $\varepsilon << 1$ is a small parameter.

In the derivation a further limitation is made to first order potentials only, it being hypothesized that components resulting from first order quantities or combinations thereof will, for the most part, make up the mean value of the hydrodynamic force that we are interested in for the wave added resistance.

The free-surface condition and the body-boundary condition to be satisfied on, respectively, the unknown actual free surface and the unknown actual position of the body are linearized with respect to the known mean position of, respectively, the waterplane and the body. We obtain for the free-surface condition and the body-boundary condition:

$$-\left(\varphi_t^{(1)} + \overline{W}\cdot\nabla\varphi^{(1)}\right)\left[\tfrac{1}{2}\frac{\partial}{\partial x_3}\left(\overline{W}\cdot\nabla W^2\right) + g\varphi_{x_3 x_3}^{(0)}\right] \Big/ \left[g + \overline{W}\cdot\overline{W}_{x_3}\right] +$$

$$+ \varphi_{tt}^{(1)} + 2\overline{W}\cdot\nabla\varphi_t^{(1)} + \overline{W}\cdot\nabla\left(\overline{W}\cdot\nabla\varphi^{(1)}\right) +$$

$$+ \tfrac{1}{2}\nabla\varphi^{(1)} \cdot \nabla(W^2) + g\varphi_{x_3}^{(1)} = 0 \qquad \text{on } x_3 = \zeta^{(0)} \quad \text{(A-44)}$$

$$\varphi_n^{(1)} = \left[\dot{\overline{\alpha}} + \left(\overline{W}\cdot\nabla\right)\overline{\alpha} - \left(\overline{\alpha}\cdot\nabla\right)\overline{W}\right]\cdot\overline{n} \qquad \text{on } \overline{A} \quad \text{(A-51)}$$

In Section 8.3 it is explained why and where in the derivation of Section A.4 the 'dynamic swell-up' effect so much in evidence around the ship's bow as observed in numerous experiments is lost. To rectify this it is explained that a further linearization with respect to a second parameter is needed, this being the local

undisturbed relative motion between ship and water surface. If we denote the total free-surface condition by {A} it is written:

$$\{A\}_{x_3=\zeta} = \{A\}_{\substack{x_3=0\\ s=0}} + \left(\zeta^{(0)} + \zeta^{(1)}\right)\frac{\partial}{\partial x_3}\{A\}_{\substack{x_3=0\\ s=0}} + \left(s^{(0)} + s^{(1)}\right)\frac{\partial}{\partial s}\{A\}_{\substack{x_3=0\\ s=0}} \tag{8-8}$$

The thus linearized body condition becomes:

$$\left[\dot{\overline{\alpha}} + (\overline{W}\cdot\nabla)\,\overline{\alpha} - (\overline{\alpha}\cdot\nabla)\,\overline{W} - \zeta^{(1)}\frac{\partial}{\partial x_3}(\overline{W}) - s^{(1)}\frac{\partial}{\partial s}(\overline{W}) - \varphi^{(1)}\right]\cdot n = 0 \tag{8-15}$$

This second linearization introduces an interaction between the steady and the unsteady potentials, which leads to a formulation for the unsteady problem that can only be solved after some further reduction.

This further reduction is brought about by examination of the boundary conditions and assumptions on the relative importance of the various terms, leading to discarding some terms, while retaining what are assumed to be the most important terms.

This leads to a free-surface condition and a body-boundary condition containing terms that appear more accessible to a solution.

At this stage the unsteady boundary conditions on the free surface and on the body each contain three terms that have features that we recognize in relation to the flow effects observed. Guided by observations of experiments and experimental data it is assumed that the boundary conditions can be grouped in pairs thus leading to three separate unsteady boundary value problems, for which solutions can be found. The free-surface conditions and the body conditions of the three problems are respectively:

Problem A:

$$\left\{\left(\frac{\partial}{\partial t} - U\frac{\partial}{\partial x_1}\right)^2 + g\frac{\partial}{\partial x_3}\right\}\varphi^{(1)} = 0 \tag{8-21}$$

$$\varphi_n^{(1)} = \left\{\dot{\overline{\alpha}} - U\left(\overline{\Omega} * \overline{i}\right)\right\}\cdot n \tag{A-54}$$

Problem B:

$$\left\{\left(\frac{\partial}{\partial t}-U\frac{\partial}{\partial x_1}\right)^2+g\frac{\partial}{\partial x_3}\right\}\varphi^{(1)}=-\zeta^{(1)}\frac{\partial}{\partial x_3}\left\{g\varphi_{x_3}^{(0)}+U^2\varphi_{x_1x_1}^{(0)}\right\} \tag{8-22}$$

$$\varphi_n^{(1)}=-\zeta^{(1)}\frac{\partial}{\partial x_3}\overline{W}\cdot n \tag{8-17}$$

Problem C:

$$s^{(1)}\frac{\partial}{\partial s}\left(g\varphi_{x_3}^{(0)}+U^2\varphi_{x_1x_1}^{(0)}\right)=0 \tag{8-20}$$

$$s^{(1)}\frac{\partial}{\partial s}(\overline{W})\cdot n=0 \tag{8-18}$$

The solutions to the three separate unsteady problems is further pointed out in Section 8.3. It is indicated that the first problem {A} can be solved by a Green's functions solution, while the second and the third problem can be solved by assuming a low frequency modulation of the steady forward speed solution, so that diffraction effects and radiation effects can, in this part of the solution, be neglected relative to the 'dynamic swell-up' effects.

In Section 8.4 the unsteady potential is decomposed into a number of linear superimposed unsteady potentials:

$$\varphi^{(1)}=\left\{\zeta_0(\varphi_0+\varphi_7)+\sum_{j=1}^{6}\xi_j\varphi_j-\zeta_{s1}\frac{\partial}{\partial x_3}\varphi^{(0)}+s\frac{\partial}{\partial s}\varphi^{(0)}\right\}\cdot e^{-i\omega_e t} \tag{8-33}$$

in which we identify separately:

- incident wave potential,
- diffraction potential,
- radiation potentials,
- first swell-up potential, associated with extrapolation of the steady velocity gradient,
- second swell-up potential, associated with the change in steady flow with the relative motion.

In Section 8.5 the pressure in the fluid is worked out down to the second order. Utilizing the power series expansion for the potential, and utilizing similar

expressions for the ship motions we obtain expressions for the zero, first order, and second order pressure components.

$$p = p^{(0)} + \varepsilon p^{(1)} + \varepsilon^2 p^{(2)} + \ldots\ldots \tag{8-42}$$

In Section 8.6 the appropriate expressions for the integration boundary are derived. This has been done by using Bernoulli's equation to derive the free-surface elevation, which after a linearization with respect to the calm waterplane and substitution of the power series expansion for the potential can also be written as a power series. Based on this derivation an expression is obtained for the first order free-surface elevation and eventually for the first order relative motion.

In Section 8.7 an explanation is given of the relation between the first order pressure and the first order free-surface elevation, which are closely related.

$$p^{(1)} = -\rho\left(\varphi_t^{(1)} + W\cdot\nabla\varphi^{(1)}\right) + \rho g\, s\left\{1 - \frac{\partial}{\partial s}\left(\frac{W^2}{2g}\right)\right\}\left(\frac{g + \overline{W}\cdot\overline{W}x_3}{g}\right) \tag{8-61}$$

$$\zeta^{(1)} = -\frac{1}{g}\left(\varphi_t^{(1)} + W\cdot\nabla\varphi^{(1)}\right)\left(\frac{g}{g + \overline{W}\cdot\overline{W}x_3}\right) + \left[\zeta_i\left\{1 - \frac{\partial}{\partial s}\left(\frac{W^2}{2g}\right)\right\} + \alpha_3\frac{\partial}{\partial s}\left(\frac{W^2}{2g}\right)\right] \tag{8-62}$$

Both these terms play a prominent role in the expression for the force. It is indicated that the differences arise from the interaction with the steady flow field.

In Section 8.8 the hydrodynamic force is worked out to zero, first and second order. This is based on the appropriate expressions for the pressure and the integration boundary each in terms of a zero, first and second order contribution.

$$\overline{F} = \overline{F}^{(0)} + \varepsilon\overline{F}^{(1)} + \varepsilon^2\overline{F}^{(2)} + \ldots\ldots\ 0(\varepsilon^3) \tag{8-65}$$

The zero order mean value in the longitudinal direction represents the total resistance of the ship, from which after subtraction of the calm water resistance the 'wave added resistance' is obtained. In line with the derivation this wave added resistance contains contributions from up to second order pressures, which itself only contain contributions from first order motions and flow velocities. A summary table to show the make-up of the forces is provided.

In Section 8.9 the practical implementation is explained. With the use of the expressions as derived the 'wave added resistance' was numerically computed for which use was made of existing computer codes for the steady flow field (DAWSON), and for the unsteady flow field (PRECAL). The steady flow field program utilizes more refined boundary conditions than we have obtained in the derivation, which can be obtained by further elaboration of the steady problem proper.

8.2 Introduction

In the present chapter 8 a formulation is derived for the mean added resistance of a ship sailing in waves.

A ship sailing amongst waves experiences forces from the waves in all six degrees of freedom, i.e. three forces and three moments. These forces are composed of a mean value plus an oscillatory component, varying in time. We concern ourselves here with the mean value of the longitudinal force since it is this force component that impedes the sailing of the ship through the water, slows the ship down and is rightly called 'mean added resistance due to waves'.

It should be understood that the presence of waves contributes to the slowing down of the ship in many ways, directly and indirectly. Directly through exerting a force on the ship hull that represents a 'drag' force and indirectly because of deterioration of propulsion efficiency and even voluntary speed reduction. We concern ourselves here with the direct effect.

Following the empirical observation in model experiments as set forth in Chapters 6 and 7 in which a close relation was observed between the mean added resistance and the relative motion of the fluid surface with respect to the hull, the formulation of the mathematical model is sought in the description of the near field as an integration of the pressure over the hull.

$$\overline{F} = -\iint_A p\,\overline{n}\,dA \tag{8-1}$$

in which: $\overline{F}$ = force vector
p = hydrodynamic pressure
$\overline{n}$ = direction normal on the hull
A = wetted area.

In order to carry out the integration, expressions have to be found for the pressure, the normal and the integration area, all of which vary with space and time.

The fluid flow about the ship is supposed to be described by a potential flow and a scalar potential subject to assumptions on the fluid and the flow as a continuum, homogeneous, isotropic, inviscid, irrotational and incompressible.

The potential is hypothesized as a linear superposition series of components due to uniform flow, steady perturbation due to forward speed and time-dependent oscillatory potentials of first and higher order:

$$\Phi = \varphi^{(0)} + \varepsilon\varphi^{(1)} + 0(\varepsilon^2) \tag{8-2}$$

in which: $\varphi^{(0)}$ = steady flow potential (uniform flow plus perturbation potential)

$\varphi^{(1)}$ = first order oscillatory potential.

The oscillatory potential is to contain the effect of the incident harmonic wave, the reflected or diffracted wave and the radiated waves due to the ship motions. In the formulation an interaction effect is introduced between the steady and unsteady potential, which describes the dynamic swell-up effect of the water so very much in evidence around the bow of a ship sailing in waves.

The potential is to satisfy the Laplace equation throughout the fluid domain and a set of suitably defined boundary conditions on the hull, on the free fluid surface, on the sea bottom and at infinity. A boundary value problem is formulated which can be solved by numerical means.

In view of the assumed series for the potential a similar series is assumed for the derived quantities like fluid velocity, free-surface elevation, pressure on the hull and eventually also ship motions.

A fundamental step, taken early in the formulation, is the selection of a suitable system of axes in which to formulate the problem. We can identify a space-fixed system of axes and a body-fixed system of axes. In addition we can identify a 'go-between' as a system of axes with the origin in the waterplane, the axes remaining parallel to the space-fixed axes at all times. This system of so-called 'travelling axes' can be used to advantage for the formulation of the problem.

Having solved for the potential, the quantities required for the force can be obtained.

The pressure is obtained from the Bernoulli equation, which relates the pressure to the kinetic energy and the potential energy of the fluid and the local acceleration potential, all of which in turn depend on the velocity potential.

$$\Phi_t + \tfrac{1}{2}V^2 + \frac{p}{\rho} + gX_3 = c(t) \tag{8-3}$$

in which: Φt = time-wise derivative of the potential

V = velocity of the fluid

p = pressure

ρ = fluid density

g = acceleration due to gravity

X_3 = vertical coordinate with respect to earth-fixed axes
c(t)= a constant, that may depend upon time.

The normal on the ship hull can be taken in a body-fixed system of axes after taking due account of the ship motions.

The area of integration is to be defined on the ship hull. In principle the pressure is to be integrated over the wetted area of the hull, yet this is composed of parts that are wet all the time and parts that become alternatively wet and dry because of ship motions and the passing of the wave crest along the ship. A clear distinction is to be made between these areas and likewise between the components of the integration.

Through a suitable linearization scheme the surface integral can be expressed as the sum of a surface integral to be taken over the static, continuously wetted, area of the submerged body and a line integral to be taken along the waterline.

A point of interest arises with respect to the order to which the series expansion of the potential and the derived quantities are to be extended. The mean added resistance stems from the time-averaging of the second order force. This second order force in turn depends on zero, first and second order quantities. On basis of experimental observations the mean force is thought to be so strongly related to the mean and first order quantities that the second order quantities arising from second order potentials alone can in this respect be neglected.

Finally, we are not so much concerned with the force as a function of time as with the mean value which is obtained through time-averaging of the force.

8.3 The boundary value problem

General

We pursue the derivation as set forth in the Appendix on hydrodynamic theory. In the derivation of the free-surface condition eq. (A-43) it was assumed that the oscillatory potential is an order of magnitude smaller than the potential of the steady-state disturbance. This is a quite common approach in seakeeping analysis to preserve linearity, and has proven to give very good results, even for not-so-very-small oscillations. As a consequence also the amplitude of the instationary free-surface elevation is considered to be small as compared to the amplitude of the steady-state free-surface elevation (the bow and stern wave system). In this concept the small amplitude of the oscillatory free-surface elevation is thought to be superimposed on the steady-state elevation. In the linearization applied in deriving eq. (A-44) the equation to be satisfied on the actual free-surface ζ is 'brought down' to the steady elevation $\zeta^{(0)}$ through a Taylor expansion of the equation with respect to the vertical *(x3)* coordinate.

The free surface is in this approach considered to be the sum of the steady elevation and the unsteady elevation without interaction. This is the result of linear decomposition of the total potential.

Another important point is that the assumption inherent in this linearization (like any linearization) is that the various functions (potentials and their derivatives) as a function of field coordinates remain the same when the boundary condition is removed from ζ to the lower level of $\zeta^{(0)}$.

As explained in Chapters 6 and 7 experimental evidence tells us this is clearly not the case and it is at this point in the derivation that the 'dynamic swell-up' effect of the free surface, so much in evidence at the ship's bow, is lost. Consequently any free-surface condition (simplification) derived from this one equation (A-44), whether it be (A-45) or (A-46) also lacks the 'dynamic swell-up' effect.

We may further illustrate this point by considering again the unsteady free-surface condition at the actual instantaneous surface: eq. (A-43). This equation stems from the complete equation, eq. (A-28), for the unsteady and steady potential:

$$\Phi_{tt} + 2\nabla\Phi\cdot\nabla\Phi_t + \tfrac{1}{2}\nabla\Phi\cdot\nabla(\nabla\Phi\cdot\nabla\Phi) + g\Phi_{x_3} = 0 \quad on\ X_3 = \zeta \qquad \text{(A-28)}$$

When we consider an entirely steady potential, the first two terms can simply be set to zero. If we consider a time-dependent slowly oscillating potential, with a frequency so low that at any one moment an almost static condition were to exist, then the first two terms cannot be dropped, but they can be neglected with respect to the other two terms.

In physical terms one can think of a ship sailing in flat calm water and making heave oscillations with very low frequency. At any moment, if we neglect the dynamics, the static terms that determine the steady bow wave system are retained and since the expression has to be satisfied at the actual - yet unknown - free surface, the 'dynamic well-up effect' is still present in this description.

In order to retain the 'dynamic swell-up effect' in the free-surface condition we have to back-track to eq. (A-43) and apply a modified linearization scheme to incorporate the interaction between steady and unsteady flow that - interesting enough - has features that are linear with the unsteady oscillation amplitudes.

The rationale underlying this point has been discussed in Chapter 6 where it was concluded that a double linearization scheme was required to include all the observed physicalities in the first order oscillatory potential.

In the modified linearization scheme we utilize two linearization parameters. The first is the space-fixed vertical field coordinate X_3 (or x_3 in travelling axes). The second is the body-fixed parameter s. This parameter represents the undisturbed -nominal- relative motion between the ship and the free surface and is composed of rigid body motions as well as incident sinusoidal waves. One can

most easily think of parameter s as being the instantaneous variation of the local draft, that varies with time. We have chosen for the 'nominal' relative motion, without disturbances, because this can be viewed as an input quantity, and the disturbances, like radiated waves, as the output quantities.

Because of this parameter s the steady bow wave will be evaluated with respect to the instantaneous draft and hence will 'swell up and down' with the draft. The dependency of the steady bow wave on this additional parameter is in all contemporary literature neglected and all expressions are simply evaluated for the mean nominal draft. As shown in Chapter 7 it is not a small quantity that is lost in such an approach. In the following sections the modified linearization scheme will be further explained.

The modified linearized free-surface condition

We take the linear free-surface condition as expressed in eq. (A-43) as departure point, in which the second order terms have been neglected, and interaction between steady and unsteady terms is retained. This expression is to be evaluated on the unknown surface $x_3 = \zeta$, which is to be reduced to an expression to be satisfied on $x_3 = 0$ through a suitable Taylor expansion. The unsteady potential contains components related to the non-uniform steady velocity field and components related to the dynamic swell-up effect which we may wish to separate at a later stage; for the moment we keep them combined.

Another point of interest is the coordinate system. The free-surface condition is most suitably expressed in a coordinate system that travels with the mean position of the trisection of the three main planes of the ship, the axes of which are at all times parallel to the space-fixed axes: $O(\bar{x})$.

Although in the derivation a dependency on the relative motion s in a truly body-fixed system of axes is identified, this does not necessitate us to transpose the expressions onto body-fixed field coordinates. Indeed in the free-surface condition we adhere to the travelling axes $O(\bar{x})$.

For ease of reference we repeat the free-surface condition of expression (A-43):

$$\begin{aligned} &\tfrac{1}{2}\overline{W}\cdot\nabla(W^2) + g\varphi_{x_3}^{(0)} + \varphi_{tt}^{(1)} + 2\overline{W}\cdot\nabla\varphi_t^{(1)} + \overline{W}\cdot\nabla(\overline{W}\cdot\nabla\varphi^{(1)}) \\ &+ \tfrac{1}{2}\nabla\varphi^{(1)}\cdot\nabla(W^2) + g\varphi_{x_3}^{(1)} = 0 \qquad \text{on } x_3 = \zeta \end{aligned} \tag{A-43}$$

For the sake of brevity we denote this full expression by {A} and the collection

of steady and unsteady terms by {B} and {C} respectively, so that the above expression can be written as:

$$\{A\} = 0 \quad \text{or} \tag{8-4}$$

$$\{B + C\} = 0 \quad \text{in which} \tag{8-5}$$

$$\{B\} = g\varphi_{x_3}^{(0)} + \tfrac{1}{2}\overline{W}\cdot\nabla(W^2) \tag{8-6}$$

$$\{C\} = \varphi_{tt}^{(1)} + 2\overline{W}\cdot\nabla\varphi_t^{(1)} + \overline{W}\cdot\nabla\left(\overline{W}\cdot\nabla\varphi^{(1)}\right) + \tfrac{1}{2}\nabla\varphi^{(1)}\cdot\nabla(W^2) + g\varphi_{x_3}^{(1)} \tag{8-7}$$

to be satisfied on $x_3 = \zeta$

$$= \zeta^{(0)} + \zeta^{(1)}$$

in which: $\zeta^{(0)}$ = steady free-surface elevation

$\zeta^{(1)}$ = unsteady free-surface elevation.

The quantity {A} contains terms of O(1) and O(ε), quantity {B} contains solely quantities of O(1) and finally quantity {C} contains terms of O(ε).

Now we introduce the concept that the various functions present in the free-surface condition depend on the space-fixed field coordinates as well as the nominal vertical relative motion between the ship hull and the water surface, which is in fact the free-surface elevation taken in a body-fixed system of axes.

In the above expression the functions contained in {A} are also made dependent upon a second variable s because the term thus added is thought to have the same order of magnitude as the other terms, as experimental evidence has indicated.

Applying a Taylor's expansion in two variables and truncating after the first order, we obtain:

$$\{A\}_{x_3=\zeta} = \{A\}_{\substack{x_3=0\\ s=0}} + \left(\zeta^{(0)} + \zeta^{(1)}\right)\frac{\partial}{\partial x_3}\{A\}_{\substack{x_3=0\\ s=0}} + \left(s^{(0)} + s^{(1)}\right)\frac{\partial}{\partial s}\{A\}_{\substack{x_3=0\\ s=0}} \tag{8-8}$$

In this expansion the derivatives are only taken up to the first order; unless the contrary will be shown, this is thought to suffice.

At this point it may be useful to reconsider the power series expansion for the potential with respect to the small parameter ε, eq. (A-34) and the subsequent

split-up of the potential in eq. (A-36). It will be useful in the sequel to make the following decomposition:

$$\varphi = \varphi^{(0)} + \varepsilon\varphi^{(1)} + 0(\varepsilon^2) \tag{A-34}$$

$$\varphi^{(1)} = \varphi_i + \varphi_d + \varphi_r + \varphi_s \tag{8-9}$$

in which: $\varphi^{(0)}$ = steady potential, including uniform flow
φ_i = potential of incident wave
φ_d = potential of diffracted (scattered) wave
φ_r = potential of radiated waves
φ_s = potential of dynamic swell-up effect.

In a likewise manner we decompose the free-surface elevation as follows:

$$\zeta = \zeta^{(0)} + \zeta^{(1)} \tag{8-10}$$

$$\zeta^{(1)} = \zeta_i + \zeta_d + \zeta_r + \zeta_s \tag{8-11}$$

If the expression (A-34) for the potential is substituted in the free-surface condition of eq. (8-8) and the terms of order O(1) and O(ε) are separated we obtain the following expressions.

For order O(1):

$$\left(1 + \zeta^{(0)}\frac{\partial}{\partial x_3} + s^{(0)}\frac{\partial}{\partial s}\right)\{B\} = 0 \qquad \text{at } \begin{matrix} x_3 = 0 \\ s = 0 \end{matrix} \tag{8-12}$$

This expression can be interpreted as the linearization of the exact steady free-surface condition at the level $x_3 = \zeta^{(0)}$ which is expanded with respect to $x_3 = 0$ and $s = 0$.

For order O(ε): Referring to expressions (8-6) and (8-7) for the meaning of the quantities {B} and {C} we obtain:

$$\left(1 + \zeta^{(0)}\frac{\partial}{\partial x_3} + s^{(0)}\frac{\partial}{\partial s}\right)\{C\} + \left(\zeta^{(1)}\frac{\partial}{\partial x_3} + s^{(1)}\frac{\partial}{\partial s}\right)\{B\} = 0$$

$$\text{at } \begin{matrix} x_3 = 0 \\ s = 0 \end{matrix} \tag{8-13}$$

In order to reduce this expression to manageable proportions we need to make a number of assumptions.

In expression (8-13) we make the following assumptions noting that the expression is composed of five terms.

First we assume that the second and third terms can be neglected with respect to the first, fourth and fifth terms. The major interaction between the unsteady and the steady flow has features that we recognize in the first term {C} and in the last terms, where the steady free-surface condition is modulated by the first

order free-surface rise and by the relative motion parameter $s^{(1)}$. The rationale behind this assumption is based on the observation that terms related to the unsteady flow (like heave and pitch motions, exciting forces and reaction forces) are not strongly dependent on the ship's draft (or for that matter on the position of the boundary level at $x_3 = \zeta^{(0)}$ or $x_3' = s^{(0)}$) and that in those cases where the flow is strongly related to draft, for instance in the case of dynamic swell-up at the bow, the flow effects appear to be more related to the fourth and fifth terms.

Secondly we assume that $\varphi_i + \varphi_s > \varphi_r + \varphi_d$ which means that the ship is a 'weak scatterer'. It is to be understood that the radiated and diffracted waves and their potentials are not really smaller by an order of magnitude as that would have meant deletion of these terms altogether as being $O(\varepsilon^2)$. Rather for practical reasons we assume that the incident wave effect and related rigid body motions and related 'dynamic swell-up' effects prevail. As a result we put $\varphi_i + \varphi_s > \varphi_r + \varphi_d$ and neglect the smaller in the unsteady free-surface condition.

Thirdly we assume $\overline{W} = -U\bar{i}$ in the expression for the unsteady condition {C} and we assume a base flow $\overline{W} = -U\bar{i}$ in the expression for the steady condition {B}. In doing this the latter condition reduces to the so-called Neumann-Kelvin condition.

On the basis of these three assumptions we obtain the following expression for the unsteady free-surface condition:

$$\left\{\left(\frac{\partial}{\partial t} - U\frac{\partial}{\partial x_1}\right)^2 + g\frac{\partial}{\partial x_3}\right\}\varphi^{(1)} +$$

$$+\left(\zeta^{(1)}\frac{\partial}{\partial x_3} + s^{(1)}\frac{\partial}{\partial s}\right)\left\{g\varphi_{x3}^{(0)} + U^2\varphi_{x_1x_1}\right\} = 0 \qquad \text{for } \begin{matrix} x_3 = 0 \\ s = 0 \end{matrix} \qquad (8\text{-}14)$$

in which: $\zeta^{(1)} = \zeta_i + \zeta_s$.

The modified linearized body boundary condition

We take the linear body boundary condition as expressed in eq. (A-50) as point of departure:

$$\left(\dot{\bar{\alpha}} - \overline{W} - \varphi^{(1)}\right)\cdot \bar{n} = 0 \qquad (A\text{-}50)$$

to be satisfied on the instantaneously wetted surface A.

This expression implies that the first order unsteady potential has to counteract the two other terms which are there anyway. The first term represents the first order motion through the undisturbed flow, the second term contains two first order contributions that we can easily imagine:

- the rotation of the ship-bound coordinate system in the otherwise undisturbed steady flow;
- the movement of a body-fixed point through the gradient field of the steady flow.

To use this expression in the formulation of a boundary value problem we shall have to invoke a linearization with respect to the ship in its mean position and use the mean nominal wetted surface.

However, as we linearize another contribution comes into being. As the ship rotates through an undisturbed fluid or as the body point moves through the steady gradient field a surface elevation and a relative motion are set up that alters the steady flow in a first order manner. These changes in the flow pattern should not be neglected and need also be incorporated in the linearized expression. We obtain:

$$\left[\dot{\bar{\alpha}} + (\overline{W} \cdot \nabla)\,\bar{\alpha} - (\bar{\alpha} \cdot \nabla)\overline{W} - \zeta^{(1)} \frac{\partial}{\partial x_3} (\overline{W}) - s^{(1)} \frac{\partial}{\partial s} (\overline{W}) - \varphi^{(1)} \right] \cdot n = 0 \tag{8-15}$$

to be satisfied on $\overline{A}$, the mean wetted surface.

On account of a reasoning similar to that invoked for the free-surface condition we assume certain interactions to be negligible and split up the expression in parts to be satisfied by the various potentials piecemeal:

$$\varphi_n^{(1)} = \left(\dot{\bar{\alpha}} + (W \cdot \nabla)\bar{\alpha} - (\bar{\alpha} \cdot \nabla)\overline{W} \right) \cdot n \tag{8-16}$$

$$\varphi_n^{(1)} = -\zeta^{(1)} \frac{\partial}{\partial x_3} (\overline{W}) \cdot n \tag{8-17}$$

$$s^{(1)} \frac{\partial}{\partial s} (\overline{W}) \cdot n = 0 \tag{8-18}$$

to be satisfied on $\overline{A}$.

The first part above can be further simplified if we assume $\overline{W} = -U\bar{i}$, it then follows:

$$\varphi_n^{(1)} = \left[\dot{\bar{\alpha}} - U(\overline{\Omega} * \bar{i}) \right] \cdot \bar{n} \tag{A-54}$$

It will be shown in the following section how these expressions are combined with the free-surface boundary condition to define a number of boundary value problems.

Splitting up the unsteady free-surface condition

We have obtained an expression for the unsteady first order free-surface condition that is not amemable to a solution without further reduction. Guided by observations of experiments and experimental data - Chapters 6 and 7 - we propose to separate the expression into three parts that will be treated separately. In principle each component potential should satisfy the whole expression so in separating it, it is tacitly assumed that interactions between the solutions is only weak and may be neglected.

One of the components is to contain time-dependent parts and will lead to a solution that represents propagating waves. The other two conditions will be further reduced and in the process an assumption on low frequency is made. These represent quasi-stationary modulations of the steady potential on which the time-dependency is enforced by the relative motion. Yet at each instant the solution is in fact a stationary one and is in itself time independent.

$$\left\{\left(\frac{\partial}{\partial t}-U\frac{\partial}{\partial x_1}\right)^2+g\frac{\partial}{\partial x_3}\right\}\varphi^{(1)}=-\zeta^{(1)}\frac{\partial}{\partial x_3}\left(g\varphi_{x_3}^{(0)}+U^2\varphi_{x_1x_1}^{(0)}\right) \qquad (8\text{-}19)$$

$$s^{(1)}\frac{\partial}{\partial s}\left\{g\varphi_{x_3}^{(0)}+U^2\varphi_{x_1x_1}^{(0)}\right\}=0 \qquad (8\text{-}20)$$

The first expression (8-19) is further split up into:

$$\left\{\left(\frac{\partial}{\partial t}-U\frac{\partial}{\partial x_1}\right)^2+g\frac{\partial}{\partial x_3}\right\}\varphi^{(1)}=0 \qquad (8\text{-}21)$$

$$\left\{\left(\frac{\partial}{\partial t}-U\frac{\partial}{\partial x_1}\right)^2+g\frac{\partial}{\partial x_3}\right\}\varphi^{(1)}=-\zeta^{(1)}\frac{\partial}{\partial x_3}\left(g\varphi_{x_3}^{(0)}+U^2\varphi_{x_1x_1}^{(0)}\right) \qquad (8\text{-}22)$$

These expressions should all be evaluated at $x_3 = 0$ and $s = 0$. For the homogeneous eq. (8-21) we shall have to find a general solution, and for the inhomogeneous equation we shall have to obtain a particular solution.

It should be noted that in eq. (8-22) the quantity $\zeta^{(1)}$ contains the surface elevation of the incident wave and the swell-up potential, since these are the dominant terms in the unsteady free-surface elevation, see eq. (8-14).

Splitting up the unsteady boundary value problem

Drawing upon the foregoing we have obtained the following three components for free-surface conditions:

$$\left\{\left(\frac{\partial}{\partial t}-U\frac{\partial}{\partial x_1}\right)^2+g\frac{\partial}{\partial x_3}\right\}\varphi^{(1)}=0 \tag{8-21}$$

$$\left\{\left(\frac{\partial}{\partial t}-U\frac{\partial}{\partial x_1}\right)^2+g\frac{\partial}{\partial x_3}\right\}\varphi^{(1)}=-\zeta^{(1)}\frac{\partial}{\partial x_3}\left\{g\varphi_{x_3}^{(0)}+U^2\varphi_{x_1x_1}^{(0)}\right\} \tag{8-22}$$

$$s^{(1)}\frac{\partial}{\partial s}\left\{g\varphi_{x_3}^{(0)}+U^2\varphi_{x_1x_1}^{(0)}\right\}=0 \tag{8-20}$$

Also we have in a likewise manner obtained the body boundary condition on which we effect a split-up as follows in similar fashion:

$$\varphi_n{}^{(1)}=\left(\dot{\overline{\alpha}}+(W\cdot\nabla)\overline{\alpha}-(\overline{\alpha}\cdot\nabla)\overline{W}\right)\cdot n \tag{8-16}$$

$$\varphi_n{}^{(1)}=-\zeta^{(1)}\frac{\partial}{\partial x_3}(\overline{W})\cdot n \tag{8-17}$$

$$s^{(1)}\frac{\partial}{\partial s}(\overline{W})\cdot n=0 \tag{8-18}$$

Finding solutions for the unsteady potentials

If we combine the three free-surface conditions and the three body boundary conditions, as we have proposed before, we will obtain three sets of expressions that define three boundary value problems:

Problem A:

$$\left\{\left(\frac{\partial}{\partial t}-U\frac{\partial}{\partial x_1}\right)^2+g\frac{\partial}{\partial x_3}\right\}\varphi^{(1)}=0 \tag{8-21}$$

$$\varphi_n{}^{(1)}=\left\{\dot{\overline{\alpha}}+(W\cdot\nabla)\,\overline{\alpha}-(\overline{\alpha}\cdot\nabla)\,\overline{W}\right\}\cdot n \tag{8-16}$$

Problem B:

$$\left\{\left(\frac{\partial}{\partial t}-U\frac{\partial}{\partial x_1}\right)^2+g\frac{\partial}{\partial x_3}\right\}\varphi^{(1)}=-\zeta^{(1)}\frac{\partial}{\partial x_3}\left(g\varphi_{x_3}^{(0)}+U^2\varphi_{x_1x_1}^{(0)}\right) \tag{8-22}$$

$$\varphi_n{}^{(1)}=-\zeta^{(1)}\frac{\partial}{\partial x_3}(\overline{W})\cdot n \tag{8-17}$$

Problem C:

$$s^{(1)}\frac{\partial}{\partial s}\left(g\varphi_{x_3}^{(0)}+U^2\varphi_{x_1x_1}^{(0)}\right)=0 \tag{8-20}$$

$$s^{(1)}\frac{\partial}{\partial s}(\overline{W})\cdot n=0 \tag{8-18}$$

In splitting up the boundary conditions and combining them in the above fashion we neglect a good deal of interaction between the terms involved, yet it is thought to describe the major first order flow effects that were observed in the experiments.

The solution to problem A

This set of boundary conditions define a solution for the radiation and the diffraction problem and the solution has been obtained elsewhere. The solution is possible by such numerical tools as for instance the source distribution method. Reference is made to Section 8.9 for the practical implementation.

The solution to problem B

If we attempt to construct a solution to problem B it should be noted that the free-surface elevation $\zeta^{(1)}$ on the right-hand side contains in principle the free-surface elevations due to all unsteady first order potentials. Yet as mentioned earlier it is assumed that $\varphi_i + \varphi_s > \varphi_r + \varphi_d$, so that only the effect of the incident wave and the swell-up potentials - of both problems B and C - are to be retained.

A solution cannot be obtained in a simple way. We make therefore a further

reduction to obtain a 'base-line' solution and assume the frequency $\omega \rightarrow 0$, so that the expressions reduce to:

$$\left(g\varphi_{x_3}^{(1)} + U^2\varphi_{x_1x_1} \right) = -\zeta^{(1)} \frac{\partial}{\partial x_3} \left(g\varphi_{x_3}^{(0)} + U^2\varphi_{x_1x_1}^{(0)} \right) \tag{8-23}$$

$$\varphi_n^{(1)} = -\zeta^{(1)} \frac{\partial}{\partial x_3} (\overline{W}) \cdot n \tag{8-17}$$

Since the surface elevation is not dependent upon x_3 and only very weakly on x_1 (for low frequency) it can be shown that the following potential suffices the boundary conditions:

$$\varphi_{s1} = -\zeta^{(1)} \frac{\partial}{\partial x_3} \varphi^{(0)} \tag{8-24}$$

$$\text{with } \zeta^{(1)} = \left\{ \zeta_i \left(1 - \frac{\partial}{\partial x_3} \frac{W^2}{2g} \right) + \xi_3 \frac{\partial}{\partial s} \frac{W^2}{2g} \right\} \tag{8-25}$$

which represents a quasi-stationary solution, and is denoted the first swell-up potential. See also the following section.

In order to show that the potential φ_{s1} leads to a surface elevation described by (8-25) we draw upon Section 8.6 where the general expression for the free-surface elevation is derived:

$$\zeta^{(1)} = -\frac{1}{g} (\varphi_t^{(1)} + \overline{W} \cdot \nabla\varphi^{(1)}) \cdot \left(\frac{g}{g + \overline{W} \cdot \overline{W}_{x_3}} \right) \tag{8-55}$$

The elevation contains contributions from the incident wave φ_i, from the swell-up potential φ_{s1} of problem B and also from the swell-up potential φ_{s2} of problem C. The latter represents an important coupling between the solutions. We obtain:

from φ_i : $-\frac{\varphi_t}{g} = \zeta_i$ incident wave elevation

$W \cdot \nabla\varphi = 0$ because long waves are implied

from φ_{s1} : $\varphi_t = 0$ because $\omega \rightarrow 0$

$$W \cdot \nabla\varphi = -\left\{ \zeta_i \left(1 - \frac{\partial}{\partial s} \frac{W^2}{2g} \right) + \xi_3 \frac{\partial}{\partial s} \left(\frac{W^2}{2g} \right) \right\} \frac{\partial}{\partial x_3} \left(\frac{W^2}{2} \right)$$

from φ_{s2} : $\varphi_t = 0$

$$W \cdot \nabla\varphi = s^{(1)} \frac{\partial}{\partial s}\left(\tfrac{1}{2} W^2 \right)$$

if we substitute these terms into the expression (8-55) we obtain after some algebra:

$$\zeta^{(1)} = \zeta_i \left(1 - \frac{\partial}{\partial s} \frac{W^2}{2g} \right) + \xi_3 \frac{\partial}{\partial s} \frac{W^2}{2g} \tag{8-25}$$

which represents a quantity significantly greater than the incident wave.

The solution to problem C

The boundary conditions defining problem C show a modulation of the steady boundary condition with the relative motion. Since the unknown unsteady potential is not included it does not seem to lead to a first order potential. However, the flow effect that it describes is an important first order effect which can perhaps be illustrated by the following reasoning in which we for simplicity only deal with the free-surface condition.

We again refer to Section 6.5 for the 'long wave case', where the wave length is so long so as to result effectively into a deeper draft. If we denote the linearized steady free-surface condition of eq. (A-40) by $\overline{FSC}$ then:

$$\text{for the deep draft: } \overline{FSC} \Big|_{s=s} = 0 \tag{8-26}$$

Linearization with respect to the nominal draft leads to:

$$\overline{FSC} \Big|_{s=0} + s^{(1)} \frac{\partial}{\partial s} \overline{FSC} \Big|_{s=0} = 0 \tag{8-27}$$

Since $s^{(1)}$ does not depend on spatial coordinates it follows that if $\varphi^{(0)}$ satisfies $\overline{FSC}$ (for s=0) and $\varphi^{(0,s)}$ satisfies $\overline{FSC}$ for s=s then the increment potential $s^{(1)}(\partial/\partial s)\varphi^{(0)}$ satisfies the term $\overline{FSC}$ at s=0, since the derivatives can be exchanged.

To find a solution to problem C it was necessary to assume low frequency, hence long waves, so that the time dependency could be removed, and a space-wise solution can be constructed. It is assumed that $s^{(1)}$ contains only the governing quantities, incident wave elevation and ship motions.

The flow effect that it is meant to describe can be shaped in the form of a first order potential:

$$\varphi_{s2} = s^{(1)} \frac{\partial}{\partial s} \varphi^{(0)} \Big|_{s=0} \tag{8-28}$$

As the relative motion s is independent of x_3 and x_1 space coordinates, the derivatives with respect to the field coordinates and the relative motion can be exchanged so that:

$$\left(g\frac{\partial}{\partial x_3} + U^2\frac{\partial^2}{\partial x_1^2}\right)\left(s^{(1)}\frac{\partial}{\partial s}\varphi^{(0)}\right) =$$

$$s^{(1)}\frac{\partial}{\partial s}\left(g\frac{\partial}{\partial x_3} + U^2\frac{\partial^2}{\partial x_1^2}\right)\varphi^{(0)} = 0 \qquad (8\text{-}29)$$

In Chapter 6, and in the reasoning invoked above, a dependency of the potentials upon the parameter s was indicated. At that stage where only a long wave or uniform heaving motion was involved the relative motion s was the same all over the ship length and can be viewed as a scalar quantity or a leading order parameter of relative motion at the fore perpendicular.

The parameter s may, however, with some approximation also be taken locally, i.e. section wise, for which we invoke the following reasoning:

$$\varphi_{s2} = s^{(1)}\frac{\partial}{\partial s}(\varphi^{(0)}) \text{ satisfied } \overline{FSC} = 0$$

because we assumed that s does not depend on spatial coordinates, so that the derivatives could be exchanged.

The relative motion as some point along the ship length can be written as:

$$s^{(1)} = \zeta_i - \alpha_3 \qquad (8\text{-}30)$$

at any station along the length of the ship.

It can also approximately be written as:

$$s = s_{a20} \cdot f(x_1,\omega,\omega_e) \cdot e^{-ikx_1} \cdot e^{-i\omega_e t} \qquad (8\text{-}31)$$

in which s_{a20} represents the amplitude of the relative motion at the fore perpendicular (*station* 20) and $f(x_1)$ represents the envelope of amplitudes of

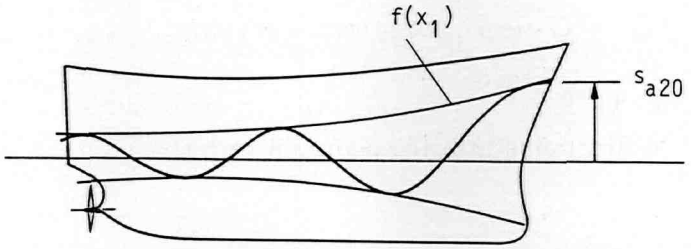

Figure 8-1: Relative motion in a body-fixed reference frame.

relative motion along the length of the ship, as shown in figure 8-1.

It should be noted that $f(x_1)$ depends on both wave length and ship speed, hence (ω,ω_e).

It is assumed that the x_1 derivative of $f(x_1)$ is small and that the wave number k is small, at least smaller than the x_1 derivatives of $\varphi^{(0)}$, then it can approximately be stated, that also in the case that $s^{(1)}$ is defined as the local relative motion we may set:

$$\overline{FSC}\left(s^{(1)} \frac{\partial}{\partial s}\varphi^{(0)} \right) = s^{(1)} \frac{\partial}{\partial s} \overline{FSC}\ \varphi^{(0)}$$

and by the same token the thus defined swell-up potential satisfies the boundary conditions.

With the assumption on local relative motion the expression (8-25) also involves the local vertical motion α_3 in lieu of ξ_3.

8.4 Linear decomposition of the unsteady potential

In keeping with the assumption of linear superimposed unsteady potentials we have decomposed the potential in eq. (8-9) as follows:

$$\varphi^{(1)} = \varphi_i + \varphi_d + \varphi_r + \varphi_{s1} + \varphi_{s2} \tag{8-32}$$

which we can further express as:

$$\varphi^{(1)} = \left[\zeta_0(\varphi_0 + \varphi_7) + \sum_{j=1}^{6} \xi_j\varphi_j - \zeta_{s1} \frac{\partial}{\partial x_3} \varphi^{(0)} + s \frac{\partial}{\partial s}\varphi^{(0)} \right] \cdot e^{-i\omega_e t} \tag{8-33}$$

so that:

$$\varphi_i = \frac{-i \cdot \zeta_0 \cdot g}{\omega} \cdot exp\left[k(x_3 + ix_1 \cos\mu + ix_2 \sin\mu) - i\omega_e t \right] \tag{8-34}$$

= incident wave potential with wave elevation

$$\zeta_i = \zeta_0 \cdot exp\left[k(ix_1 \cos\mu + ix_2 \sin\mu) - i\omega_e t \right]$$

$$\varphi_d = \zeta_0 \cdot \varphi_7 \cdot e^{-i\omega_e t} \tag{8-35}$$

= diffraction scattering potential such that:

$$\frac{\partial}{\partial n}(\varphi_0 + \varphi_7) = 0 \qquad \text{on } \bar{A}$$

$$\varphi_r = \sum_{j=1}^{6} \xi_j \varphi_j \cdot e^{-i\omega_e t} \tag{8-36}$$

= sum of six radiation potentials associated with the six basis ship motions, ϕ_j being the radiation potentials for unit motion

$$\varphi_{s1} = -\zeta_{s1} \frac{\partial}{\partial x_3} \varphi^{(0)} \cdot e^{-i\omega_e t} \tag{8-37}$$

= first swell-up potential, associated with extrapolation of the velocity gradient, where zs1 is equal to eq. (8-25) except for the time-dependent part

$$\varphi_{s2} = -s \frac{\partial}{\partial s} \varphi^{(0)} \cdot e^{-i\omega_e t} \tag{8-38}$$

= second swell-up potential, associated with the change in steady flow with the relative motion

The incident wave potential is a given quantity. The diffraction and the radiation potentials are solutions to problem A of Section 8.3, equations (8-21) and (8-16), the first swell-up potential φ_{s1} is the solution to the problem B of Section 8.3, while the second swell-up potential φ_{s2} is the solution to the problem C of Section 8.3.

8.5 The pressure in the fluid

The pressure in the fluid at a point fixed with respect to the steady translating axes is governed by the Bernoulli equation:

$$p = -\left\{ \rho\Phi_t + \tfrac{1}{2}|\nabla\Phi|^2 + \rho g x_3 \right\} + \tfrac{1}{2}\rho U^2 + c(t) + p_a \tag{8-39}$$

We may set $c(t)$ to zero and if all pressures are taken relative to the constant atmospheric pressure p_a then the last two terms may be deleted.

We are, however, not so much interested in the pressure at a fixed point in translating axes; our first interest lies more with the pressure at a point on the hull. Such a point, fixed with respect to body axes, carries out an oscillatory motion on the system of travelling axes. This oscillatory motion is, in principle, composed of all orders:

$$\bar{x} = \bar{x}' + \bar{\alpha}^{(0)} + \varepsilon\bar{\alpha}^{(1)} + \varepsilon^2\bar{\alpha}^{(2)} + \ldots\ldots \tag{8-40}$$

The pressure at the point on the hull can be expressed in the pressure at its

mean position (hence fixed in translating axes), by using the following vector form of the Taylor's expansion:

$$p(\bar{x}) = p(\bar{x}' + \bar{\alpha}) = p(\bar{x}') + (\bar{\alpha}\cdot\nabla)\,p\,(\bar{x}') + \frac{1}{2!}(\bar{\alpha}\cdot\nabla)^2 p(\bar{x}') \qquad (8\text{-}41)$$

Utilizing the power series expansion for the potential eq. (A-34) we can work out the appropriate expression for the pressure which as a result can also be written as a power series:

$$p = p^{(0)} + \varepsilon p^{(1)} + \varepsilon^2 p^{(2)} + \ldots\ldots \qquad (8\text{-}42)$$

in which:

$p^{(0)}$ = sum of the terms containing no ε: (8-43)

$-\rho g x_3^{(0)}$	hydrostatic term
$-\frac{1}{2}\rho W^2 + \frac{1}{2}\rho U^2$	kinetic term

$p^{(1)}$ = sum of the terms containing ε: (8-44)

$-\rho\varphi_t^{(1)}$	local acceleration term
$-\rho\overline{W}\cdot\nabla\varphi^{(1)}$	kinetic term
$-\rho g\nabla X_3^{(0)}\cdot\bar{\alpha}^{(1)}\ (=-\rho g\alpha_3^{(1)})$	hydrostatic term
$-\frac{1}{2}\rho\nabla(W^2)\cdot\bar{\alpha}^{(1)}$	interaction between stationary flow field and instationary ship motion

$p^{(2)}$ = sum of the term containing ε^2: (8-45)

$-\rho\varphi_t^{(2)}$	local acceleration term
$-\frac{1}{2}\rho\ \nabla\varphi^{(1)}\cdot\nabla\varphi^{(1)}$	kinetic term
$-\rho\overline{W}\cdot\nabla\varphi^{(2)}$	interaction stationary-instationary
$-\rho g\nabla X_3^{(0)}\cdot\bar{\alpha}^{(2)}\ (=-\rho g\alpha_3^{(2)})$	hydrostatic term
$-\rho\nabla\varphi_t^{(1)}\cdot\bar{\alpha}^{(1)}$	instationary interaction

$-\frac{1}{2}\rho\nabla(W^2)\cdot\overline{\alpha}^{(2)}$ interaction stationary-instationary

$-\rho\nabla\left\{\overline{W}\cdot\nabla\varphi^{(1)}\right\}\cdot\overline{\alpha}^{(1)}$ interaction term

$-\frac{1}{2}\rho\nabla^2(W^2)\,(\overline{\alpha}^{(1)}\cdot\overline{\alpha}^{(1)})$ interaction term

It should be noted that four of the terms of the second order pressure are similar to the terms of the first order pressure, and the other four terms contain cross products of first order quantities.

It may be well to remember that the zero and first order pressure components on the left pertain to a fixed point on the hull. The terms on the right, however, are written in field coordinates of the travelling axes and are evaluated at a point fixed in those travelling axes.

The meaning of the various terms can be obtained if we back-track from where they came. For the zero order terms the meaning will be obvious, see also Section 6.3.

For the first order we have the following:

$\rho\varphi_t^{(1)}$ is the pressure component obtained from the unsteady potential and is associated with local acceleration of the fluid particles,

$\rho g\alpha_3^{(1)}$ is the pressure component that stems from the vertical movement of the body-fixed point in the hydrodynamic field,

$\rho\overline{W}\cdot\nabla\varphi^{(1)}$ is the first order pressure component that stems from the velocity squared term in the Bernoulli equation,

$\frac{1}{2}\rho\overline{\alpha}^{(1)}\cdot\nabla(W^2)$ which can also be written as $\overline{\alpha}^{(1)}\cdot\nabla\,(\frac{1}{2}\rho W^2)$ is the first order pressure component associated with the fact that the body-fixed point moves through the steady flow field (which is thought not to be interfered by such movement).

In the modified linearization scheme for the first order potential we have obtained a solution that is composed of radiation and diffraction potentials and swell-up potentials, each satisfying the appropriate boundary conditions.

As a result we obtain the following expressions.

It will turn out useful to separate the effect of the radiation and diffraction potential from the incident wave and swell-up parts. We obtain:

$$p^{(1)} = -\rho\left\{\varphi_t + \overline{W}\cdot\nabla\varphi\right\} \qquad \textit{for}\ \varphi = \varphi_r + \varphi_d \qquad (8\text{-}46)$$

and

$$p^{(1)} = -\rho\left\{\varphi_t + W\cdot\nabla\varphi + g\alpha_3^{(1)} + \overline{\alpha}^{(1)}\cdot\nabla(\tfrac{1}{2}W^2)\right\}$$

$$for\ \varphi = \varphi_i + \varphi_{s1} + \varphi_{s2} \qquad (8\text{-}47)$$

The first expression needs no further reduction. The latter expression can be evaluated as follows, using eqs. (8-34), (8-37) and (8-38) we obtain:

$$\frac{p^{(1)}}{\rho} = g\zeta_i - gs\frac{\partial}{\partial s}\left(\frac{W^2}{2g}\right) + \zeta_i\left\{1-\frac{\partial}{\partial s}\left(\frac{W^2}{2g}\right)\right\}\cdot\frac{\partial}{\partial x_3}\left(\frac{W^2}{2}\right)+$$

$$-g\alpha_3^{(1)} - \overline{\alpha}^{(1)}\cdot\nabla(\tfrac{1}{2}W^2) + \alpha_3\frac{\partial}{\partial s}\left(\frac{W^2}{2g}\right)\cdot\frac{\partial}{\partial x_3}\left(\frac{W^2}{2}\right) \qquad (8\text{-}48)$$

If it is assumed that the vertical motion component of $\overline{\alpha}^{(1)}$ is of prevailing importance, then we obtain:

$$\frac{p^{(1)}}{\rho g} = s - s\frac{\partial}{\partial s}\frac{W^2}{2g} + s\left(1-\frac{\partial}{\partial s}\frac{W^2}{2g}\right)\frac{\partial}{\partial x_3}(\tfrac{1}{2}W^2)$$

$$= s\left(1-\frac{\partial}{\partial s}\frac{W^2}{2g}\right)\left(\frac{g + \overline{W}\cdot\overline{W}_{x_3}}{g}\right) \qquad (8\text{-}49)$$

This expression can be interpreted as the relative motion, increased with dynamic swell-up, being extrapolated along the vertical component of the gradient of the velocity squared term ($\frac{1}{2}W^2$).

For the meaning of the various terms of the second order pressure we first note that the first four terms are similar in appearance to the terms. The terms of the first order pressure and the meaning is equivalent.

The meaning of the remaining four terms follows from the relevant first order quantities as products of first order velocities.

8.6 The free-surface elevation and relative motion

The elevation of the free surface at a point in the undisturbed free surface can be obtained in the travelling system of axes from the Bernoulli equation.

$$\zeta = -\frac{1}{g}\left\{\Phi_t + \tfrac{1}{2}|\nabla\Phi|^2\right\} + \frac{1}{2g}U^2 \qquad \text{at } x_3 = \zeta \qquad (8\text{-}50)$$

This expression has to be evaluated on the actual (unknown) free surface. In order to arrive at a useful expression we have to reduce this expression to a fixed level in $x_3 = 0$. To this end we apply a Taylor's expansion with respect to coordinate x_3 so that:

$$\zeta = -\frac{1}{g}\left\{ \Phi_t + \tfrac{1}{2}|\nabla\Phi|^2 \right\} + \frac{1}{2g}U^2 + \\ -\left(\zeta^{(0)} + \zeta^{(1)} \right)\frac{1}{g}\frac{\partial}{\partial x_3}\left\{ \Phi_t + \tfrac{1}{2}|\nabla\Phi|^2 \right\} \qquad at\ x_3 = 0 \qquad (8\text{-}51)$$

If we substitute the power series expansion for the potential and apply the same assumptions as for the free-surface condition we can work out the appropriate expression for the free-surface elevation, which as a result can also be written as a power series:

$$\zeta = \zeta^{(0)} + \varepsilon\zeta^{(1)} + \varepsilon^2\zeta^{(2)} + \ldots\ldots \qquad (8\text{-}52)$$

It follows that:

$$\left(\zeta^{(0)} + \zeta^{(1)} \right)\left\{ 1 + \frac{\partial}{\partial x_3}\cdot\frac{1}{g}\left(\varphi_t + \frac{1}{2}W^2 + W\cdot\nabla\varphi \right) \right\} = \\ -\frac{1}{g}\left(\varphi_t + \frac{1}{2}W^2 + W\cdot\nabla\varphi \right) + \frac{1}{2g}U^2 \qquad (8\text{-}53)$$

If we assemble like powers of ε we obtain:

For order O(1):

$$\zeta^{(0)} = -\frac{1}{2g}\left(W^2 - U^2 \right)\cdot\left(\frac{g}{g + \overline{W}\cdot\overline{W}_{x_3}} \right) \qquad at\ x_3 = 0 \qquad (8\text{-}54)$$

For order O(ε):

$$\zeta^{(1)} = -\frac{1}{g}\left(\varphi_t + W\cdot\nabla\varphi \right)\cdot\left(\frac{g}{g + \overline{W}\cdot\overline{W}_{x_3}} \right) \qquad \text{at } x_3 = 0 \qquad (8\text{-}55)$$

The first order potential is composed of the components mentioned in equations (8-32) through (8-38).

Like the pressures we can separate the contribution to the radiation and

diffraction potential from the incident wave and swell-up parts, and we obtain for the first order:

$$\zeta^{(1)} = -\frac{1}{g}\left(\varphi_t + W \cdot \nabla\varphi\right) \cdot \left(\frac{g}{g + \overline{W} \cdot \overline{W}_{x_3}}\right) \text{ for } \varphi = \varphi_r + \varphi_d$$

$$at\ x3 = 0 \qquad (8\text{-}56)$$

$$\zeta^{(1)} = -\frac{1}{g}\left(\varphi_t + W \cdot \nabla\varphi\right) \cdot \left(\frac{g}{g + \overline{W} \cdot \overline{W}_{x_3}}\right) \text{ for } \varphi = \varphi_i + \varphi_{s1} + \varphi_{s2}$$

$$at\ x3 = 0 \qquad (8\text{-}57)$$

The first expression needs no further reduction. The latter expression can be evaluated as follows, using eqs. (8-34), (8-37) and (8-38) we obtain:

$$\zeta^{(1)} = \left[\zeta_i - s\frac{\partial}{\partial s}\left(\frac{W^2}{2g}\right) + \frac{1}{g}\left[\left\{\zeta_i\left(1 - \frac{\partial}{\partial s}\left(\frac{W^2}{2g}\right)\right) + \alpha_3 \frac{\partial}{\partial s}\left(\frac{W^2}{2g}\right)\right\}\frac{\partial}{\partial x_3}(\tfrac{1}{2}W^2)\right]\right] \cdot$$

$$\cdot \left[\frac{g}{g + \overline{W} \cdot \overline{W}_{x_3}}\right] \qquad (8\text{-}58)$$

After some algebra we obtain:

$$\zeta^{(1)} = \zeta_i\left\{1 - \frac{\partial}{\partial s}\left(\frac{W^2}{2g}\right)\right\} + \alpha_3 \frac{\partial}{\partial s}\left(\frac{W^2}{2g}\right) \qquad (8\text{-}59)$$

This expression can be interpreted as the incident wave augmented by the dynamic swell-up, complemented by the swell-up due to the vertical ship motion.

In order to evaluate the relative vertical motion we have to introduce the rigid body motion of the ship and we obtain:

$$s^{(1)} = \zeta^{(1)} - \alpha_3^{(1)} \qquad (8\text{-}60)$$

This quantity can be evaluated at any station along the hull.

8.7 Some notes on the first order pressure and free-surface elevation

In the foregoing we have obtained expressions for the pressure on the hull at some point in or below the free surface. We have also obtained expressions for

the free-surface elevation, relative to the zero datum level. These expressions are to some extent related, as we can show below:

For the pressure at some location on the hull:

$$p^{(1)} = -\rho\left(\varphi_t^{(1)} + W\cdot\nabla\varphi^{(1)}\right) + \rho g\, s\left\{1 - \frac{\partial}{\partial s}\left(\frac{W^2}{2g}\right)\right\}\left(\frac{g + \overline{W}\cdot\overline{W}_{x_3}}{g}\right) \qquad (8\text{-}61)$$

↑ Elastic energy

↑ Acceleration potential

↑ Kinetic energy

↑ Relative motion (nominal hence incident wave + motion)

↑ Dynamic swell-up augmenting relative motion

↑ Extrapolation along vertical derivative of steady kinetic energy

Time-dependent part due to radiation and diffraction

Quasi-stationary part due to incident wave and dynamic swell-up

For the free-surface elevation we obtain:

$$\zeta^{(1)} = -\frac{1}{g}\left(\varphi_t^{(1)} + W\cdot\nabla\varphi^{(1)}\right)\left(\frac{g}{g + \overline{W}\cdot\overline{W}_{x_3}}\right) + \left[\zeta_i\left\{1 - \frac{\partial}{\partial s}\left(\frac{W^2}{2g}\right)\right\} + \alpha_3\frac{\partial}{\partial s}\left(\frac{W^2}{2g}\right)\right]$$

↑ Acceleration potential

↑ Kinetic energy

↑ Extrapolation along vertical derivative of steady kinetic energy

↑ Incident wave

↑ Dynamic swell-up

Wave part

↑ Surface elevation due to vertical motion

Quasi-stationart part due to incident wave and dynamic swell-up

Time-dependent part due to radiation and diffraction

(8-62)

The pressure at some location underwater depends on the above terms, without taking account of the free-surface elevation above the point in question, which is already incorporated in the other flow terms.

The expression for the first order pressure is shown to be equivalent for the case of a very slow heaving motion in an otherwise calm fluid and for the case of a very long wave passing a restrained ship.

So from scrutinizing these terms we may conclude that the expression for the first order pressure is 'symmetric' in the sense that the effect of a very slow heaving motion or a very long wave give rise to the same pressure variation. In essence, this statement supports the relative motion hypothesis albeit for low frequency only.

8.8 The hydrodynamic forces

In the foregoing we have obtained expressions for the pressure on the hull and the relative motion of the water surface relative to the hull. The expressions extend to the zero and first order quantities, neglecting second and higher orders because of their lesser magnitude.

In order to obtain the wave forces the pressure has to be integrated over the appropriate wetted surface area, which on account of the fluctuating free surface, is also a dynamic quantity.

Yet, in deriving the force expression we have to extend the series expansion of the force up to and including the second order, which seems to be inconsistent. The reason is that the quantity we are interested in, the wave added resistance, constitutes the time average value of the wave force. This average value is for the greater part the result of the second order force.

The second order force, in turn, is as we shall show, composed of a number of terms of which the products of first order quantities are the most important, and

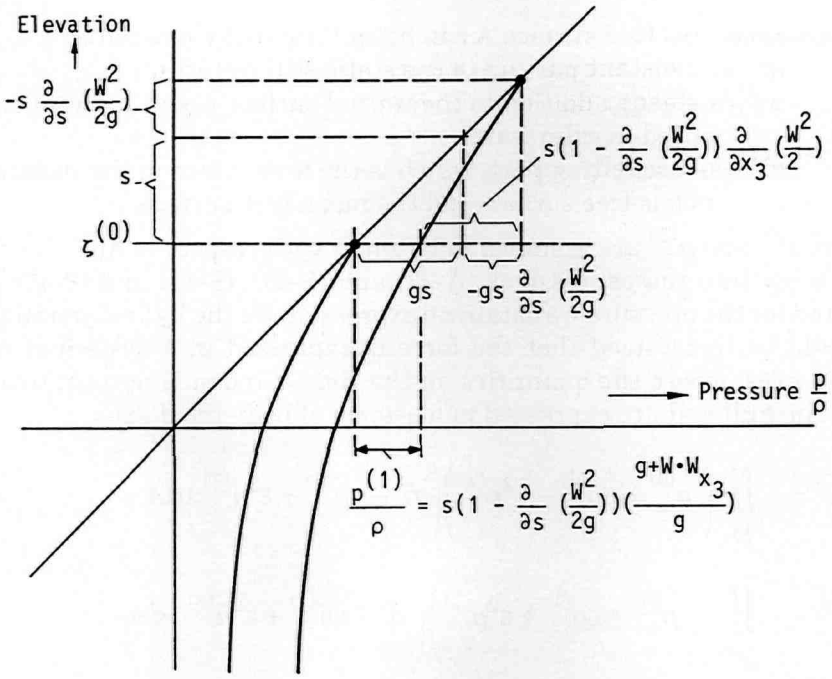

Figure 8-2: Diagram relating quasi-static pressure to relative motion for the forebody.

can be obtained from the zero and first order pressures and relative motions obtained thus far. That is the reason why thus far we have only worked up to the first order whilst now we have to consider the second order force as well.

In order to deal correctly with the second order wave force we have to give due consideration to the system of axes to which we shall refer. We choose to express the wave force in the system of travelling axes which has the origin in the calm water plane and travels with the mean ship velocity and of which the axes remain horizontal at all times: the $O(\bar{x})$ system, see Figure A-1.

The fluid exerts a force on the ship in this system of axes that follows from:

$$\overline{F} = -\iint_{\underline{A}} p\,\overline{n}\,dA \tag{8-63}$$

in which: $\underline{A}$ =instantaneous wetted surface
$\overline{n}$ =instantaneous normal vector to the surface element dA, and expressed in the $O(\bar{x})$ system, see expression (A-20)
p =instantaneous pressure, which follows from expression (8-42).

The instantaneous wetted surface A can be split up into three parts:

A_0 =a constant part up to the static still waterline

$a^{(0)}$=a steady addition to the wetted surface resulting from forward speed in calm water

$a^{(1)}$=an oscillating part, which is the area between the instantaneous free surface and the mean free surface.

The areas $a^{(0)}$ and $a^{(1)}$ are assumed to be small with respect to A_0.

If we substitute the expressions (A-23) and (8-43), (8-44) and (8-45) of the normal and for the pressure we obtain an expression for the hydrodynamic force.

It should be understood that the force is expressed in a system of steady travelling axes, where the quantities on the right-hand side pertain to a fixed point on the hull and are expressed in a system of body-fixed axes.

$$\overline{F} = -\iint_{A_0} \left(p^{(0)} + \varepsilon p^{(1)} + \varepsilon^2 p^{(2)} \right) \left(\overline{n}' + \varepsilon \overline{n}^{(1)} + \varepsilon^2 \overline{n}^{(2)} \right) dA +$$

$$-\iint_{a^{(0)}} \left(p^{(0)} + \varepsilon p^{(1)} + \varepsilon^2 p^{(2)} \right) \left(\overline{n}' + \varepsilon \overline{n}^{(1)} + \varepsilon^2 \overline{n}^{(2)} \right) dA +$$

$$-\iint_{a^{(1)}} \left(p^{(0)} + \varepsilon p^{(1)} + \varepsilon^2 p^{(2)} \right) \left(\overline{n}' + \varepsilon \overline{n}^{(1)} + \varepsilon^2 \overline{n}^{(2)} \right) dA + \qquad (8\text{-}64)$$

which can be written as:

$$\overline{F} = \overline{F}^{(0)} + \varepsilon \overline{F}^{(1)} + \varepsilon^2 \overline{F}^{(2)} + \ldots\ldots\ 0(\varepsilon^3) \qquad (8\text{-}65)$$

If we substitute the expressions for the pressure and work out the multiplications we obtain expressions for the zero, the first and the second order force component.

The zero order component

$$\overline{F}^{(0)} = -\iint_{A_0} \left(p^{(0)} \overline{n}' \right) dA \qquad -\iint_{a^{(0)}} \left(p^{(0)} \overline{n}' \right) dA$$

$$= -\iint_{A_0} \left(\rho g X_3^{(0)} \right) \overline{n}'\ dA \qquad -\iint_{A_0} \tfrac{1}{2}\rho\ (U^2 - W^2)\ \overline{n}'\ dA$$

$$+ \iint_{a^0} \left(\rho g X_3^{(0)} \right) \overline{n}' \, dA \qquad - \iint_{a^0} \tfrac{1}{2}\rho \, (U^2 - W^2) \, \overline{n}' \, dA \quad (8\text{-}66)$$

The force component of zero order is composed of four terms.

The first term constitutes the static displacement vector which has only a vertical component directed upward, eventually making equilibrium with the ship's weight.

The second term is a flow term. If at some location on the submerged body the flow velocity drops below U so that W < U the integrand represents a pressure increase and the total integral represents a force vector with at least an upward pointing vertical force. The forebody contributes to a negative force, i.e. an additional drag force. With a view to Figure 8-3 the integration can be approximated by assuming the distribution is linear, hence triangular:

$$= -2 \int_0^L \tfrac{1}{2} \left(\tfrac{1}{2}\rho \, (U^2 - W^2) \cdot \frac{\zeta^{(0)} - a_3^{(0)}}{\sqrt{n_1^2 + n_2^2}} \right) \cdot \overline{n}' \, dl \quad (8\text{-}67)$$

The factor 2 is included to include both port and starboard side, the factor ½ stems from the triangular distribution. The contour integral is to be taken in the $x_3' = 0$ plane along the waterline.

The third term is a hydrostatic term taken over the extra wetted surface that - paradoxically - contains a vertical component pointing downward into the fluid. However, for a better understanding this third term should be viewed together with the fourth term. The pressure on the extra steady wetted portion of the hull above the still water level is equal to the drop in kinetic energy of the flow minus the increase in potential energy (see Section 8.5).

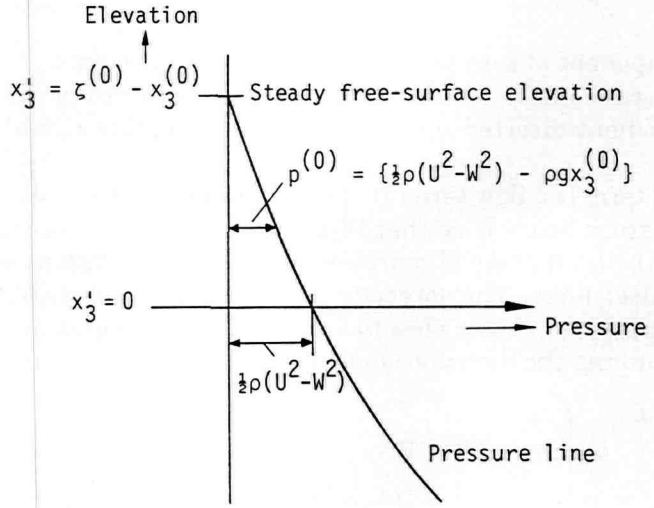

Figure 8-3: Diagram to illustrate pressure integration in a body-fixed reference frame.

If we take the two terms together we can simplify the integral expression:

$$-\iint_{a^0} \left(\tfrac{1}{2}\rho\,(U^2 - W^2) - \rho g X_3^{(0)} \right) \overline{n}'\, dA \text{ to be evaluated at } x_3' = 0 \qquad (8\text{-}68)$$

The first order term

For the first order force we have to collect the terms associated with ε. We obtain the following terms:

$$\overline{F}^{(1)} = -\iint_{a} (p^{(0)}\,\overline{n}')\, dA - \iint_{A_0+a^{(0)}} (p^{(0)}\overline{n}^{(1)})\, dA - \iint_{A_0+a^{(0)}} (p^{(1)}\overline{n}')\, dA \qquad (8\text{-}69)$$

The first term represents a steady force integrated over the infinitesimally small wetted surface $a^{(1)}$. Since this surface is small with respect to $A_0+a^{(0)}$ we may neglect this term relative to the other steady terms.

The second and third term can be worked out if we substitute the appropriate expressions for pressure and normal.

$$\overline{F}^{(1)} - \iint_{A_0} \left\{ -\rho g x_3^{(0)} + \tfrac{1}{2}\rho\,(U^2 - W^2) \right\} \left(\overline{\Omega}^{(1)} * \overline{n}' \right) dA$$

$$- \iint_{a^{(0)}} \left\{ -\rho g x_3^{(0)} + \tfrac{1}{2}\rho\,(U^2 - W^2) \right\} \left(\overline{\Omega}^{(1)} * \overline{n}' \right) dA$$

$$+ \iint_{A_0} \rho \left\{ + \varphi_{u_t}^{(1)} + g\alpha_3^{(1)} + \overline{W} \cdot \nabla \varphi_u^{(1)} + \tfrac{1}{2}\overline{\alpha}^{(1)} \cdot \nabla (W^2) \right\} \overline{n}'\, dA$$

$$+ \iint_{a^{(0)}} \rho \left\{ + \varphi_{u_t}^{(1)} + g\alpha_3^{(1)} + \overline{W} \cdot \nabla \varphi_u^{(1)} + \tfrac{1}{2}\overline{\alpha}^{(1)} \cdot \nabla (W^2) \right\} \overline{n}'\, dA \tag{8-70}$$

The expression (8-70) can be explained as follows.

The first integral involves an integration of the zero order pressure over the nominal submerged hull surface rotated with the first order motion:

$$- \iint_{A_0} \left(p^{(0)} \overline{n}^{(1)} \right) dA = \overline{\Omega}^{(1)} * \left\{ - \iint_{A_0} (p^{(0)}\, \overline{n}')\, dA \right\} \tag{8-71}$$

A similar integral showed up in the zero order force and no approximation is required.

The second integral involves a correction of the first integral, to be taken over the steady additionally wetted surface. A similar term showed up in the zero order force and we can use the same approximation:

$$- \iint_{a^{(0)}} \left(p^{(0)} \cdot \overline{n}^{(1)} \right) dA = \overline{\Omega}^{(1)} * \left\{ - \iint_{a^{(0)}} (p^{(0)}\, \overline{n}')\, dA \right\}$$

$$= \overline{\Omega} * \left[-2 \int_0^L \tfrac{1}{2} \left\{ \tfrac{1}{2}\rho\,(U^2 - W^2)\, \frac{\zeta^{(0)} - a_3^{(0)}}{\sqrt{n_1^2 + n_2^2}} \right\} \overline{n}'\, dl \right] \tag{8-72}$$

The third integral $- \iint_{A_0} (p^{(1)} \overline{n}')\, dA$ represents the integration of the first order pressure over the nominal submerged hull surface. No approximation is required.

The fourth integral $-\iint_{a^{(0)}} (p^{(1)}\overline{n}')\,dA$ represents a correction to the third integral, to be taken over the steady additionally wetted surface. It can be approximated by:

$$= -2\int_0^L \left\{ p^{(1)} \frac{\zeta^{(0)} - a_3^{(0)}}{\sqrt{n_1^2 + n_2^2}} \right\} \overline{n}'\,dl \tag{8-73}$$

The second order force

For the second order force we need to collect the terms preceded by ε^2. We obtain the following terms:

$$\overline{F}^{(2)} = -\iint_{A_0} \left(p^{(0)}\overline{n}^{(2)} + p^{(1)}\overline{n}^{(1)} + p^{(2)}\overline{n}' \right) dA$$

$$-\iint_{a^{(0)}} \left(p^{(0)}\overline{n}^{(2)} + p^{(1)}\overline{n}^{(1)} + p^{(2)}\overline{n}' \right) dA$$

$$-\iint_{a^{(1)}} \left(p^{(0)}\overline{n}^{(1)} + p^{(1)}\overline{n}' \right) dA \tag{8-74}$$

This expression contains eight terms. In keeping with Section A.4 it is hypothesized that the mean forces are the result of the second order oscillatory force, which in turn is to leading order governed by the first order pressures and first order motions.

In that case, on that assumption, some of the terms can be deleted; for instance terms containing $\overline{n}^{(2)}$. On the other hand the terms containing $p^{(2)}$ are made up of eight terms, some of which can be discarded on account of second order effects, still other terms are composed of products of first order terms which should be retained.

We can briefly survey the meaning of the various integrals in formula (8-74) as follows.

The first integral in formula (8-74) is due to the product of the first order pressure and the first order normal taken over the static wetted surface. Since angular motions are the same for all surface elements it can be written as

$$-\iint_{A_0} p^{(1)}\overline{n}^{(1)}\,dA = \overline{\Omega}^{(1)} * \left(-\iint_{A_0} p^{(1)}\,\overline{n}'\,dA \right) \tag{8-75}$$

The integral corresponds to a similar integral in the first order force.

The second integral is a similar expression, but taken over the extra wetted surface due to steady forward motion:

$$-\iint_{a^{(0)}} p^{(1)}\overline{n}^{(1)}\,dA = \overline{\Omega}^{(1)} * \left(-\iint_{a^{(0)}} p^{(1)}\,\overline{n}'\,dA \right) \tag{8-76}$$

The third integral is due to the second order pressure being integrated over the static wetted surface, up to the calm water plane.

$$-\iint_{A_0} (p^{(2)}\overline{n}')\,dA \tag{8-77}$$

The fourth integral is due to the second order pressure being integrated over the extra wetted surface due to forward motion.

$$-\iint_{a^{(0)}} (p^{(2)}\overline{n}')\,dA \tag{8-78}$$

The fifth integral is an integration of the steady pressure $p_{(0)}$ taken over the oscillatory wetted surface.

$$-\iint_{a^{(1)}} p^{(0)}\overline{n}^{(1)}\,dA \tag{8-79}$$

The sixth integral results from the first order pressure fluctuations taken over the oscillatory surface.

$$-\iint_{a^{(1)}} (p^{(1)}\overline{n}')\,dA \tag{8-80}$$

The surface represents that part of the hull that becomes wet and dry in a 'first order oscillatory fashion'.

Approximation of the second order force

The six aforementioned integrals can be evaluated with some approximation. They all have the form of an integration of the pressure over some surface area, the latter being defined by the surface element and the direction normal. The pressure as well as the normal are functions of the three space coordinates on the hull; the pressure is also a function of time.

If we assume that the sides of the ship above the waterplane are straight, not necessarily vertical, and under an angle defined in the waterplane, and if we assume the pressure curves to be fairly straight lines, at least over the extra wetted surface, we can remove the vertical coordinate of the integration in some of the integrals. In this way the integration over an area above the calm water

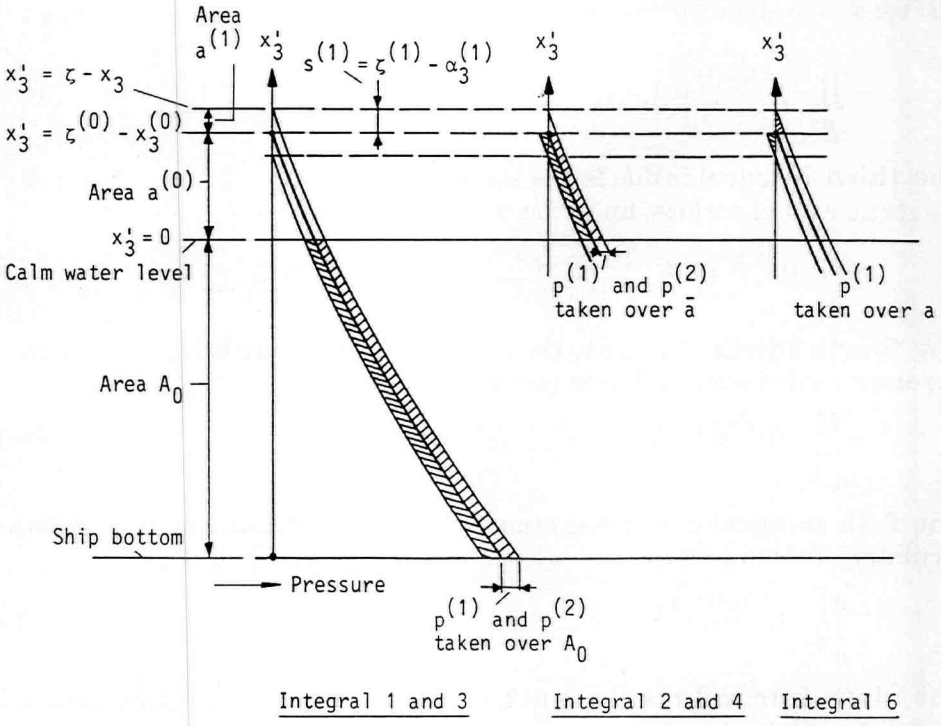

Figure 8-4: Illustration of the integration domains for second order force components.

surface (or occasionally below) is transformed into an integration over the waterline, taking due account of the direction normals.

For the shape of the pressure line we refer to some examples, for instance in Sections 6.3 and 7.5. For a further explanation of the approximations we refer to Figure 8-5.

The first integral involves a straightforward integration of the first order pressure over the mean wetted surface and no approximation seems to be necessary at this stage.

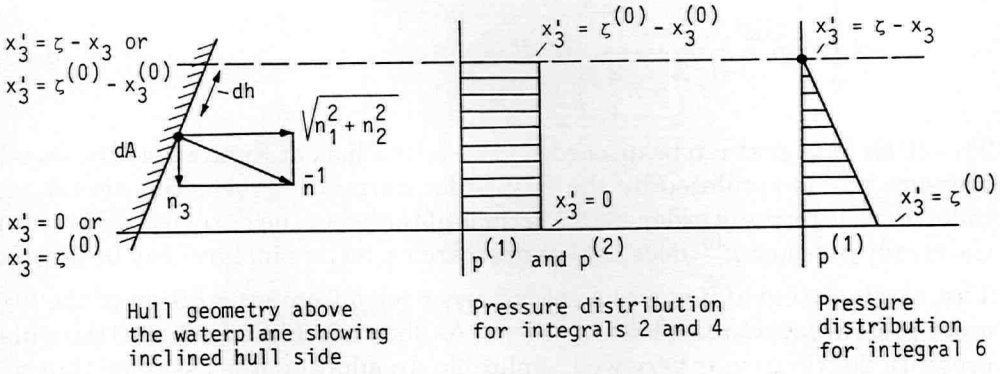

Figure 8-5: Illustration to the approximations of integrals of second order force.

The second integral involves the integration of the first order pressure over the extra steadily wetted surface and the pressure distribution can fairly well be approximated by a parallelogram.
We find:

$$-\overline{\Omega}^{(1)} * \iint_{a^{(0)}} p^{(1)} \bar{n}' \, dA =$$

$$-\overline{\Omega}^{(1)} * 2 \int_0^L p^{(1)} \frac{\zeta^{(0)} - a_3^{(0)}}{\sqrt{n_1^2 + n_2^2}} \bar{n}' \, dl \qquad (8\text{-}81)$$

This expression involves a multiplication of first order quantities to be evaluated at the calm water surface. Also it is assumed that the sides of the ship have a constant inclination angle so that the normal can be taken in the mean waterplane. The factor 2 is meant to account for port and starboard side.

The third integral involves a straightforward integration of the second order pressure over the mean wetted surface, and no approximation would seem necessary at this stage.

The fourth integral constitutes an integration of the second order pressure over the extra wetted surface and if it is assumed (like we did in the second integral) that the second order quantity does not vary all that greatly over the area of the extra steadily wetted surface a we may approximate the pressure distribution by a parallelogram, like shown in Figure 8-4 and we find in a likewise manner:

$$-2\int_0^L \left(p^{(2)} \frac{\zeta^{(0)} - a_3^{(0)}}{\sqrt{n_1^2 + n_2^2}} \right) \overline{n}'\, dl \qquad (8\text{-}82)$$

The fifth integral can be discarded if we take a look at Figure 8-4. The steady pressure $p^{(0)}$ is oscillated by the first order normal $n^{(1)}$ over the area a and collecting the terms of order ε^2 this term is obtained in the derivation. However, the steady pressure $p^{(0)}$ does not act upon area a, so this integral can be deleted.

The sixth integral involves a second order term from integration of the first order pressureover area a both of order ε. As shown in Figure 8-5 the triangular pressure distribution is very well applicable. In addition it is assumed that $p^{(1)}$ will only weakly change over the height of the steady bow wave $\overline{\zeta}$ and that as a consequence we may evaluate the components of $p^{(1)}$ at the level of $x_3 = 0$ instead of at $x_3 = \overline{\zeta}$. We obtain the following expression:

$$-\iint_a p^{(1)} \overline{n}'\, dA =$$

$$-\int_{H0}^{L} \int p^{(1)} \overline{n}'\, dh\, dl =$$

$$-2\int_0^L \tfrac{1}{2} \left(p^{(1)} \frac{\zeta^{(1)} - a_3^{(1)}}{\sqrt{n_1^2 + n_2^2}} \right) \overline{n}'\, dl \qquad (8\text{-}83)$$

This expression involves $p^{(1)}$, $\zeta^{(1)}$ and $\overline{n}'$ to be evaluated in the calm water plane. The factor 2 is meant to account for the port and starboard side.

Table 8-1: Summary of hydrodynamic forces
Integrals over submerged body and around waterline

Integral term	Integral expression	Integral approximation	Term C	Term A	Term B
I_1	$\iint_{A_0} (p^{(0)}\,\bar{n}')\,dA$	exact	$p^{(0)}$	–	–
I_2	$\iint_{a^{(0)}} (p^{(0)}\,\bar{n}')\,dA$	$\int_{WL}\left\{ \tfrac{1}{2}\frac{p^{(0)}s^{(0)}}{\sqrt{n_1^2+n_2^2}}\right\}\bar{n}'\,dl$	$\tfrac{1}{2}\frac{p^{(0)}s^{(0)}}{\sqrt{n_1^2+n_2^2}}$	–	–
I_3	$\iint_{A_0} (p^{(1)}\,\bar{n}')\,dA$	exact	1	$p^{(1)}$	–
I_4	$\iint_{a^{(0)}} (p^{(1)}\,\bar{n}')\,dA$	$\int_{WL}\left\{ \frac{s^{(0)}}{\sqrt{n_1^2+n_2^2}}p^{(1)}\right\}\bar{n}'\,dl$	$\frac{s^{(0)}}{\sqrt{n_1^2+n_2^2}}$	$p^{(1)}$	–
I_5	$\iint_{A_0} (p^{(2)}\,\bar{n}')\,dA$	$= I_{51} + I_{52}$			
I_{51}	$\iint_{A_0} (p_1^{(2)}\,\bar{n}')\,dA$	exact	$-\frac{\rho}{2}$	$\nabla\varphi^{(1)}$	$\nabla\varphi^{(1)}$
I_{52}	$\iint_{A_0} (p_2^{(2)}\,\bar{n}')\,dA$	exact	$-\rho$	$\nabla\varphi_t^{(1)}$	$\bar{\alpha}^{(1)}$
I_6	$\iint_{a^{(0)}} (p^{(2)}\,\bar{n}')\,dA$	$= I_{61} + I_{62}$			
I_{61}	$\iint_{a^{(0)}} (p_1^{(2)}\,\bar{n}')\,dA$	$\int_{WL}\frac{s^{(0)}}{\sqrt{n_1^2+n_2^2}}p_1^{(2)}\,\bar{n}'\,dl$	$\frac{-\tfrac{1}{2}\rho\, s^{(0)}}{\sqrt{n_1^2+n_2^2}}$	$\nabla\varphi^{(1)}$	$\nabla\varphi^{(1)}$
I_{62}	$\iint_{a^{(0)}} (p_2^{(2)}\,\bar{n}')\,dA$	$\int_{WL}\frac{s^{(0)}}{\sqrt{n_1^2+n_2^2}}p_2^{(2)}\,\bar{n}'\,dl$	$\frac{-\rho\, s^{(0)}}{\sqrt{n_1^2+n_2^2}}$	$\nabla\varphi_t^{(1)}$	$\bar{\alpha}^{(1)}$
I_7	$\iint_{a^{(1)}} (p^{(0)}\,\bar{n}')\,dA$	deleted	–	–	–
I_8	$\iint_{a^{(1)}} (p^{(1)}\,\bar{n}')\,dA$	$\int_{WL}\left(\frac{\tfrac{1}{2}}{\sqrt{n_1^2+n_2^2}}p^{(1)}\,s^{(1)}\right)\bar{n}'\,dl$	$\frac{1}{2\sqrt{n_1^2+n_2^2}}$	$p^{(1)}$	$s^{(1)}$

Table 8-2: Standard form of integrals
Summary of integrals and forces/moments

Integral term	Standard form	Mean		First order		Second order	
		Force	Moment	Force	Moment	Force	Moment
I_1	$\iint_{A_S} (c\,\overline{n}')\,dA_S$	$F_1^{(0)}$	$M_1^{(0)}$				
I_2	$\int_{WL} (c\,\overline{n}')\,dl$	$F_2^{(0)}$	$M_2^{(0)}$				
I_3	$\iint_{A_S} (c\,A\,\overline{n}')\,dA_S$			$F_3^{(1)}$	$M_3^{(1)}$		
I_4	$\int_{WL} (c\,A\,\overline{n}')\,dl$			$F_4^{(1)}$	$M_4^{(1)}$		
I_5	$\iint_{A_S} c(\overline{A}\cdot\overline{B})\,\overline{n}'\,dA_S$	$F_5^{(0)}$	$M_5^{(0)}$			$F_5^{(2)}$	$M_5^{(2)}$
I_6	$\int_{WL} c(\overline{A}\cdot\overline{B})\,\overline{n}'\,dl$	$F_6^{(0)}$	$M_6^{(0)}$			$F_6^{(2)}$	$M_6^{(2)}$
I_7							
I_8	$\int_{WL} c(A\,B)\,\overline{n}'\,dl$	$F_8^{(0)}$	$M_8^{(0)}$			$F_8^{(2)}$	$M_8^{(2)}$
$\overline{\Omega} * I_1$				$F_9^{(1)}$	$M_9^{(1)}$		
$\overline{\Omega} * I_2$				$F_{10}^{(1)}$	$M_{10}^{(1)}$		
$\overline{\Omega} * I_3$		$F_{11}^{(0)}$	$M_{11}^{(0)}$			$F_{11}^{(2)}$	$M_{11}^{(2)}$
$\overline{\Omega} * I_4$		$F_{12}^{(0)}$	$M_{12}^{(0)}$			$F_{12}^{(2)}$	$M_{12}^{(2)}$
TOTAL FORCE/MOMENT		$F_T^{(0)}$	$M_T^{(0)}$	$F_T^{(1)}$	$M_T^{(1)}$	$F_T^{(2)}$	$M_T^{(2)}$

= minus {sum of the appropriate columns (complex vectors)}

8.9 Practical implementation

In the foregoing derivation, Section 8.3, a modified linearization scheme was developed in which account was taken of the dynamic swell-up effect which has been found in experiments to be most in evidence around the bow of the ship. In current linearization schemes this effect is invariably omitted. In doing so we have arrived at expressions for the forces and the pressures that in turn depend on a number of potentials, steady and unsteady.

In order to obtain tangible results we have made use of two existing computer programs, one for the steady flow computations (DAWSON) and one for the unsteady flow computations (PRECAL).

For steady flow we have given the free-surface condition in expression (8-6) further developed in (8-12). These are to be combined with the body boundary condition (A-47) and the Laplace equation. For the actual steady flow computations we have made use of the program DAWSON, initially developed by Dawson [8-1] and further refined into a computer program by Raven [8-2].

This program utilized a different expression for the free-surface condition, which is discussed in the references. The program has shown to yield good results on a great number of ships and for the purpose to obtain steady pressures and flow vectors it was considered to be the best tool available.

For the unsteady flow we have split the boundary condition into three separate sets to be solved separately, viz. expressions (8-16) to (8-22).

The boundary problem A for the unsteady potential of radiation and diffraction forms the basis of an existing computer program developed in a joint effort by four companies (American Bureau of Shipping, British Maritime Technology, Lloyd's Register and Maritime Research Institute Netherlands) working together in the context of the CRS (Cooperative Research on Ships), ref. [8-3].

The program PRECAL uses a source distribution method and Green's functions to solve for the unknown potentials complying with the boundary conditions as given in problem A. The program has two options, the full forward speed option that complies with the boundary conditions in problem A, and an approximate method in which the speed effect term in the free-surface condition is neglected on the assumption that the frequency is sufficiently larger than $U\,\delta/\delta x$ so that the latter term can be dropped as most strip theories do.

The influence of ship speed on the calculation of the hydrodynamic forces on a ship then takes place through the modification of the pressure expression and the body boundary condition. Also an additional contour integral along the intersection of the hull surface and the free surface arises. This approximate method employs a much simpler Green's function that satisfies the approximate free-surface condition.

For the computations of the unsteady radiation and diffraction potentials we have used the program PRECAL in its approximative form for two reasons; first in the validation of the program little difference was found to exist in the results, and secondly the full forward speed takes about 24 hours CPU time on a Cray computer for just one combination of ship speed and frequency, which precluded any extensive use of this option.

For the unsteady problems B and C the boundary conditions are given in Section 8.3 and in the sequel it was shown that some expressions could be derived that could be fully evaluated on basis of steady flow computations as set forth above. Thus the swell-up and its potential and its derivatives could be obtained on basis of computations utilizing the steady flow program DAWSON.

By carrying out the steady flow calculations for three different even keel drafts the derivatives of the flow quantities with respect to draft variations, hence relative motions, could be obtained and used in the expressions for the unsteady pressures.

In a practical context the computational steps for each combination of ship speed and wave frequency were:

- Three runs with 'DAWSON' to obtain steady flow quantities and derivatives of those quantities with respect to draft;
- one run with 'PRECAL' to obtain the unsteady radiation and diffraction quantities;
- one run with 'RAWSHIP' to obtain the pressure and the forces (see Sections 8.5 and 8.8).

The computational results thus obtained are correlated with experimental data for a number of ships in the following Chapter 9.

Chapter 9

Correlation of measured and computed results

9.1 Correlation of Wigley 1 model data

-references

The model test results obtained for the slender Wigley 1 model (L/B = 10) were compared with the results of computations. For the test results we refer to Ref. (9-1) for the pressure and relative motion measurements and to Ref. (9-3) for the wave added resistance. A summary of the most important results is given in Section 7.5.2. The computations were carried out following the theory as outlined in Chapter 8.

-computation discretization scheme

For the computations it was required to discretize the hull form in a large number of facets. The facet scheme is given in Figure 9.1-1. In the upper half of the underwater hull the panels were required to be arranged in line with the waterlines in order to facilitate computer runs to be made for three even keel drafts. The calculations of the stationary flow field and bow wave system were done for three draughts: the nominal draft and a greater and a lesser draft. This allowed us to obtain the derivatives of stationary flow quantities with respect to the draft. In total 800 panels were used in the computations.

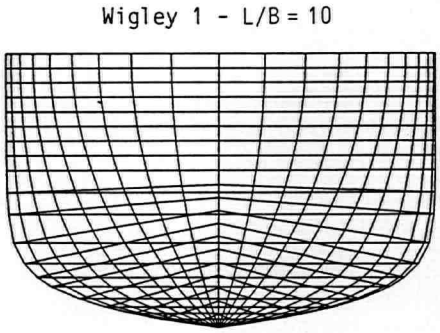

Figure 9.1-1: Bodyplan and panel distribution for slender Wigley 1.

-steady bow wave system

The steady bow wave as measured is given in Figure 7.5.2-3 of Section 7. In Figure 9.1-2 we have included the prediction of the bow wave height for the various speeds and drafts. For the Fn. = 0.20 speed case the bow wave as computed is very nearly zero as it coincides with the cross-over point of the bow wave system. The measurement has its bow wave crest further forward, more in the vicinity of Section 19 for which case a swellup coefficient of 1.07 is found. For the Fn. = 0.30 speed case the prediction is fairly well in line, as is the swellup

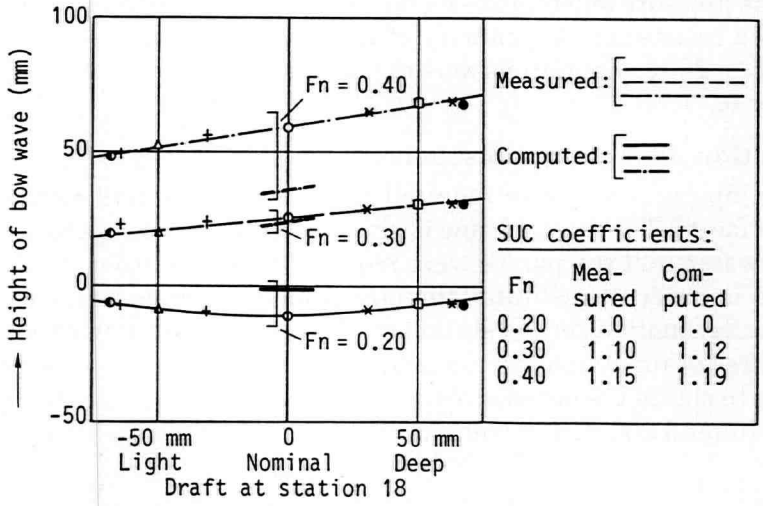

Figure 9.1-2: Measured and calculated steady bow wave height at Station 18 for three drafts and three speeds.

coefficient. For the Fn. = 0.40 the prediction is lower than the measurements. It is shown in the figure that, although the bow wave height prediction was in some cases smaller than the measured value, the predicted swellup coefficient (SUC) was reasonably well in line.

-added resistance components

The added resistance as computed is built up from 7 different terms, as described in Chapter 8. Of these 7 terms only 4 terms are really significant as illustrated in Figure 9.1-3. It is shown that the integrals I_{51} (kinetic energy), I_{52} (motion through pressure gradient field), I_8 (relative motion along the waterline) and I_{11} (coupling between heave and pitch motions) are the larger ones. It is shown in Figure 9.1-3 that I_{51}, I_{52} and I_{11} are all positive thus constituting a propulsive force rather than a resistance. However I_8 is a resistance that exceeds them all and the resulting difference is indeed a resistance.

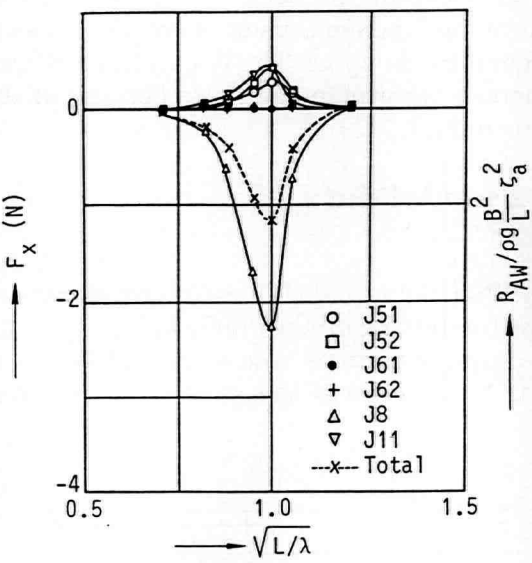

Figure 9.1-3

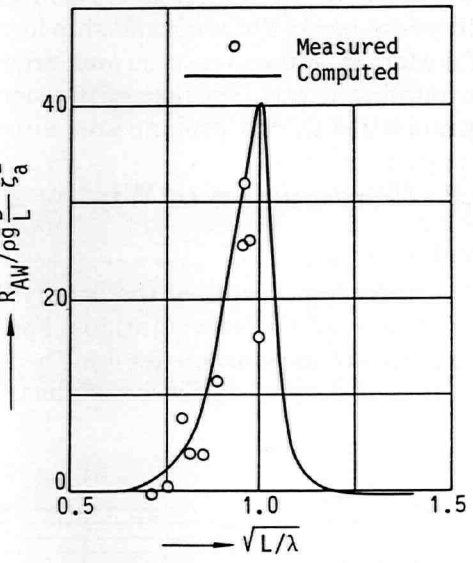

Figure 9.1-4

Added resistance components and transfer function for Fn = 0.20.

The positive sense of I_{51} can be understood from Bernoulli's equation, as being the kinetic term. This term brings about a suction force which is larger at the bow than at the stern on account of larger water disturbance velocities at the bow. The sense of I_{52} varies and can be either positive or negative. Because of the harmonic motion it can also be understood as the inner product of the fluid velocity and the rigid body motion. If in phase they contribute to a suction force which is larger at the bow than at the stern, thus causing a propulsive force. The

sign of I_8 is invariably negative, as the relative motion at the bow exceeds that at the stern, thus causing a resistance force. This relative motion integration represents the largest contribution to the added resistance. Finally the integral I_{11} depends on the coupling between heave and pitch. At pitch resonance the phasing between heave and pitch is such that when the bow is in a downward position the centre of gravity is being accelerated upward. The upward fluid force effecting this acceleration has a forward component that has the sign of a propulsive force. The remainder of the integrals are small and can be viewed as corrections to the other four main terms.

-added resistance

The total added resistance force as computed is compared to the measured force for Fn. = 0.20 in Figure 9.1-4. The computed values at pitch resonance are well in line with the measured values. It is shown that the added resistance transfer function is an extremely narrow filter, attaining its peak at the frequency of pitch resonance. For a normal ship form the function is usually broader because of the larger waterplane area and larger pitch damping. The Wigley hulls behave in a different way, because of the slender waterplane and also because of the symmetry of the waterplane area fore and aft.

9.2 Correlation of Wigley 2 model data

- references

The model test results of the beamy Wigley 2 model (L/B = 5) were compared with the results of computations. For the test results we refer to Ref. (9-2) for the pressure measurements and the relative motions, and to Ref. (9-3) for the motions and wave added resistance. A summary of the most important test

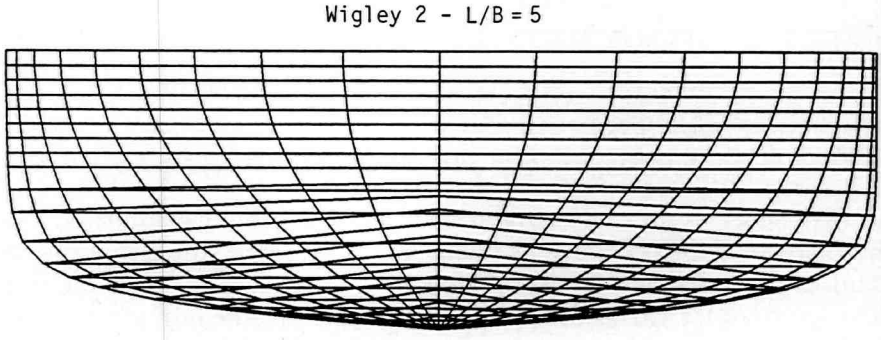

Figure 9.2-1: Bodyplan and panel distribution for beamy Wigley 2.

results is given in Section 7.5.2. The computations were carried out following the theory as outlined in Chapter 8.

- computation discretization scheme

The panel facet discretization scheme as used for the present hull form is given in Figure 9.2-1. Underwater the panels were arranged in an inclined fashion as shown in the figure to fit in with the requirements for steady flow calculations, while around the water line in the upper region the panel layers were arranged in a horizontal fashion to allow a deeper draft and a lesser draft to be obtained by adding and stripping a layer of panels to obtain the derivatives with respect to the draft. In total 800 panels were used.

- steady bow wave system

The steady bow wave was measured at station 18½ which happened to almost coincide with the bow wave crest-trough cross-over point so that the calm water swellup coefficient obtained was small and not representative of the other stations at the bow. When we compare the bow wave system for the three drafts at Fn. = 0.20 a noticable difference is observed, in particular at station 19 and 20, leading to a swellup coefficient of about 1.12 at the peak of the bow wave crest, see Figure 9.2-2.

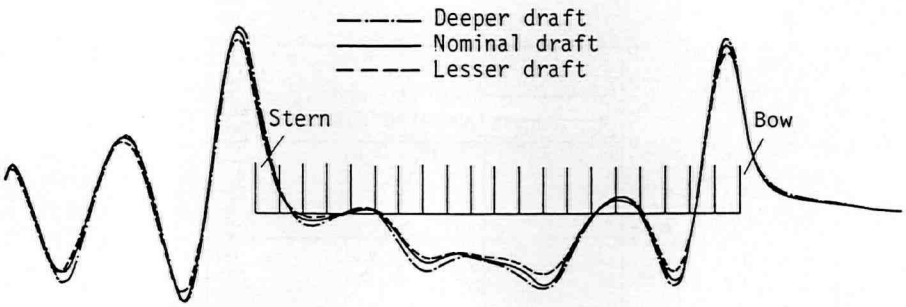

Figure 9.2-2: Stationary bow wave profile for three drafts (Fn = 0.20).

- ship motions heave and pitch

In the comparison of added resistance data and relative motion data the ship motions play an important role. The measured data and the computed data are compared in Figure 9.2-3 and 9.2-4. It shows that the heaving motion is predicted reasonably well, but the pitching is overpredicted. Comparison of the measured and predicted motion coefficients in the equations of motion show that mainly the damping is responsible for this difference. With reference to Journée Ref.

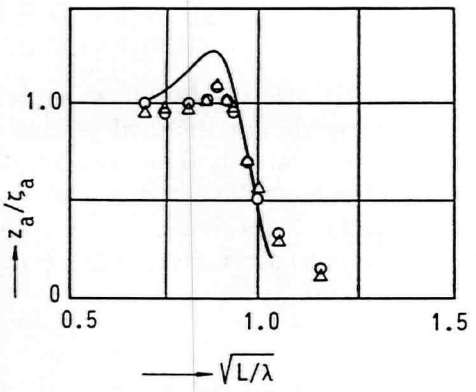

Figure 9.2-3

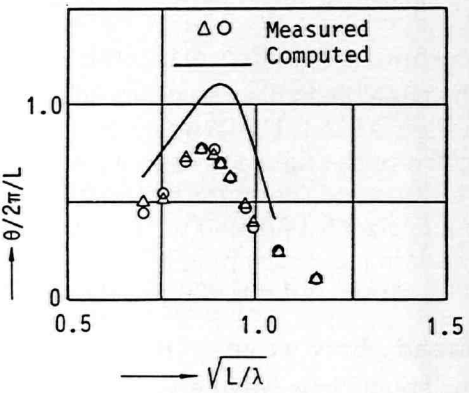

Figure 9.2-4

Transfer functions of heave and pitch.

(9-3) it will be clear that the difference in pitching is very similar to the prediction of strip-theory using a close-fit approximation. Nevertheless, it will have a bearing on the relative motions, for which not only the pitch amplitude but also the phasing relative to the waves is to be taken into account.

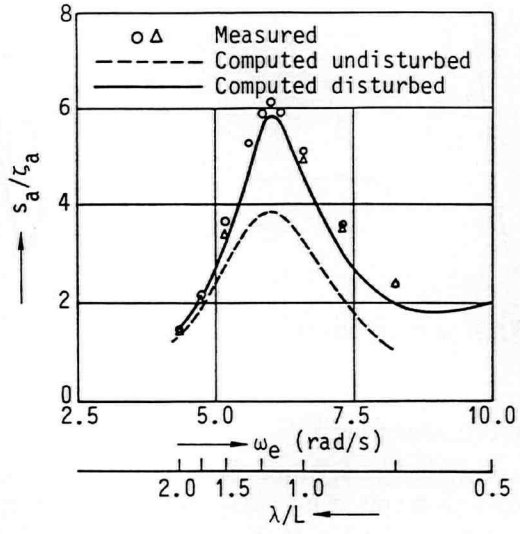

Figure 9.2-5: Transfer function of relative motion (Station 18 1/2, Fn = 0.20).

- relative motion forward

In the model test program the relative motion at station 18½ on the forebody was measured as shown in Figure 9.2-5. The peak of the function attains a high value of six times the wave amplitude which is more than for usual ship hull forms. This is to be attributed to the fore and aft symmetry of the hull, and the pointed waterline in the aftbody, quite unlike normal hull forms. The calculation of the nominal relative motion at this station, taking account only of ship motions and incident undisturbed wave is also given in Figure 9.2-5. In addition the relative motion is predicted including the dynamic swell-up as obtained from calm water steady bow wave computations together with radiation and diffraction wave effects. It is shown that the fit of the relative motion is fairly close if radiation and diffraction waves together with dynamic swellup wave are taken into account.

- added resistance components

The results of the various integrations are shown in Figure 9.2-6. As shown, only the integrals I_{51}, I_{52} and I_8 are of interest, the relative motion integration I_8 again being the largest and most important, because it is the only term that yields added resistance. It is interesting to note also in this case the importance of I_{51} and I_{52} indicating a considerable influence of the kinetic energy term that causes a suction force to forward. It is also noteworthy that for this hull form, quite unlike the Wigley 1 of the foregoing Section 9.1 the integral I_{11} does not

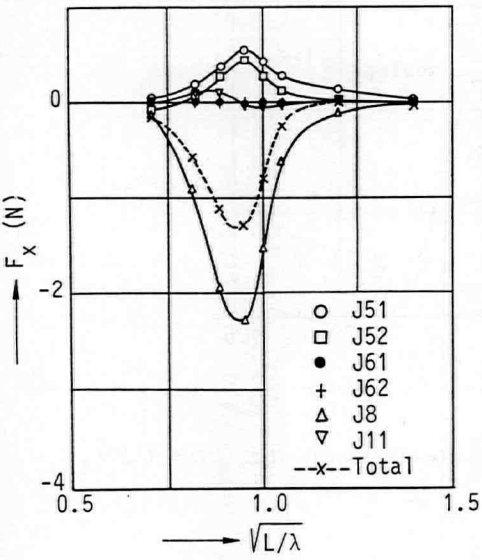

Figure 9.2-6

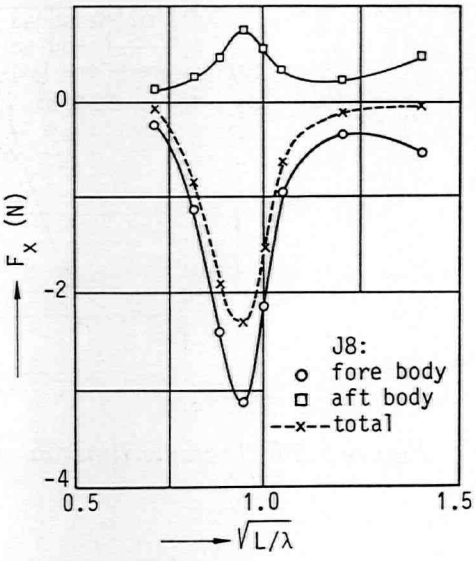

Figure 9.2-7

Added resistance components (Fn = 0.20).

have a significant influence on the added resistance. This is so because the heaving motion does barely exceed unity and as a consequence the heave-pitch coupling fails to gain importance. In Figure 9.2-7 a separation is made between the integration I8 of forebody and aftbody. It is shown that the forebody force is about four times larger than the aftbody force. It is also shown that for the short wave length range where the waves are much shorter than the ship length the contribution of the aftbody is equal and opposite to the forebody. In experiments it is observed that in such short waves the ship 'irons-out' the waves at the stern so that very little relative motion is left at the aftbody. So the aftbody contribution is considered too large in this wave length range and should be suppressed.

- added resistance

The predicted added resistance is shown in Figure 9.2-8. The fit is clearly very good for long and medium waves. On the short wave length side we have seen that the I8 integral contribution of the aftbody (relative motion) remains to large, thus leading to a too small added resistance. For these wave lengths it would suffice to use just the contribution of the relative motion at the forebody, which is shown as separate data. It is not shown in the experimental data here presented, but as can be seen in Section 7.6.1 the added resistance operator will increase again for very short wave length. This corresponds with the trend of the forebody I8 shown in Figure 9.2-8.

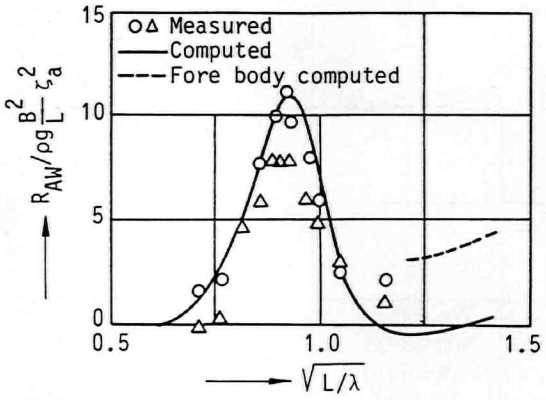

Figure 9.2-8: Transfer function of added resistance (Fn = 0.20).

9.3 Correlation of cargo ship data

-references

The experimental results of the cargo ship hull were compared with the results of computations. For the test results we refer to Ref. 9-4 and 9-5. A summary of the most important test results is given in Section 7.4 and 7.5.1. The computations were carried out following the theory as outlined in Chapter 8.

-computation discretization scheme

The panel facet discretization scheme is shown in Figure 9.3-1. Like in the foregoing cases the upper strips could be stripped off to enable the derivatives with respect to draft to be obtained. In total 714 panels were used. As can be seen in the panel scheme the bilge radius in the forebody in particular is represented by only one panel under a 45 degree angle. The hull shape indeed has a fairly small bilge radius as designed. Initially the facet distribution had two facets on the bilge radius, with devastating effect on the computational results. It was changed into one bigger panel and the results were much improved.

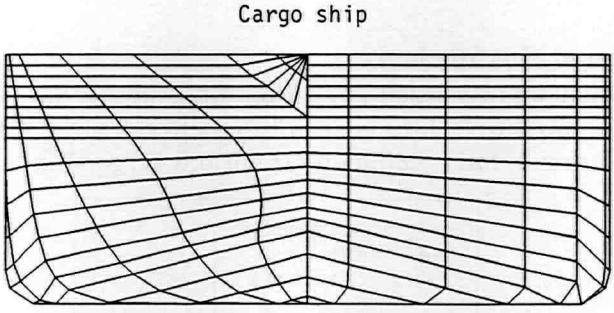

Figure 9.3-1: Bodyplan and panel distribution of cargo ship.

-steady bow wave system

The steady bow wave was measured at station 19½ on the forebody, which is at the bow wave crest. The bow is not very good from the steady flow point of view, since the forebody sections remain wall-sided all the way down to the bilge, thus forcing the water to follow the waterlines rather than the buttocks. This made for a large bow wave in the experiments and a conspicuous bow wave trough at the forward shoulder. From the Figure 9.3-2 or from the numerical data we can obtain a dynamic swellup coefficient of 1.10 for the speed of Fn. = 0.20 which is rather low. From model tests on the restrained model a value of 1.6 was obtained for the long waves, increasing to 2.0 for short waves. This would lead to the

conclusion that wave reflection on the bow is for this hull and speed more important than dynamic swellup associated with the bow wave dependency on the instantaneous draft.

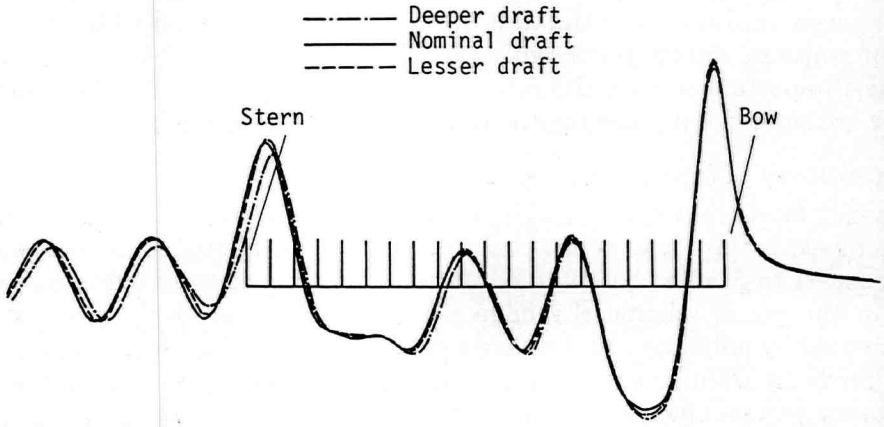

Figure 9.3-2: Stationary bow wave profile for three drafts (Fn = 0.20).

-relative motion at the forebody

The relative motion was recorded at station 19½ on the forebody as given in Figure 9.3-3. The measured data is seen to reach a peak of 4 times the wave amplitude at resonance, fairly common for normal cargo ship hulls. The undis-

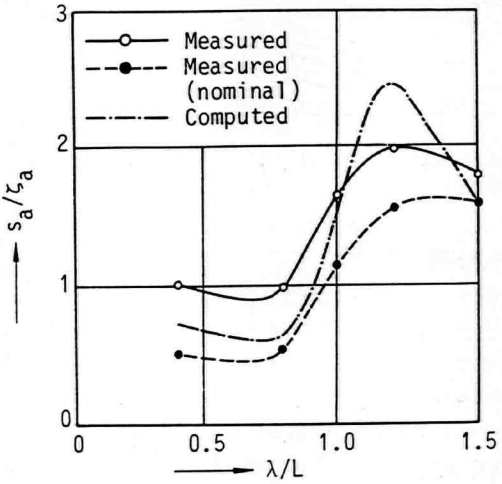

Figure 9.3-3: Transfer function of relative motion at Station 19½ for Fn = 0.20.

turbed relative motion being compiled of measured heave, pitch and undisturbed incident wave is also shown and is considerably lower. The computed relative motion is seen to overpredict for wave lengths a little longer than the ship length and to underpredict for wave length shorter than the ship length.

-added resistance components

In Figure 9.3-4 we have shown the various integrations that are relevant to this case. It was found that I_{61}, I_{62} and I_{12} were very small indeed and have been omitted from the diagram. It is shown that the integration of the relative motion around the waterline (I_8) is again the largest component, and also virtually the only component that generates resistance, all others producing a forward force. Like in the foregoing cases of the Wigley hulls it is interesting to note the importance of I_{51} and I_{52} being the kinetic energy terms that generate a suction force to forward. In the figure it is also shown that the kinetic energy term I_{52} is almost as large and opposite in sign to the relative motion term I_8. Also the kinetic term I_{51} maintains a considerable magnitude up to short wave lengths. The nett result of all these components is a total added resistance which is smaller than the measurements and which is even positive in short waves, such unlike the measurements. It would seem that in particular the I_{51} and I_{52} must

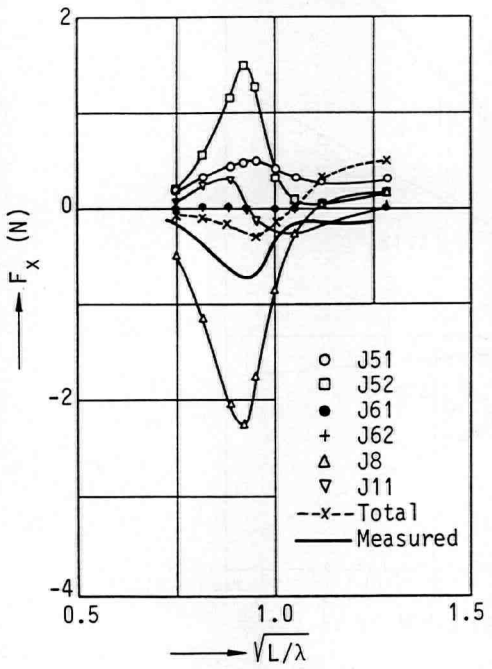

Figure 9.3-4

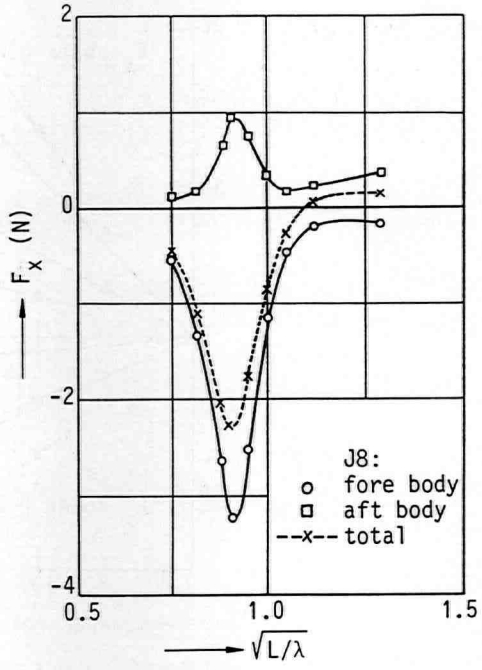

Figure 9.3-5

Added resistance components (Fn = 0.20).

be held responsible for this effect. Probably the sharp bilge radius of the forebody still produces too high local pressure variations leading to too high mean values of pressure. In Figure 9.3-5 the contribution of fore and aftbody to the total I8 is shown. As expected the aftbody contributes a forward positive force. It is also shown that in the short wave range the total I8 becomes positive, due to the fact that for short waves the wave oscillations at the aftbody are apparently not sufficiently suppressed in the computation.

-added resistance of segments

Further insight is furnished by Figure 9.3-6 where we have plotted the forces on the various segments of this model. On the abscisse the squared relative motion at the forebody is used as 'input' parameter and the resistance components as the output are shown on the ordinate. When we compare like with like we find that the upper bow force as computed is fairly well in line with the measurement, yet the lower bow and the stern forces are overpredicted.

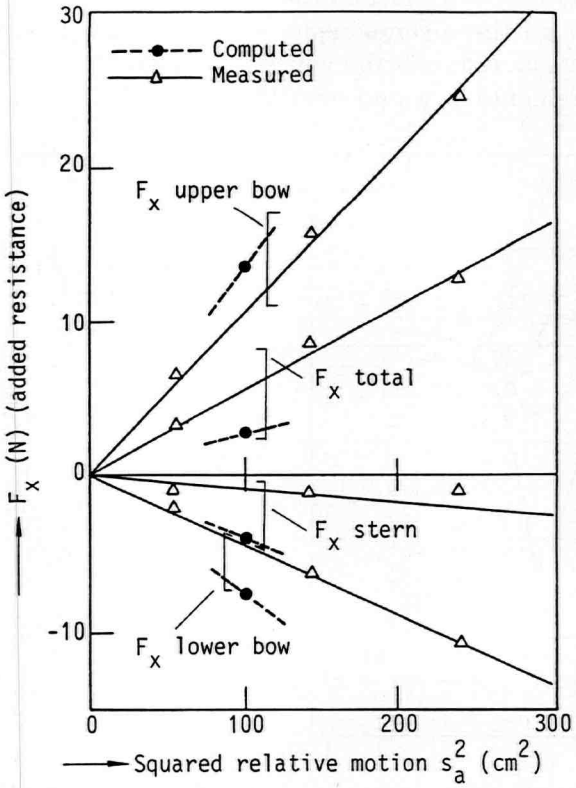

Figure 9.3-6: Comparison of added resistance contributions of various ship segments (Fn = 0.20).

Since the latter are positive they greatly affect the computed total added resistance which then becomes considerably smaller than the measured total force. In the main both the experiments and the computations support the conclusion that the upper bow determines the wave added resistance and is the governing part of the ship in this respect. Both approaches also support the finding that the lower bow and the stern produce a propulsive force, i.e. a reduction of their contribution to the steady calm water resistance.

9.4 Correlation of high-speed frigate data

-references

The model test results obtained for the high-speed frigate were compared with the results of computations. For the experimental results we refer to Ref. (9-7), a summary of some of the most interesting test results is given in Sections 7.2.2 and 7.6.2. The computations were carried out following the theory as outlined in Chapter 8.

-computation discretization scheme

The hull form was discretized in a large number of facets (748). The facet scheme is given in Figure 9.4-1. In a likewise manner as for the other hulls the top layers of panels could be stripped off to obtain derivatives of stationary flow quantities with respect to draft.

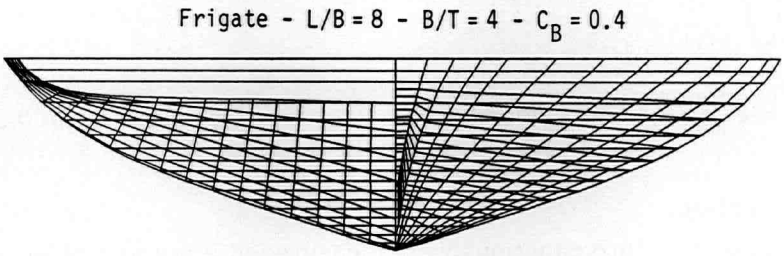

Figure 9.4-1: Bodyplan and panel distribution of high speed frigate.

-steady bow wave system

The steady bow wave as computed is given in Figure 9.4-2 for the three drafts used in the computations, which were 13 percent of the draft apart. From the steady bow wave crests we can calculate a swellup coefficient of 1.17 which would appear to be on the low side. We do not have direct measurements to compare with, yet we may compare this value to the values obtained by experiment for the Compact Frigate discussed in Section 7.3 which has very similar forebody

sectional shape. We then observe in Figure 7.3-4 that the compact frigate had a similar coefficient, as can be read off the ordinate for the speed of Fn. = 0.30. We also see that for increasing speed the swellup coefficient goes up dramatically. Unlike in the foregoing ship hulls the frigate had no stern wave sitting under the stern, owing to the flat transom stern. The program computed a large stern wave, but at some distance abaft the stern, where it did not interfere with the computation of the relative motion aft.

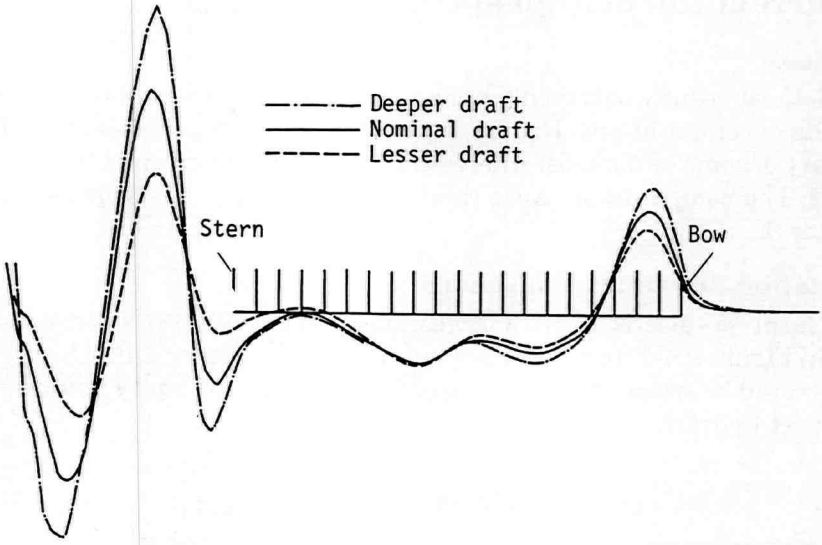

Figure 9.4-2: Stationary bow wave profile for three drafts (Fn = 0.285).

-relative motions

For the frigate the relative motions were measured at a number of locations on the forebody. These results can be compared with the computations. When we consider relative motions it should not pass unnoticed that the sides of the forebody hull are extremely inclined at the waterline, as can be judged from Figure 9.4-1 and 7.6.2-1 for model 5a. The inclined side-walls of the hull above the water will most probably have interfered with the crests of the incoming waves so as to increase the reflection and causing an increase of the relative motion. In Figure 9.4-3 we have compared the relative motion as measured and computed at station 19 and the fit is remarkable for the greater part of the frequency range.

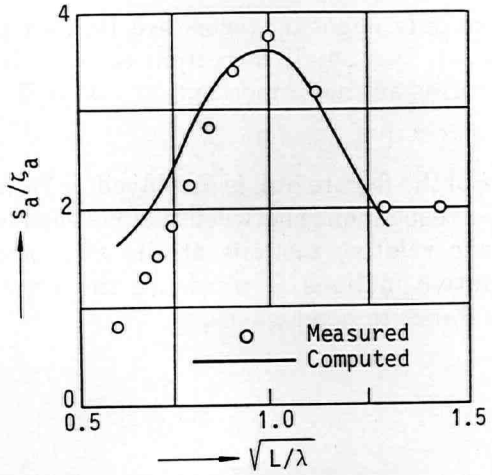

Figure 9.4-3: Transfer function of relative motion (Station 19, Fn = 0.285).

-added resistance components

In Figure 9.4-4 we have plotted the various components of the added resistance. It is again shown that the forebody contribution of the relative motion gives by far the largest contribution, the aftbody part of I8 representing only 10 percent

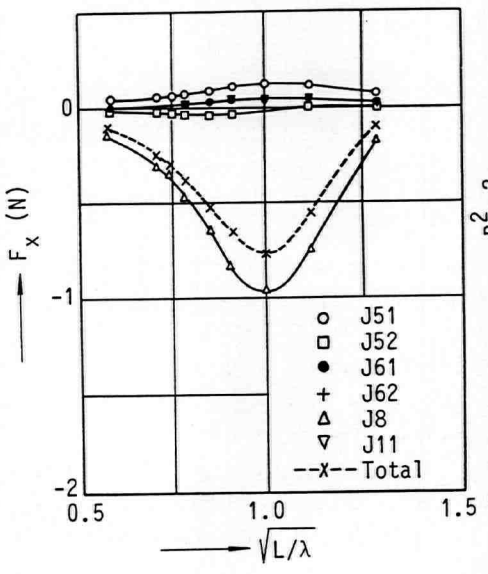

Figure 9.4-4

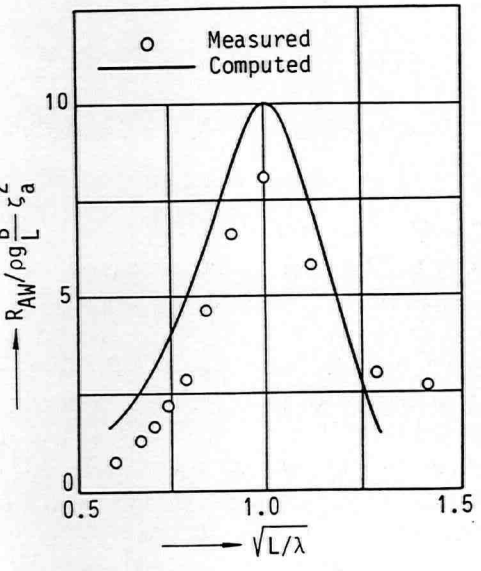

Figure 9.4-5

Added resistance components and transfer function (Fn = 0.285).

of the total of I_8. The only opposing terms are I_{51}, the kinetic energy at the forebody, and I_{61} which is a small correction term to I_{51}, taken around the waterline. All other terms are not important for this hull.

-added resistance

The added resistance of the frigate hull is displayed in Figure 9.4-5 as measured and computed. The correspondence between them is good as may be expected on basis of the fit of the relative motions at the forebody. This supports the supposition that relative motions forward are the driving mechanism with respect to added resistance in head waves.

Chapter 10

Conclusions

On basis of the research described in the foregoing chapters the following can be concluded:

1. The hypothesis as posed in Chapter 4, stating that the resistance increase of a ship in waves is for the most part due to the relative vertical water motion at the bow, can in view of the results of this research be accepted. (Chapter 4, Section 7.2, section 9)

2. The resistance increase of a ship in waves is mainly of potential origin, frictional forces playing only a minor role. (Chapter 5)

3. The relative vertical water motion at the bow of a ship contains a considerable contribution from the interaction between the instationary and the stationary flow. The interaction makes its presence manifest at the water surface through the 'dynamic swell-up' effect. (Section 7.3)

4. The 'dynamic swell-up' effect turns out to be dependent upon the local undisturbed relative water motion, made up of vertical ship motions and undisturbed incident wave. It is strongly dependent on speed and on bow form, and only weakly dependent on frequency. (Section 7.3)

5. The forces responsible for the resistance increase in waves from ahead are for the most part applied at the bow. The upper part of the bow which becomes alternatingly wet and dry was found to contribute most to the resistance increase while the underwater part of the bow and also the stern

have a negative contribution to the resistance increase in waves. (Section 7.4)

6. It was shown that the 'relative motion hypothesis', which forms one of the 'building bricks' of ship motion theory, is not only valid for instationary vertical forces, but also for the instationary pressures. (Section 7.5)

7. The instationary pressure distribution at the bow depends on the relative motion irrespective of how the relative motion is brought about, either through heaving, pitching, incident wave or a combination of these. (Section 7.5)

8. In order to incorporate the 'dynamic swell-up' effect in the mathematical model based on linear potential theory, and also to extrapolate the velocity field from the domain under the undisturbed waterplane surface to the actual free surface, it is necessary to use a double linearization scheme, i.e. to linearize with respect to the vertical field coordinate and also, in addition, with respect to the undisturbed relative motion. (Chapter 6, Section 7.5, Chapter 8)

9. The main particulars of a ship have a large influence on the behaviour of a ship in waves in general, and on the resistance increase in waves in particular. The ship length is the quantity that causes the 'tuning' of the ship's pitching with the wave length in head waves. The beam is mainly responsible for the magnitude of the added resistance force. The resistance increase is shown to be proportional with beam squared in longer waves and with linear beam in short waves. (Section 7.6)

10. Experiments on models having different bow forms show that to minimize the resistance increase due to waves from ahead, a sharp bow form should be favoured in short waves, whilst in long waves a cylindrical bow is better. Since most ships operate in comparatively short waves for most of the time, it is in general recommended to choose a rather sharp bow form. (Section 7.7)

11. For oblique wave headings from the bow quarter the experimental data also shows a good correlation between resistance increase and relative motions at the bow, indicating that also for oblique wave headings the relative motion at the bow remains the governing quantity. (Section 7.8)

12. To obtain insight into the make-up of the resistance increase in waves a mathematical model based on linear potential theory is a useful tool. (Chapter 8)

13. The correlation of the computational results to the experimental results of four different ship forms is satisfactory enough to accept the mathematical model as a useful description of the physics involved. (Chapter 9)

This page intentionally left blank

Appendix

Hydrodynamic theory

In the present appendix we will give a brief derivation of the exact and the linearized boundary value problem that we have invoked and modified to describe the physical findings of the experiments.

Also in this chapter the selection of system of axes and rigid body motions is made.

A.1 Coordinate systems

In the following sections as well as in Chapter 8 use is made of three right-handed Cartesian coordinate systems, defined by:

$\bar{X} = (X_1, X_2, X_3)$	fixed in space
$\bar{x}' = (x'_1, x'_2, x'_3)$	fixed with respect to the ship
$\bar{x} = (x_1, x_2, x_3)$	moving in steady translation with the mean forward velocity of the ship

The first system has its origin in O in the undisturbed free surface, taking $X_3=0$ as the free-surface plane, the X_1-axis positive in the direction of the ship's forward velocity, the X_3-axis positive upward and X_2-axis to make the system right-handed.

The second system is fixed in the ship. When the ship is at rest the origin O' is the point of trisection of the calm water plane, the ship's centre plane of symmetry and the vertical plane passing through the centre of gravity of the

ship. For the ship at rest the $O'x_1'$-axis points horizontally towards the bow, the $O'x_2'$-axis points horizontally to port and the $O'x_3'$-axis points upwards.

The third system of axes has its origin in the same point as the second system, when the ship is at rest. The axes remain parallel to the space-fixed axes at all times. The third system translates at the mean forward velocity of the ship.

The steady moving coordinate system $\bar{x}$ is defined by the transformation:

$$\bar{x} = (X_1 - Ut, X_2, X_3) \tag{A-1}$$

with U the mean velocity of the ship. The ship-fixed system is defined such that $\bar{x} = \bar{x}'$ in steady-state equilibrium.

The space-fixed system $\bar{X}$ is the simplest in which to express the free-surface boundary condition, whereas the ship-fixed system $\bar{x}'$ is the best in which to derive the boundary condition on the ship's wetted surface. The steady moving coordinate system $\bar{x}$ is an inertial reference frame in which the motions are periodic.

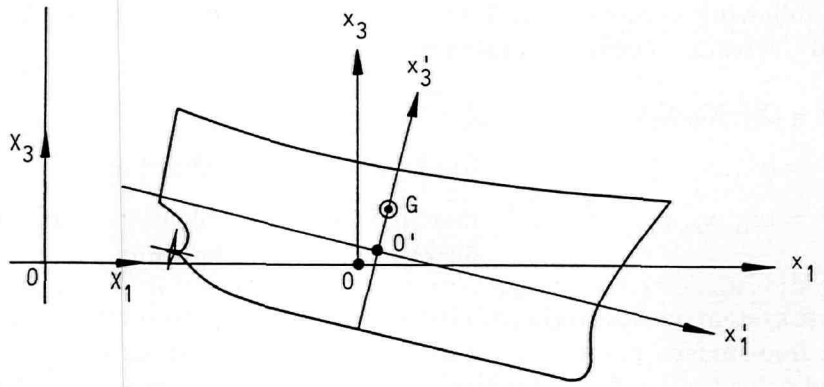

Figure A-1: Definition of systems of axes.

The angular motions of the body about the travelling axes $\bar{x}$ and about the body-fixed axes $\bar{x}'$ are assumed to be small.

A.2 Rigid body motions

Suppose the body is moving in steady translation and carrying out small amplitude motions in six degrees of freedom. The position vector of a point on the hull of the body relative to the three systems of axes can be written as follows:

- in body-fixed axes : $\bar{x}'$ (A-2)

which is of course independent of the motions of the ship

- in translating axes: $\bar{x} = \bar{x}' + \bar{\alpha}$ (A-3)

which $\bar{\alpha}$ represents a small oscillatory quantity which can itself be decomposed into:

$$\bar{\alpha} = \bar{\xi} + \bar{\Omega} * \bar{x}' \tag{A-4}$$

where $\bar{\xi}$ and $\bar{\Omega}$ denote respectively the unsteady translation and rotation of the ship relative to the origin of the steady translating axes. Their components can be enumerated as:

$$\bar{\xi} = (\xi_1, \xi_2, \xi_3) \qquad \text{(surge, sway, heave)} \tag{A-5}$$

$$\Omega = (\Omega_1, \Omega_2, \Omega_3) \qquad \text{(roll, pitch, yaw)} \tag{A-6}$$

- in space-fixed axes: $\bar{X} = Ut\bar{i} + \bar{x}$ (A-7)

$$= Ut\bar{i} + \bar{x}' + \bar{\alpha} \tag{A-8}$$

If we then define the oscillatory motion to be composed of first order and second order oscillations we obtain for the oscillatory motion:

- first order : $\bar{\alpha}^{(1)} = \bar{\xi}^{(1)} + \bar{\Omega}^{(1)} * \bar{x}'$ (A-9)

- second order: $\bar{\alpha}^{(2)} = \bar{\xi}^{(2)} + \bar{\Omega}^{(2)} * \bar{x}'$ (A-10)

For the position vector of a point on the hull of the ship we obtain:

- in body-fixed axes : $\bar{x}'$ (A-11)

- in translating axes: $\bar{x} = \bar{x}' + \varepsilon\bar{\alpha}^{(1)} + \varepsilon^2\bar{\alpha}^{(2)}$ (A-12)

- in space-fixed axes: $\bar{X} = Ut\bar{i} + \bar{x}' + \varepsilon\bar{\alpha}^{(1)} + \varepsilon^2\bar{\alpha}^{(2)}$ (A-13)

For the velocities of a point on the hull we obtain likewise:

- in body-fixed axes : $\dot{\bar{x}}' = 0$ (A-14)

- in translating axes: $\bar{v} = \dot{\bar{x}} = \varepsilon\dot{\bar{\alpha}}^{(1)} + \varepsilon^2\dot{\bar{\alpha}}^{(2)}$ (A-15)

- in space-fixed axes: $\bar{V} = \dot{\bar{X}} = U\bar{i} + \varepsilon\dot{\bar{\alpha}}^{(1)} + \varepsilon^2\dot{\bar{\alpha}}^{(2)}$ (A-16)

We can also write for the oscillatory velocities:

- first order : $\dot{\bar{\alpha}}^{(1)} = \dot{\bar{\xi}}^{(1)} + \dot{\bar{\Omega}}^{(1)} * \bar{x}'$ (A-17)

- second order: $\dot{\bar{\alpha}}^{(2)} = \dot{\bar{\xi}}^{(2)} + \dot{\bar{\Omega}}^{(2)} * \bar{x}'$ (A-18)

Finally, having defined the position, motions and velocities of a point fixed on the hull of the ship, there remains to be defined the orientation of a surface element of the hull. This orientation is defined by the outward pointing normal vector, outward from the hull.

This normal vector can also be defined in the various systems of axes:

- in body-fixed axes : $\bar{n}'$ (A-19)

which is constant in these axes

- in translating axes: $\bar{n} = \bar{n}' + \bar{\Omega} * \bar{n}'$ (A-20)

- in space-fixed axes: $\bar{N} = \bar{n} = \bar{n}' + \bar{\Omega} * \bar{n}'$ (A-21)

In view of the first and second order oscillatory motions the latter can also be written as:

$$\overline{N} = \overline{n} = \overline{n}' + \varepsilon\overline{\Omega}^{(1)} * \overline{n}' + \varepsilon^2\overline{\Omega}^{(2)} * \overline{n}' \tag{A-22}$$

or

$$\overline{N} = \overline{n} = \overline{n}' + \varepsilon\overline{n}^{(1)} + \varepsilon^2\overline{n}^{(2)} \tag{A-23}$$

A.3 The boundary value problem: the exact formulation

In order to come to an exact formulation of the fluid behaviour within the framework of potential theory, we have to make the following assumptions. We assume the fluid to be:

- a continuum, so that the molecular mean free path is many orders of magnitude smaller than the typical length scale of the problem we concern ourselves with;
- homogeneous, so no spatial variations of fluid characteristics occur;
- isotropic, so that the fluid characteristics are independent of direction;
- inviscid, so no shear stresses develop, nor can they set up rotation;
- irrotational, so that no rotation, not even initial rotation, is present in the fluid;
- incompressible, so that the specific density is a constant.

With these assumptions the fluid velocity vector $\overline{V}\ (\overline{X},\ t)$ is equal to $\nabla\Phi$, with the velocity potential $\Phi(\overline{X},t)$ governed by Laplace's equation $\nabla^2\Phi = 0$ throughout the fluid domain.

The fluid pressure $p(\overline{X},t)$ is given by Bernoulli's equation:

$$p = -\rho\,(\Phi_t + \tfrac{1}{2}V^2 + gX_3) + p_a \tag{A-24}$$

In this formulation as well as hereinafter, when independent variables $(\bar{x},t)$ appear as subscripts partial differentiation is indicated.

The fluid domain is bounded by the free surface, the surface of the body, the sea floor and a boundary at infinity. Within the fluid domain the Laplace equation governs the fluid behaviour. In addition suitable conditions have to be imposed on the boundaries in order to solve for the velocity potential Φ.

Free-surface condition in space-fixed coordinates

The free surface is defined by the elevation $X_3 = \zeta(X_1, X_2, t)$. On this surface the

kinematic boundary condition is expressed by means of the substantial derivative $D/Dt = \partial/\partial t + \overline{V}.\nabla$ in the form:

$$(D/Dt)\,(\zeta - X_3) = 0 \qquad \text{on } X_3 = \zeta \quad \text{(A-25)}$$

Since the position of the free surface is unknown, an additional dynamic boundary condition is imposed, stating that the pressure on the free surface is atmospheric. From Bernoulli's equation it follows that:

$$\Phi_t + \tfrac{1}{2}V^2 + gX_3 = 0 \qquad \text{on } X_3 = \zeta \quad \text{(A-26)}$$

This boundary condition can be used to determine the free-surface elevation from the implicit equation:

$$\zeta = -\,(1/g)\,(\Phi_t + \tfrac{1}{2}V^2) \qquad \text{on } X_3 = \zeta \quad \text{(A-27)}$$

Since this condition holds on the free surface for all time, its substantial derivative can be set equal to zero. This gives an alternative boundary condition for the velocity potential:

$$\Phi_{tt} + 2\nabla\Phi \cdot \nabla\Phi_t + \tfrac{1}{2}\nabla\Phi \cdot \nabla(\nabla\Phi \cdot \nabla\Phi) + g\Phi_{X_3} = 0$$

$$\text{on } X_3 = \zeta \quad \text{(A-28)}$$

Free-surface condition in translating axes

An alternative formulation for the free surface condition can be found if we transpose the above equation onto steady translating axes. There are various ways to do this, one is to apply the substantial derivative for steady forward speed to the Bernoulli equation for the forward speed case:

$$\left(\frac{\partial}{\partial t} - U\frac{\partial}{\partial x_1} + \nabla\Phi \cdot \nabla\right)\left(\varphi_t - U\varphi_{x_1} + \tfrac{1}{2}\nabla\varphi \cdot \nabla\varphi + gx_3\right) = 0 \qquad \text{(A-29)}$$

which yields:

$$\varphi_{tt} + 2\nabla\varphi \cdot \nabla\left(\varphi_t - U\varphi_{x_1}\right) + \tfrac{1}{2}\nabla\varphi \cdot \nabla\,(\nabla\varphi \cdot \nabla\varphi)$$

$$+ g\varphi_{x_3} - 2U\varphi_{x_1 t} + U^2\varphi_{x_1 x_1} = 0 \qquad \text{on } x3 = \zeta \quad \text{(A-30)}$$

If we set the ship speed to zero we obtain the zero speed case again.

Boundary condition on the ship's hull

On the submerged portion of the ship's surface A, the normal velocity is equal to that of the adjacent fluid. The appropriate boundary condition is:

$$(\overline{V}_S - \overline{V}) \cdot \overline{N} = 0 \qquad \text{(A-31)}$$

on A, the instantaneous wetted surface where $\overline{V}_S$ is the local velocity of the ship's wetted surface, the unit normal $\overline{N}$ is defined to point outward of the hull.

Essentially this means that the relative motion between the hull and the adjacent water particle is zero in the direction normal to the hull so that no water passes through the hull. The boundary condition is to be imposed on the instantaneous position of the body.

Boundary condition on the sea floor

On the bottom of the sea, if not infinitely far away from the body, the same condition of zero fluid transport in the normal direction is to be imposed as on the hull. In this case it reads:

$$\nabla\Phi \cdot \overline{N} = 0 \qquad \text{on } X_3 = -d \text{ (water depth)} \qquad \text{(A-32)}$$

Boundary condition at infinity

In order to close the fluid region an appropriate outer boundary is to be defined.

This condition is most usefully applied in a limit form stating that the energy flux of the waves associated with the disturbance of the ship is directed away from the ship at infinity. The incoming wave signified by its potential Φ_0 already has a well-defined direction of travel, entering the fluid domain on one side and leaving it on the other side, so that this one potential need not be subjected to the energy flux condition.

The condition is known as the Sommerfeld radiation condition, and takes the form:

$$\lim_{kR\to\infty} (kR)^{1/2} \left(\frac{\partial}{\partial R} - ik\right) \varphi_i \qquad (i = 1 \ldots 7) \qquad \text{(A-33)}$$

This condition imposes an uniqueness on the problem and its solution that would not otherwise be present; proof was given by John (1950) [A-1].

As pointed out by J. Wehausen (1971) [A-4] for motion generated by an incident monochromatic wave in which transients have died out, the appropriate radiation condition is not known for all cases.

For the case that we concern ourselves with infinite fluid depth and a body bounded in extent the condition is known; yet it is one of the limited number of cases where the radiation condition is known.

A.4 The boundary value problem: the linearized formulation

General

The problem formulation stated above is exact within the limitations of an ideal incompressible fluid. However, the non-linear free-surface condition precludes solutions without further simplifications. Further progress requires the fluid motion to be small in some sense, which leads to a linearization of the problem as set forth in the sequel.

Power series expansion

An additional assumption, in accordance with classical hydrodynamic theory, see for instance Stoker [A-2], is to be made implying that the velocity potential of the flow and all quantities to be derived from it, fluid velocity, pressure, wave height, hydrodynamic forces and motions of the ship, may be expanded in a convergent power series with respect to a small parameter ε so that for example for the potential:

$$\varphi = \varphi^{(0)} + \varepsilon\varphi^{(1)} + \varepsilon^2\varphi^{(2)} + 0(\varepsilon^3) \tag{A-34}$$

where $\varepsilon << 1$ is a small parameter.

The wave elevation would be:

$$\zeta = \zeta^{(0)} + \varepsilon\zeta^{(1)} + \varepsilon^2\zeta^{(2)} + 0(\varepsilon^3) \tag{A-35}$$

where the affix (0) denotes the static *(DC)* value, (1) denotes the first order quantity and (2) denotes second order quantities. The first order quantities will be preceded by ε, the second order quantities by ε^2. If an expression or equation contains only first or only second order quantities the ε or ε^2 factor is deleted. In such cases the order of the components can still be determined by the affix. It should be noted that the product of the first order quantities is itself a second order quantity.

Higher order terms

In monochromatic sinusoidal waves the first order quantities are oscillatory quantities with the wave frequency. In the most general case, where a number of sinusoidal waves are superimposed, the second order quantities contain components at frequencies much lower and much higher than the range of wave

frequencies. These frequency components are no doubt important. Low frequency components give rise to wave excitation usually called slowly varying drift forces, which for a ship moored in the open sea can give rise to large motions if its resonance frequency in the mooring system is excited. For a free sailing ship this component is of lesser importance, if any. At the other end of the scale the high frequency components may produce excitation of vibratory modes of the ship's hull, which is called 'springing'.

Mean value

Although interesting in their own right these high and low frequency components may be, the present study is concerned with the wave added resistance, which involves the mean value of the longitudinal hydrodynamic force. This mean value is the result of combinations of higher order quantities and in principle the power series expansion should extend to orders higher than two. However, two considerations can be brought forward on basis of which a rejection of orders higher than two is deemed justified.

First, the mean value component associated with a higher order oscillation is proportional to the amplitude of that higher order quantity. In the postulated power series the amplitude of the higher order quantities diminish rapidly, if - in keeping with the assumption - the series is convergent. Secondly, experimental evidence like shown in Chapter 7 shows a strong correlation between the mean value and the second order wave frequency component, so that for the present case we could restrict ourselves to orders up to and including the order two.

Further limitation to first order only

Moreover there is a consideration to reduce this even further. The ship at speed in sinusoidal regular waves does not exhibit any dominant or even discernible second order motions as far as in particular heaving and pitching are concerned. Yet, as analysis of relevant experiments at model scale bear out, cases where the ship was subjected to wave forces without appreciable second order input, the force on the ship did contain a second order term, and also a close relation was present between mean value, first order term and second order term (e.g. Chapter 7).

Consequently we need not take along all information up to and including the second order, all the more so in view of the fact that solutions - even partial solutions - to the second order problem of a ship at forward speed are non-existent. Even more, for the first order, solutions exist only for simplified cases.

So, in summary, it is hypothesized that components resulting from first order quantities or combinations thereof will, for the most part, make up the mean value of the hydrodynamic force that we are interested in.

The linearized free-surface condition

If the amplitude ζ_a of the incident wave system is small, the oscillatory motions of the ship and the surrounding fluid will be proportional to ζ_a. Linearization of the unsteady problem can be justified on this basis.

We assume that the total potential can be written as:

$$\Phi(\overline{X}, t) = \varphi(\overline{x}, t)$$
$$= \varphi^{(0)}(\overline{x}) + \varepsilon\varphi^{(1)}(\overline{x}, t) \qquad \text{(A-36)}$$

where the unsteady potential is assumed small. The zero order potential is used to denote the velocity potential due to the steady forward motion of the ship, inclusive of the uniform parallel flow potential:

$$\overline{\Phi}(\overline{X}, t) = \varphi^{(0)}(\overline{x}) \qquad \text{(A-37)}$$

The velocity vector of the steady flow relative to the moving frame of reference is:

$$\overline{W} = \nabla\varphi^{(0)} \qquad \text{(A-38)}$$

In the moving reference frame the non-linear free-surface condition for the steady flow is:

$$g\varphi^{(0)}_{x_3} + \nabla\varphi^{(0)} \cdot \nabla\left(\tfrac{1}{2}(\nabla\varphi^{(0)})\right)^2 = 0 \qquad \text{on } x_3 = \zeta^{(0)} \quad \text{(A-39)}$$

which can be further linearized to:

$$g\varphi^{(0)}_{x_3} + U^2\varphi^{(0)}_{x_1x_1} = 0 \qquad \text{on } x_3 = 0 \quad \text{(A-40)}$$

In principle this free-surface condition (eq. (A-40)) applies to the perturbation potential solely. However, the uniform flow can be added since its derivatives are zero and eq. (A-40) can also be thought to apply to the total steady potential.

The steady free-surface elevation associated with this condition is:

$$\zeta^{(0)} = -\frac{1}{2g}(W^2 - U^2) \qquad \text{on } x_3 = \zeta^{(0)} \quad \text{(A-41)}$$

which can like the associated free-surface condition be linearized to:

$$\zeta^{(0)} = -\frac{1}{2g}(W^2 - U^2) \cdot \left(\frac{g}{g + \overline{W} \cdot \overline{W}_{x_3}}\right) \qquad \text{on } x_3 = 0 \quad \text{(A-42)}$$

For the unsteady problem we have to take the formula (A-28) as the departure point for the free-surface condition. If we substitute the total potential (eq. (A-36) above) and neglect second order terms in the unsteady potential $\phi^{(1)}$, the free-surface condition becomes:

$$\tfrac{1}{2}\overline{W}\cdot\nabla(W^2)+g\varphi_{x_3}^{(0)}+\varphi_{tt}^{(1)}+2\overline{W}\cdot\nabla\varphi_t^{(1)}+\overline{W}\cdot\nabla(\overline{W}\cdot\nabla\varphi^{(1)})$$
$$+\tfrac{1}{2}\nabla\varphi^{(1)}\cdot\nabla(W^2)+g\varphi_{x_3}^{(1)}=0 \qquad \text{on } x_3=\zeta \quad \text{(A-43)}$$

to be satisfied on the unknown free surface. The contributions from the steady terms in the above expression can be evaluated by expanding from ζ to $\zeta^{(0)}$ and by using the expression for the steady free-surface condition, eq. (A-39).

Thus, the unsteady velocity potential is governed by the first order free-surface condition:

$$-\left(\varphi_t^{(1)}+\overline{W}\cdot\nabla\varphi^{(1)}\right)\left[\tfrac{1}{2}\frac{\partial}{\partial x_3}(\overline{W}\cdot\nabla W^2)+g\varphi_{x_3x_3}^{(0)}\right]\Big/\left[g+\overline{W}\cdot\overline{W}_{x_3}\right]$$
$$+\varphi_{tt}^{(1)}+2\overline{W}\cdot\nabla\varphi_t^{(1)}+\overline{W}\cdot\nabla(\overline{W}\cdot\nabla\varphi^{(1)})$$
$$+\tfrac{1}{2}\nabla\varphi^{(1)}\cdot\nabla(W^2)+g\varphi_{x_3}^{(1)}=0 \qquad \text{on } x_3=\zeta^{(0)} \quad \text{(A-44)}$$

The free-surface condition for the unsteady velocity potential is intimately related to the condition for the steady flow. The steady problem is to be solved first and thereafter the unsteady problem involving a free-surface condition to be evaluated on the steady surface elevation $\zeta^{(0)}$.

The eq. (A-44) above is a combination of steady and unsteady effects and its general solution is at present impossible. This stems from the impossibility to separate the time and space variables or more general to construct a fundamental velocity potential for a translating pulsating source that satisfies the full unsteady free-surface condition set forth above.

It is fair enough to derive expressions that we would very much like to solve, but equally important it is to proceed to expressions that can be solved and can lead us to practical applications. If the perturbation of the steady flow due to the ship is neglected such that $\overline{W}=-U\bar{i}$, then the free-surface boundary condition in the unsteady velocity potential reduces to a much more simple expression:

$$\varphi_{tt}^{(1)}-2U\varphi_{x_1t}^{(1)}+U^2\varphi_{x_1x_1}^{(1)}+g\varphi_{x_3}^{(1)}=0 \qquad \text{on } x_3=0 \quad \text{(A-45)}$$

For an unsteady potential harmonic with time this can also be expressed as:

$$U^2\varphi^{(1)}_{x_1x_1} - 2i\omega_e U\varphi^{(1)}_{x_1} - \omega_e^2\varphi^{(1)} + g\varphi^{(1)}_{x_3} = 0 \qquad \text{on } x_3 = 0 \quad \textit{(A-46)}$$

in which ω_e is the circular frequency.

The velocity potential that satisfies the speed and frequency-dependent free-surface boundary condition is that of the fundamental travelling pulsating source, the formulation of which can be found for instance in Wehausen and Laitone [A-5].

The linearized body boundary condition

Like the free-surface boundary condition we will derive the body boundary condition for the steady and unsteady flow and put it in a linearized form. The boundary condition on the hull in its steady state position $\overline{A}$ takes the form:

$$\overline{W} \cdot \overline{n} = 0 \qquad \text{on } \overline{A} \quad \text{(A-47)}$$

For the unsteady boundary condition the local velocity of the ship's wetted surface can be decomposed in the following form, as expressed in the space-fixed reference frame:

$$\overline{V}_s = U\overline{i} + \dot{\overline{\alpha}}^{(1)} \qquad \text{(A-48)}$$

where $\overline{\alpha}^{(1)} = \overline{x}^{(1)} - \overline{x}'$ represents the first order local (small) oscillatory displacement of the ship's surface in translating axes and the dot represents time differentiation in the moving reference frame. Since we are dealing with first order quantities solely we may as well drop the superscript (1).

Like shown before (eq. (A-4)) the oscillation can be decomposed into:

$$\overline{\alpha} = \overline{\xi} + \overline{\Omega} * \overline{x}' \qquad \text{(A-49)}$$

in which $\overline{\xi}$ and $\overline{\Omega}$ denote the unsteady translation and rotation vectors respectively, relative to the origin of the steady translating axes.

If we combine the expressions (A-38), (A-36) and (A-48) and substitute these in expression (A-31) we obtain the unsteady boundary condition:

$$\varphi_n^{(1)} = \dot{\overline{\alpha}} \cdot \overline{n} - \overline{W} \cdot \overline{n} \qquad \text{on } \overline{A} \quad \text{(4-50)}$$

This expression is exact, since it is to be evaluated on the actual moving fluctuating wetted surface A. The expression can be reduced to a more tangible form through a Taylor's expansion with respect to the hull in its mean position, so that we obtain:

$$\varphi_n^{(1)} = \left[\dot{\bar{\alpha}} + (\overline{W} \cdot \nabla)\,\bar{\alpha} - (\bar{\alpha} \cdot \nabla)\overline{W} \right] \cdot \bar{n} \qquad \text{on } \bar{A} \quad \text{(A-51)}$$

which can be written in a more compact form as:

$$\varphi_n^{(1)} = \left[\dot{\bar{\alpha}} + \nabla * (\bar{\alpha} * \overline{W}) \right] \cdot \bar{n} \qquad \text{on } \bar{A} \quad \text{(A-52)}$$

This boundary condition was derived by Timman and Newman in 1962 [A-3].

If we apply the same simplification as done before for the free-surface boundary condition and neglect the perturbations of the uniform steady flow field and set $\overline{W} = -U\bar{i}$ we obtain:

$$\varphi_n^{(1)} = \left[\left(\frac{\partial}{\partial t} - U\frac{\partial}{\partial x_1} \right) \bar{\alpha} \right] \cdot \bar{n} \qquad \text{(A-53)}$$

$$= \left[\dot{\bar{\alpha}} - U(\overline{\Omega} * \bar{i}) \right] \cdot \bar{n} \qquad \text{(A-54)}$$

We can interpret the term proportional to U as the product of the ship's forward velocity and the angle of attack due to pitch and yaw.

This page intentionally left blank

References

References of Section 1:

1-1 KENT, J.L.: *"Ships in Rough Water"*, Thomas Nelson and Sons Ltd., 1958, New York.

1-2 MÖCKEL, W.: *"Fahrtverlust der Schiffe im Seegang aus Fahrtbeobachtungen"*, Schiff und Werft, Heft 19/20, October 1944, pp 224-228.

1-3 LEWIS, E.V.: *"Ship Speeds in Irregular Seas"*, Transactions SNAME, Vol. 63, 1955, pp 134-202.

1-4 LEWIS, E.V. AND MORRISON, M.: *"Preliminary Analysis of Moore-McCormack Log Data"*, SNAME bulletin, Vol. 9, No. 3, October, 1954, pp 15 and 18.

1-5 LEWIS, E.V. AND MORRISON, M.: *"Additional Partial Analysis of Moore-McCormack Log Data"*, International Shipbuilding Progress, Vol. 2, No. 7, 1955, pp 132-133.

1-6 DIWALD, HELLMUT,: *"Der Kampf um die Weltmeere"*, DroemerischVerlagsanstelt Munchen, 1980.

1-7 BEKKER, C.: *"Verdammte See"*, Gerhard Stalling Verlag, Oldenburg, 1971.

1-8 KEHOE, J.W.: *"Destroyer Seakeeping: Ours and Theirs"*, United States Naval Institute Proceedings, November 1973.

1-9 COMSTOCK, E.N., BALES, S.L. AND KEANE, R.G.: *"Seakeeping in Ship Operations"*, SNAME STAR Symposium, 1980.

References of Section 2:

2-1 ADACHI,H.: *"On the calculation of wave exciting forces on ship translating in head sea waves"*, Journal of the society of naval architects of Japan, Vol. 143, 1978, pp. 34-40.

2-2 ANKUDINOV, V.K.: *"The added resistance of a moving ship in waves"*, International Shipbuilding Progress 1972, Vol. 19, No. 220.

2-3 ANKUDINOV, V.K.: *"Non-periodical forces and moments on a ship in waves"*, International shipbuilding Progress, Vol. 16, 1969, No. 174.

2-4 BECK, R.F.: *"The added resistance of ships in waves"*, Department of naval architecture and marine engineering, MIT report No. 67-9, Cambridge, Mass., June 1967.

2-5 BECK, R.F.: *"A computerized procedure for prediction of seakeeping performance"*, Dept. of naval architecture and marine engineering, MIT Report 69-2, Cambridge, Mass., March 1969.

2-6 BEUKELMAN,W.: *"Added resistance and vertical hydrodynamic coefficients of oscillating cylinders at speed"*, Delft University of Technology, Ship hydromechanics laboratory, Report No. 510, September 1980.

2-7 BEUKELMAN,W.: *"Vertical motions and added resistance of a rectangular and triangular cylinder in waves"*, Delft University of Technology, Ship Hydromechanics Laboratory, Report No. 594, July 1983.

2-8 BEUKELMAN,W. AND BUITENHEK,M.: *" Full Tscale measurements and predicted seakeeping performance of the containership 'Atlantic Crown' "*, International Shipbuilding Progress, Vol. 21, November 1974, No. 243.

2-9 BLUME,P.: *"Widerstandserhöhung volliger Schiffe in kurzen Wellen bei sehr kleinen Geschwingigkeiten"*, FDS-Bericht No. 91-1979, Hamburg, 1979.

2-10 BLUME,P. AND KRACHT,A.M.: *"Prediction of the behaviour of ships with bulbous bow in waves"*, The society of naval architects and marine engineers, Annual meeting, November 1985.

2-11 BOESE,P.: *"Eine einfache Methode zur Berechnung der Widerstandserhohung eines Schiffes im Seegang"*, Schiffstechnik Bd 17, 1970, Heft 86.

2-12 BROWN, S.H.,WAHAB, R.,YEH, H.Y.H. AND VASSILOPOULOS, L.: *"Prediction of destroyer added drag in head waves from Maruo's theory"*, International Shipbuilding Progress, Vol. 19, December 1972, No. 220.

2-13 DALZELL, J.F.: *"Application of cross-bi spectral analysis to ship resistance in waves"*, Davidson laboratory, Stevens institute of technology, Report SIT- DL-72-1606 (may 1972)

2-14 DALZELL, J.F.: *"Some additional studies of the application of cross-bi-spectral analysis to ship resistance in waves"*, Stevens Institute of Technology, Davidson laboratory, Report SIT-DL-72-1641 (December 1972).

2-15 DALZELL,J.F.: *"Application of the functional polynomial method to the ship added resistance problem"*, 11th ONR Symposium on Naval Hydrodynamics, London, 1976.

2-16 FALTINSEN,O.M., MINSAAS, K.J., LIAPIS, N. AND SKJORDAL, S.O.: *"Prediction of Resistance and propulsion of a ship in a seaway"*, 13th ONR symposium on Naval Hydrodynamics, October 1980, Tokyo.

2-17 FALINSEN, O.M.: *"Bow flow and added resistance of slender ships at high Froude nunber and low wave lengths"*, Journal of Ship Research Vol. 27, No. 3, September 1983, No. 3, pp 160-171.

2-18 FUJI, H.AND TAKAHASHI, T.: *"On the increases in the resistance of a ship in regular head waves"*, Mitsubishi Heavy Industries Technical Review, Vol. 4, December 1967, No. 6, pp 644-650.

2-19 FUJI,H.AND TAKAHASHI, T.: *"Experimental study on resistance increase of a large full ship in regular oblique waves"*, Journal of the society of naval architects of Japan, Vol. 137, 1975, pp 132.

2-20 FUJI, H. AND TAKAHASHI, T.: *"Experimental study on the resistance increase of a ship in regular oblique waves"*,Proceedings 14th ITTC, Ottawa, 1975.

2-21 GADD, G.E.: *"Some experiments on the incremental resistance due to rolling with and without bilge keels and vanes"*, RINA Transactions 1967.

2-22 GATZER, H. AND FRÖHLICH, M.: *"Experimentelle und theoretische Untersuchungen zum seegangsbedingten Zusatzwiderstand eines schnellen Frachtschiffes"*, Schiffbauforschung 23 2/1984.

2-23 GERRITSMA, J.: *"Some recent advances in the prediction of ship motions and ship resistance in waves"*, Delft University of Technology, Ship hydromechanics Laboratory Report No. 345, February 1972.

2-24 GERRITSMA, J. AND BEUKELMAN, W.: *"Analysis of the resistance increase in waves of a fast cargo ship"*, International Shipbuilding Progress, Vol. 19, No. 217, 1972 and 13th ITTC, Vol. 2, 1972.

2-25 GERRITSMA, J., BEUKELMAN, W. AND GLANSDORP, C.C.: *"The effect of beam on the hydrodynamic characteristics of ship hulls"*, 10th ONR Symposium of Naval Hydrodynamics, 1974.

2-26 GERRITSMA, J., VAN DEN BOSCH, J.J. AND BEUKELMAN, W: *"Propulsion in regular and irregular waves"*, International Shipbuilding Progress, Vol. 8, No. 82, 1961.

2-27 GERRITSMA, J., AND JOURNÉE, J.M.J.: *"Resistance increase in oblique waves"*, Proceedings 15th ITTC Part 2, 1978, Contribution to the report of the Seakeeping Committee.

2-28 HANAOKA, T.: *"The motion of a ship among waves and theory of wave resistance"*, Journal of the society of naval architects of Japan, Vol. 98, February 1956, pp1-5.

2-29 HAVELOCK, T.H.: *"The resistance of a ship among waves"*, Proceedings Royal Society of Arts, Vol. 161, 1937, p. 299.

2-30 HAVELOCK, T.H.: *"The pressure of water waves upon a fixed obstacle"*, Proceedings Royal Society of Arts, No. 963, Vol. 175, July 1940.

2-31 HAVELOCK, T.H.: *"The drifting force of a ship among waves"*, Philosofical Magazine Vol. 33, 1942, pp 467-475.

2-32 HESS, J.L. AND SMITH, A.M.D.: *"Calculation of potential flow about arbitrary bodies"*, Progress in Aeronautical Science Vol. 8, 1967.

2-33 HOSODA, R.: *"The added resistance of ships in regular oblique waves"*, Journal of the society of naval architects of Japan, No. 113, June 1973. Also : Selected papers JSNA of Japan Vol. 12, 1974.

2-34 JINKINE, V. AND FERDINANDE, V.: *"A method for predicting the added resistance of fast cargo ships in head seas"*, International Shipbuilding Progress, 1974.

2-35 JOOSEN,W.P.A.: *"Added resistance of ships in waves"*, 6th ONR Symposium on Naval Hydrodynamics, Washington, 1966.

2-36 JOURNÉE,J.M.J.: *"Motions and resistance of a ship in regular following waves"*, Delft University of Technology, Ship hydromechanics Laboratory, Report No. 440, September 1976.

2-37 KHOLODILIN,A.N. AND YURKOV,N.N.: *"On added resistance of ships in head waves"*, Proceedings 14th ITTC, Vol. 4, Ottawa, 1975.

2-38 KIM, Y.: *"Computation of the second order steady forces acting on a surface ship in an oblique wave"*, DTNSRDC Rept. SPD-0964-01, March 1981.

2-39 KREITNER,J.: *"Heave,pitch and resistance of ships in seaway"*, RINA Transactions Vol. 87, 1939, pp 203.

2-40 KWON, Y.J.: *"The effect of weather, particularly short waves, on ship performance"*, PhD Thesis, University of Newcastle, 1982.

2-41 LEE, K-Y.: *"Ein beitrag zur Berechnung der Widerstandserhöhung in von vorn kommender Wellen"*, Institut fur Schiffbau, Hamburg, Bericht Nr. 431, October 1982.

2-42 LEE, K-Y.: *"Widerstandserhöhung in kurzen Wellen"*, Schiffstechnik, Bd. 30, Heft 3, Sept. 1983.

2-43 LIN, W.L. AND REED, A.M.: *"The second order steady force and moment on a ship moving in an oblique seaway"*, 11th ONR Symposium on Ship Naval Hydrodynamics, London, March 1976.

2-44 LOUKAKIS, T.A.: *"Computer aided prediction of seakeeping performance in ship design"*, Dept. of naval archtecture and marine engineering, MIT, Report 70-3.

2-45 LOUKAKIS, T.A.: *"Theoretical evaluation of ship added resistance in waves"*, Dept of Ocean Engineering, August 1972 MIT Report 72-17.

2-46 LOUKAKIS, T.A. AND SCLAVOUNOS, P.D.: *"Some extensions of the classical approach to strip theory of ship motions, including the calculation of mean added forces and moments"*, Journal of ship research, Vol. 22, 1978, No. 1.

2-47 MARUO, H. AND HANAOKA, T. ET AL: *"Resistance in waves"*, Researches on seakeeping qualities of ships in Japan, Chapter 5, 60 th Anniversary series, The Society of Naval Architects of Japan, Vol. 8, 1963. pp 67-102.

2-48 MARUO, H.: *"On the increase of the resistance of a ship in rough seas (1)"*, Journal of the society of naval architects of Japan, No. 101, August 1957, pp 33-39.

2-49 MARUO, H.: *"On the increase of the resistance of a ship in rough seas (2)"*, Journal of the society of naval architects of Japan, No. 108, August 1960, pp 5-13.

2-50 MARUO, H.: *"The excess resistance of a ship in rough seas"*, International Shipbuilding Progress, Vol. 4, No. 35, July 1957, pp 337-345.

2-51 MARUO, H.: *"Energy relations for the wave resistance of ships in a sea-way"*, Seminar on theoretical wave resistance, 1963.

2-52 MARUO, H.: *"The drift of floating bodies in waves"*, Journal of ship research, December 1960.

2-53 MARUO, H.: Written contribution to the 15th ITTC, The Hague, Sept 1978, Proceedings Part 2, pp 67-69.

2-54 MARUO, H. AND ISHII, T.: *"Calculation of added resistance in head waves by means of a simplified formula"*, Journal of the society of naval architects of Japan, Vol. 140, 1976.

2-55 MARUO, H. AND IWASE, K.: *"Calculation of added resistance in oblique waves"*, Journal of the society of naval architects of Japan, Vol. 147, pp 79-84, June 1980.

2-56 MARUO, H.: *"Wave resistance of a ship on regular head seas"*, Bulltin of the Faculty of Engineering Yokohama National University, Vol. 9, 1960, pp73-91.

2-57 MARUO, H. AND SASAKI, N.: *"On the wave pressure acting on the surface of an elongated body fixed in head seas"*, Journal of the society of naval architects of Japan, Vol. 136, 1974, pp. 107-114.

2-58 MARUO, H.: *"Formulae for theoretical predictions of added resistance, side drift force and steady turning moment in oblique waves"*, Discussion to report of Seakeeping Committee 16th ITTC, Vol. 2. 1981, pp 131-132.

2-59 NAITO, S., NAKAMURA, S. AND NISHIGUCHI, A.: *"Added resistance in regular head waves of a ship with blunt bow"*, PRADS Trondheim, June 22-26, 1987.

2-60 NAKAMURA, S. AND SHINTANA, A.: *"On ship motions and resistance increase of mathematical ship forms in regular waves"*, Journal of the society of naval architects of Japan, Vol. 118, pp 24-35, December 1965.

2-61 NAKAMURA, S. AND NAITO, S.: *"Added resistance in short length waves on ship forms with blunt bow"*, Discussion on paper of Seakeeping committee on ITTC 1984.

2-62 NAKAMURA, S., NAITO, S., MATUMOTO, K., SUSUKIDA K . AND NISIGUCHI, A.: *"Experimental study on resistance increase in regular head waves of a ship with blunt bow"*, Journal of the kansai society of naval architects of Japan, No.190, 1983, pp73.

2-63 NETSVETAEV, Y.A.: *"An approximation for calculating the additional resistance of a ship in rough seas"*, Int. Symp. on Ship Hydrodynamics and Energy Saving, El Pardo, September 1983.

2-64 NEWMAN, J.N.: *"The damping and wave resistance of a pitching and heaving ship"*, Journal of Ship Research, Vol. 3, No. 1, June 1959, pp 1-19.

2-65 NEWMAN, J.N.: *"The drift forces and moments on a ship in waves"*, Journal of ship research, Vol. 11, No. 1, March 1967.

2-66 NEWMAN, J.N.: *"The interaction of stationary vessels with regular waves"*, 11th ONR Symposium on Naval Hydrodynamics, London, 1976.

2-67 OHKUSU, M.: *"Analysis of waves generated by a ship oscillating and running on a calm water with forward velocity"*, Jounal of the society of naval architects of Japan, Vol.142,1977, pp. 36.

2-68 OHKUSU,M.: *"Added resistance in waves in the light of unsteady wave pattern analysis"*, Proceedings 13th ONR Symposium on Ship Naval Hydrodynamics, Tokyo, October 1980.

2-69 OHKUSU,M.: *"Added resistance of blunt bow ships in very short waves"*, Journal of the kansai society of naval; architects of Japan, No. 202, September 1986.

2-70 OHKUSU,M.: *"Added resistance in waves of hull forms with blunt bow"*, Proceedings 15th ONR Symposium on naval hydrodynamics, Hamburg, pp 135, 1984.

2-71 SAKAMOTO,T. AND BABA, E.: *"Minimization of resistance of slowly moving full hull forms in short waves"*, 16th ONR Symposium on Naval Hydrodynamics, USA, July 1986.

2-72 SALVESEN,N.: *"Second order steady-state forces and moments on surface ship in oblique regular waves"*, Symposium on the dynamics of marine vehicles in waves, London, 1974.

2-73 SALVESEN,N.: *"Added resistance of ships in waves"*, Journal of Hydronautics, Vol. 12, No. 1.

2-74 SCHIFRIN: *"An approximate calculation of added resistance of ship in regular waves"*, Sudostroenie, No. 12 Leningrad, 1973.

2-75 SHINTANI,A.: *"Comparison of computed and measured added resistance in waves"*, Journal of the Kansai society of naval architects, Vol. 137, 1970.

2-76 SIBUL, O.J.: *"Ship resistance in uniform waves"*, Institute of Engineering Research, University of California, Report No. NA-64-1, January 1964.

2-77 SIBUL, O.J.: *"Increase of ship resistance in waves"*, Report NA-67-2, 1967, College of Engineering, University of California.

2-78 SIBUL, O.J.: *"Constant thrust versus constant velocity method for resistance measurements in waves"*, College of Engineering, University of California, Report No. NA-71-1, June 1971.

2-79 SIBUL, O.J.: *"Measurements and calculations of ship resistance in waves"*, College of Engineering, University of California, Report No. NA-71-2, December 1971.

2-80 SIBUL, O.J.: *"Ship resistance and motions in uniform waves as a function of block coefficient"*, Institute of engineering Research, University of California, Series 61, Issue 19, June 1961.

2-81 SIBUL, O.J.: *"Ship resistance in irregular waves"*, College of engineering, University of California, Report No.NA-69-5, October 1969.

2-82 SIBUL, O.J. AND REICHERT, G.: *"Ship resistance in uniform waves as a function of wave steepness"*, Institute of Engineering Research, University of California, Series 61, Issue 14, Date June 1957.

2-83 SIBUL, O.J.: *"Ship resistance in uniform waves as a function of wave steepness and beam of the ship"*, University of california, Institute of Engineering Research Report Series 61, Issue 18, September 1959.

2-84 STROM-TEJSEN, J., YEH, H.Y.H. AND MORAN, D.D.: *"Added resistance in waves"*, SNAME transactions 1973.

2-85 TAKAGI, M., HOSODA, R. AND HIGO, Y.: *"An investigation into Gerritsma's formula of the resistance increase by Energetics"*, Journal of the Kansai society of naval architects of Japan, No. 170, September 1978, pp 59.

2-86 TAKAGI, M., HOSODA, R. AND SHIMASAKI, H.: *"An improvement for the calculation of added resistance in waves"*, Journal of the kansai society of naval architects, Japan, No. 141, pp. 33-44, June 1971.

2-87 THIEL, R., *"Assessment of two empirical methods for the calculation of resistance and power increase of ships in a seaway based on experimental results"*, Schiffbauforschung, Heft No. 3, 1982.

2-88 UENO, K. ET AL.: *"Some experiments of heaving effect on ahead resistance of ships"*, Journal of the Society of naval Architects of West Japan, No. 37, February 1969, and 12th ITTC 1969, p.112.

2-89 UENO, K. ET AL.: *"Some experiments of pitching effect on ahead resistance of ships"*, Journal of the Society of Naval Architects of West Japan, No. 37, February 1969, and 12th ITTC 1969, p.114.

2-90 UENO, K. ET AL.: *"Some experiments of Yawing effect on ahead resistance of ships"*, Journal of the Society of Naval Architects of West Japan, No. 23, March 1962.

2-91 UENO, K. ET AL.: *"Further experiments of yawing effect on ahead resistance of ships"*, Journal of the Society of Naval Architects of West Japan, No. 27, March 1964.

2-92 UENO, K. ET AL.: *"Some experiments of rolling effect on ahead resistance of ships"*, Journal of the Society of Naval Architects of West Japan, No. 31, March 1966.

2-93 VASSILOPOULOS,L.A.: *"Wave induced added drag of destroyer type ships in head random seas"*, Report No.70-4-7002-1, Maritech Inc., 1970.

2-94 VOSSERS,G.: *"Resistance propulsion and steering of ships-C-Behaviour of ships in waves"*, The technical publishing company, The Netherlands, 1962.

2-95 VOSSERS,G.: *"Behaviour of ships in waves"*, International Shipbuilding Progress 1961.

2-96 WAHAB,R. AND MOSS, L.W.: *"On the added drag of destroyers in regular head waves"*, NSRDC report 3704, August 1971.

2-97 WANG, S.: *"Experiments on added resistance of a ship among waves"*, Dept of naval architecture and marine engineering, MIT Report 65-1, March 1965.

2-98 YAMANOUCHI,Y. AND ANDO, S.: *"Experiments on a series 60, Cb = 0.70 ship model in oblique regular waves"*, Eleventh International Towing Tank conference, Tokyo (1966), p. 404.

2-99 YEH, H.Y.H., SHUTZ, H. AND PLAIA, P.: *"Powering characteristics of a low block displacement hull form in head seas"*, NSRDC report 4059, February 1973.

2-100 YOSHIOKA, I.: *"On the increase of the towing resistance of a ship model due to rolling motion"*, Bulletin of the Faculty of Engineering, Yokohama National University, Vol. 2, March 1953, pp. 137.

2-101 BEUKELMAN, W.: *"Added resistance and vertical oscillations for cylinders at forward speed in still water and waves"*, Discussion to 19th ITTC, Madrid.

2-102 VASSILOPOULOS,L.: *"The application of statistical theory of non-linear systems to ship motion performance in random seas"*, ISP Vol. 14, No. 150, February 1967.

2-103 FALTINSEN, O.M., HELMERS, J.B., MINSAAS, K.J. AND ZHAO, R.: *"Speed loss and operability of Catamarans and SES in a seaway"*, Proceedings from the first international conference on fast sea transportation, FAST '91, Trondheim, Norway, 1991.

2-104 WADA, Y AND BABA, E.: *"Calculation of resistance increase of large full ships in short waves"*, Proceedings of the third international symposium

on practical design of ships and mobile units, PRADS '87, Trondheim, Norway, 1987.

2-105 SAKAMOTO,T. AND BABA, E.: *"Minimization of resistance of slowly moving full hull forms in short waves"*, Proc. of 16th Symposium on Naval Hydrodynamics, 1986.

2-106 NAITO, S. AND TAKAGI, K.: *"Practical estimation method for added resistance, wave induced steady lateral force and turning moment in oblique waves"*, Proceedings of the fifth international symposium on practical design of ships and mobile units, PRADS '92, Newcastle upon Tyne, UK, May 1992.

2-107 HEARN, G.E., KOON CHUNG TONG AND SIEW MING LAU: *"Hydrodynamic models and their influence on added resistance predictions"*, Proceedings of the third international symposium on practical design of ships and mobile units, PRADS '87, Trondheim, Norway, 1987.

2-108 NAKOS, D.E. AND SCLAVOUNOS, P.D.: *"Ship motions by a three-dimensional rankine panel method"*, 18th ONR Symposium on naval hydrodynamics, Michigan, 1990.

2-109 NAKOS, D.E. AND SCLAVOUNOS, P.D.: *"On steady and unsteady ship wave patterns"*, Journal of fluid mechanics, 1990. Vol. 215, pp 263-288.

2-110 LIAPIS, S. AND BECK, R.F.: *"Seakeeping computations using time-domain analysis"*, 4th International conference on numerical ship hydrodynamics, Washington, 1985.

References of Section 3:

3-1 GERRITSMA, J.; VAN DEN BOSCH, J.J. AND BEUKELMAN, W.: *"Propulsion in regular and irregular waves"*, International Shipbuilding Progress, Vol. 8, No. 82, June 1961.

3-2 VOSSERS, G.; SWAAN, W.A. AND RIJKEN, H.: *"Experiments with series 60 models in waves"*, Transactions SNAME 1961.

3-3 SIBUL, O.J.: *"Ship resistance and motions in uniform waves as a function of block coefficient"*, Institute of Engineering Research, University of California, Series 61, Issue 19, June 1961.

3-4 GERRITSMA, J.; BEUKELMAN, W.; AND GLANSDORP, C.C.: *"The effect of beam on the hydrodynamic characteristics of ship hulls"*, 10th ONR Symposium of Naval Hydrodynamics, 1974.

3-5 BLOK, J.J. AND BEUKELMAN, W.: *"The High-Speed Displacement Ship Systematic Series Hull Forms-Seakeeping Characteristics"*, Transactions SNAME 1984.

References of Section 4:

4-1 JOHN, F.: *"On the motion of floating bodies"*, Communications on pure and applied mathematics", Part I-2, 1949, pp 13-57; Part 2-3, 1950, pp 45-100.

4-2 OORTMERSSEN, G. VAN: *"The motions of a moored ship in waves"*, PhD Thesis, Publication No. 510 Maritime Research Institute Netherlands, Wageningen, The Netherlands.

4-3 NEWMAN, J.N.: *"Interaction of stationary vessels with regular waves"*, 11th Symposium on Naval Hydrodynamics, London, 1976.

References of Section 5:

5-1 FROUDE, W.: *"On experiments with HMS 'Greyhound'"*, Transactions I.N.A., 1874.

5-2 CANHAM, H.J.S.: *"Resistance,Propulsion and Wake Tests with HMS 'Penelope' "*, Transactions RINA, 1975, Vol. 117, pp 61.

5-3 STROM-TEJSEN, J.; YEH, H.Y.H. AND MORAN, D.D.: *"Added Resistance in Waves"*, Transactions SNAME 1973.

5-4 MOOR, D.I. AND MURDEY, D.C.: *"Motions and Propulsion of single screw models in head seas"*, Part 2, Transactions RINA, 1970, Vol. 112, No. 2.

5-5 SLUIJS, M.F. VAN AND DOMMERSHUIJZEN, R.J.: *"Investigations into the effect of model scale on the performance of two geosim ship models"*, Monograph published by the Netherlands Maritime Institute, M20, July 1977.

5-6 JOURNÉE, J.M.J.: *"Prediction of speed and behaviour of a ship in a seaway"*, International Shipbuilding Progress, Vol.23, Sept. 1976, No. 265.

References of Section 6:

6-1 LAMB, SIR HORACE.: *"Hydrodynamics"*, Dover Publication, 1945, Cambridge University Press.

6-2 BATCHELOR, G.K.: *"An Introduction to Fluid Dynamics"*, Cambridge University press, 1967..

6-3 NEWMAN,J.N.: *"Marine Hydrodynamics"*, 1977, MIT Press, Cambridge, Massachusetts.

References of Section 7:

7-1 BLOK, J.J. AND HUISMAN, J.: *"Relative Motions and Swell-up for a Frigate Bow"*, Transactions Royal Institution of Naval Archtects, London, 1983.

7-2 SLUIJS, M.F. VAN: *"Ship Relative Motions and Related Phenomena"*, International Symposium on the dynamics of Marine Vehicles and Structures in waves, London, 1974.

7-3 BLOK, J.J. AND BEUKELMAN, W.: *"The High Speed Displacement Ship Systematic Series Hull Forms-Seakeeping Characteristics"*, Transactions Society of Naval Architects and Marine Engineers, New York, 1984.

7-4 BLOK, J.J.: *"Added Resistance in Waves, Volume I: Five wave directions"*, MARIN Report 50332-1-OE, December 1983.

7-5 BLOK, J.J.: *"Added resistance in Waves, Volume 2: Four Forebody Forms"*, MARIN Report 50332-1-OE, December 1983.

7-6 BLOK ,J.J.: *"Model Experiments with TU-Delft Wigley 1 Model"*, MARIN Report 50731-1-OE, June 1988.

7-7 BLOK, J.J.: *"Model Experiments with TU-Delft Wigley 2 Model"*, MARIN Report 50935-1-OE, December 1989.

7-8 BLOK, J.J.: *"Model Experiments on Wave added resistance of a Segmented Model"*, MARIN Report 50935-2-ZT, Oktober 1989.

7-9 BLOK, J.J.: *"Model Experiments on the Instationary Pressure Distribution at the Bow of a Model in Waves"*, MARIN Report 50935-3-ZT, April 1992.

7-10 OOSSANEN,P. AND PIEFFERS,J.B.M.: *"NSMB-Systematic Series of High Speed Displacement Hull Forms"*, Workshop on the Development of Hull Form Design, MARIN, October 1985.

7-11 ROBSON, B.L.: *"Systematic Series of High Speed Displacement Hull Forms for Naval Combatants"*, RINA-Autralian Division, September 1987.

7-12 *"High Speed Hull Forms"*, MARIN Report No. 11, July 1982.

7-13 *"MARIN High Speed Displacement Hull Form Designs"*, MARIN Report No. 30, December 1987.

7-14 TASAI, F.: *"Wave height at the side of two-dimensional body oscillating on the surface of a fluid"*, Reports of the research Institute for Applied Mechanics, Vol. IX, No. 35, 1961.

7-15 VUGTS, J.H.: *"The hydrodynamic coefficients for swaying, heaving and rolling cylinders in a free surface"*, Technical University of Delft, Hydromechanics Laboratory Report No. 194, January 1968.

References of Section 8

8-1 DAWSON, C.W.: *"A Practical Computer Method for solving Ship-Wave Problems"*, Proceedings 2nd International Conference on Numerical ship hydrodynamics, September 1977, University of California, Berkeley.

8-2 RAVEN, H.C.: *"Variations on a theme by Dawson"*, 17th Symposium on Naval Hydrodynamics, The Hague, 1989.

8-3 CHEN, H.H., TORNG, J.M. AND SHIN, Y.S.: *"Formulation, method of solution and procedures for hydrodynamic pressure project"*, ABS Research and Development Division, Technical Report RD-85026, November 1985, (Distribution restricted to CRS).

References of Section 9:

9-1 BLOK, J.J.: *"Model experiments with TU Delft Wigley 1 model"*, MARIN report 50731-1-OE, June 1988.

9-2 BLOK, J.J.: *"Model experiments with TU Delft Wigley 2 model"*, MARIN report 50935-1-OE, December 1989.

9-3 JOURNÉE, J.M.J.: *"Experiments and calculations on four Wigley hull forms"*, TU Delft Publication MEMT 21, 1992.

9-4 BLOK, J.J.: *"Model experiments on wave added resistance of a segmented model"*, MARIN report 50935-2-ZT, October 1989.

9-5 BLOK,J.J.: *"Model experiments on the instationary pressure distribution at the bow of a model in waves"*, MARIN report 50935-3-ZT, April 1992.

9-6 BLOK,J.J.: *"Added resistance in waves, Volume 1: Five wave directions"*, MARIN report 50332-1-OE, December 1983.

9-7 BLOK, J.J.AND BEUKELMAN, W.: *"The High-Speed Displacement Ship Systematic Series Hull Forms- Seakeeping Characteristics"*, Transactions SNAME, New York, 1984.

9-8 LEE, C.M., O'DEA, J.F. AND MEYERS, W.G.: *"Prediction of Relative Motions of Ships in waves"*, 14th Symposium on Naval Hydrodynamics, Ann Arbor, Michigan, August 1982.

References of Appendix A:

A-1 JOHN,F.: *"On the Motions of Floating Bodies"*, Communications on Pure and Applied Mathematics, Part I:2, 1949 and Part 2:3, 1950.

A-2 STOKER, J.J.: *"Water Waves"*, Interscience Publishers Inc., New York, 1957.

A-3 TIMMAN, R. AND NEWMAN, J.N.: *"The Coupled Damping Coefficients of a Symmetric Ship"*, Journal of Fluid Mechanics, 1962.

A-4 WEHAUSEN, J.V.: *"The Motion of Floating Bodies"*, Annual Review of Fluid Mechanics, No. 3, 1971, pp 237-268.

A-5 WEHAUSEN, J.V. AND LAITONE, E.V.: *"Handbuch der Physik"*, Vol. 9, Springer Verlag, Berlin, 1960

This page intentionally left blank

Nomenclature

A	=	wetted surface area
dA	=	element of wetted surface area
$\overline{A}$	=	mean wetted surface area
A_0	=	static wetted surface area up to static waterline
$a^{(0)}$	=	steady addition to the wetted surface area resulting from forward speed in calm water
$a^{(1)}$	=	unsteady part of instantaneous wetted surface
$\{A\}$	=	total free-surface condition expression of eq. (A-43)
B	=	ship beam
$\{B\}$	=	steady term of the free-surface condition in eq. (A-43)
$\{C\}$	=	instationary parts of the free-surface condition expression of eq. (A-43)
C_B	=	block coefficient
C_{WP}	=	waterplane coefficient
$c(t)$	=	constant, dependent upon time
d	=	water depth
$\partial/\partial t$	=	local derivative
D/Dt	=	substantial derivative
Fn	=	Froude number
$\overline{F}$	=	force vector
$\overline{FSC}$	=	steady part of linearized free-surface condition

$f(x_1)$	=	envelope of amplitudes of relative motion along the ship length
g	=	acceleration due to gravity
h (Tq)	=	steady bow wave height at station q for local draft Tq
i	=	complex number
j	=	index to ship motion modes j = 1-6
k	=	wave number
L	=	ship length
$\overline{n}$	=	normal vector outward from hull
$\overline{n}'$	=	normal vector, body fixed
$\overline{n}$	=	normal vector relative to travelling axes
$\overline{N}$	=	normal vector relative to space-fixed axes
O	=	origin of $\overline{X}$ system of space-fixed axes
o'	=	origin of $\overline{x}'$ system of body-fixed axes
o	=	origin of $\overline{x}$ system of travelling axes
p	=	pressure in the fluid
p_a	=	atmospheric pressure
R	=	radius
RAW	=	added resistance in waves
$\overline{X}\,(X_1, X_2, X_3)$	=	system of axes fixed in space
$\overline{x}' = (x_1', x_2', x_3')$	=	system of axes fixed in the ship
$\overline{x} = (x_1, x_2, x_3)$	=	system of axes moving in steady translation with the mean forward velocity of the ship
s	=	vertical relative motion between ship and water surface
$\overline{S}$	=	stationary bow wave height
s_a	=	relative motion amplitude
s_{a20}	=	amplitude of relative motion at the fore perpendicular
SUC	=	swell-up coefficient

t	=	time
σ_s	=	standard deviation of relative motion
TAW	=	added thrust in waves
T_m	=	mean draft
$\overline{U}$	=	ship's mean velocity
V	=	velocity of the fluid
$\overline{V}$	=	velocity of a body-fixed point
$\overline{V}_s$	=	local velocity of ship's wetted surface
$\overline{W}$	=	steady flow velocity vector
$\bar{\alpha} = (\alpha_1, \alpha_2, \alpha_3)$	=	vector of unsteady body motion
∇	=	nabla operator
∇^2	=	nabla operator squared
ΔTq	=	increment of local draft Tq
ρ	=	fluid density
ε	=	small perturbation parameter
Φ	=	total potential space fixed
$\phi^{(0)}$	=	potential of steady flow
$\phi^{(1)}$	=	first order unsteady potential
$\phi^{(2)}$	=	second order unsteady potential
ϕ_i	=	potential of incident wave
ϕ_d	=	potential of diffracted (scattered) wave
ϕ_r	=	potential of radiated wave
ϕ_s	=	potential of dynamic swell-up effect
ϕ_{s1}	=	first dynamic swell-up potential
ϕ_{s2}	=	second dynamic swell-up potential
$\bar{\xi} = \xi_1, \xi_2, \xi_3$	=	vector of unsteady translations
$\bar{\xi}_B$	=	stationary bow wave height

$\overline{\Omega} = \Omega_1, \Omega_2, \Omega_3$	=	vector of unsteady rotations
ζ	=	free-surface elevation of the fluid
ζ_a	=	regular wave amplitude
ζ_i	=	free-surface elevation due to incident wave
ζ_d	=	free-surface elevation due to diffracted wave
ζ_r	=	free-surface elevation due to radiated wave
ζ_s	=	free-surface elevation due to swell-up wave
ω	=	circular frequency
ω_e	=	circular frequency of encounter
λ	=	wave length
(0)	=	superscript to denote steady zero order quantity
(1)	=	superscript to denote first order quantity
(2)	=	superscript to denote second order quantity
$\bullet$	=	vector inner product
*	=	vector outer product
index 0	=	index to incident wave potential
index 1 to 6	=	index to radiation potentials
index 7	=	index to diffraction potential

List of Tables

This page intentionally left blank

List of Figures

This page intentionally left blank

Summary

In this thesis a detailed investigation is described of the resistance increase of a ship in waves.

For a ship sailing in flat calm water the resistance force is due to the flow of the water along the hull setting up frictional forces and pressure forces.

For a ship sailing on a stormy sea the resistance is increased due to contributions from a whole range of sources: waves, wind, rudder drag, drift angle as a result of which often the speed is reduced. One of the most important contributions to the resistance increase stems from the forces of the waves on the ship. These forces set up impressive ship motions but they also cause an average mean resistance increase. This may either cause a speed loss if the power is kept constant, or may necessitate increased fuel consumption if the speed is to be maintained.

It can be shown that the resistance increase due to waves, or the 'wave added resistance' as it is often called, is predominantly of potential origin, the frictional contribution being only small. This opens up the possibility to invoke the Froude scaling law to convert experimental data from model scale to the full ship scale, and it allows the use of potential theory to describe the behaviour of the flow.

Based on some initial observations it was hypothesized that the wave added resistance is for the most part the result of the relative water motions predominantly at the bow, and the study had the objective to validate this hypothesis through model experiments and mathematical modelization.
An extensive suite of model test programs was carried out to obtain insight into the behaviour of the flow, the pressures and the free surface around a ship model in motion in waves, in the end including 10 model test series covering 19 hull forms.

On basis of the detailed experimental investigation a mathematical model based on linear potential theory was setup to describe the observed effects. The mathematical model was converted into a computer program and correlation computations were made for 4 hull forms, a slender and a beamy Wigley hull, a cargo ship and a frigate.

The key aspects of the study are the analysis of the relative water motion at the bow in which a strong interaction between the stationary and the instationary flow field was discovered leading to the definition of the 'dynamic swell-up'.

This 'swell-up' is an effect brought about by the influence of local draft on the steady bow wave, and it was shown to be remarkably independent of frequency.

The interaction was also shown to exist deeper in the fluid, as evidenced by the behaviour of the instationary pressures and forces. The dynamic variations about the steady mean value contained a significant contribution of the swell-up.

These observations led to the adoption in the mathematical model of a double linearization scheme using the field coordinates and the local undisturbed relative motion as variables.

In the global sense the upper part of the bow of the model was found to contribute the greater part of the extra resistance, the lower bow and the stern making only minor contributions.

Both the model experiments and the mathematical model based computations supported the hypothesis posed in the beginning, namely that the relative vertical water motion at the bow is the governing factor for the added resistance in waves from ahead.

This page intentionally left blank

Een uitgebreide reeks model experimenten werd uitgevoerd om inzicht te verkrijgen in het gedrag van de stroming, de drukken en van het vrije vloeistof oppervlak rond een schip dat beweegt in golven. Er werden 10 series experimenten uitgevoerd met in totaal 19 rompvormen.

Op basis van het gedetaileerde experimentele onderzoek werd een mathematisch model opgesteld om het gedrag van de stroming te beschrijven. Het model werd op de computer geprogrammeerd en correlatie berekeningen zijn uitgevoerd voor vier scheepstypen, een slanke en een brede WIGLEY vorm, een vrachtschip, en een fregat.

De belangrijkste aspecten van de studie behelsen de analyse van de relatieve waterbeweging rond de boeg waarin een sterke interactie tussen het stationaire en het instationaire stromingsveld werd aangetoond, hetgeen leidde tot de definitie van de 'dynamische swell-up'. Deze 'swell-up' is het gevolg van de invloed van locale diepgangsveranderingen op het boeggolfsysteem en deze interactie is zoals getoond opmerkelijk onafhankelijk van de frequentie.

De interactie tussen het stationaire en het instationaire veld bleek ook dieper onder water te bestaan, zoals bleek uit het gedrag van de dynamische drukken. De dynamische variaties van de druk rond de gemiddelde stationaire waarde bleek een aanzienlijke bijdrage te bevatten van de 'swell-up'. Deze observaties leidden in het mathematisch model tot het kiezen van een dubbel lineariseringsschema waarbij de veldcoordinaat en de ongestoorde relatieve beweging als variabelen genomen zijn.

Over het geheel genomen bleek dat het bovenste gedeelte van de scheepsboeg de grootste bijdrage levert aan de extra weerstand, terwijl het onderste gedeelte van de boeg alsmede het achterschip slechts een kleine bijdrage leveren.

Zowel de modelexperimenten als de berekeningen gebaseerd op het mathematische model bevestigen de hypothese welke in het begin gesteld was, namelijk dat de relatieve verticale waterbeweging aan de boeg de grootste bijdrage levert aan de toegevoegde weerstand ten gevolge van golven welke recht van voren komen.

Curriculum Vitae

The author was born on June 13, 1947 in Voorburg, The Netherlands. He attended school in Rijswijk, and completed the HBS-B from the 'Gemeentelijk Lyceum Rijswijk' in 1964. He commenced his professional education at the Dordrecht Technical Institute where he obtained his batchelor's degree in naval architecture in 1967. He continued at the Delft University of Technology and obtained his master's degree in naval architecture in 1974, on a thesis on the optimization of automatic steering control of large tankers, receiving the 1974 study award of the Naval Architecture Department.

In 1974 he joined the staff of the Maritime Research Institute Netherlands,Wageningen as project manager on the staff of the Seakeeping Laboratory. He has been working in the Industrial Projects Division and the Ocean Engineering Division and he is currently engaged as a senior project manager of the Ship Research Department of MARIN.

Samenvatting

In deze thesis wordt een gedetaileerde beschrijving gegeven van de weerstands verhoging van een schip in golven.

Wanneer een schip in kalm water vaart treedt een weerstands kracht op tengevolge van de stroming van het water langs de romp hetgeen leidt tot wrijvingskrachten en drukkrachten.

Wanneer een schip in een stormachtige zee vaart neemt de weerstand toe door een reeks factoren: golven, wind, roerwerking, drift hoek ten gevolge waarvan veelal de snelheid zal verminderen. Eén van de belangrijkste bijdragen aan de extra weerstand wordt geleverd door de krachten van de golven op het schip. Deze krachten veroorzaken niet alleen indrukwekkende bewegingen maar zij veroorzaken ook een gemiddelde verhoging van de weerstand. Deze weerstandsverhoging leidt tot snelheidsverlies indien het vermogen constant gehouden wordt, of noodzaakt tot extra brandstofverbruik indien de snelheid constant gehouden moet worden.

Het kan aangetoond worden dat de weerstandsverhoging ten gevolge van golven hoofdzakelijk een potentiaal effect is, en dat het aandeel van wrijving klein is. Dit schept de mogelijkheid om resultaten van model experimenten met de schaalwet van Froude te verschalen naar de ware grootte, en het biedt de mogelijkheid om potentiaal theorie te benutten om het gedrag van de stroming te beschrijven.

De werkhypothese welke in het begin gesteld was veronderstelde dat de extra weerstand in golven voor het grootste deel het gevolg is van de relatieve verticale water beweging aan de boeg, en deze studie had tot doel om deze hypothese te onderbouwen met model experimenten en mathematische modelvorming.

Acknowledgement

I should like to thank my promotor Prof. Ir. J. Gerritsma who, after having introduced me to the realm of ship hydrodynamics two decades earlier, offered continual support and encouragement during the progress of this study.

I am indebted to the Board of Directors of the Maritime Research Institute Netherlands for their permission to undertake this work and to publish the results in the form of a thesis, and for affording me the time and funds to complete the work.

A special word of thanks is extended to the staff members of MARIN who have contributed to the experiments, the analysis and the software programming. They have all been loyal fellow-workers and their whole-hearted cooperation has greatly encouraged me.

I also gratefully acknowledge the support of the staff of the Ship Hydromechanics Laboratory of the Delft University of Technology for their enthousiastic support and their generosity in letting me use their facility for part of the experimental work.

My gratitude is also extended to the sponsor companies of the Co-operative Research on Ships (CRS) group and to the sponsors of the Fast Displacement Ship (FDS)project, for their permission to use some interesting experimental data in this study. As platforms of exchange of views and experiences these international groups have proven to be invaluable.

A personal word of appreciation goes to the trio that prepared the manuscript for printing. The graphic artwork by Mr. H.J. Keukens, the doyen of MARIN's 'seakeeping family', nicely matches the text-processing by Mrs. M.L.N.A. Drinoczy-Jansen and the type-setting by Miss Rixta van den Hoofdakker on the Ventura software package. I am very pleased with their result.

Finally, and most importantly, I wish to thank my wife Annejuul and daughters Marloes and Merle for bearing with my absence, my absent-mindedness and numerous 'just-a-few-more-weeks' assurances.